THESIS

to be presented on October 6, 2014 at

Universidad de La República, UdelaR

for achieve the degree of

MAGISTER EN INGENIERÍA MATEMÁTICA

to

Ing. Guillermo RELA MUSIANI

Investigation Institute: DPI – IIMPI
University components:
UNIVERSIDAD DE LA REPÚBLICA
FACULTAD DE INGENIERÍA

Thesis title:

Unsolved Accidents in Fuel Storage Tanks: Resolution Methodology by Mathematical Modeling under Systemic Approach

Committee of examiners:

Dr. Franco	ROBLEDO	Thesis Director
Dr. Gerardo	RUBINO	President
Dr. Pedro	PIÑEYRO	
Ing. Gabriel	PISCIOTTANO	
Dra. Soledad	GUTIERREZ	

Acknowledgement

I wish to thank Doctor Franco Robledo Amoza, Thesis Director, for his dedication, without which this thesis would not have been possible.

To my beloved wife Graciella Chirico for her unconditional support of an entire life, I never properly rewarded, particularly including this thesis.

My sons María Fernanda Rela Chirico and Martin Rela Chirico by admitting low quality of care of his father during the development of this thesis, and more broadly during the development of their father's profession.

I want to thank Gerardo Rubino, Gabriel Pisciottano, Pedro Piñeyro and Soledad Gutierrez for the honor of judging this work.

Index

Content Index

Part I – INTRODUCTION **3**

Abstract 11

Introduction 15

Part II – PROCEDURE THEORETICAL FRAMEWORK **19**

Chapter 1 – Theoretical Framework 21

1.1 Introduction 21

1.2 Procedure 21

Part III – CASE STUDY **31**

Chapter 2 – Description of the Accident 33

Chapter 3 – Fuel Air Mixture 39

3.1 Calculation of Air-Fuel Mixture in the Tank 39

3.2 Monitoring of Explosive Atmospheres Test Description 43

3.3 Estimate Calculation of the Sudden Inflammation Energy within the Tank 35

Chapter 4 – Process of Tank Explosion Model 49

4. 1 Evolution of Internal Pressure from the Lit of the Flame to the Tank Burst 49

4.2 Mathematical Model of Simulation of Tank Behavior from Lit of the Flame to Burst . . 65

Chapter 5 – Tank Burst 93

5.1 Tank Burst Pressure 93

5.2 Burst Energy Distribution 93

5.3 Tank Burst Modelling 93

Chapter 6 – Consequences of Explosion Effects on Persons in Accident 119

6.1 Effects of Burst 119

6.2 Effects of Body Displacement 124

6. 3 Consequences of Explosion Effects on Persons in Case of Tank Burst by Detonation. . 128

Chapter 7 – Displacement of a Body Standing on the Tank 135

Chapter 8 – Movement of a Body Initially on the Loading Port Lighting a Flame 139

Chapter 9 – Detonation and Shockwave Creation 153

Chapter 10 – Interaction Between Shockwave and a Liquid Layer 159

Chapter 11 – Conclusions 163

Part IV - APPENDIX **167**

Appendix A: Chapter 4 - Tank Behavior Model I to Model X 169

Appendix B: Chapter 5 Tables 201

Appendix C: Chapter 6 Tables. 235

Appendix D: Chapter 7 Tables. 269

Appendix E: Chapter 8 Tables 279

Appendix F: Chapter 10 Tables 325

Bibliography **329**

Figures Index **331**

Glosary of Terms

Burning Velocity. The rate of flame propagation relative to the velocity of the unburned gas that is ahead of it.

Fundamental Burning Velocity. The burning velocity of a laminar flame under stated conditions of composition, temperature, and pressure of the unburned gas.

Combustion. A chemical process of oxidation that occurs at a rate fast enough to produce heat and usually light in the form of either a glow or flame.

Deflagration. Propagation of a combustion zone at a velocity that is less than the speed of sound in the unreacted medium.

Detonation. Propagation of a combustion zone at a velocity that is greater than the speed of sound in the unreacted medium.

Enclosure. A confined or partially confined volume.

Explosion. The bursting or rupturing of an enclosure or a container due to the development of internal pressure from a deflagration.

Flame Speed. The speed of a flame front relative to a fixed reference point.

Flammable Limits. The minimum and maximum concentrations of a combustible material, in a homogeneous mixture with a gaseous oxidizer, that will propagate a flame.

Flash Point. The minimum temperature at which a liquid gives off vapor in sufficient concentration to form an ignitable mixture with air near the surface of a liquid, as specified by test.

Gas. The state of matter characterized by complete molecular mobility and unlimited expansion; used synonymously with the term vapor.

K_G. The deflagration index of a gas cloud.

Maximum Pressure (Pmax). The maximum pressure developed in a contained deflagration of an optimum mixture.

Rate of Pressure Rise (dP/dt). The increase in pressure divided by the time interval necessary for that increase to occur.

Maximum Rate of Pressure Rise [(dP/dt)max]. The slope of the steepest part of the pressure-versus-time curve recorded during deflagration in a closed vessel.

Reduced Pressure (Pred). The maximum pressure developed in a vented enclosure during a vented deflagration.

Vent. An opening in an enclosure to relieve the developing pressure from a deflagration.

Vent Closure. A pressure-relieving cover that is placed over a vent.

Part I

INTRODUCTION

RESUMEN

Las mezclas basadas en hidrocarburos pesados con componentes más livianos se utilizan en la construccion de carreteras (diluido asfaltico), en la energia para la produccion industrial (hornos, calderas, generadores electricos) y en la generación de potencia de accionamiento para el transporte internacional por barco de enormes cantidades de bienes (motores de combustion interna de gran porte).

Esto permite el desarrollo de una serie de actividades, ofrece el apoyo a la produccion de bienes y servicios a nivel mundial, aunque su contribucion aparece invisible para el mundo que nos rodea tal como lo percibimos.

Para su uso, los combustibles de hidrocarburos pesados se manipulan, almacenan, transportan y transfieren.

Todas estas operaciones tienen un alto riesgo de explosion.

Esta tesis se centra en las explosiones dentro de los tanques de almacenamiento de combustible pesado. Particularmente los que ocurrieron hace mucho tiempo y no han tenido una explicacion completa.

En la misma se ha establecido una metodología genérica para la determinación de las atmósferas explosivas en el interior de tanques de combustible, el modelado del proceso de combustión en su interior a partir de la ignición ante la presencia de una chispa o llama en el entorno de una abertura del tanque, así como las consecuencias de esta combustión (derivando en una posible explosión) sobre las personas en el entorno del tanque.

Este trabajo fue realizado con la expectativa de hacer una contribucion a la investigacion de este tipo de accidentes no resueltos.

Palabras clave: explosion, tanque, combustible, accidente, modelado.

ABSTRACT

Storage of mixtures of heavy hydrocarbon fuels with lighter components is a worldwide necessity because of their use for the construction of roads (asphalt diluted), the energy for industrial production (furnaces, boilers, electrical generators) and power for international transportation by ship of huge amounts of goods (big size internal combustion engines).
This allows the development of a number of activities, provides the support for the production of goods and services worldwide, although its contribution appears invisible to the life as we know and for the world surrounding us as we perceive it.
For its use, the heavy hydrocarbon fuels need to be handled, stored, transported, and transferred.
All this operations have high risk of explosion.
This thesis focuses on the explosions inside heavy fuel storage tanks. Particularly those that occurred long ago and have not had a full explanation.
In this Thesis a generic methodology for determining hazardous atmospheres inside fuel tanks has been set, the modeling the combustion process inside the tank from the ignition in the presence of a spark or flame in the vicinity of an opening of the tank, and the consequences of this combustion (resulting in a possible explosion) on persons in the vicinity of the tank.
This job was done in the expectative of be making a contribution to the investigation of such kind of unsolved accidents.

Keywords: explosion, tank, fuel, accident, modeling

INTRODUCTION

This work will encourage the seeking of an explanation to some type of unsolved accidents involving storage of heavy hydrocarbon fuels, and also contribute to improve support systems and managerial decisions, to eliminate the accident's cause from the root.

One key of this thesis aproach is the systemic perspective of the problem along its resolution, because in the accident all the nature's law must be followed.

Being the heavy fuel combustibles ubiquitous debt to their use for the construction of roads, energy generation, among others, the risk of accident is everywhere this fuels are needed.

The content of this thesis is presented as follows.

Chapter 1 shows the theoretical framework as an algorithm to be processed in order to study the accident without take in account the amount of time between the accident and the moment of the study.

The theoretical framework chapter is composed of a twenty steps procedure that would enable to achieve the accident resolution.

From Chapter 2 to Chapter 10 the algorithm explained in Chapter 1 was tested in a real case.

Chapter 2 is centered in the description of the tank and circumstances where the accident happened.

Chapter 3 determines the air fuel mixture at explosion moment in this particular case, and Chapter 4 applies the mathematical model of flammable mixture behavior inside tank.

Chapter 5, 6, 7 and 8 explains the consequences of the accident in the nearby area including the possible effects in persons.

Finally, Chapters 9 and 10 analyzes the effect of shock wave in tank's body and fuel spill in order to have more elements that could match with the accident's explanation.

As a sum of all this elements, deployed in sequence, an explanation similar to what really would happened was found, no matter the year passed.

Consistently with this, as it was said, the systemic approach of the problem, considering as much as possible all nature's laws involved in the accident, and its effects on the people and materials in the influence area of the accident, is the key to solve the problem.

Mathematical models allow to show the accident's evolution in time steps. Each step last one hundredth of a second. Also enables to establish the synchronicity of events and effects with the area nearby the accident.

The reliability level of the results achieved in the case study are different according to the topic.

Explosive atmospheres evaluation in Chapter 3 Fuel Air Mixture, is the most reliable result in this work. In this Chapter, a theoretical calculation of the air-fuel mixture inside the tank was compared with a monitoring of explosive atmospheres test. The results of calculus and test are quite similar.

The process of explosion model of the tank in Chapter 4 Process of Tank Explosion Model, is next in reliability order. This Chapter studies the evolution in time of the internal pressure and other variables, from the lit of a flame to the tank burst moment.

The internal pressure evolution in time obtained in Chapter 4, was no so different of the internal pressure evolution in time obtained by the Russian scientist Vladimir Molkov [4] in a study using a tank quite similar to the tank that suffer the accident.

Next in less reliable order in the study of the tank burst. Chapter 5 Tank Burst, studies this phenomenon using two different models, and arrives to converging conclusions.

The following subject in reliability decreasing order, is the study of the injuries suffered by the people around the tank. Chapter 6 Consequences of Explosion Effects on Persons in the Accident, for estimate the injury use the international technical reference theories only.

Less reliable is the study of the movement of the bodies in the accident's nearby area. In Chapter 7 Displacement of a Body Standing on the Tank the movement ; this is debt to fact that they use the general law of the mechanical (cardinal equations of rigid bodies).

Finally, tank rupture and deformation as well as fuel spill around the tank are atemps to have more reference elements in order to enhace the systemic perspective as a way to arrive to a solid conclusion.

0.1 References

This thesis join from the stand point of view of a systemic aproach of these aspects:

- behavior, in terms of air fuel mixture, of a heavy fuel type flamable/ combustible inside a tank
- development of pressure and temperature inside tank of the burned and unburned air fuel mixture along the time
- detonation, if that is the case, of the unburned mixture
- flow of gases through the tank openings
- efect of flow of gases through the tank openings in the neighborhood of the tank, people and objects
- efect of explosion in the neighborhood of the tank, people and objects
- tank deformation due to the internal pressure
- tank rupture time
- interaction between the explosion shock wave and liquid inside the tank

- spill of fuel in the neighborhood of the tank

Each one of them requires an specific tratment, and as a whole, they would provide an explanation for a heavy fuel explosion accident.

To the best of our knowledge, it has not been possible to find a scientific work that brings together all disciplines requires the study of this type of accident from a single systemic approach.

It has not been found any technical article that comprise all these aspects at the same time with the purpose of give a general methodollogy for these kind of problems.

It has been found technical articles and books that comprise each aspect separately.

The behavior, in terms of air fuel mixture, of a heavy fuel type flamable/ combustible inside a tank is a subject widely studied.

For the development of pressure and temperature inside tank of the burned and unburned air fuel mixture along the time, as well for detonation, there are several works, among these it have been found:

The National Fire Protection Agency standard NFPA 68 Guide for Venting of Deflagrations – Edition 2002, is a Standard that guides the design, location, installation, maintenance, and use of devices and systems that vent the combustion gases and pressures resulting from a deflagration within an enclosure so that structural and mechanical damage is minimized. The guide should be used as a companion document to NFPA 69, Standard on Explosion Prevention Systems, which covers explosion prevention measures.

According to these Standards, the choice of the most effective and reliable means for explosion control should be based on an evaluation that includes the specific conditions of the hazard and the objectives of protection. Venting of deflagrations only minimizes the damage that results from combustion.

NFPA 30, Flammable and Combustible Liquids Code - Sixth Edition, its provisions are intended to reduce the hazard to a degree consistent with reasonable public safety, without undue interference with public convenience and necessity, of operations that require the use of flammable and combustible liquids. Thus, compliance with this standard does not eliminate all hazards in the use of flammable and combustible liquids.

For the efect of explosion in the neighborhood of the tank, people and objects, as well as the flow of gases through the tank openings study, the book Lee´s Loss Prevention in the Process Industries [2] have several chapters studing explosion types and consequences.

The efect on persons and object is very well treated in the GreenBook [3].

Gas Explosion Handbook [4] is a useful guide for the study of gas explosion.

All these references not consider the possibility of a detonation or explosion inside a tank. According to these and other works the transition from detonation to explosion

would be produced after a long pipe traveling, seen a cylindrical tank as a pipe.

The way this thesis study the problem of the combustion inside the tank, that is, using a mathematical model that registered the unburned air fuel mixture pressure and temperature inside the tank, allow arrive to the conclusion that the mixture will reached the self ignition temperature.

This conclusion is opposite to the Gas Explosion Handbook and so many other reference sources.

So, this thesis methodology allow to find an explanation that fits better with some heavy fuel tank internal explosion accidents.

The efect of the flow of gases through the tank openings in the neighborhood of the tank related to body movement, is based on drag and lift coeficients for human body at different positions. A good reference was found in The Evaluation of de Human Body as an Airfoil by William P. Schane, LTC, MC - U. S. Army Aeromedical Research Laboratory and U. Dean C. Borgman, Research Scientist U.S. Army Aeronautical Research Laboratory Moffett Field, California MAY 1969.

Nevertheless, a better aproach to the first movement of the body over the loading port would be found. That is when considering a flow of gases in the order of a comercial jet airplane turbine exhaust. There is a lack of information about it, but, an article, [6] Aircraft Jet Engine Exhaust Atlantic City international Airport Blast Effects on Par-56 Runway. Threshold Lamp Fixtures, was helpful in match the conclusions of the body over the loading port considering that flow of gases in the order of a comercial jet airplane turbine exhaust and the conclusions of this thesis about the subject.

Talking about detonation/explosion inside tank, when the shock wave advances inside and outside the tank, there is an interation between the shock wave and the liquid inside the tank that is well described in the Interaction of a Shock Wave with a Water Layer [7].

The work Venting of Gaseous Explosions: Turbulization Aspect [8], study the case of a tank with similar volume of the tank and its relief opening to the one of the case of study. This study didn't consider the self ignition.

For the problem of evaluate the tank burst time, two articles were found: Development of a Simplified Theoretical Model for Dynamic Burst Time and Pressure of a Cylindrical Shell [9] and Research on Bursting Pressure Formula of Mild Steel Pressure Vessel [10].

In the study of fuel spill no study about it was found, but useful ideas came from the article Flashing Liquid Jets and Two-phase Dispersion [11].

Part II

THEORETICAL FRAMEWORK

Chapter 1

Theoretical Framework

1.1 Introduction

This theoretical framework Chapter enables to understand the twenty steps procedure to achieve the accident resolution.
The main subjects are the estimation of fuel vapor – air mixture at the explosion moment, the estimation of the sudden inflammation energy within the tank, the evolution of the explosion inside the tank and outside the tank, and the efect on people and materials in the neighborhood of the accident.
The objective is to study a combustion process inside a fuel tank, and its consequences in the neighborhood of the accident area if an explosion happen.
In some conditions an explosion inside the tank can happen, the study try to determine when this can be possible.

1.2 Procedure

Step #1: Estimation of Free Tank Volume

The procedure starts with the determination of the free volume of the tank.
Inside the tank there is liquid up to certain level and the rest is ocupated by air and hydrocarbon vapor.
Free tank volume is the volume of the tank ocupated by air and hydrocarbon vapor.

Step #2: Estimation of Fuel Temperature at the Explosion Moment

If the accident happened during a filling or a withdraw process is necessary to evaluate the temperature of the fuel, because there's a strong relationship between fuel temperature and pressure vapor of the fuel.
Any fuel is a mixture of hundreds of different types of hydrocarbons, and if have an specific pressure vapor.

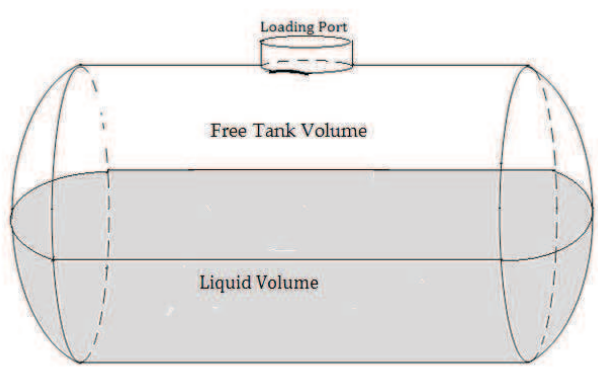

Figure 1.1 – Free Tank Volume

Previous concepts to Steps #3 and #4:

- To estimate the amount of vapor of fuel that was in the tank at the explosion moment, it must resort to the concept of vapor pressure; by the Dalton's Law, determines the amount of fuel vapor relative to air there.

- The vapor pressure for any substance, particulary a fuel, is characteristic of the fuel and it depends only on the temperature at which it is located.

- The total pressure of a mixture is equal to the sum of the partial pressures of itscomponents.

- The partial pressure in a gas mixture is equal to the mol fraction of each component in the mixture.

- Assuming ideal gas behavior, if each of these gases (air and fuel vapor) were studied separately, the contribution to the pressure of each component is directly related to the number of mols of the component.

- Similarly it can be set that the volume percentage is given by the Amagat Law of Partial Volumes, which states that in a mixture of gases, each gas occupies the volume as if the other gases were not present.

Step #3: Estimation of Fuel Vapor Pressure from Vapor Pressure of Hydrocarbon Products of Equal Length of Carbons than the Characteristically Components of Fuel

The fuel can be characterized by over sever hundred of different types of hydrocarbons.

Among these, there are different types of hydrocarbons according to the type of bond between hydrogen and carbon.

Each fuel particularly comprises a certain percentage of paraffinic hydrocarbon type, of naphthenic type, and of the aromatic type.

Using the vapor pressure of a hydrocarbon that was taken as representative of each type, the result of calculating the vapor pressure of a mixture of three types of hydrocarbon in the above mentioned percentages, gives approximately the vapor pressure of the fuel.

If the total pressure is equal to atmospheric pressure, the volume percent of fuel vapor relative to air in a tank can be determinate easy from the fuel vapor pressure.

This value corresponds to conditions of equilibrium which is achieved after some time, so this value could be lower if it had not reached equilibrium.

If the fuel is a mix of two of more kind of commercial fuels (like in the case of study) is necessary to study the compound effect of the two fuel types.

Previous Concepts to Step #4:

The way to measure the amount of hydrocarbon vapor in air is with a Gas Detector device.

Gas detectors are calibrated for certain hydrocarbons, and within a validity date of calibration.
To be calibrated with certain hydrocarbon, the value indicated in the instrument reading should be corrected to be used with other hydrocarbons.
The read value at the instrument must be corrected with the correction factor.
The corrected value is compared to determine if it would be in the lower explosive limit.

Step #4: Estimated Percentage of Fuel Vapor in the Interior of the Tank from the Explosive Atmosphere Tests
Each tank has one or more openings. These openings can be used for filling the tank with fuel (loading port), for inspection (man hole), among other aplications.
For start a fire inside a fuel tank it is necessary to have an ignition service and put this ignition source close to one of these openings of the tank.
For these purpose it is necessary to recreate the tank area near the opening or the point where the ignition start.
It is important to recreate the geometry of the area at the same fuel vapor temperature that when the ignition start.
Using an indicator of fuel vapor concentration in air it is possible determine if reaches the minimum value of fuel vapor in the air to ignite.
Monitoring of explosive atmospheres test consisted of three parts.

Previous Concepts to Step #5 and Step #6:
The measurement of vapor fuel concentration in several points inside the tank, and or the openings on the tank, is called monitoring of fuel vapor concentration inside the tank and or the openings the tank.

Step #5: Monitoring of Fuel Vapors Concentration in the Interior of the Tanks
For determine where the explosion start, is necessary found where inside the tank the porcentage of fuel vapors in air is in the explosion range for that kind of fuel.

Step #6: Monitoring of Fuel Vapors Concentration on the Surface of the Tanks
Another test is necessary to be conducted on the surface of the recreate tank area in order to determine if the explosion is only possible if the flame burns inside the tank or also could be produced outside of it.

Step #7: Monitoring Fuel Vapors Concentration at Environment Temperature
Vapor concentration it is also needed to be measured at room temperature if the fuel object of study is moved hot (heavy fuel) in order to record the vapor concentration values.
This measure gives the idea of how near or how far of the flash point, the vapor fuel concentration at room temperature is.

<u>Previous concepts to Step #8:</u>

- 22,4 liters is the volume occupied by 1 mol at atmospheric pressure and temperature 15 °C, so it is possible to calculate the number of air and vapor fuel

mols inside the tank.

- Considering that the ambient air is a mixture of gases (mainly oxygen and nitrogen) that are at atmospheric pressure, and applying the Amagat's Law, the volume percentage follow the molar fraction.

Step #8: Estimate Calculation of the Sudden Inflammation Energy within the Tank

Considering the percentage volume of fuel and percentage volume of air scenario, considering that the molecular weight of the air is 28 g / mol and the molecular weight of the fuel can be estimated in g / mol from the molecular weight of the hydrocarbon most representatives.

The energy that can release 1000 grams of fuel if it reacts with all the necessary air is obtained from its specific heat power.

Knowing the mass of fuel and air mix inside the tank is possible to determine the explosion energy.

Step #9: Process of Tank Explosion Model - Evolution of Internal Pressure from the Lit of the Flame to the Tank Burst

After lit a flame inside the tank, the sudden inflammation inside the tank generated a rapid increase in pressure in few time.

The case of a sudden inflammation of fuel vapor and air in a closed vessel has been studied extensively and there is enough technical information to characterize their behavior.

Due to the fact that there is sufficient information for the case of closed tanks, to study the evolution of the internal pressure from the ignition of the flame to the outbreak in the damaged tank, first it have been studied the behavior of the tank if the loading port it had been closed.

Step #10: Process of Tank Explosion Model - Interior Pressure Variation for Closed Tank

It is considered in this case a tank as the damaged tank but without the loading port acting as a pressure relief device.

According to NFPA 68 [1] when a closed tank has a mixture of air and fuel vapor, each type of gaseous fuel has a value K_G constant that establishes the maximum pressure variation over time in terms of the constant and the volume of the tank.

Knowing this constant value for the type of fuel and the free volume of the tank is possible to determine the profile of variation pressure vs time.

Also is needed to correct the values according to the Fundamental Burning Velocities of the fuel considered.

The maximum pressure developed inside the tank according to the literature would be between 0,6 MPa and 0,9 MPa, in case that it has the capacity to contain the pressure.

The reaction time of a person is something greater than the explosion development time, so from the moment that lit the flame until the explosion occurred each protagonist in this scene of the accident had been subject to the forces associated with

its development, showing individually a behavior completely out of his personal will.

Step #11: Process of Tank Explosion Model -Effect of Loading Port or Active Opening in the Internal Pressure Variation from the Lit of the Flame to Tank Burst

Is possible calculate the vent area for maintaining internal pressure of 0,2 MPa (absolute).

If the value of vent area in the tank (including all the opening acting at the explosion moment) is smaller than required to maintain an absolute pressure in the tank in the vicinity of 0,2 MPa (absolute), the pressure inside the tank should rise.

Once reached the condition of maximum variation in pressure over time, $(dp/dt)_{max}$, the pressure inside the tank will increased far beyond the possibilities of evacuation through the active openings.

It's also possible to estimate the time it would take to relieve a reduced pressure inside the tank P_{red} = 0,2 MPa.

Step #12: Process of Tank Explosion Model -Mathematical Model of Simulation of the Tank Behavior from the Lit of the Flame to the Burst

For the purpose of determining the behavior in the tank during the explosion, a mathematical model simulating the behavior of the tank can be made from flame ignition to the explosion moment.

In order to consider possible errors in accident's records information is advisable to also manage the possibility that the free volume was 33% more and 33% less.

<u>The Model</u>

For the model is necessary to use time intervals of 0,01 s calculating all the model's variables (pressure, temperature, density, of burned and unburned mass, mass inside and leaving the tank) for it and then advancing one interval each time.

As the flame starts an inflammation, the variation in time of the flammable mixture burned, can be modeled as a function of the radius of the sphere of flammable mixture that has burned, the turbulence factor, the density of the flammable mixture and the speed of the flame front (see Figure 4.8 and Figure 4.14).

At any arbitrary time i, the volume of the flammable mixture that has already been burned, plus the volume of the flammable mixture that has not been burned totals the inner volume of the tank occupied by the unburned combustible mixture at the moment of lit a flame.

Inside the tank, once inflammation of flammable mixture begins, the pressure starts to increase.

The increase in pressure is regulated by the differential pressure maintained between the inside and the outside of the tank as a consequence of outgassing of flammable mixture (burned as unburned) through the active openings.

Both the flammable mixture and ignited mixture will increase the pressure as a polytrophic type process.

<u>Calculation Procedure</u>

Initially it takes an interval of time dt=0,01 s.

A sphere centered at the point where the flame started and radio calculated by unburned mixture density, turbulence factor, and fundamental flame velocity.
A control volume in the vicinity of the major tank opening maybe it have to be established. In it, the mixture of air fuel evolves from all unburned to all burned along the process (see Figure 4.13)
It's advisable to use more than one control volume in order to better characterize the model, and also use more than one turbulence factor for same reason. That is, supose that one specific value of volume in the vicinity of the major tank opening can characterizise better than others the behaviour of the combustion process starting in the major opening.
When calculate the mass exiting the active openings it is necessary to consider when to use the critical ratio of pressures to calculate the flow through it.
Also is needed to make a thermal balance inside the tank considering the heat energy of the combustion, and the mass and specific heat of the gases; this allow obtain the temperature inside the tank, and the correspondent densities for burned and unburned gases.
Running the model for different free volumes, control volumes, turbulence factors, it is possible to characterize the case studied model adequately.

<u>Previous concepts to Steps #13 and #14:</u>
Tank Burst Pressure
Three possible causes arises as possible: 1) overpressure inside the tank (later in this thesis it shows that is for detonation), 2) general failure at operating pressure due to corrosion or general tank failure due to bad maintenance, 3) blast for being the tank surrounded by flames.

Burst Energy Distribution
The way burst energy was distributed it is divided as follows: 1) tank expansion, 2) tank rupture, 3) burst 4) fragments.
The energy due to the expansion tank can be neglected because it is very small. Some energy is required also for breakage of the tank but is also very small, some studies shown in Lee´s Loss Prevention in the Process Industries [2], estimate the energy in the order of 10000 Joules, while the burst energy can be was estimated in 1000 times.
The burst can occur for the internal pressure rise or a detonation debt to self-ignition In order to determine if it happened one or another is necessary to study the unburned air and fuel vapor mixture temperature inside the tank. To evaluate the consequences of the tank burst two methods were used:

- Method of Baker et al.
- The Multienergy method

Step #13: Study the pressure variation in time outside tank – Tank Burst Modelling/ Baker et al. Method. Basic Method
The method was developed by W. E. Baker et al. (1975), and refers to spherical tank containing ideal gas.

Explosion energy is calculated by the equation by burst pressure, volume of the selfignition mixture, and polytrophic index of air and fuel vapors mixture not inflamed yet. For each Model of the tank behavior it is needed to calculate the explosion energy values.
Each explosion energy value lead to pressure and impulse value of the explosion shockwave for each point of the exterior of the tank according to this method.
The method consider several explosion severities describing one curve each one, that according to the explosion energy, sound speed at gas conditions, and free tank volume is necessary to select.

Step #14: Study the pressure time outside tank – Tank Burst Modelling/ Multi-Energy Method

The TNO Multi-Energy method is based on the concept of multi-energy, which is the presentation of a deflagration of gas so that the development of the blast and overpressure obtained only under certain boundary conditions, where only flammable mixture is partially confined or obstructed.
Through a lot of explosion experiments, it has been established a explosions curves family known as "TNO blast curves" for explosions
The Mult-energy method does not strictly apply to the case of the explosion of a tank, but it will in the case of a cloud of explosive mixture contained, which approximately is the case under study considering:
- The energy consumed by tank rupture is negligible
- That confinement by the tank is too high

Based on the concept of Multi-Energy, the explosion of gas clouds have been modeled for a number of models of hemispheric loads. The load of each model is characterized by the load size and load stress.
Load size is related to the combustion heat present in the source, while the load stress is related to the explosion overpressure.
Based on these characteristics, scaled blast parameters were calculated (peak overpressure, positive phase duration) as a function of the scaled distance, a number between 1 and 10 representing categories from "negligible" to "detonating".
Again it is assumed that the center of the outbreak corresponds to the center of the opening in the tank caused by the outbreak.
To calculate the explosion energy was considered that in every Model, the amount of flammable mixture that was burned since the flame lit until the tank burst, assuming that the tank burst at the maximum pressure in each of the ten Models considered.

<u>Previous concepts to Steps #15 and 16</u>

The human body can adapt to significant changes in pressure if it is given enough time to compensate for pressure changes in the organs in which air is present.
If this change occurs suddenly, the difference in pressure can damage organs. The most vital organ containing air are the lungs.
In the technical literature it pays more attention to lung damage since lung damage can cause death.
A less vital organ, however more sensitive to pressure changes, it is the ear.

Step #15: Evaluation of the effects on people the tank - Effects of Burst/ Lung Injury

When a pressure difference between the outside and the inside of the lungs is established, with greater pressure outside, the chest is pressed inward, which can lead to lung damage. Since this pressed inward process required time besides the value of overpressure, the duration of this situation is important.

The Greenbook have charts that describes the probability of survival by pulmonary damage depending on the incident overpressure and duration of the pressure pulse.

The correct chart choose is determined by establishing the position of the person relative to the direction of propagation of the pressure wave.

This is necessary, because the pressure exerted by the pressure wave on the person as a result of reflection of it on the person's body and the flow surrounding to the person may be greater than the maximum overpressure incident in pressure wave.

It also provides equations that allow relate this lung injury with the dynamic pressure, side pressure, and impulse on the body that the Baker et. al. method and Multienergy method previously gave.

With this information it is possible to obtain tables of survival probability and lung injury vs person distance to the explosion origin point.

Step #16: Evaluation of the accident effects on people's body - Effects of Burst/ Ear Damage

Similarly to Lung Damage, the Greenbook allows to calculate the percentage of probability of ruptured eardrums as a function of the pressure on them.

It should be considered here as the exerted pressure the reflected pressure.

The reflected pressure can be calculated an equation, that lead to obtain eardrum rupture probability by overpressure according to the Baker et al. method and eardrum rupture probability for overpressure for multienergy method.

Step #17: Effects of Body Displacement

Air particles behind the shock wave have a specific speed and the direction of the burst.

Consequently this called "wind of the explosion," can take a person and move it a particular distance. It is necessary for that to assume a person position in order to use the Greenbook chart of flow around a person and the relative position to pressure wave direction.

Displacement creates risks of collision with solid objects with probability of death by impact to the skull or body in general.

The dynamic stress or pressure exerted by the wind of the explosion on a stationary object or person can be calculated as a function of drag coefficient, perpendicular surface to the propagation of the shock wave, air density behind the shockwave, and velocity of particles in the wave.

This lead to a differential equation involved acceleration of the person's body, mass of the person's body, and velocity of the person's body.

The particle velocity and air density are dependent on the atmospheric pressure p_0

and the density of air $_0$ in front the shock wave according to same equations that Greenbook gives.
The maximum body displacement can be determined by solving the differential equation, using particle velocity and density.
The solution can bring tables with values of: Lateral Pressure, Lateral Impulse, Scaled Time, Pulse Duration, Particles Speed, Air Density, Corporal Speed of persons in the accident.
For the Baker et. al method and c for Multienergy method applied to each Model created previously in the explosion study.
Then, with the impulse and lateral pressure the Greenbook also provides Landing Speed of Body Displacement Based on Lateral Pressure and Impulse for a 70 kg Weight Person.
This landing speed can be checked with the tables obtained, simulating the body movement in the space.
This simulation gives the distance traveled by each body of persons present in the accident.

Step #18: Body Displacement by Flow Trough Active Opening
Another aspect to study is the long displacement of persons without important lung or ear damage.
That could be the case if the person was near an active opening during the explosion.
In this analysis is valuable to study the explosion energy limit from the stand point of view of the property damage, as for example glass breakage. For this consider the non broken glass distance to explosion origin point, and calculate breakage pressure according to Greenbook data.
This analysis allow separate body translation debt to explosion and consider only body translation debt to gas flow through the active tank openings.
Knowing the final position of each body, and considering the lung and ear injury degree in each case, it is possible to obtain the body position at the explosion moment, moved just for flow of gases through the active tank openings.
Once again for this study it have to be considered the explosion models applying the Baker et al method and the Multienergy method.
With the information obtained in the last step of this procedure, assuming an initial position of a person nearby an active opening, it is possible to determine the person movement. For this it is possible to use equations that model the flow through the active opening as a function of density of exhaust gases through it, speed of exhaust gases through active opening, diameter of the active openning , density of gas in the exit condition of the active opening, discharge coefficient of the active opening.
To evaluate the effect that the gas flow has on the body should apply the first and second cardinal equation, to thereby obtain the equations of motion of the body.
It has to be done this work for all models that cover the range of possible explosion behavior. The flow of gases exiting the active opening, passes through external vicinity of the body generating efforts of drag and lift.
The application of these stresses on the body allow establish body position debt to explosion. This allow to obtain as a function of the time, pressure in the tank, temperature of the not inflamed mixture, body surface area impacted by the exhaust

gases of the active opening, the dynamic pressure corrected for the height of the body above the active opening, vertical acceleration and vertical velocity, height of centroid above the active opening, horizontal acceleration and velocity and, horizontal position of the body from its initial position, body's trunk angular acceleration, angular velocity, rotation over time, and initial position respect to the horizontal, the lift and drag coefficients, and the angle of attack.
Al this variables have to be modeled for the different Control Volume, Turbulence Factor, Initial Angle, and Free Volume, obtained in the Baker et. al. method and Multienergy method.
With this information is possible to calculate body movement in air from the moment of departure from the loading port opening until landing for all models created.
Horizontal and vertical acceleration, speed, and body position with one hundredth of second accuracy respect to initial position.
Finally, horizontal displacement in the air, sliding on the ground, and the total displacement can be obtain.
For calculate the movement sliding on the ground it have to be considered the proper factor of friction between the ground and the person, an applied the proper equations.

Step #19: Mathematical model of tank deformation - Detonation and Shockwave Creation

If it have a detonation occurrence, would have formed a shock wave.
According to Chapman Jouget equations shown in Lee´s Loss Prevention in the Process Industries [2], the shockwave characteristics can be modeled as a function of polytrophic index, gas pressure entering shockwave, specific volume gas entering shockwave, gas pressure leaving shockwave, specific volume gas living shockwave, energy added per mass unit.
To consider the reaction force on the tank, it is necessary to know of assimilate the type to a Design Standard, and determine the original steel sheet thickness.
From that stand point of view it is possible to calculate the yield stress value of the material, and study the regions in which would be produced a permanent depression or brake.
After that the results can be compared with the tank accident photographs or records.

Step #20: Mathematical model of the fuel spill - Interaction between Shockwave and a Liquid Layer

As the flow progressed on the surface, a surface wave of large amplitude have been formed; its size depends on the Mach number.
The equations governing the phenomenon can lead to characterize the wave as a function of wave mass, wave horizontal velocity, pressure in wave vicinity, pressure far from the wave, wave height, liquid height, wave width, gas density far from the wave, liquid density, shockwave velocity.
This can lead to explain the fuel spill configuration in the damaged tank vicinity. After that the results can be compared with the tank accident photographs or records.
For the liquid fuel that flowed through the actives openings it is possible to make an flow breakdown analysis in order to calculate the droplet size, speed, and final position.

Part III

CASE STUDY

Chapter 2

Conceptual Description of Accident

2.1 Introduction

The accident happened in an asphalt emulsion tank, used to road repair.

The tank was filled from time to time according to the tank level. Tanker truck were used for that purpose, and originally came from a tank placed in another city, at the asphalt emulsion supplier company.

On a tank of 22000 liters of capacity containing about 10000 liters of asphaltic emulsion RC 2 at 10 º C, a process of filling with the same product at 50 ° C was in progress; suddenly an explosion happened.

Asphaltic emulsion RC 2, is a fast curing emulsion of asfalt diluted in gasoline.

The product at 50 °C came from a tanker truck.

At this moment, 5000 liters of this product at 50 °C there where in the tank plus the initial 10000 liters (see Figure 4.13).

Tank, almost symmetrical, has a loading port opening in the upper mid point, and a vent hole to the side near the loading port opening.

Every tank of this kind has a vent hole in order to equalize the pressure inside and outside the tank during the liquid filling and withdraw process in the tank.

The RC2 is an emulsion of asphalt and heavy naphtha.

Usually the tank filling operations are at daylight, but in this case the filling operation was starting the night.

To check the level inside the tank, one person with a cigarette lighter or a similar device made an igneous focus in the vicinity of the loading port opening, causing a combustion process inside the tank.

The pressure in the tank reached the minimum value of rupture in one extreme of it, causing a sudden pressure relief inside.

An outside observer would have appreciated the following stages in sequence, in this process:

1. Incandescent gases flowing out of the loading port opening in vertical flow.
2. Asphalt spray accompanying the flow of incandescent gases leaving the loading port.
3. Projection of asphalt in a 6-8 meters radius centered in the loading port.
4. Explosion in a side of the tank vessel, with asphalt release into the surrounding

area.

5. Advancement of an explosive wave, centered on the side of the tank, moving radially in multiple directions, reflecting the tanker truck and tank vessel.
6. Formation of a cloud of flowing gas with flames of a few tens of meters in height approximately.
7. Spontaneous ignition of the heavy naphtha emulsified with asphalt released to the environment at those points where radiation has provided enough heat to vaporize the heavy naphtha and achieved self-ignition energy, or the igneous focus has ignited the vapors nearby.

2.2 Brief Accident Description

Before the filling operation, the tank of 22,000 liters capacity, contained about 10,000 liters of diluted asphalt RC2 inside at room temperature, 10 °C approximately. RC2 diluted asphalt comprises a mixture of 20% of heavy naphtha and 80% asphalt.

Heavy naphtha vapors when mixed with air in certain percentage generate an explosive mixture.

The free volume inside the tank was completely occupied by air at atmospheric pressure and room temperature before starting the transfer, which was determined in one test of explosive atmospheres to which reference will be made later.

When lighting a flame on the tank loading port opening, the free volume inside the tank contained an explosive mixture of air and vapor heavy naphtha.

This can be stated because the asphalt diluted RC2 that was in the tank before the start of the transfer was at room temperature, which at that temperature has a quite solid aspect, so when the asphalt diluted RC2 entered from the tank at approximately 40 °C to 50 ° C, heavy naphtha vapors were released into the surrounding air inside the tank.

The amount of heavy naphtha vapors in air in the tank can be estimated from the vapor pressure of the heavy naphtha to a temperature of approximately 40 ° C. It has been estimated that the time for transfer of 4500 lt asphalt diluted RC2, that is, when accident happened was approximately 5 minutes from the start of fill tank process.

Three different assays of measure of explosive atmospheres in two asphalt diluted RC2 tanks property of the supplier company were conducted. These have revealed that the only way to generate an explosion is completely placing a hand with a flame into the loading port of the tank, and is not possible that a person standing in the vicinity of the loading port of the tank could have caused an explosion.

These tests were decisive for the location of the initial position of the body of the person who lit a flame in the loading port of the tank.

The third test allowed us to determine that at the start of the filling process there was no explosive mixture. A mathematical model to see later allowed study the evolution

of the internal pressure of the tank from the ignition flame to the burst. It was first studied if the tank had been closed (without loading port opening) when ignite a flame inside.

Then it have been studied the effect of the loading port opening in the variation of internal pressure from the ignition of the flame until the burst of the tank.

The results obtained in both cases were similar to the literature reference.

It has been corroborated that the time from ignition of the flame until the burst of the tank was below the reaction time of a person, so from the moment that the flame start until the explosion occurred, each person was subjected to forces related to the pressure development, individually exhibiting each person a behavior completely independent to his personal will.

Calculated by an international reference method, in the next chapter, the outcome was that the area of the loading opening was less than one third of the needed to relieve the pressure inside the tank without significantly increased pressure, leading to the tank burst.

The mathematical model, in the Chapter 4, of the simulation of tank behavior from the lit of the flame to the tank explosion determined:

- The evolution of the pressure inside the tank from the moment that lit the flame until the tank exploded.
- The variation of gas flow through the loading port opening from the moment that lit the flame until the tank exploded.
- The instant of the tank burst from the moment that lit the flame.
- The bursting pressure of the tank.
- The amount of burned and unburned mass inside the tank at the time of the tank burst, and the amount of flammable mass that flowed out through the loading port opening at the moment of the explosion.

Reference values of duration of the explosion by the calculation formulas of international technical regulations and the ones arising from mathematical modeling were coincident.

The burst pressure of the tank, along with the amount of burned and unburned mass inside the tank and its exit through the loading port when the tank burst, were the basis for the calculation of energy and pressure distribution in the space and time in the area around the point of explosion of the tank.

With this information it was possible to determine the different trajectories and final positions for who had been standing at different parts of the tank at the time of the tank burst.

A technical paper was found, that study the changes in internal pressure of a tank similar of the damaged tank. It is a study by the Russian scientist V. Molkov that during the pre-detonation is similar to this thesis model.

All fuel behavior through its Turbulence Factor, the possible variations on the information available in the accident records about the free volume of the tank, and the possibility that the energy of the explosion was the greatest possible have been studied.

This resulted in ten different models which were describing the process of explosion in steps of one hundredth of a second.

The modeling of tank burst was performed by two methods of the highest international importance.

Intentionally these methods were selected from well considering different methodologies in order to compare results.

Through them it was possible to determine the pressure and momentum of a person standing at 1, 2, 3 meters from the center of the outbreak in the tank.

The coincidence of results between the two methods confirms the validity of the results.

The tank would have exploded by increased pressure without detonation, which is what the literature indicates that occurs in general.

Without the mathematical modeling of the explosion process it would not have been possible to propose the existence of a detonation.

In this particular case the cylindrical shape of the tank, and the onset of inflammation in the center of it, were compressing the unburned flammable mixture to the end of the tank achieving self-ignition of the flammable mixture, suddenly generating a shock wave.

In Section 5. is explained why the detonation occur at one end particularly.

In Section 6. consequences of the effects of the explosion on the people in the accident, and particularly in Section 7. the displacement of a body standing on the tank were studied.

The burst pressure on the windshield of the truck and its position relative to the center of explosion was estimated, which allowed discarding some explosion energies too high, the coincidence of the two methods used on the ten models used was total. Consequently, studied the situation described in the accident proceedings, and possible changes to inaccuracies in such information has been established that for positions 1, 2, 3 meters respectively with respect to the center of the explosion, for Models I to X, the initial velocities of a body standing on the tank would be: If it had been the case with the explosion of the tank without detonation, the person on the tank had experienced a slight shift, ending a few meters from its original position.

If it had been the case of tank explosion with detonation, the person on the tank had experienced a slight shift, ending a few meters from its original position also.

A person who had a displacement between tens of meters and one hundred of meters caused by an explosion, would have had experienced lung damage or death from severe lung damage, in addition to rupture eardrums or hearing damage of high

severity.

The person surviving the accident, which suffered a major displacement in the accident, according to medical reports and statements contained in the proceedings had none of the health problems listed above.

Consequently, the presence of this person in any standing position on the tank is discarded.

The variation of gas flow through the loading port from the moment that lit the flame until the tank exploded, was the basis for calculating the stresses on the body of the person who was in the area of the loading port igniting a flame.

In Chapter 8, based on that it was possible to calculate the trajectory and end position of the person who lit the flame, not reaching conclusive results because depending on the model used the person on the loading port opening of the tank could have stayed from distances of the order of the survivor final position, to distances more near of the tank.

Based on the Chapter 8 studies, it has obtained an estimate of the whole body position changes every hundredth of a second, which is recorded in Tables 8-1 to 8-19 near the loading port to detonation, and the movement in the air after it, which is expressed in Tables 8-20 to 8-36.

Based on studies and listed in Chapter 8, the maximum displacement of a person on the loading port could go from 4,9 meters to 68 meters the typical values being within 30 meters, depending on the scenario studied.

The person surviving the accident, told in the accident records had suffered a horizontal shift in the air by 50 meters.

Some witnesses place him farther from the accident, in the order of 150 meters, but at the time of arrival of these witnesses.

After exhaustive embodiment of the above studies, we conclude that it was not possible to find any scenario in which the person surviving the accident had been standing on the tank.

The other possible location for this person, is lighting a flame on the loading port of the tank. Not on all models studied for a person there are coincident with the shift really experienced by that person.

It is not possible to express with certainty the position of the deceased person, at the time of start of the accident.

The formation of a wave of liquid generated inside the tank by the detonation, part of which would flowed through the loading port opening, may be the cause of the staining of product found in the soil and on the tank truck.

Chapter 3

Fuel Air Mixture

3.1 Calculation of Air-Fuel Mixture in the Tank

3.1.1 Before the Tank Filling Process Starts the Tank Contained Only Air Inside

Before the tank filling process starts, the tank with 22,000 lt of capacity contained about 10,000 liters of diluted asphalt RC2 inside at room temperature.

The vapor level of heavy naphtha was almost zero inside the tank.

The free space inside the tank consisting of the part of the interior volume that was not occupied by asphalt diluted RC2 initially contained in the tank, it can assumed that was completely occupied by air at atmospheric pressure and room temperature.

This can be stated because a measure of explosive atmosphere was made into a bucket of 30 liters approximately containing asphalt diluted RC2 at room temperature (about 10 ° C) and the vapor level heavy naphtha on the surface of asphalt diluted RC2 was virtually zero.

3.1.2 At the Moment of Lighted a Flame on the Loading Port, the Free Volume Inside the Tank Contained an Explosive Mixture of Air and Heavy Naphtha Vapor

The asphalt diluted RC2 that was in the tank before the start of the transfer process was at room temperature.

As was entering the asphalt diluted RC2 in to the tank at a temperature of 50 ° C, the temperature of the asphalt diluted RC2 which was initially in the tank increased, as well as the temperature of the entering one was decreasing as a result of the operation of transfer.

The higher the temperature of the asphalt diluted RC2 the greater the quantity of vapors of heavy naphtha which were released into the surrounding air. Progressively, as the transfer process progressed, the amount of heavy naphtha vapors released inside the tank were increasing.

To estimate the amount of vapor of heavy naphtha that was in the tank when light a flame inside of it, it must resort to the concept of vapor pressure.

The vapor pressure for a given temperature, by the Dalton's Law, determines the amount of fuel vapor relative to air there.

The vapor pressure for any substance, in particular in this case the asphalt diluted RC2, is characteristic of it and it depends only on the temperature at which it is located.

This means that the vapor pressure of the asphalt diluted RC2 at the supplier company tanks and in the damaged tank was the same as if they were at the same temperature.

The total pressure of a mixture is equal to the sum of the partial pressures of its components.

The partial pressure in a gas mixture is equal to the mol fraction of each component in the mixture.

Assuming ideal gas behavior, if each of these gases (air and heavy naphtha vapor) were studied separately, the contribution to the pressure of each component is directly related to the number of mols of the component.

Since each component has the same volume and the same temperature, the difference of the pressures exerted by the two different gases will be due to their numbers of mols.

If the partial pressure of each component is known, it is possible to calculate the number of mols of each of the gases found in the mixture in a given enclosed volume and at a given temperature.

Similarly it can be set that the volume percentage is given by the Amagat Law of Partial Volumes, which states that in a mixture of gases, each gas occupies the volume as if the other gases were not present.

The specific volume of a particular gas in a mixture is called partial volume.

The total volume of the mixture is calculated simply by adding the partial volumes of all gases that compose it.

To estimate the amount of heavy naphtha vapors present inside the tank at the time of lighting a flame it has been established two ways.

3.1.3 Estimation of Heavy Naphtha Vapor Pressure a Temperature of 40 °C approximately

Has been established at 40 °C because the asphalt diluted RC2 that was initially in the tank at room temperature was in a semi-solid state and does not mix easily with the being poured from the tanker truck that is liquid and flowed easily.

Therefore, we can assume that liquid asphalt diluted RC2 was admitted at 50 ° C, it was deposited on the inside of the tank and it's temperature descended as it gave heat to asphalt diluted RC2 that was at the bottom tank. It has been estimated transfer time of 4500 lt of asphalt diluted RC2 from the tank truck to the tank vessel, taking into account the difference in piezometric level between tank truck and tank vessel and the pressure drop in the hose.

The time is about 5 minutes. It has also been evaluated the thermal transfer in 5 minutes of asphalt diluted RC2 liquid entering the tank to which it is semi-solid at the bottom of the tank.

The asphalt diluted RC2 comprises 80% of asphalt whose vapor pressure is practically

zero at 40 ° C, and 20% of heavy naphtha whose vapor pressure is estimated from:

- distillation curve
- vapor pressure hydrocarbon carbon chains of equal length that of the typical components of heavy naphtha.

3.1.4 Estimation of Heavy Naphtha Vapor Pressure from Vapor Pressure of Hydrocarbon Products of Equal Length of Carbons than the Characteristically Components of Heavy Naphtha

The heavy naphtha consists of over 200 different types of hydrocarbons from a 7 carbons chain up to 10 carbons chain. Particularly affecting the vapor pressure are the 7 carbon chain, called C7.

Among these, there are different types of hydrocarbons according to the type of bond between hydrogen and carbon.

Heavy naphtha particularly comprises approximately 50% paraffinic hydrocarbon type, 40% of naphthenic type, and 10% of the aromatic type.

In the following **Table 3.1 -** *Vapor Tensions of Hydrocarbons Representative of Each Type* is indicated the vapor pressures of a hydrocarbon that was taken as representative of each type.

In the rightmost column it shows the result of calculating the vapor pressure of a mixture of three types of hydrocarbon in the above mentioned percentages.

The calculation performed shows that the vapor pressure of the heavy naphtha is in the order of 15 000 Pa. Since the total pressure is equal to atmospheric pressure, that is, 101 300 Pa, the volume percent of heavy naphtha vapor relative to air in a tank that has a 100% Heavy Naphtha is in the order of 15%.

This value corresponds to conditions of equilibrium which is achieved after some time, which could be higher than the time of transfer, so this value of 15% could be lower if it had not reached equilibrium.

Hydrocarbon Type	Aromatic	Naphthenic	Paraffinic	Weighted Mixture
Representative	Toluene	Dimethylcyclopentane	1-Heptane	
Composition	C7H8	C7H14	C7H16	
Percentage	10	40	50	
Vapor Pressure at 40 ° C	7887	16723	14918	14937

Table 3.1 - Vapor Pressure of Hydrocarbon Representative of Each Type

The following **Table 3.2 -** *Distillation Curves of Asphalt Diluted RC2 and Heavy Naphtha*

distillation curves of asphalt diluted RC2 and heavy naphtha are appreciated.

Distillation Curve	Heavy Naphtha	Asphalt Diluted RC2
Initial	94 º C	
10%	110 ° C	
30%	120 ° C	190 ° C
60%	150 ° C	225 ° C
100%	250 º C	360 º C

Table 3.2 - Distillation Curves of Asphalt Diluted RC2 and Heavy Naphtha

After distillation of 100% of asphalt diluted RC2 there is a residue of around 80%, that is, asphalt.

In them, the effect of the mixture of 80% asphalt and 20% of heavy naphtha is appreciated, reducing the volatility with respect to the case of 100% of heavy naphtha.

The vapor pressure of asphalt at 40 ° C is practically zero, and the heavy naphtha was estimated at 15000 Pa.

For example at a temperature of 150 ° C was estimated that the asphalt dilute RC2 would distillate less than 10% while the heavy naphtha distillates 60%, this would be approximately 6 times less the level of vaporization.

Translating as an estimation this ratio, it is possible to estimate the vapor pressure at 2500 Pa for the heavy naphtha contained in the asphalt diluted RC2.

Therefore, the volume of heavy naphtha vapors present inside the tank at the time of lighting a flame would have been of the order of 2.5%.

The explosive range for heavy naphtha is between the explosive range of the Gasoline that is 1,4% to 8%, and that of Kerosene that is 0,7% to 5%.

It is reasonable to locate the explosive range of the heavy naphtha from 1% to 7% range.

At the moment of ignite a flame inside the tank, according to this estimation, it would happened a sudden inflammation in a burst mode.

3.1.5 Estimated Percentage of Heavy Naphtha Vapor in the Interior of the Tank from the Explosive Atmosphere Tests

Measurement tests of explosive atmospheres were conducted in the two tanks of asphalt diluted RC2 of the supplier company (see paragraph 3.2).

When the indicator of fuel vapor concentration in air reaches the value 0,4 means that this is the minimum value of fuel vapor in the air to ignite that is in the order of 1%.

Reach 1% of heavy naphtha vapors in the air means that heavy naphtha vapors reached the flash point, or the temperature at which if approached a flame a sudden inflammation of the vapors would occur.

In one of the tanks the value 0,4 is obtained and the other 0,7.

That is, one of the tank was find the threshold value of explosiveness, was in the flash point; while in the other one it was above the threshold value.

This is quite consistent with the theoretical estimation of that could be in the order of 2.5%.

3.2 Monitoring of Explosive Atmospheres Test Description

Monitoring of explosive atmospheres test consisted of three parts.

3.2.1 Monitoring of Heavy Naphtha Vapors Concentration in the Interior of Asphalt Diluted RC2 Tanks.

The supplier company has two tanks of asphalt diluted RC2, which maintain the product between 50 ° C and 60 ° C using a system of internal heating, and thermal insulation in their sidewalls.

At the top of each tank there is an opening called "manhole" to access the interior. This opening is very similar to the loading port opening of the damaged tank in the accident.

This means that having been on the manhole of each tank of the supplier company with the manhole open, is very similar to being on the loading port opening of the damaged tank at the moment that somebody lit a flame.

The main difference is in the temperature, since in the tanks of the supplier company the temperature is the highest possible, because for there the truck was loaded and then it had to make a trip to the damaged tank area and then fill in that initially cold tank.

This means that the temperature of the asphalt diluted RC2 in the damaged tank at the time of the accident could not exceed the temperature of the tank of the supplier company on which the monitoring of explosive atmospheres test was conducted.

Thus the vapor pressure and consequently the level of heavy naphtha vapor present in relation to the amount of air was lower in the damaged tank at the moment of the accident that the quantity measured during the monitoring of explosive atmospheres test performed at the supplier company.

In the test, consisting in put the gas detector instrument in different positions in the space, it was found that in one tank the atmosphere was the minimum necessary to cause an explosion, that is, 1% of heavy naphtha vapors in relation to the air, and the other tank was found superior levels perhaps of the order of 2.5% as stated in the theoretical estimation explained above.

Considering that the vaporization is reduced with the temperature and the vapors in the tank of the supplier company would be about 10 °C above the vapor inside the damaged tank when ignite a flame, the vapor level of heavy naphtha present inside the tank at the time of lighting a flame can be estimated between 1% and 2.5%.

This means that heavy naphtha vapors would then have had available all the necessary air to ignite suddenly.

3.2.2 Monitoring of Heavy Naphtha Vapors Concentration on the Surface of the Asphalt Diluted RC2 Tanks. Vapor concentration of heavy naphtha was measured outside the tank, around the manhole. In either case a value close to 0,4 (see paragraph 3.2.3) did not appear, which means it was found that:

a) The explosion is only possible if the flame burns inside the tank.

b) The person who lit a flame would not have been surrounded by flames from heavy naphtha vapors present in the tank surface. The flames only would come from the inside of the tank.

c) The only way to generate an explosion is placing flame inside the loading port opening, for which the person it must be much crouched inside the tank.

d) Converging to the above is the fact that to light should be squatting well over the loading port of the tank, because the asphalt dilute RC2 is very dark, it is not possible to see clearly the difference of level through the manhole opening with daylight, so it is necessary to bring the flame deep into the tank.

3.2.3 Monitoring Heavy Naphtha Vapors Concentration at Environment Temperature.

Vapor concentration was measured in a bucket at room temperature. The result was very low vapor concentration heavy naphtha. The instrument recorded values lower than 0,1 on a minimum value of 0,4 for explosiveness.

Then, a dumping on that bucket was made with asphalt dilute RC2 at about 30 º C.. The recorded values were not significantly different.

This allows to state that, consistent with the calculations performed, the level of heavy naphtha vapors inside the damaged tank before the transfer process, was practically zero at atmospheric pressure and room temperature; only air was present.

3.2.4 Technical Features of the Test Equipment

Gas detector Biosystems brand Multipro model, which was calibrated with methane, and within the validity date of the calibration, was used.

To be calibrated with methane, the value indicated in the instrument reading should be corrected to be used with other hydrocarbons.

References within the Correction Factor is 0,4 for n-octane, 0,45 to n-hexane, and the values increase in inverse proportion to the length of the hydrocarbon chain.

For gasoline the correction factor is 0,65.

Based on the foregoing, it seems reasonable to assume that for heavy naphtha the correction factor is about 0,4.

For this correction factor was obtained for each tank

0.4 / 0.4 = 1.0 that is it would be in the lower explosive limit, this is about 1% by volume of heavy naphtha in the air volume inside the tank in which the measurement was made.

0.7 / 0.4 = 1.75 that is higher than the lower explosive limit. Maybe it can be estimated in the order of about 2% volume of heavy naphtha in the air volume inside the tank in which the measurement was made.

Figure 3.1 - Gas Detector Biosystems - Multipro

3.3 Estimate Calculation of the Sudden Inflammation Energy Within the Tank

It was indicated by the accident records that the tank had 22000 lt capacity, with 10000 lt initially contained and had been dumped in it 4500 lt the time of the explosion.

Consequently, the free volume was 7500 lt.

In the damaged tank, the initial temperature was 10 °C, in it were poured approximately 4500 lt at 50 °C.

If the cold and hot asphalt dilute RC2 were totally mixed to the temperature of the mixture would be 22 °C, which would be below the flash point.

During the tests performed on the occasion of explosive atmospheres test it was found that the asphalt dilute RC2 when is at room temperature has a semi-solid state.

Already explained that transfer time of about 5 minutes the heat transfer liquid asphalt diluted RC2 was not significant.

Therefore when depositing asphalt dilute RC2 at approximately 50 °C from the tank truck to the tank, the asphalt dilute RC2 at approximately 50 °C initially behaves as if it had been deposited on a tank whose volume is equal to the free tank volume.

The floor initially solid was beginning to migrate to the liquid state with input temperature of the asphalt diluted RC2 poured from the tanker truck.

As there was an explosion, it is understood that the mixture was explosive, the amount of air contained in the tank was able to react with fuel vapors which would be of the order of 1% to 8% of the total volume.

In a 1% volume of heavy naphtha and 99% of air scenario, considering that the molecular weight of the air is 28 g / mol and the molecular weight of the heavy naphtha can be estimated at 120 g / mol (average between C8H18 - C9H20).

Whereas 22,4 lt is the volume occupied by 1 mol at atmospheric pressure and temperature 15 °C, and assuming that the temperature correction is much smaller, so it will work with this relationship, the tank would have the following number of air mols:

7500 lt / 334 lt = 22,4 mols of air

If the concentration of vapors heavy naphtha would be of 1%, it would have been there 75 lt of such vapors inside the tank at the time of lighting a flame.

This represents

75 lt / 22.4 lt = 3,3 mols of heavy naphtha vapor

Expressed in grams:

334 x 28 = 9352 grams of Air

3,3 x 120 = 396 grams of Heavy Naphtha

It will be assumed that the reaction between air and fuel into the tank was fully realized when the tank explode. This is the most conservative assumption, that is, it would develop all the energy that the air contained in the tank is able to allow release.

Assimilating the heavy naphtha (which has a range of C7 through C10) at an average of C8H18 and C9H20 it is possible to estimate the stoichiometric ratio as follows:

$$C_8H_{18} + \frac{25}{2}\,O_2 = 8CO_2 + 9H_2O \qquad [3.1]$$

$$C_9H_{20} + 14\ O_2 = 9CO_2 + 5H_2O \qquad [3.2]$$

This implies that 1 mol fuel chemically reacts with approximately 13 mols of oxygen.

Air is composed in volume by a 21% of oxygen.

Considering that the ambient air is a mixture of gases (mainly oxygen and nitrogen) that are at atmospheric pressure, and applying the Amagat's Law:

$$p\sum V_i = \sum n_i RT \qquad [3.3]$$

the volume percentage follow the molar fraction, so 13 mols of oxygen represent:

13 / 0,21 = 62 mols of air.

The enclosed volume in the tank contains 334 mols of air.

Thus the exact reaction (stoichiometric) air and vapor between heavy naphtha if it had used all the air inside the tank as oxidizing

334/62 = 5,4 mol of heavy naphtha

In the mixture between air and heavy naphtha of 334 mols of air and 5,4 mols of heavy naphtha, the molar fraction determined the volumes, following the Amagat's Law.

This would be equivalent to 1.5% of heavy naphtha vapors in the air inside the tank.

5,4 mols of heavy naphtha are 600 grams of that fuel.

The energy that can release 1000 grams of heavy naphtha if it reacts with all the necessary air is 40000000 Joules (heat power of heavy naphta).

In this case the air within the tank can chemically react with approximately 600 g of heavy naphtha, releasing about 24 million of Joules.

The tests performed and the calculations are convergent in that inside the tank at the time of the explosion would have been an explosive mixture with an amount of heavy naphtha vapors ranging between 1% and 2.5%.

The amount of fuel that allows to fully utilize all the air inside the tank is of the order of 1.5% heavy naphtha vapor in the air.

A higher quantity of heavy naphtha vapor, for example, up to 2.5% does not significantly change the fact that the sudden inflammation used all the air contained in the tank when somebody light a flame.

Therefore it can be estimated the energy in Joules 24000000 debt to the sudden inflammation inside the tank.

Chapter 4

4. Process of Tank Explosion Model

4.1 Evolution of Internal Pressure from the Lit of the Flame to the Tank Burst

After lit a flame inside the tank, the sudden inflammation inside the tank generated a rapid increase in pressure in short time.

The case of a sudden inflammation of fuel vapor and air in a closed vessel has been studied extensively and there is enough technical information to characterize their behavior.

There is sufficient information for the case of closed tanks. Then in order to study the evolution of the internal pressure from the ignition of the flame to the outbreak in the damaged tank, first it have been studied the behavior of the tank if the loading port it had been closed.

Methodologically, in Section 4.1 *Interior Pressure Variation for Closed Tank* it will be considered first if the tank had been closed without loading port opening when ignite a flame inside. Then in Section 4 .2 *Effect of Loading Port Opening in the Internal Pressure Variation from the Lit of the Flame to Tank Burst.* The influence of the loading port opening, relieving some of the pressure inside the tank, will be assessed.

4.1.1 Interior Pressure Variation for Closed Tank

It is considered in this case a tank as the damaged tank but without the loading port acting as a pressure relief device.

According to NFPA 68 [1] when a closed tank has a mixture of air and fuel vapor, each type of gaseous fuel has a value K_G constant that establishes the maximum pressure variation over time in terms of the constant and the volume of the tank:

$$K_G = \left(\frac{dp}{dt}\right)_{\max} V^{\frac{1}{3}} \qquad [4.1]$$

In **Figure 4.1** - *Effect of Test Volume in K_G Measure for Spherical Tanks*, of all hydrocarbons that are represented, the one that appears next to the heavy naphtha is Pentane (hydrocarbon composed of a chain of five carbons).

Pentane values are taken as reference, and then the theory states that should be corrected their values based on the fundamental flame speed.

Values of flame speed appearing in Table 4-1, *Fundamental Burning Velocities for Selected Flammable Gases in Air*, for hydrocarbons containing in the heavy naphtha are about pentane speed.

Thus it is understood that such correction is not necessary.

It will not be considered at this point 4.1 of these thesis the influence corresponding to the difference in shape, that is, the tests correspond to spherical tanks and the damaged tank was cylindrical.

This is because at this point 4.1 the objective is a first approach to the subject that shows convergence of results with the more detailed results that will be showed later with the specific calculations in section 4.2 .

It can be seen in **Figure 4.2** - *Explosions in Closed Tanks: Effect of Volume. Propane at Stoichiometric Concentration*, that there is a first phase in which the pressure variation is reduced, which to the free volumes of the order of the damaged tank (from 5 m^3 and 10 m^3) can be estimated between 0,20 s and 0,30 s, followed by a sudden pressure change corresponding to the maximum variation of pressure over time, according to equation **[4.1]** .

The maximum pressure developed inside the tank according to the literature would be between 0,6 MPa and 0,9 MPa, in case that it has the capacity to contain the pressure.

This means that if the damaged tank would have been closed, that is, without the loading port open, and assuming that the mixture of air and heavy naphtha would have the same behavior of stoichiometric propane, from the time the flame begins until the time of the explosion, would will occur between 0,20 and 0,30 s at a low pressure, and then 0,20 s 0,30 s until the maximum pressure is reached.

So is estimated at about 0,60 s or less the time from ignition of the flame until the outbreak of the tank if it had a stoichiometric mixture of propane and air inside.

The reaction time of a person is something greater than 0,60 s, so from the moment that lit the flame until the explosion occurred each protagonist in this scene of the accident of propane and closed tank had been subject to the forces associated with its development, showing individually a behavior completely out of his personal will.

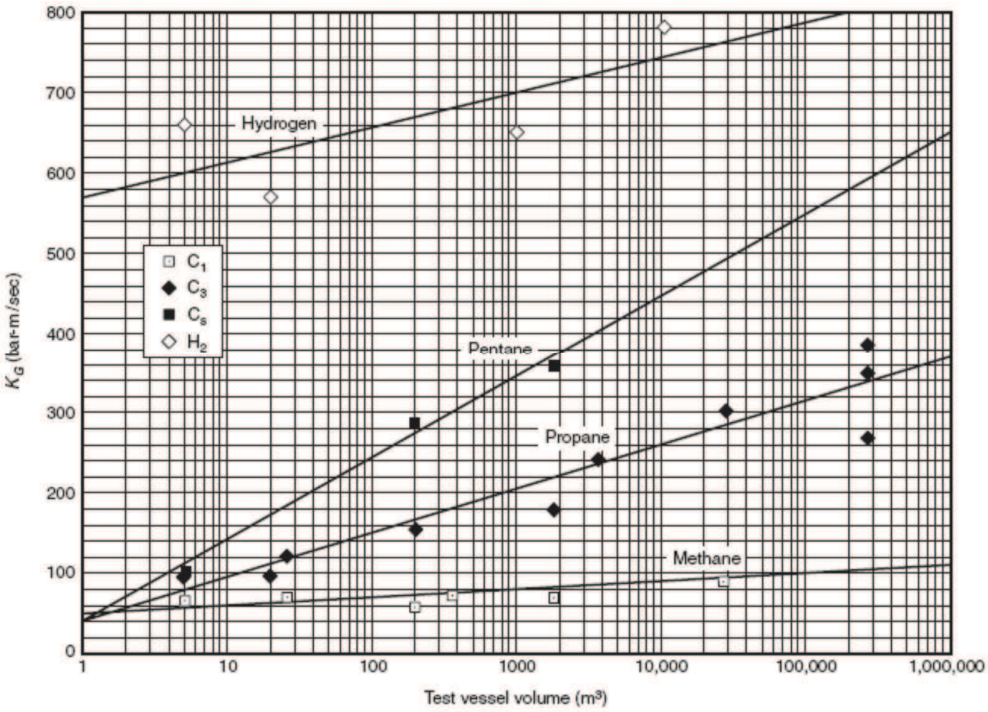

Figure 4.1 - Effect of Essay Volume K_G Measure for Spherical Tanks

Annex C Fundamental Burning Velocities for Selected Flammable Gases in Air

This annex is not a part of the recommendations of this NFPA document but is included for informational purposes only.

C.1 General. The values of fundamental burning velocity given in Table C.1(a) are based on NACA Report 1300 [82]. For the purpose of this guide, a reference value of 46 cm/sec for the fundamental burning velocity of propane has been used. The compilation given in Perry's *Chemical Engineers' Handbook* [83] is based on the same data (NACA Report 1300) but uses a different reference value of 39 cm/sec for the fundamental burning velocity of propane. The reason for using the higher reference value (46 cm/sec) is to obtain closer agreement with more recently published data as presented in Table C.1(b).

Table C.1(a) Fundamental Burning Velocities of Selected Gases and Vapors

Gas	Fundamental Burning Velocity (cm/sec)
Acetone	54
Acetylene	166*
Acrolein	66
Acrylonitrile	50
Allene (propadiene)	87
Benzene	48
,*n*-butyl-	37
,tert.obutyl-	39
,1,2-dimethyl-	37
1,2,4-trimethyl-	39
1,2-Butadiene (methylallene)	68
1,3-Butadiene	64
2,3-dimethyl-	52
2-methyl-	55
n-Butane	45
2-cyclopropyl-	47
2,2-dimethyl-	42
2,3-dimethyl-	43
2-methyl-	43
2,2,3-trimethyl-	42
Butanone	42
1-Butene	51
2-cyclopropyl-	50
2,3-dimethyl-	46
2-ethyl-	46
2-methyl-	46
3-methyl-	49
2,3-dimethyl-2-butene	44
2-Buten 1-yne (vinylacetylene)	89
1-Butyne	68
3,3-dimethyl-	56
2-Butyne	61
Carbon disulfide	58
Carbon monoxide	46
Cyclobutane	67
ethyl-	53
isopropyl-	46

Table C.1(a) *Continued*

Gas	Fundamental Burning Velocity (cm/sec)
methyl-	52
methylene	61
Cyclohexane	46
methyl-	44
Cyclopentadiene	46
Cyclopentane	44
methyl-	42
Cyclopropane	56
cis-1,2-dimethyl-	55
trans-1,2-dimethyl-	55
ethyl-	56
methyl-	58
1,1,2-trimethyl-	52
trans-Decalin (decahydronaphthalene)	36
n-Decane	43
1-Decene	44
Diethyl ether	47
Dimethyl ether	54
Ethane	47
Ethane (ethylene)	80*
Ethyl acetate	38
Ethylene oxide	108
Ethylenimine	46
Gasoline (100-octane)	40
n-Heptane	46
Hexadecane	44
1,5-Hexadiene	52
n-Hexane	46
1-Hexene	50
1-Hexyne	57
3-Hexyne	53
Hydrogen	312 *
Isopropyl alcohol	41
Isopropylamine	31
Jet fuel, grade JP-1 (average)	40
Jet fuel, grade JP-4 (average)	41
Methane	40*
diphenyl-	35
Methyl alcohol	56
1,2-Pentadiene (ethylallene)	61
cis-1,3-Pentadiene	55
trans-1,3-Pentadiene (piperylene)	54
2-methyl-(cis or trans)	46
1,4-Pentadiene	55
2,3-Pentadiene	60
n-Pentane,	46
2,2-dimethyl-	41
2,3-dimethyl-	43
2,4-dimethyl-	42
2-methyl-	43
3-methyl-	43
2,2,4-trimethyl-	41
1-Pentene	50
2-methyl-	47
4-methyl-	48
cis-2-Pentene	51

Table 4.1 - Fundamental Burning Velocities for Selected Flammable Gases in Air

From the **Figure 4.2 -** *Explosions in Closed Tanks: Effect of Volume. Stoichiometric Propane Concentration,* were determined maximum pressure variations versus time, $\left(\frac{dp}{dt}\right)_{max}$, for the cases of 1 m³ volume, and 20 m³ volume.

Has also been studied, as discussed below, the possibility of errors in the information on the accident records the of free volume inside the tank, which supposedly would be 7,5 m^3 could be 10 m^3 or either 5 m^3.

Based on the hypothesis that a near stoichiometric value of air and vapors of heavy naphtha mixture inside the wrecked tank when the explosion happened, would had a behavior similar to the stoichiometric propane, the following values would be obtained of $\left(\frac{dp}{dt}\right)_{max}$ and of mean time from the ignition of the flame to the explosion.

Free Tank Volume [m^3]	$(dp/dt)_{max}$ [bar/s]	Time from Ignition to Flame Burst [s]	Observations
1,0	75	0,40	Figure 4-2 Experiment.
5,0	44	0,54	Wrecked Tank - $K_G = 75$
7,5	38	0,59	Wrecked Tank - $K_G = 75$
10,0	35	0,62	Wrecked Tank - $K_G = 75$
20,0	27	0,70	Figure 4-2 Experiment.

Table 4.2 - Values of $\left(\frac{dp}{dt}\right)_{max}$ for a Tank with Stoichiometric Propane and for the Wrecked Tank with Stoichiometric Propane

To estimate the pressure values it was considered that a linear relationship follows between $\left(\frac{dp}{dt}\right)_{max}$ and the cube root of the volume.

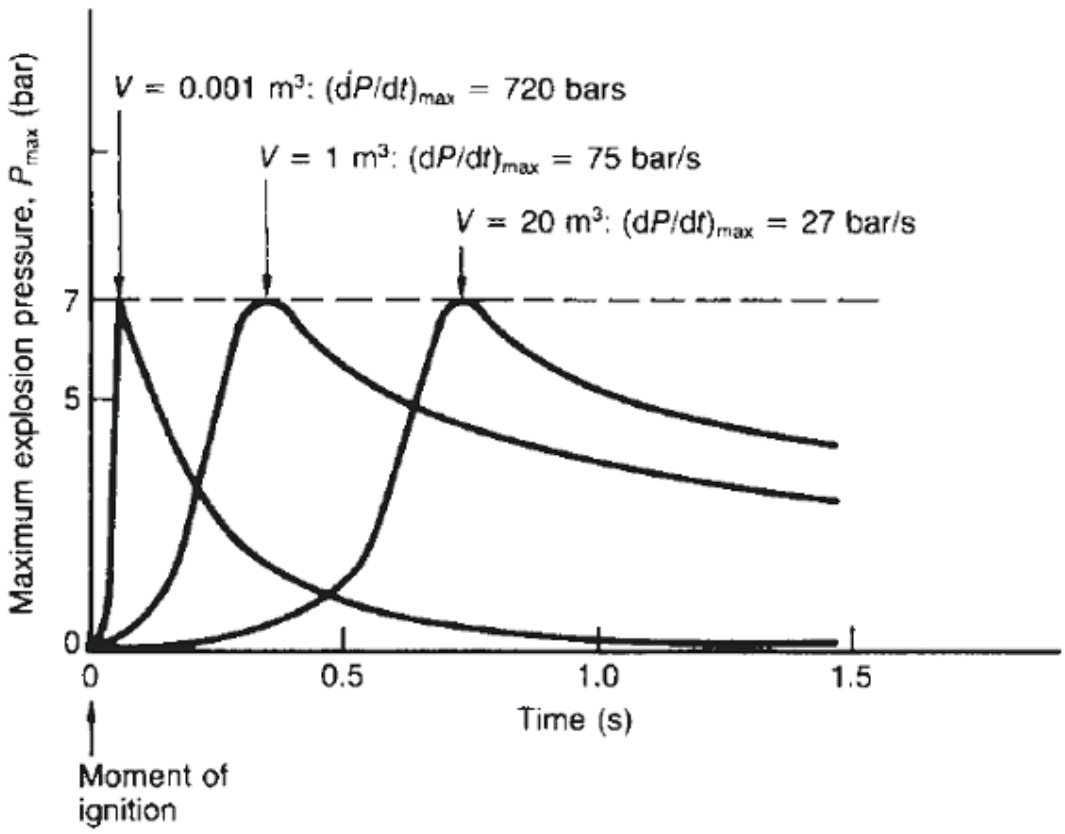

Figure 4.2 - Explosions in Closed Tanks: Effect of Volume. Propane at Stoichiometric Concentration.

As previously indicated, in the damaged tank case is assumed that the behavior of the heavy naphtha vapors is more comparable to that of pentane to propane since the pentane have an hydrocarbon chain of 5 carbons while propane has an hydrocarbon chain of 3 carbons.

Previously it had been noted that heavy naphtha is a mixture of more than 200 types of hydrocarbons ranging from hydrocarbon chains of 7 carbon to hydrocarbon chains in the order of 10 carbons.

Accordingly, due to in the case of pentane the coefficient $K_G = 120\ bar\,.\,{}^{m}/_{s}$, the values of $\left(\frac{dp}{dt}\right)_{max}$ would be as follows:

Free Tank Volume [m^3]	$(dp/dt)_{max}$ [bar/s]	Observations
5,0	71	Wrecked Tank - $K_G = 120$
7,5	62	Wrecked Tank - $K_G = 120$
10,0	56	Wrecked Tank - $K_G = 120$

Table 4.3 - Values of $\left(\frac{dp}{dt}\right)_{max}$ for a Closed Wrecked Tank with Stoichiometric Pentane

A mathematical model was developed simulating the process of inflammation in the damaged tank, to which the dimensions of it were considered, as well as the amount of explosive mixture of air and fuel vapors in the tank.

As a result, the pressure variation versus time was obtained, which is expressed by the graph in **Figure 4.3 -** *Variation of Pressure in Wrecked Tank as Function of Time. Case # 1: Volume 7.5 m^3 - Factor Turbulence 3* and **Table 4.4 -** *Variation of Pressure in Wrecked Tank as Function of Time. Case # 1: Volume 7.5 m^3 - Factor Turbulence 3.*

Equations or calculations are not shown here because they are the same of the model that was developed for the case where the damaged tank count with the loading port opening, but in this case by imposing the restriction that that port is closed (closed tank).

Note the similarity relationship between the graphical model of Figure 4.3 and in the Figure 4.2 corresponding to similar volumes of spherical shapes.

This suggests that the model developed for this particular case, responds well to the description of what would have been the pressure value inside the tank if it would not had the loading port as an element of pressure relief by a way of escape of gas through it, and if the tank would have no burst.

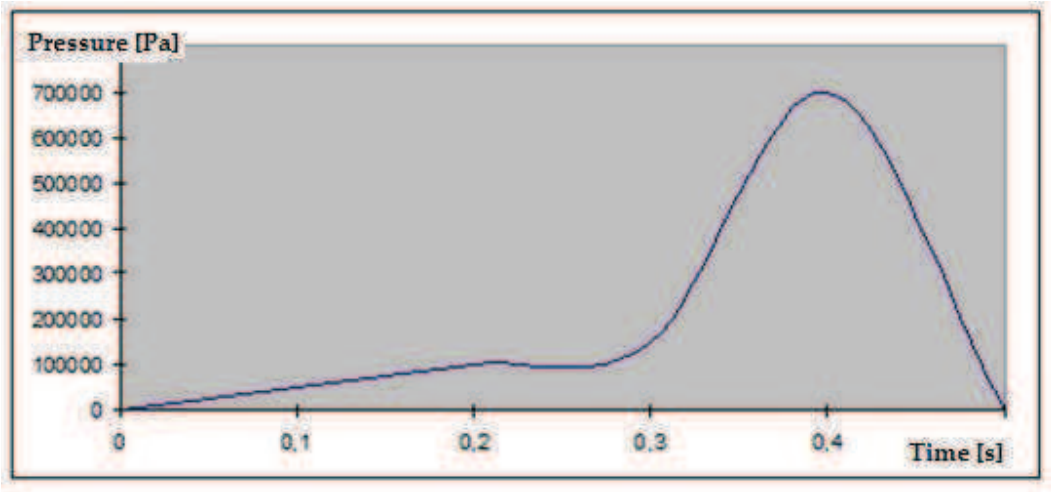

Figure 4.3 - Variation of Pressure in Wrecked Tank as a Function of Time. Case # 1: Volume 7.5 m³ - Factor Turbulence 3.

Time [s]	Gauge Pressure [Pa]
0	0
0,1	50000
0,2	100000
0,3	150000
0,4	700000
0,5	0

Table 4.4 - Variation of Pressure in Wrecked Tank as a Function of Time. Case # 1: Volume 7.5 m³ - Factor Turbulence 3.

4. 1. 2 Effect of the Loading Port in the Internal Pressure Variation from the Lit of the Flame to Tank Burst

In this section, will be addressed first, in Section 4.1.2.1 the assessment of the inadequacy of the loading port to relieve the pressure inside the tank, showing that despite the existence of a pressure relief, the pressure continued increase inside the tank.

After that, Section 4.2 developed the mathematical model that explains:

- The evolution of the pressure inside the tank from the moment that lit the flame until the tank exploded.

- The variation of gas flow through the loading port from the moment that lit the flame until the tank exploded.

- The instant of the burst from the moment that lit the flame.

- The bursting pressure of the tank.

- The amount of burned and unburned mass inside the tank at the time of the blast, and the amount of flammable mass out of the loading port at the time of the explosion.

The variation of gas flow through the loading port from the moment that lit the flame until the tank exploded, is the basis for calculating the stresses on the person who was in the area of the loading port at the moment of lighting a flame.

From this it was possible to calculate the trajectory and final position of the person who lit the flame.

The burst pressure of the tank, along with the amount of burned and unburned mass inside the tank and exit through the loading port when the outbreak, were the basis for the calculation of energy and pressure distribution in the space and time in the area around the point of explosion of the tank.

Since then it was possible to determine the different trajectories and final positions of a person been standing in different parts of the tank at the time of the outbreak.

4.1.2.1 Assessment of Impairment of the Loading Port to Relieve the Interior Pressure of the Tank

Following the trend of the experimental values shown in Figure 4.2 above, it is assumed that during the first 0,3 s the pressure inside the tank will increase proportionally with time at 50,000 Pa each every 0,1 s, being the initial pressure atmospheric pressure.

The initial absolute pressure was set at 101300 Pa.

From an absolute pressure slightly lower than 200000 Pa inside the tank, regardless of the pressure outside the tank, the dislodging capacity through the loading port (acting as a nozzle) is related to the speed of sound, which depends on the temperature.

$$a_1 = \left(\gamma . R_g . T_1\right)^{\frac{1}{2}} \qquad [4.2]$$

a_1 = speed of sound inside the tank

γ = ratio of specific heats of the mixture of air and fuel vapors

R_g = gas constant for the mixture of air and fuel vapors

T_1 = the temperature of the mixture of air and fuel vapors in the tank

$\gamma \quad = 1{,}36$

$R_g \quad = 240$

Considering the equation of state of an ideal gas:

$$p_1 \,.\, V_1 = m_1 \,.\, R_g \,.\, T_1 \qquad [4.3]$$

being the gas density ρ_1 equal to $\frac{m_1}{V_1}$, the equation of state can write:

$$\rho_1 = \frac{m_1}{V_1} \qquad [4.4]$$

$$\frac{p_1}{\rho_1} = R_g T_1 \qquad [4.5]$$

the speed of sound within the tank can be expressed as:

$$a_1 = \left(\frac{\gamma p_1}{\rho_1}\right)^{\frac{1}{2}} \qquad [4.6]$$

Whereby the dislodging through the tank after the pressure inside thereof exceeds a critical pressure, it becomes dependent on the pressure inside the tank and not to the pressure difference between inside and outside the tank.

Momentarily leaving the effect of the leakage of gases and liquid from the loading port, it can be assumed that the volume inside the tank is constant, and the mass is constant inside the tank.

In that scenario, and approximating the behavior of the mixture of air and heavy naphtha vapor to ideal gas:

$$\frac{p_1 V}{n_1 T_1} = \frac{p_0 V}{n_0 T_0} \qquad [4.7]$$

and $\quad n_0 = n_1$

thus:

$$T_1 = \frac{p_1}{p_0 T_0} \qquad [4.8]$$

$p_0 = 101300$ Pa

$T_0 = 283$ °K

During the time interval 0,35 s – 0,45 s the temperature of the gases within the tank would be:

$T_1 = 1990$ °K

It is only necessary to show that the internal pressure continues to rise despite having the loading port relieving tank pressure by venting through it.

This is determined as follows:

According to NFPA 68 - Guide for Venting of Deflagrations; Edition 2002, for maintaining internal pressure of 200000 Pa (absolute) surface vent should be 0.72 m^2 as it results from the calculations discussed below, but the charging port is about 0.20 m^2.

Because the area of the loading port is smaller than required to maintain an absolute pressure in the tank in the vicinity of 200 000 Pa (absolute), the pressure inside the tank should rise.

From the value of critical pressure, the flow out of the loading port depends on the internal pressure and not of the pressure difference between inside and outside the tank.

As already stated, by the difference in vent areas established in NFPA 68 the pressure rose generated in the tank burst conditions.

Once reached the condition of maximum variation in pressure over time, $\left(\frac{dp}{dt}\right)_{max}$, the pressure inside the tank increased far beyond the possibilities of evacuation through the loading port.

As indicated in NFPA 68 point 4.3.3.2, the composition of the fuel-air mixture that achieves the highest values of maximum pressure and maximum pressure rise, $\left(\frac{dp}{dt}\right)_{max}$, for a deflagration, are usually on the side richer of the stoichiometric fuel mix. It should be noted that the concentration that achieves the highest rate of increase in pressure over time and achieves the maximum pressure may differ.

Effect of turbulence The turbulence causes the flames to be stretched, which causes the increase of the not ignited mixture area exposed to flame, resulting in an increase in flame speed.

The initial turbulence in closed tanks results in higher rates of pressure rise and maximum pressure somewhat greater than would occur if the mixture of air and fuel were initially subject to quiescent conditions.

The turbulence results in an increase of the area required for venting. Figure 4.4 illustrates the effects of the turbulence and the fuel concentration.

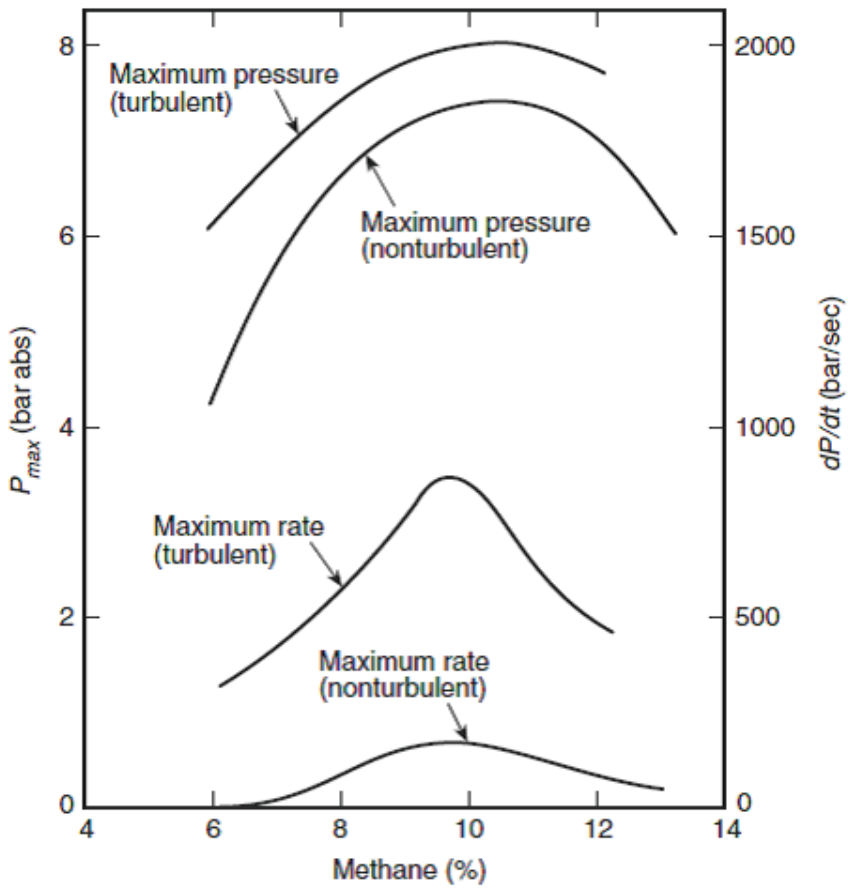

Figure 4.4 - Effect of Turbulence on the Maximum Rate Rising in Pressure vs. Time for Mixtures of Methane and Air.

The explosion vent is an opening in the tank through which the material (gas and liquid) expands and flows, thereby relieving the pressure.

If no vent is provided, the maximum pressure developed during an explosion is typically between 6 and 10 times atmospheric pressure.

The greater the increase in pressure over time, the greater the need for a vent area, with all other factors being equal.

For a ratio between length and diameter tank, L/D less than 2, one can estimate the surface of venting by the following equation:

$$A_V = \left[(0{,}127 \log_{10} K_G - 0{,}0567)P_{red}^{-0{,}582} + 0{,}175P_{red}^{-0{,}572}(P_{stat} - 0{,}1)\right]V^{\frac{2}{3}} \qquad [4.9]$$

where

A_V = vent area [m2]

K_G < 550 bar-m / s

P_{red} $\leq$ 2 bar and at least 0,05 bar> Pstat

P_{stat} $\leq$ 0.5 bar

V = volume [m^3]

$A_V = 0.53$ m^2

In the case of the damaged tank the L/D ratio is 3,5 which is must be added to the next surface ΔA.

$$\Delta A = \frac{A_V K_G \left(\frac{L}{D} - 2\right)^2}{750} \qquad [4.10]$$

$\Delta A = 0{,}19\ m^2$

Finally:

$A_V = 0{,}72\ m^2$

Another method for the calculation of the required venting area is the application of graphics of the following Figures 4.5 to 4.7, which are based on equations [4.8] and [4.9].

This will verified by calculations such equations.

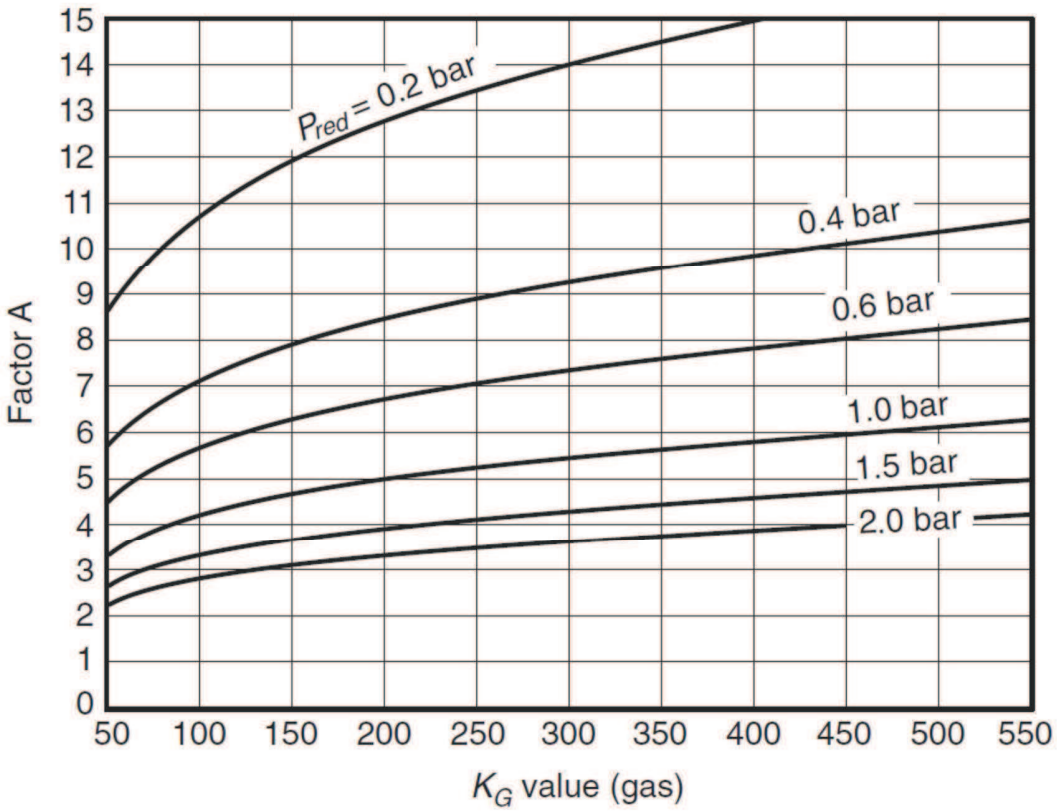

Figure 4.5 - Sizing for Gas Venting Area. Pstat = 0.1 bar.

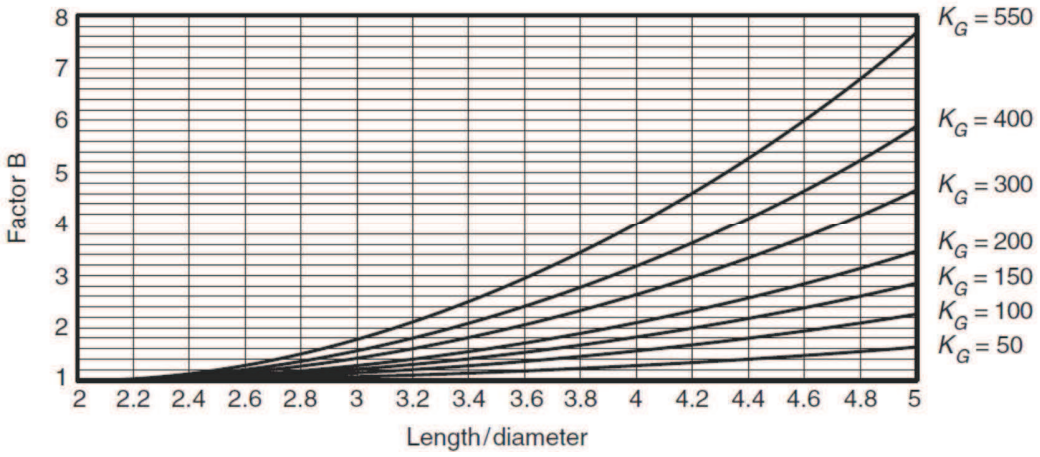

Figure 4.6 - Elongated Tank Correction. Factor B - for Gas.

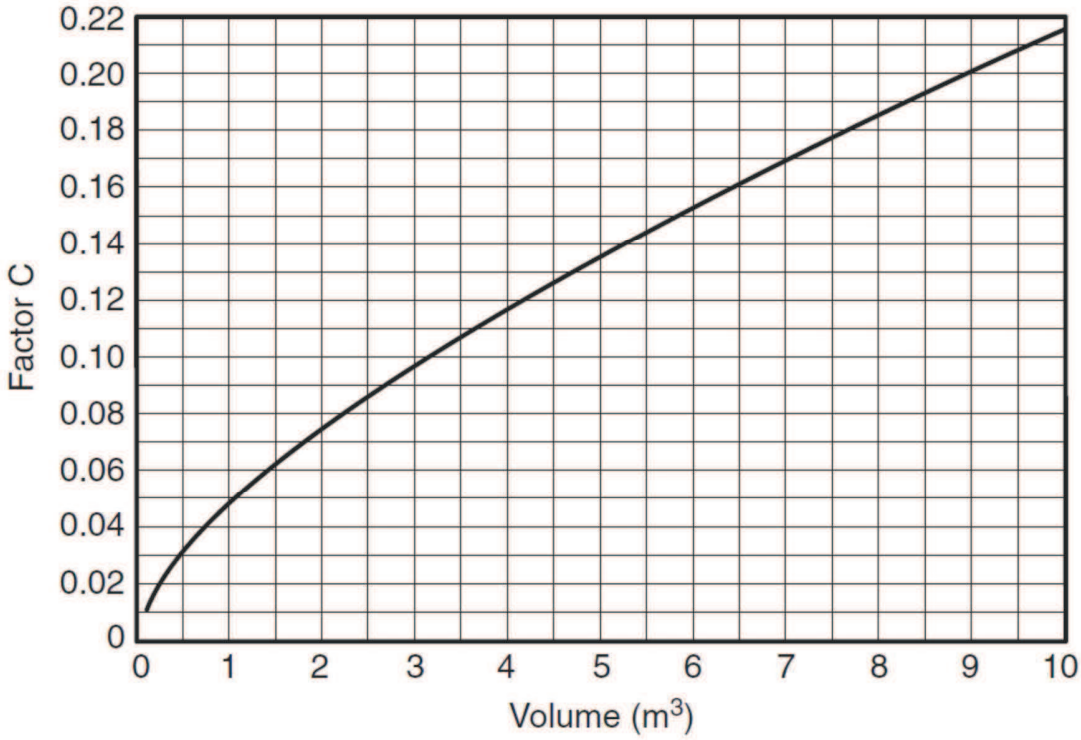

Figure 4.7 - Volume Correction. Factor C - for Gas (0 m³ to 10 m³)

Factor A. Is determined by the curves in Figure 4-5. Sizing for Gas Venting Area. Pstat = 0,1 bar, from the value of K_G of the corresponding gas, and with the appropriate $P_{stat.}$ In the case of the damaged tank:

$K_G = 120\ bar\ \frac{m}{s}$

$P_{stat} = 0$ bar, because the vent opening (loading port) was open at the time of the accident.

Factor B. In the case of the damaged tank the L / D ratio is greater than 2 and less than 5, and P_{red} is assumed for the purposes of being able to use this method of calculation is less than 2 bar.

This factor is determined by Figure 4-6. *Elongated Tank correction. Factor B - for Gas.*

Factor C. This factor is determined by Figure 4-7. *Correction Volume. Factor C - for Gas (0 m3 - 10 m3).*

The required venting area is calculated by the formula:

$$A_V = Factor\ A\ \ Factor\ B\ Factor\ C \qquad [4.11]$$

$A_V = 2.9\ .\ 1{,}4\ .\ 0{,}178$

$A_V = 0{,}72\ m^2$

Therefore, calculated by two different methods the vent surface for pressure relief to maintain 2 bar (200,000 Pa) in the interior of the tank should be on the order of 0.72 m^2.

As the surface of the loading port is on the order or less than 0.20 m^2 could not maintain the pressure in the damaged tank in that value, and continued to rise.

An estimate of the time it would take to relieve a reduced pressure inside the tank P_{red} = 2 bar, can be obtained by the following formula, which gives a value between 39% less and 118% more.

$$t_f = b\left(\frac{P_{max}}{P_{red}}\right)^{0,5}\left(\frac{V}{A_v}\right) \qquad [4.12]$$

Where:

t_f = duration of the pressure pulse through the vent (loading port)

b = $4.3.\ 10^{-3}$

P_{max} = developed into a high pressure is not vented explosion [bar]

P_{red} = developed in a vented explosion peak pressure [bar]

V = tank volume [m^3]

A_V = vent area [m^2]

The maximum explosion pressure developed in a similar non-vented tank is in the order of 6 to 10 bar, in accordance with the provisions of NFPA 68 point 5.1.1. It can be assumed an average value of 8 bar.

The maximum pressure developed in a vented explosion as will show the mathematical model that represents the pressure in the damaged tank versus time during the accident, could be in the order of 3 bar.

According to equation [4.12] :

$t_f = 4{,}3.10^{-3}.\left(\frac{8}{3}\right)^{0,5}\left(\frac{7{,}5}{0{,}2}\right)$

$t_f = 0{,}26\ s$ (less 39% plus 118%) that is, $0{,}16\ s < t_f < 0{,}57\ s$

As discussed below, the range of values obtained from the mathematical model of the tank pressure versus time, are within the range of values that Equation [4.12] indicates.

4.2 Mathematical Model of Simulation of the Tank Behavior from the Lit of the Flame to the Burst

For the purpose of determining the behavior in the tank during the explosion, a mathematical model simulating the behavior of the tank was made from flame ignition to the explosion moment.

The tank initially contained an explosive mixture consisting of 7,5 m^3 of air and vapors of heavy naphtha, according to the information available in the proceedings.

In order to consider possible errors in such information is also managed the possibility that the free volume was 10 m^3 to 5 m^3.

As the flame stars an inflammation with the following characteristics begins:

The variation in time of the flammable mixture burned or flame propagation speed inside the tank, corresponds to the following equation [2]:

$$\frac{dm_{bi}}{dt} = 4\pi r^2 \chi \rho_u S_u \qquad [4.13]$$

Where,

$\frac{dm_{bi}}{dt}$ = variation in time of the flammable mixture burned in the time interval i.

r = radius of the sphere of flammable mixture that has burned

χ = turbulence factor

ρ_u = density of the flammable mixture

S_u = speed of the flame front

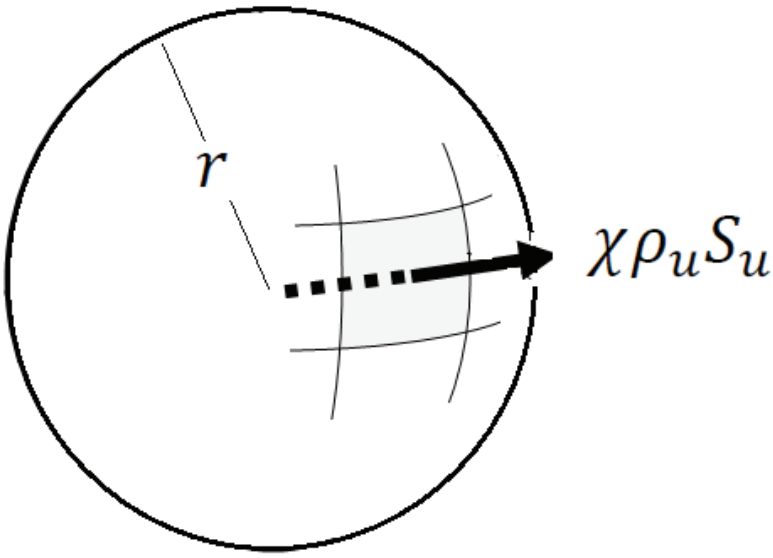

Figure 4.8 - Evolution of Inflamed Mix $\frac{dm_{bi}}{dt}$. Equation [4. 13]

The mass ratio satisfies the following equations:

$$m_{bi} = -dm_{sbi} + dm_{bi} + m_{bi-1} \qquad [4.14]$$

$$m_{ui} = -dm_{bi} - dm_{sui} + m_{ui-1} \qquad [4.15]$$

$$m_{si} = m_{si-1} + dm_{sbi} + dm_{sui} \qquad [4.16]$$

where,

m_{bi} = mass of flammable mixture burned since lit a flame to the interval i

m_{ui} = mass of flammable mixture not burned yet since lit a flame to the interval i

m_{si} = mass out the tank since lit a flame to the end of interval i

dm_{bi} = mass of flammable mixture burned in the interval i

dm_{sbi}= mass of flammable mixture burned that had left the tank during the interval i

dm_{sui}= mass of flammable mixture that had left the tank without burn in the interval i

m_{ui-1} = mass of flammable mixture present in the tank before the start of interval i

m_{si-1} = mass out of the tank from the lit of a flame lit up to before the interval i

m_{bi-1} = mass of flammable mixture that had been burned before interval **i** begin

Note that adding the three equations the mass conservation is verified, that is:

$$m_{bi} + m_{ui} + m_{si} = m_{b0} + m_{u0} + m_{s0} \qquad [4.17]$$

By definition, the total mass of flammable mixture exiting at a given time is the sum of the mass leaving burned and unburned:

$$dm_{si} = dm_{sui} + dm_{sbi} \qquad [4.18]$$

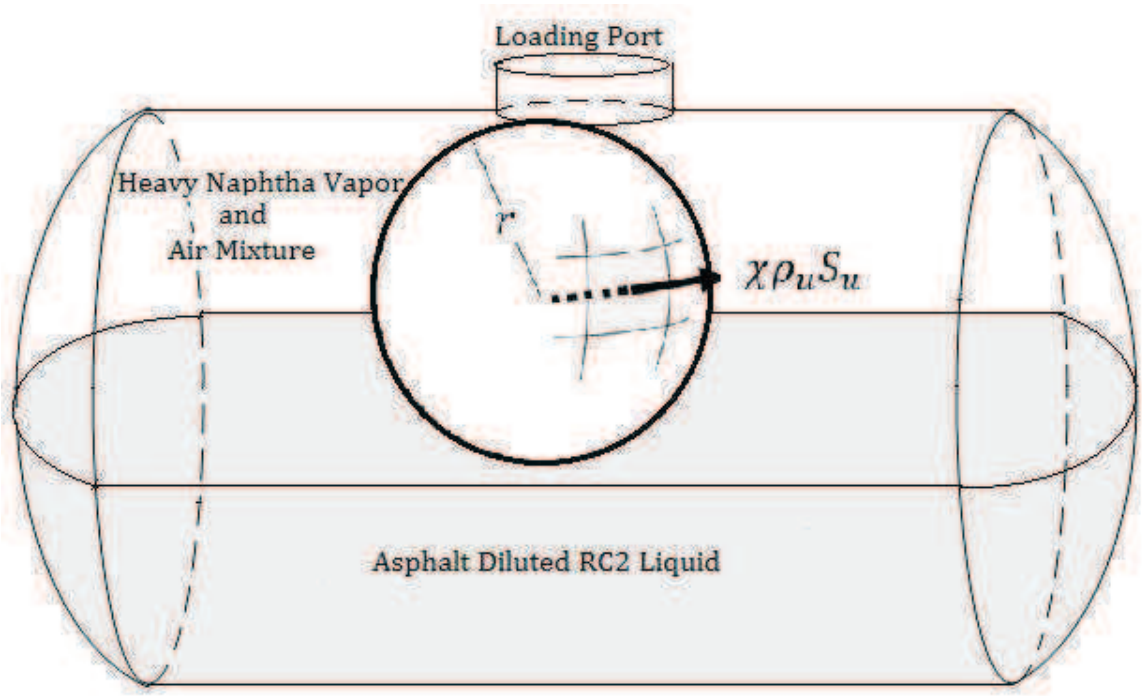

Figure 4.9 - Evolution of Inflamed Mix dm_{bi}/dt at the Tank.

At any arbitrary time i, the volume of the flammable mixture that has already been burned, plus the volume of the flammable mixture that has not been burned totals the inner volume of the tank occupied by the unburned combustible mixture at the moment of lit a flame.

As already indicated, this volume, according to the information contained in the proceedings is estimated in 7,5 m^3 and it is consider also the values of 5 m^3 and 10 m^3.

$$V_0 = V_{ui} + V_{bi} \qquad [4.18]$$

where,

V_0 = 7,5 m^3

V_{ui} = volume of the flammable mixture that has not been burned at the instant i

V_{bi} = volume of the flammable mixture burned up to the instant i

then

$$V = \frac{m_{ui}}{\rho_{ui}} + \frac{m_{bi}}{\rho_{bi}} \qquad [4.20]$$

where,

m_{ui} = mass of flammable mixture not burned at instant **i** and present in the tank

m_{bi} = mass of flammable mixture burned at instant **i** and present in the tank

ρ_{ui} = density of flammable mixture not burned at instant **i** and present in the tank

ρ_{bi} = density of flammable mixture burned at instant **i** and present in the tank

Inside the tank, once inflammation of flammable mixture begins, the pressure starts to increase.

The increase in pressure is regulated by the differential pressure maintained between the inside and the outside of the tank as a consequence of outgassing of flammable mixture (burned as unburned) through the loading port.

Both the flammable mixture and ignited mixture will increase the pressure as a polytrophic process of the type

$$pv^{\gamma} = constant \qquad [4.21]$$

that is, between instant 0 in which lit the flame inside the tank, and an arbitrary state i:

$$p_i v_i^{\gamma} = p_0 v_0^{\gamma} \qquad [4.22]$$

where,

p = pressure inside the tank

v = specific volume inside the tank

γ = ratio of specific heats

Consequently can be established that:

$$\frac{1}{\rho_i} = \frac{1}{\rho_0}\left(\frac{p}{p_0}\right)^{-\frac{1}{\gamma}} \qquad [4.23]$$

both for the unburned flammable mixture to the already burned which is contained inside the tank

Therefore, applying this relationship in the above equation can be established that:

$$V = \frac{m_{ui}}{\rho_{u0}}\left(\frac{p}{p_0}\right)^{-\frac{1}{\gamma_u}} + \frac{m_{bi}}{\rho_{b0}}\left(\frac{p}{p_0}\right)^{-\frac{1}{\gamma_b}} \qquad [4.24]$$

Where,

ρ_{u0} = density of flammable mixture at initial pressure and temperature conditions when lit a flame

ρ_{b0} = density of burned mixture at initial pressure and temperature conditions when lit a flame

γ_u = ratio of specific heats of the flammable mixture not inflamed yet

γ_b = ratio of specific heats of the flammable mixture burned

Typical values of γ_u and γ_b cited in the literature as common are:

$\gamma_u = 1{,}36$

$\gamma_b = 1{,}25$

4.2.1 Calculation Procedure

Initially it takes an interval of time $dt = 0{,}01\ s$.

During this time interval, according to equation [4.13] it generates a sphere centered at the point where the flame started and radio:

$$r_0 = \chi S_u dt \qquad [4.25]$$

the mass of the said sphere, comprising the amount of combustible mixture burned up to this moment is:

$$dm_{b1} = \frac{4}{3}\pi\rho_u(\chi S_u dt)^3 \qquad [4.26]$$

It is considered that the loading port provides a certain influence in its environment, by which it will tend to exit through it a combination of burned and unburned flammable mixture.

A mathematical model in which leave only burned gas from the beginning was performed; it was not consistent because it not allow the formation of a volume of inflamed gases large enough to increase the pressure in the tank despite the flow through the loading port.

This would imply that the pressure inside the tank would have been very low, and the inflamed gases would have escaped the loading port without consequences.

As the tank exploded, it is understood that this assumption is not true.

In order to characterize the zone of influence, the model was run assuming that through the loading port would only flow out burned mass once the volume of the sphere were 1m^3.

Also the model was run for the case of 5 m^3.

In a control volume of 5 m^3 (the considerations are analogous to 1 m^3), the mass leaving the tank in the period considered is proportional to the volume of burned mass is present in the tank within the control volume at the beginning of the period.

A run of the parameterized model was performed for the control volume of 5 m^3 as well as for 1 m^3.

As a result, the pressure variation in time profile obtained was similar to that obtained by Russian scientist Vladimir V. Molkov of the All-Russia Scientific Research Institute for Fire Protection, Ministry of the Interior, in his article Venting of Gaseous Expansions: Turbulization Aspect [8].

This article study a tank of 10 m3 capacity, with a mixture of air and hydrocarbons near stoichiometric mixture, and a vent hole of 0,5 m diameter.

This is the closest case found to the case of the damaged tank, of all research on the subject that it have been explored.

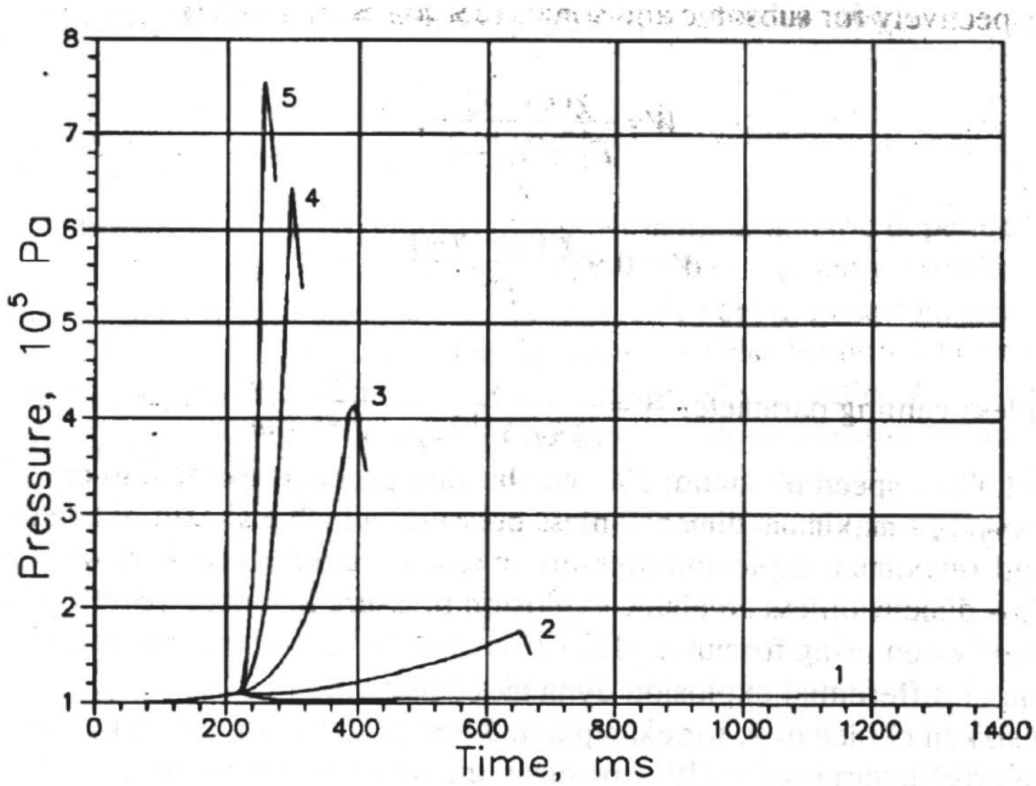

Figure 4.10 - Pressure Variation in Time for a 10 m³ tank with vent area of 0.20 m³ for Different Turbulence Factors

The values in this case were: the initial pressure is atmospheric pressure, the vent opening pressure = 0.11 MPa; initial temperature = 298 K; flame speed rate S_u = 0.34; ratios and specific heats $\gamma_u = 1{,}365$ and $\gamma_b = 1{,}248$. In the figure are plotted the values of pressure in the tank versus time for various levels of turbulence.

4.2.1.1 Estimation of Turbulence Factor for Wrecked Tank

The level that best fits turbulence is $\chi = 3$ or higher due to the relationship [1]

$$K_G = \left(\frac{dp}{dt}\right)_{max} V^{\frac{1}{3}} \qquad [4.1]$$

and considering that in this case the tank volume is 10 m³ unlike the model that was designed for the damaged tank, which initially has a free volume of 7,5 m³.

The curve identified as number 3 in **Figure 4.10 -** *Pressure Variation in Time for a 10 m³ tank with vent area of 0,20 m³ for Different Turbulence Factors* corresponds to $\chi = 3$.

It was assumed for flammable mixture inside the damaged tank that $K_G = 120\ bar\ m/s$.

For a tank with the same K_G but with a volume of 10 m³ a value of $\left(\frac{dp}{dt}\right)_{max} = 56\ bar/s$ is obtained.

To a mixture of air and hydrocarbon with $S_u = 0{,}34$ as in the case of the Figure 4.10, the corresponding K_G is a lower value, for example in the order of methane, that is $K_G = 120\ bar\ m/s$.

Therefore, for the curve number 3 would be:

$$\left(\frac{dp}{dt}\right)_{max} = \frac{56}{10^{\frac{1}{3}}}\ bar/s$$

$$\left(\frac{dp}{dt}\right)_{max} = 26\ bar/s$$

The calculation of the slope at the curve number 3 in Figure 4.10 is:

$$\left(\frac{dp}{dt}\right)_{max} = \frac{2}{0{,}08}\ bar/s$$

$$\left(\frac{dp}{dt}\right)_{max} = 25\ bar/s$$

The calculation of the slope in the curve of the damaged tank model of **Figure 4.11-** *Pressure Variation in Time for Wrecked Tank if the Volume is 7,5 m³, Venting Surface 0,20 m³, and Turbulence Factor is 3* is as follows:

$$\left(\frac{dp}{dt}\right)_{max} = 12\ bar/s$$

This difference is due to the loading port of 0,2 m³ gives proportionally greater relief capability in the reduction of the internal pressure in a tank of 7,5 m³ free volume that for of one of 10 m³.

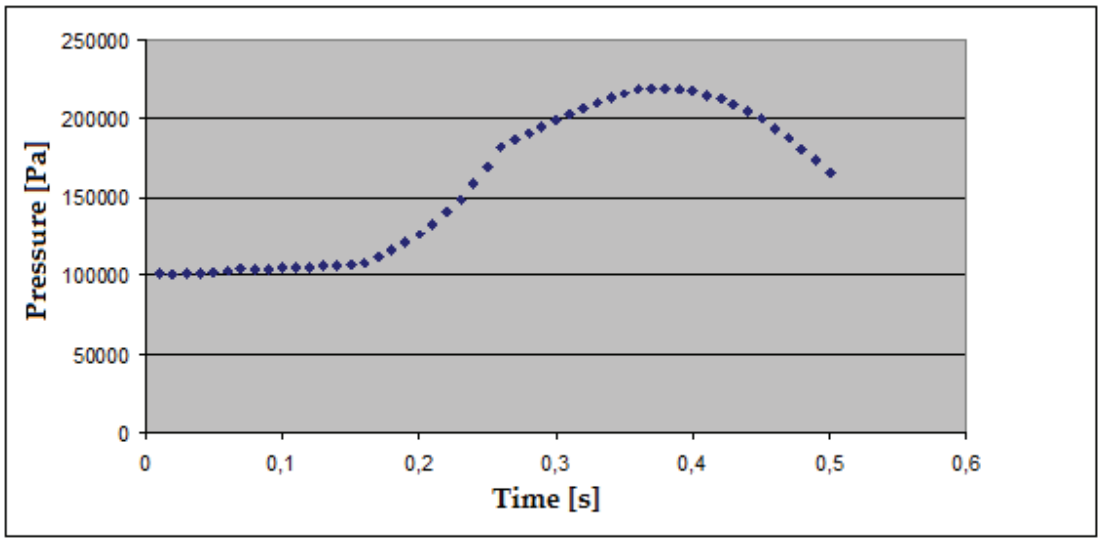

Figure 4-1 1. Pressure Variation in Time for Wrecked Tank if the Free Volume is 7,5 m³ the vent area of 0,20 m³ and Turbulence Factor is 3.

4.2.1.2 Advancement Mechanism of Pressure in Time Inside Wrecked Tank

Following the interval dt = 0,01 s, it begins to form a sphere whose center point is in the control volume and that results from the expansion of the sphere of the previous interval.

Initially the area was the one for the interval dt = 0,01 s.

Then the next sphere, corresponding to the interval dt = 0,02 s, is formed with the previous sphere, added the expansion.

The expansion is determined by

$$\frac{dm_{b1}}{dt} = 4\pi r^2 \chi \rho_u S_u \qquad [4.27]$$

from equation [4.13] for i = 1, where r is the radius of the sphere formed in the previous period.

4.2 .1.2.1 Mass Flow Through the Loading Port of Tank Calculation

The mass exiting the loading port of the tank is calculated as follows.

As the pressure ratio between atmospheric pressure and the pressure inside the tank is less than [2]:

$$\left[\frac{2}{(\gamma+1)}\right]^{\frac{\gamma}{1-\gamma}} \qquad [4.28]$$

the flow through the loading port will be regulated by the differential pressure between inside and outside the tank.

The polytrophic index for the mixture of air and heavy naphtha vapor is 1,36.

Therefore this ratio is equal to:

$$\frac{p}{p_0} = \left[\frac{2}{(1{,}36+1)}\right]^{\frac{1{,}36}{1-1{,}36}} \qquad [4.29]$$

$\frac{p}{p_0} = 1{,}87$

$p_0 = 101300\ Pa$

$p = 189300\ Pa$

In the case of $\gamma_b = 1{,}25$ the critical relation is:

$\frac{p}{p_0} = 1{,}80$

$p_0 = 101300\ Pa$

$p = 182500\ Pa$

The initial flow through the loading port is of unburned mixture and the final flow is of completely burned mixture.

As is going to show later, when it gets to that values of pressures, the flow through the loading port is composed entirely of already inflamed gases (burned).

Therefore, while the pressure does not exceed the value 182500 Pa the flow will be sonic and the mass departure in the interval dt is determined by the equation:

$$\frac{dm_{s1}}{dt} = AC_d\left\{\frac{2p\rho\gamma}{\gamma-1}\left[\left(\frac{p_0}{p}\right)^{\frac{2}{\gamma}} - \left(\frac{p_0}{p}\right)^{\frac{\gamma+1}{\gamma}}\right]\right\}^{\frac{1}{2}} \qquad [4.30]$$

Once the pressure ratio exceeds the value set in [4.30] (exceeds 182500 Pa) the following relation, corresponding to sonic flow applies:

$$\frac{dm_{s1}}{dt} = AC_d \left[p\rho\gamma \left(\frac{2}{\gamma + 1} \right)^{\frac{\gamma+1}{\gamma-1}} \right]^{\frac{1}{2}} \qquad [4.31]$$

This means that from p = 182500 Pa the mass flowed through the loading port depends on the pressure inside the tank and not to the pressure difference between inside and outside the tank.

4.2.1.2.2 Thermal Balance

The heat produced by the inflammation of the mixture of air and fuel vapor, is used for heating the gases of the already ignited mixture [14].

$$dQ = mc_p dT \qquad [4.32]$$

$$dQ = (m_{b1} - m_{s-1})c_p T_{b1} + m_{sb1} c_p T_{sb1} - m_{b1} c_p T_0 \qquad [4.33]$$

In the relationship between air and fuel vapor calculated previously had been established that for each 1 mol of fuel the chemical reaction with 62 mols of air is established.

1 mol fuel is 120 gr, and 1 mol of air is 29 gr.

Therefore, for every 120 gr of fuel provides a reaction with:

29 gr / mol. 62 mols air = 1798 gr

Consequently for every 1 gr of fuel consumed about 15 gr air approximately.

Every 16 gr air – fuel mixture have 1 gr of fuel vapors and 15 gr of air.

The calorific value of heavy naphtha is estimated at 40. 10^6 J / kg.

Therefore, for every 16 g of mixture of air - fuel vapors, that is, for every 1 g of fuel burned, released 40. 10^3 J.

In the heat balance to maintain 16:1 is formulated as follows:

$$\frac{40\,.\,10^6\,m_{b1}}{16} = (m_{b1} - m_{s-1})c_p T_{b1} + m_{sb1} c_p T_{sb1} - m_{b1} c_p T_0 \qquad [4.34]$$

Considering that T_{b1} and T_{sb1} are very close temperatures due to one of them is the temperature of the inflamed mass in the interval 1, and the other is the temperature of the inflamed mass leaving the tank in the interval 1, the equation [4.34] is:

$$\frac{40\,.\,10^6}{16} = c_p T_1 - c_p T_0 \qquad [4.35]$$

$T_0 = 283\ °K$

$c_p = 1{,}0.\,10^3\,\frac{J}{kg\ °K}$

$T_1 = 2783\ °K$

The molecular weight of the mixture of air and vapors of heavy naphtha is:

$$\frac{\left(29\,\frac{kg}{kmol}\,15 + 120\,\frac{kg}{kmol}\,1\right)}{16} = 34{,}7\,\frac{kg}{kmol} \qquad [4.36]$$

The R_g constant for this gas mixture is:

$R_g = \frac{8314}{34{,}7}\,\frac{J}{kg\ °K}$

$R_g = 240\ \frac{J}{kg\ °K}$

$$pV_{b1} = m_{b1} R_g T_1 \qquad [4.37]$$

$$p = \rho_{b1} R_g T_1 \qquad [4.38]$$

$$p = \rho_{b1}.\,240\,.\,2783 \qquad [4.39]$$

$$p = \rho_{b1}.\,66{,}7.\,10^3 \qquad [4.40]$$

4.2.1.2.3 Mass Burned by Time Interval

The mass burned in the interval i is calculated according to equation [4.13].

$$dm_{b1} = 4\pi {r_{i-1}}^2 \chi \rho_u S_u dt \qquad [4.41]$$

As already indicated, the turbulence factor to consider is $\chi = 3$

The fundamental burning velocity is assimilated to that of pentane, which is the hydrocarbon most comparable to the heavy naphtha of those listed in **Table 4.1-** *Fundamental Burning Velocities for Selected Flammable Gases in Air.*

$$S_u = 0{,}45 \frac{m}{s}$$

The interval dt in all cases is 0,01 s.

The mass burned up to the interval i-1 and that is still present in the tank, occupies a sphere of diameter r.

The mass burned in the interval i is determined by the spherical sector which is the difference between a sphere of radius $r + \chi \rho_u S_u dt$ and a sphere of radius r, as illustrated in Figure 4-11.

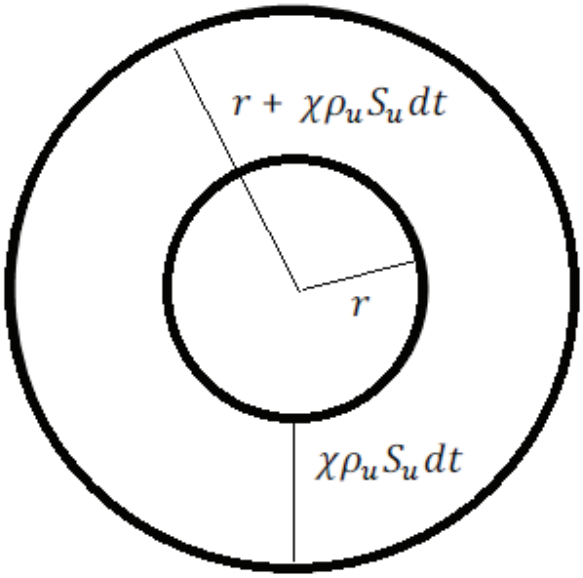

Figure 4-12. Burned Gas Volume in the Interval i.

$$dm_{bi} = 4\pi r^2 \chi \rho_{ui} S_u dt \qquad [4.42]$$

Accordingly:

$$dm_{bi} = 4\pi r^2\ 3\ \rho_{ui} 0{,}45\ dt \qquad [4.43]$$

$$dm_{bi} = 0{,}17 \rho_{ui} r^2 \qquad [4.44]$$

<u>4.2.1.2.4 Gases Flow Through the Loading Port</u>

Initially while the pressure is less than the critical ratio, that is p <189300 Pa

$$\frac{dm_{s1}}{dt} = AC_d \left\{ \frac{2p\rho\gamma}{\gamma - 1} \left[\left(\frac{p_0}{p}\right)^{\frac{2}{\gamma}} - \left(\frac{p_0}{p}\right)^{\frac{\gamma+1}{\gamma}} \right] \right\}^{\frac{1}{2}} \qquad [4.45]$$

C_d = nozzle coefficient of discharge

In this case since the loading port has an opening of straight edges the value of C_d most suitable is 0.62.

The polytrophic index γ has a value for the mixture not inflamed of 1,36 and a value for product gases of combustion, that is, the mixture already inflamed of 1,25.

$\gamma_u = 1{,}36$

$\gamma_b = 1{,}25$

The density referred ρ in the equation [4.44] is the density of the gases flowing through the loading port.

4.2.1.2.4.1 Density of the Gas Flowing Through the Loading Port Calculation

The gases leaving the loading port is assumed that consist a mixture of:

- The gaseous mixture of air and heavy naphtha vapors not inflamed yet

- The products of combustion of the said mixture but already inflamed.

For the calculation of the density of the mixture of gases leaving the loading port is considered that in a control volume of 5 m^3 originally occupied by non-ignited mixture begins to develop combustion (also will be modeled to 1 m^3).

Consequently as the control volume will be occupied by products of combustion will decrease the amount of non-inflamed mixture present in the said volume.

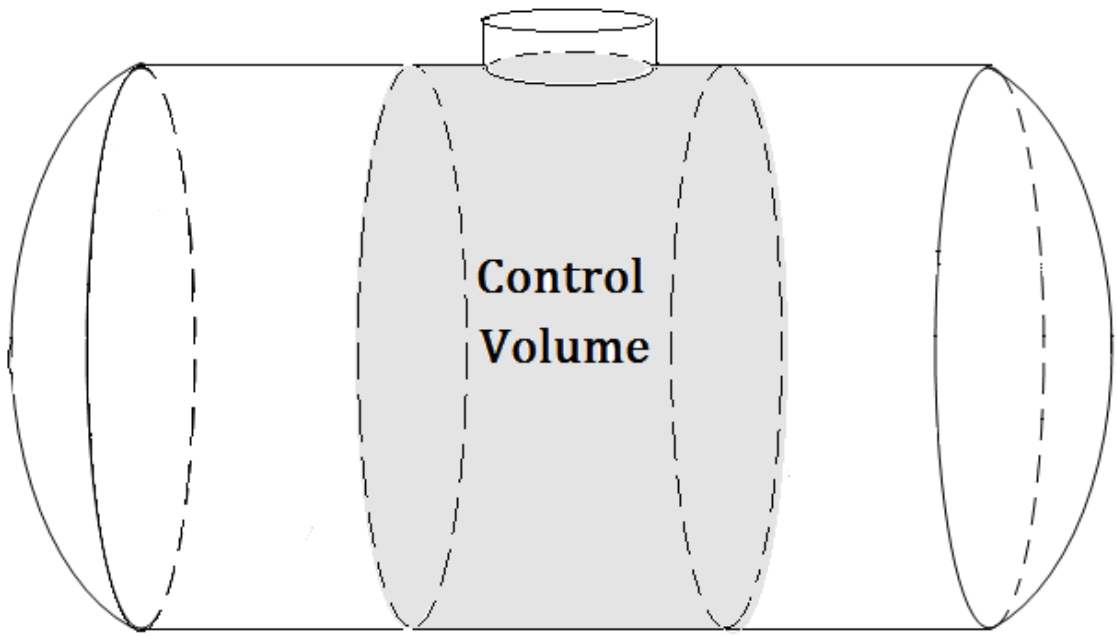

Figure 4-13. Control Volume at the Vicinity of the Loading Port

These gases are a mixture of non-inflamed and inflamed gases.

It has been established a control volume of 5 m³ (Also modeled for 1 m³) in the vicinity of the loading port as illustrated Figure 4-12. *Control Volume at the Vicinity of the Loading Port.*

It is assumed that the polytrophic index γ is a linear combination of the amount of this mass burned an unburned of fuel vapor and air in the said control volume.

Therefore, when lit the flame all the control volume is occupied by an uninflamed fuel vapor and air mixture.

As inflammation progresses over time, the volume occupied by the already inflamed gases is increased and decreases the volume of gas still not inflamed.

Once all the control volume is occupied by the gases already inflamed the polytrophic index will be the correspond to these gases.

Therefore, the polytrophic index of the gases flowing through the loading port vary from a value equal to the air - heavy naphtha vapor mixture of (at the time the flame is ignited) to a value equal to the already inflamed gases (when all the control volume has been occupied by the already inflamed gases).

The initial situation is ($i = 0$):

$$\frac{m_{b0}}{\rho_{b0}} = 0\ m^3 \qquad [4.46]$$

$$\frac{m'_{u0}}{\rho_{u0}} = 5\ m^3 \qquad [4.47]$$

Where m'_{u0} represents the mass of air and heavy naphtha vapor mixture that has not been ignited yet.

$$m'_{ui} = m_{ui} - (7{,}5 - 5)\rho_{ui} \qquad [4.48]$$

$$m'_{ui} = m_{ui} - 2{,}5\ \rho_{ui} \qquad [4.49]$$

In this mechanism, it is assumed that once you reach the interval j in which:

$$\frac{m_{bj}}{\rho_{bj}} = 5\ m^3 \qquad [4.50]$$

$$\frac{m'_{uj}}{\rho_{uj}} = 0\ m^3 \qquad [4.51]$$

inside the control volume, henceforth it will be assumed that the entire control volume will remain occupied by the combustion products, expanding into the ends of the tank.

$$\gamma_{mix} = \frac{\gamma_b m_{bi} + \gamma_u m'_{ui}}{m_{bi} m'_{ui}} \qquad [4.52]$$

for all $i \leq j$

$$\rho_{mix\ i} = \frac{m_{bi} + m'_{ui}}{5} \qquad [4.53]$$

$$\rho_{mix\ i} = \frac{m_{bi} + m_{ui} - 2{,}5\ \rho_{ui}}{5} \qquad [4.54]$$

The mass that flowed through the loading port during the interval, it will be weighted according to the volume of burned mixture and of unburned mixture, in respect to the control volume.

Similarly, the density corresponding to the gases leaving the loading port of the tank is calculated analogously to the polytrophic index, as a linear combination of the density of the flammable mixture of air and fuel vapor, and the mixture already inflamed.

Therefore, the density of the gases flowing through the loading port vary from a value equal to the air - heavy naphtha vapor mixture (at the time the flame is ignited) to a value equal to the already inflamed gases (when all the control volume has been occupied by the already inflamed gases).

$$dm_{s1} = 0{,}20\ .\ 0{,}0087 \left\{ \frac{2p\rho\gamma}{\gamma - 1} \left[\left(\frac{101300}{p} \right)^{\frac{2}{\gamma}} - \left(\frac{101300}{p} \right)^{\frac{\gamma+1}{\gamma}} \right] \right\}^{\frac{1}{2}} \qquad [4.55]$$

4.2.1.2.5 Occupied Volume by the Burned Gases and Unburned Flammable Mixture Inside the Tank

Total volume was expressed as follows using the equation [4.24].

$$V = \frac{m_{ui}}{\rho_{u0}}\left(\frac{p}{p_0}\right)^{-\frac{1}{\gamma_u}} + \frac{m_{bi}}{\rho_{b0}}\left(\frac{p}{p_0}\right)^{-\frac{1}{\gamma_b}} \qquad [4.56]$$

Initial density values for non-inflamed mixture and inflamed mixture can be calculated using the equation of state of ideal gases:

$$\rho_{u0} = \frac{p_0}{R_g T_0} \qquad [4.57]$$

$$\rho_{u0} = \frac{101300}{240\,.\,283} \qquad [4.58]$$

$$\rho_{u0} = 1{,}49 \qquad [4.59]$$

Similarly:

$$\rho_{b0} = \frac{p_0}{R_g T_0} \qquad [4.60]$$

$$\rho_{u0} = \frac{101300}{240\,.\,2783} \qquad [4.61]$$

$$\rho_{u0} = 0{,}15 \qquad [4.62]$$

$$7{,}5 = \frac{m_{u1}\left(\frac{p}{101300}\right)^{-\frac{1}{1{,}36}}}{1{,}49} + \frac{m_{b1}\left(\frac{p}{101300}\right)^{-\frac{1}{1{,}08}}}{0{,}15} \qquad [4.63]$$

4.2.1.2.6 Mass Balances

Equations [4-14], [4-15], [4-16] already established, summarize the mass balance inside and outside the tank.

The mass in the system totals the volume originally occupied by the tank in the initial conditions:

$$m_0 = V_0 \rho_{u0} \qquad [4.64]$$

$$m_0 = 7{,}5 \,.\, 1{,}49 \; kg \qquad [4.65]$$

$$m_0 = 11{,}2 \; kg \qquad [4.66]$$

$$11{,}2 = m_{u1} + m_{b1} + m_{s1} \qquad [4.67]$$

Considering the interval number 2, the area of inflamed gases formed at the end of interval 1 has the mass m_{b1} and density ρ_{b1} and its volume is accordingly V_{b1}.

$$V_{b1} = \frac{m_{b1}}{\rho_{b1}} \qquad [4.68]$$

$$V_{b1} = \frac{4}{3}\pi r_2^3 \qquad [4.69]$$

$$r_2 = \left(\frac{3m_{b1}}{4\pi\rho_{b1}}\right)^{\frac{1}{3}} \qquad [4.70]$$

$$r_2 = 0{,}62\left(\frac{m_{b1}}{\rho_{b1}}\right)^{\frac{1}{3}} \qquad [4.71]$$

EQUATIONS OF THE TANK BEHAVIOUR MODEL FROM LIT A FLAME TO THE EXPLOSION

$$p = \rho_{b1}.66{,}7.10^3 \qquad [4.40]$$

$$dm_{bi} = 0{,}17\rho_{ui}r^2 \qquad [4.44]$$

$$dm_{s1} = 0{,}20\,.\,0{,}0087\left\{\frac{2p\rho\gamma}{\gamma-1}\left[\left(\frac{101300}{p}\right)^{\frac{2}{\gamma}} - \left(\frac{101300}{p}\right)^{\frac{\gamma+1}{\gamma}}\right]\right\}^{\frac{1}{2}} \qquad [4.55]$$

$$7{,}5 = \frac{m_{u1}\left(\frac{p}{101300}\right)^{-\frac{1}{1{,}36}}}{1{,}49} + \frac{m_{b1}\left(\frac{p}{101300}\right)^{-\frac{1}{1{,}08}}}{0{,}15} \qquad [4.63]$$

$$m_{bi} = -dm_{sbi} + dm_{bi} + m_{bi-1} \qquad [4.14]$$

$$m_{ui} = -dm_{bi} - dm_{sui} + m_{ui-1} \qquad [4.15]$$

$$m_{si} = m_{si-1} + dm_{sbi} + dm_{sui} \qquad [4.16]$$

$$11{,}2 = m_{u1} + m_{b1} + m_{s1} \qquad [4.67]$$

$$dm_{si} = dm_{sui} + dm_{sbi} \qquad [4.18]$$

$$r_2 = 0{,}62\left(\frac{m_{b1}}{\rho_{b1}}\right)^{\frac{1}{3}} \qquad [4.71]$$

Resolution Mechanism of Model Equations

It begins with a radius r_0 calculated as:

$$r_0 = \chi S_u dt \qquad [4.71]$$

the volume of said sphere consisting of the amount of combustible mixture burned up to this moment:

$$dm_{b1} = \frac{4}{3}\pi\rho_{u0}(\chi S_u dt)^3 \qquad [4.72]$$

$$m_{b0} = 0 \qquad [4.73]$$

$$m_{b2} = m_{b1} + dm_{b2} - dm_{b1} \qquad [4.74]$$

then, in the interval number 2

$$dm_{b2} = 0{,}17\rho_{u1}r_1^2 \qquad [4.75]$$

The possible variants of the model or are:

a) Free Tank Interior Volume: considered three possible of Free Interior Volumes, 5 m^3, 7,5 m^3, 10 m^3.

b) Control Volume: were considered Control Volumes of 1 m^3 and 5 m^3

c) Time Interval: it was considered the time interval 0.01 s which establishes the progress from one step to the next in the model; that is, the model progresses in hundredths of a second from the lit of a flame until the outbreak of the tank.

d) Turbulence Factor: the analysis already made have established a Turbulence Factor = 3 or higher as the closest one. Notwithstanding the cases of Turbulence Factor = 2, Turbulence Factor = 4 and Turbulence Factor = 5 were also analyzed, in order to study the sensitivity of the problem under different turbulence factors.

There have been the following models:

Model No.	Free Volume	Control Volume	Time Interval	Turbulence Factor
I	7,5	5	0,010	2
II	7,5	5	0,010	3
III	7,5	5	0,010	4
IV	7,5	5	0,010	5
V	7,5	1	0,010	3
VI	7,5	1	0,010	4
VII	7,5	1	0,010	5
VIII	5,0	1	0,010	5
IX	10,0	1	0,010	3
X	10,0	1	0,010	5

Table 4-5. Types of Models for Free Volume, Control Volume, Time Interval, and Turbulence Factor

In their order, the models are described, with highlights of each outstanding features. Only is presented in detail those models leading to a closer explanation of what happened.

Column 1: $\boldsymbol{dt}$

In this column the time variation in the model is established.

The next cell takes the value of the previous and increments in 0,01 s.

Column No. 2: $\boldsymbol{r_{i-1}}$

Represents the radius of the sphere of fire and inflamed gases at time i-1.

At the instant $t = 0{,}01\ s$ is calculated as $\chi S_u dt$.

From the instant $t = 0{,}02\ s$ to onwards takes the value of r_i for the previous time interval, that is, the value contained in the cell that is in the 10th column of the table, and in the previous row to the one of the instant considerate.

Column No. 3: $\boldsymbol{m_{bi}}$

Represents the burn mass of the air and heavy naphtha vapor mixture which is inside the tank.

At the instant $t = 0{,}01\ s$ is calculated as

$$\frac{4}{3}\pi\rho_{u0}r_{i-1}^{3} \qquad [4.76]$$

From time $t = 0{,}02\ s$ to onwards is calculated as equation [4.14]:

$$m_{bi} = -dm_{sbi} + dm_{bi} + m_{bi-1}$$

For this, the value of the previous cell in the same column is taken (m_{bi-1}), it is added to the value of the mass burned in that time interval (dm_{bi}) and it is subtracted the value of burnt mass that flew through tank during the previous time interval (dm_{sbi-1}).

Column No. 4: $\boldsymbol{m_{ui}}$

Represents the mass of air and heavy naphtha vapors inside the tank and has not been burned yet.

It is calculated by two different methods, appearing in these columns number 4 and number 8 of the table respectively.

Column No. 4 is calculated as follows using equation [4.15]:

$$m_{ui} = -dm_{bi} - dm_{sui} + m_{ui-1}$$

For this, the value of the previous cell in the column (m_{ui-1}), is subtracted from the value in the same row in the 13th column (dm_{sui}), and subtract the value of the same row in the 15th column (dm_{bi}).

Column No. 5: $\boldsymbol{p_i}$

Represents the pressure inside the tank.

The values of p_i are entered manually in order to balance the values of m_{ui} obtained in 4th and 8th column.

The values of the 8th column vary with the pressure.

Once the entire table is completed, that is, once all values in all columns are loaded except the 5th column, the m_{ui} values are very different.

The process of balancing columns is to search manually for each cell in the 5th column the value of p_i that balances the values in 4th and 8th columns.

In this way tank behavior is determined from the beginning of a flame until the outbreak for different Free Interior Volume, Control Volume, Turbulence Factor, and Time Interval, supposed conditions.

Column 6: $\boldsymbol{\rho_{bi}}$

Represents the density of the burnt mass present inside the tank.

Is calculated from the equation [4.39]:

$$p = \rho_{b1}.66{,}7.10^3$$

Column 7: $\boldsymbol{m_{si}}$

Represents the mass flowed through the damaged tank from the moment that lit a flame until it exploded.

Is calculated from the equation [4.16]:

$$dm_{si} = dm_{sui} + dm_{sbi}$$

and [4.18]:

$$m_{si} = dm_{sui} + dm_{sbi} + m_{si-1}$$

hence:

$$m_{si} = dm_{si} + m_{si-1} \qquad [4.77]$$

Is calculated by adding the value of the previous cell in the same column with the value of the 14th column of the same row.

Column 8: $\boldsymbol{m_{ui}}$

Represents the mass of air and heavy naphtha vapors inside the tank and which has not been burned yet.

Unlike the calculation of the 4th column, in this case the calculation is the product of the density of the unburned mass by the volume occupied by it inside the tank.

The volume occupied by the amount of the mixture of air and heavy naphtha vapors of not inflamed mass is calculated by difference between the total free volume and the volume occupied by the already inflamed mass in the tank.

$$m_{ui} = (V_{0-}V_{bi})\rho_{ui} \qquad [4.78]$$

The calculation is made by subtracting the value of the free volume to the value of the volume already inflamed in the tank shown in the same row cell at the 9th column.

This value is multiplied by the density value of the not inflamed mixture contained in the corresponding same cell row at the 18th column.

Column 9: $\boldsymbol{V_{bi}}$

Represents the volume occupied by the mass of air and heavy naphtha vapor mixture already ignited and located inside the tank.

It is calculated as the quotient of the already inflamed mass contained in the cell in the same row of the 3th column, and the density given in the cell in the same row of 6th column.

$$V_{bi} = \frac{m_{bi}}{\rho_{bi}} \qquad [4.79]$$

Column 10: $\boldsymbol{r_i}$

Represents the radius of a sphere occupied by the already inflamed mass of air and heavy naphtha vapors.

Once the diameter of the sphere exceeds the height of the free volume (space between the top of the tank and the surface of asphalt diluted RC2 liquid) it will be assumed that the expansion of this inflamed mass remains spherical but deformed the sphere taking the shape of its container.

The value of r_i is calculated from the equation:

$$V_{bi} = \frac{4}{3}\pi r_i^3 \qquad [4.80]$$

Is calculated by taking the value of V_{bi} in the same row in 9th column, dividing it by $\frac{4}{3}\pi$ and obtaining its cube root.

Column 11: $\boldsymbol{X_i}$

Represents the position of the flame front for the volume (the deformed sphere because the diameter is greater than the height of the free volume) of burned gases with respect to each of the ends of the tank.

It is assumed here that the flame front advances symmetrically towards both ends of the tank.

It is calculated by the equation:

$$X_i = \frac{(V_{0-}V_{bi})}{2S} \qquad [4.81]$$

Being S equal to the section of the free volume inside the tank.

Calculated by dividing the free volume between the length of the tank, which is estimated at 7 m.

For $V_0 = 5{,}0\ m^3$ section S is $0{,}72\ m^2$

For $V_0 = 7{,}5\ m^3$ section S is $1{,}07\ m^2$

For $V_0 = 10{,}0\ m^3$ section S is $1{,}43\ m^2$

<u>Column 12:</u> $\boldsymbol{dm_{sbi}}$

Represents the burned mass that flowed through the tank during the differential interval.

Is calculated by the equation:

$$dm_{sbi} = dm_{si}\frac{V_{bi}}{V_c} \qquad [4.82]$$

V_c is the volume control

until $V_{bi} = V_c$

From there, by the way it was defined the concept of volume control:

$$dm_{sbi} = dm_{si} \qquad [4.83]$$

Column 13: $\boldsymbol{dm_{sui}}$

Represents the unburned mass that during the differential interval left the tank.

Is calculated by the equation:

$$dm_{sui} = dm_{si} - dm_{sbi} \qquad [4.83]$$

until $V_{bi} = V_c$

From there, by the way it was defined the concept of volume control:

$$dm_{sui} = 0 \qquad [4.84]$$

Column 14: $\boldsymbol{dm_{si}}$

Represents the mass that during the differential interval left the tank.

While the sub-sonic flow is calculated by the equation [4.30]:

$$\frac{dm_{s1}}{dt} = AC_d \left\{ \frac{2p\rho\gamma}{\gamma - 1} \left[\left(\frac{p_0}{p}\right)^{\frac{2}{\gamma}} - \left(\frac{p_0}{p}\right)^{\frac{\gamma+1}{\gamma}} \right] \right\}^{\frac{1}{2}}$$

The density is the density of the mixture of burned and unburned gases inside the control volume.

This density takes the value of the density of the burned gas once the volume of the burned gases equals the volume control.

Similarly the polytrophic index is calculated.

Once the pressure ratio reaches a critical ratio, flow becomes sonic and is calculated by the equation [4.31]:

$$\frac{dm_{s1}}{dt} = AC_d \left[p\rho\gamma \left(\frac{2}{\gamma + 1}\right)^{\frac{\gamma+1}{\gamma-1}} \right]^{\frac{1}{2}}$$

Column 15: $\boldsymbol{dm_{bi}}$

Corresponds to the scheme shown in Figure 4.11 and the corresponding equations.

Column 16: $\boldsymbol{\gamma_{mix}}$

As already indicated is obtained by weighting between the already inflamed and non-inflamed mixture.

Column 17: $\boldsymbol{\rho_{mix}}$

As already indicated is obtained by weighting between the already inflamed and non-inflamed mixture.

Column 18: $\boldsymbol{\rho_{ui}}$

Is obtained from the ratio of mass and volume of not inflamed mixture (total volume minus 8th column).

Column 19: $\boldsymbol{T_{ui}}$

Is obtained from the ideal gas equation for the non-inflamed mixture with the corresponding density value (18th column) and pressure (5th column).

The result of the calculus are in Appendix I: Tank Behavior - Model I to Model X

Chapter 5

5. Tank Burst

The tables of this Chapter are in Appendix II.

The tank has a loading port that relieves pressure during the explosion.

But this relief is very slow to release pressure quickly enough, and the tank behaves as a fully enclosed tank as the pressure increased.

The pressure increase depends mainly on the type and concentration of fuel, the initial pressure, the tank filling speed, the burn rate, the tank vent.

5.1 Tank Burst Pressure

Three possible causes arises as possible: 1) overpressure inside the tank (later in this thesis it shows that is for detonation), 2) general failure at operating pressure due to corrosion or general tank failure due to bad maintenance, 3) blast for being the tank surrounded by flames.

In this case, the tank burst happened because the tank was subjected to a pressure much higher than the operation pressure, which is practically the atmospheric pressure. It is unknown if a weak condition particularly in the burst area of the tank will lead to the failure out there.

5.2 Burst Energy Distribution

The way burst energy was distributed it is divided as follows: 1) tank expansion, 2) tank rupture, 3) burst 4) fragments.

The energy due to the expansion tank can be neglected because it is very small.

Some energy is required also for breakage of the tank but is also very small, some studies estimate the energy in the order of 10000 Joules, while the burst occurred was estimated to be 1000 times higher in energy.

5.3 Tank Burst Modelling

The most relevant study according to Lee's Lost Prevention in the Process Industry is the W.E. Baker et al. (1975), who conducted a parametric explosions exploration in tanks and developed a method for estimating the parameters similar to those used for the condensed phase explosion.

Has been taken as a reference the Adamczyk (1976) work contained in Guidelines for Vapor Cloud Explosion, Pressure Vessel Burst, BLEVE and Flash Fires of the Center for Chemical Process which indicates that the burst of a tank is approaching a condensed phase explosion only for high pressure ratios and high temperature.

Guiraio and Bach (1979) investigations blasts of air and fuel mixtures, have found that in such cases only between 27% and 37% of the combustion energy is converted into work.

To evaluate the consequences of the tank burst two methods were used:

- Method of Baker et al. [2]
- The Multienergy method [4]

5.3.1 Baker et al. Method. Basic Method

A method for estimating the burst parameters of a pressurized tank containing gas are described below.

The method was developed by W. E. Baker et al. (1975), and refers to spherical tank containing ideal gas.

5.3.1.1 Explosion Energy

Explosion energy is calculated by the equation:

$$E_{ex} = 2(p_1 - p_0)\frac{V}{\gamma_u - 1} \qquad [5.1]$$

Where

2 = coefficient for ground reflection of the pressure wave

p_1 = burst pressure

p_0 = atmospheric pressure

V = volume of the self-ignition mixture

γ_u = polytrophic index of air and heavy naphtha vapors mixture not inflamed yet

Therefore the equation [5.1] is:

$$E_{ex} = 2(p_1 - 101300)\frac{V}{1{,}36 - 1} \qquad [5.2]$$

In **Table 5.1-** *Explosion Energy Values for the Explosion Development Models*, different explosion energy values E_{ex} are set, calculated according to equation [5-1].

This Table also states the values of the potential chemical energy released E_b as a result of the mass inflammation m_b inside the tank.

To calculate E_b was considered that for every 1 kg of heavy naphtha inflamed 40.10^6 Joules are released.

Previously it had been determined that there was 1 kg of heavy naphtha in 16 kg of mixture of air and heavy naphtha vapors.

Therefore, for every 1 kg of m_b burned mass of air mixture and heavy naphtha vapors $2{,}5.10^6$ J are released.

In **Table 5.2 -** *Explosion Energy Values for the Explosion Development Models Compared with the Energy Released by the Flammable Mixture Burned in the Tank*, are established the energy values that could potentially release the mixture of air and heavy naphtha vapors burned inside the tank.

In **Table 5.3-** *Explosion Energy Values for the Explosion Development Models Compared with the Energy Releasable by the Flammable Mixture Initially Contained in the Tank*, you can see the relationship between the energy potentially available et the inflammation start (lighting the flame) and how much it materialized in increasing gas pressure inside the tank up to its outbreak.

As a reference, the technical literature generally provides an $\frac{E_{ex}}{E_0}$ ratio about 3% to 30%.

5.3.1.2 Pressure and Impulse

It will be assumed that the center of the outbreak corresponds to the center of the opening in the tank caused by the burst.

The radius is determined by the following equation:

$$R = r\left(\frac{p_0}{E_{ex}}\right)^{\frac{1}{3}} \qquad [5.3]$$

where

R = scaled distance

r = distance of the person to the center of the explosion [m]

p_0 = atmospheric pressure [Pa]

E_{ex} = explosion energy [J]

If a person is supposed to be standing on the tank at a distance r from the center of the explosion, a scaled distance R is given by the equation [5.3] for each value of r.

A person standing on the tank at a distance r will receive a maximum pressure pulse where crossed by the pressure wave.

For each value of R found it can be calculated the scaled overpressure, which by means of equation [5.3] can be converted to the value of the pressure pulse received by the said person.

$$P_s = \frac{p_s}{p_0} - 1 \qquad [5.4]$$

Where

P_s = lateral pressure scaled

p_s = lateral pressure received by a person standing on the tank

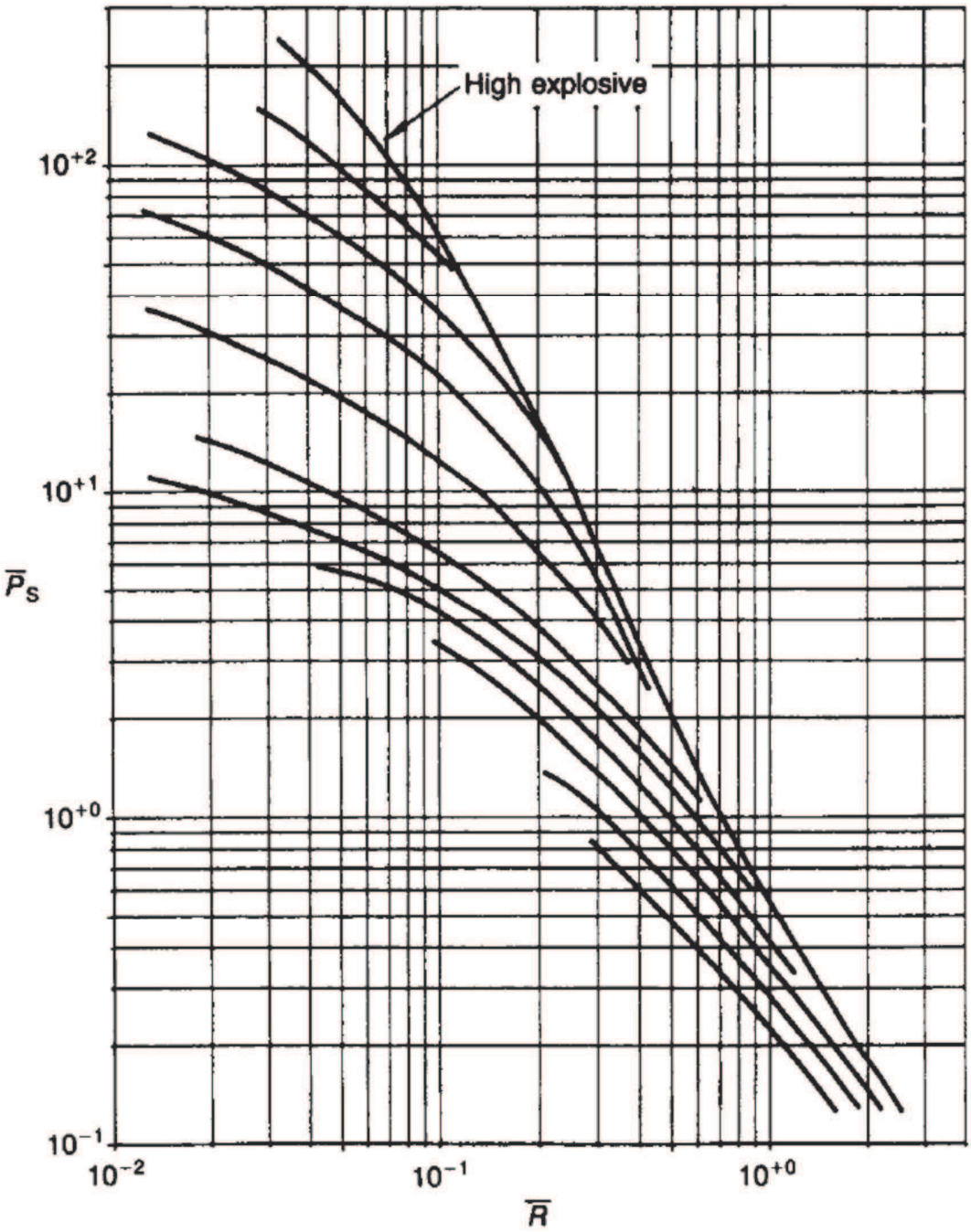

Figure 5-1. Scaled Overpressure of Tank Burst. (Baker et al. 1975)

Scaled overpressure is obtained from **Figure 5.1-** *Scaled Overpressure of Tank Burst* initially using the "high explosive" curve.

As it will see below, a correction for the case $R \leq 2$ was performed as indicated by the theory, resulting that the range that fits to the situation under study will go from the curve No. 2 to No. 5, from left to right.

This is interpreted as an average explosion, because the curve "high explosive" is represented by the curve to the right, that is, the curve No. 11.

The impulse on the body of a person standing on the tank can be obtained from equation [5.5].

$$I = \frac{i_s a_0}{p_0^{\frac{2}{3}} E_{ex}^{\frac{1}{3}}} \qquad [5.5]$$

Where

I = scaled impulse

i_s = lateral impulse [Pa. s]

a_0 = velocity of sound in the gas

The scaled impulse can be obtained from **Figure 5.2 -** *Scaled Impulse for Pentonite* and **Figure 5.3 -** *Scaled Impulse for Tank Burst*

Table 5-4. *Lateral Pressure and Lateral Impulse for 1, 2, 3 meters from the Center of the Explosion*, has expressed the result of calculating the lateral pressure p_s and the lateral impulse i_s for a person standing on the tank at three different distances r of 1, 2, 3 meters.

Equations [5.4] to [5.5] should be assigned the following correction when $R \leq 2$ as recorded in this case.

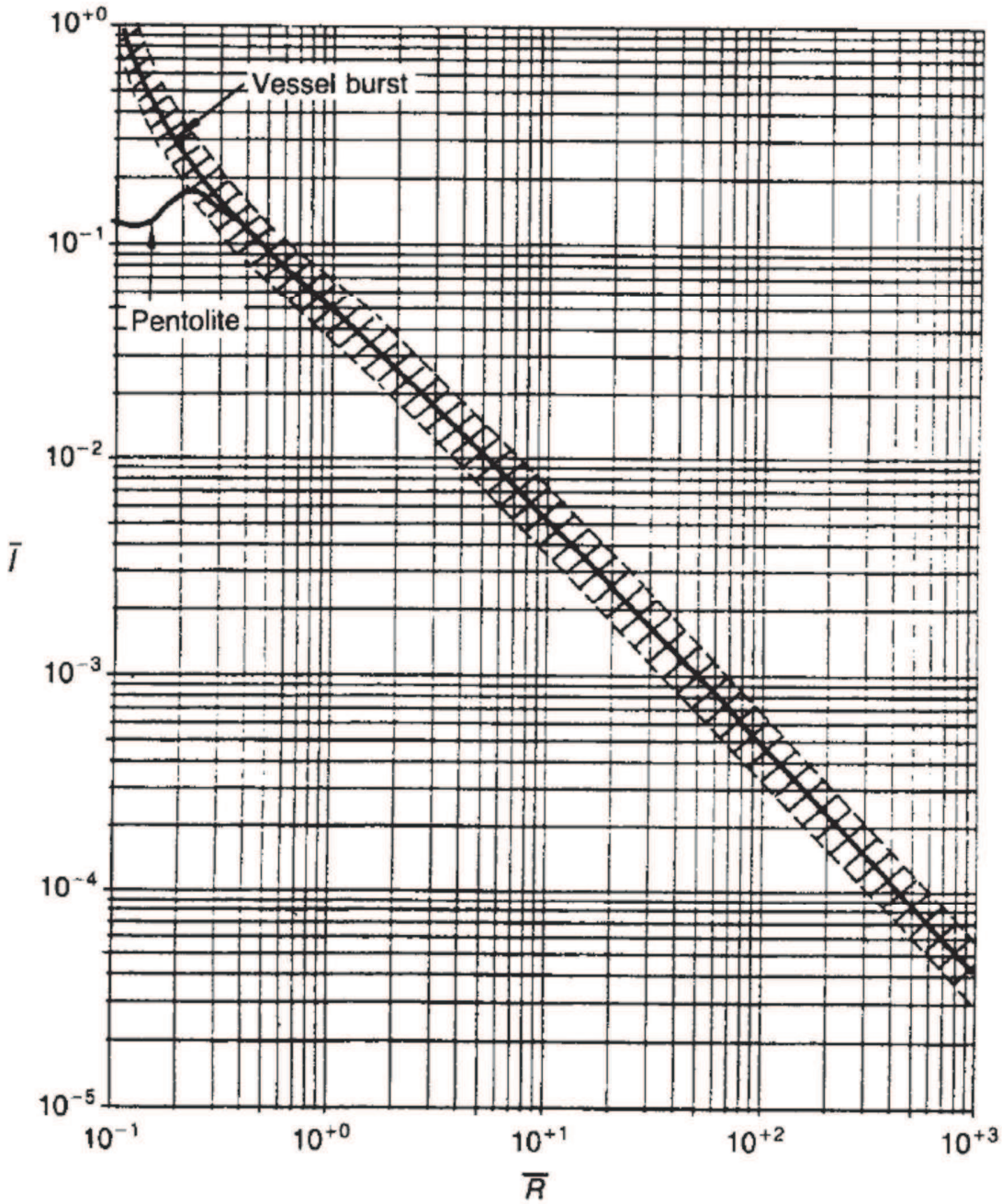

Figure 5-2. Scaled Impulse for Pentonite. (Baker et al. 1975)

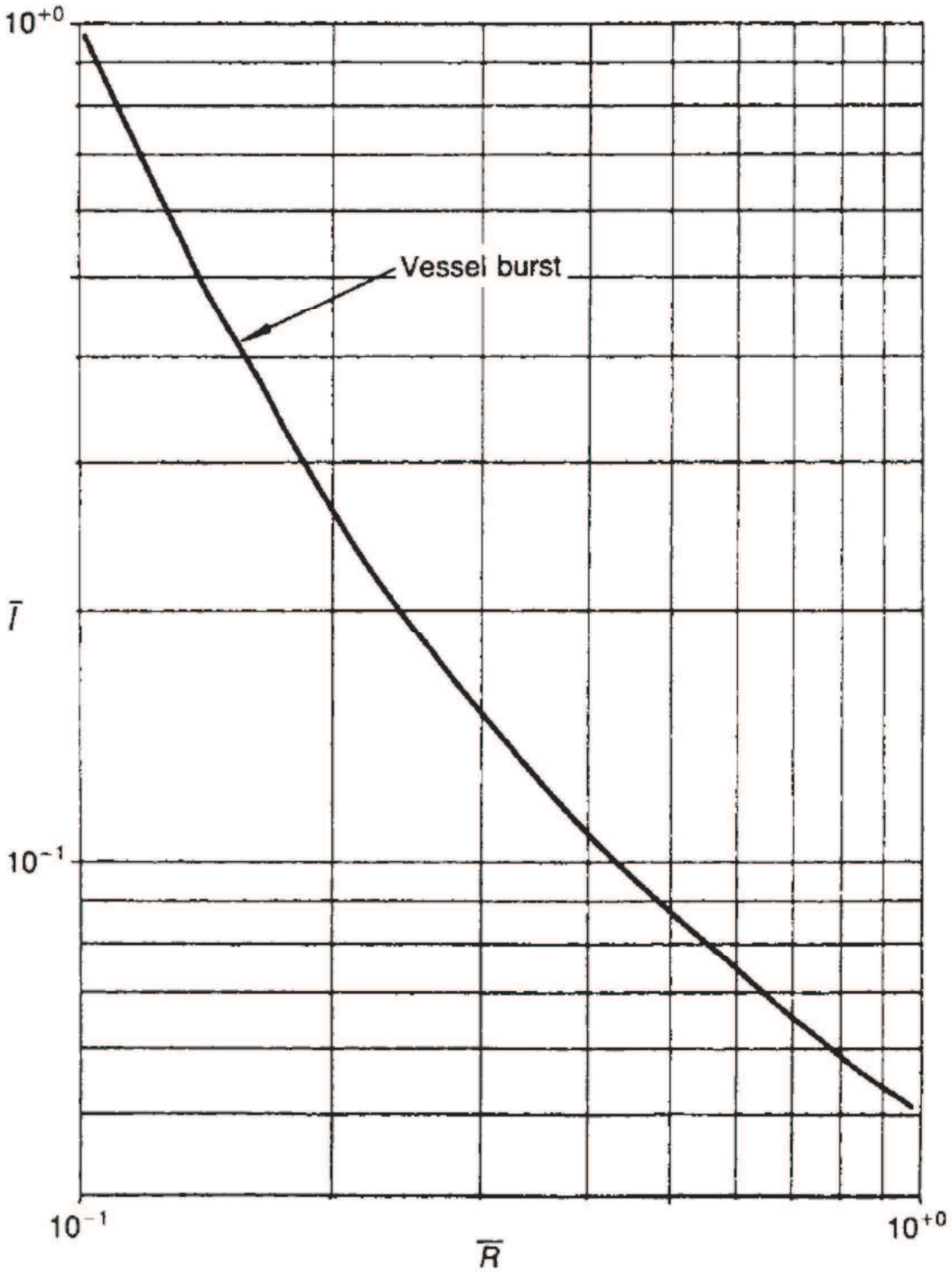

Figure 5-3. Scaled Impulse for a Tank Burst. (Baker et al. 1975)

Firstly, an effective radius r_0 is determined for the equivalent hemisphere formed by the initial gas volume:

$$r_0 = \left(\frac{3V_1}{2\pi}\right)^{\frac{3}{4}} \qquad [5.6]$$

$r_0 = 1{,}9\ m$ for a volume of 5,0 m³

$r_0 = 2{,}6\ m$ for a volume of 7,5 m³

$r_0 = 3{,}2\ m$ for a volume of 10,0 m³

As a function of r_0 can be calculated R_0 by the equation [5.7].

$$R_0 = r_0 \left(\frac{p_0}{E_x}\right)^{\frac{1}{3}} \qquad [5.7]$$

In the **Figure 5.4 -** *Scaled Peak Overpressure at Short Distance for a Tank Burst $\gamma = 1{,}4$*, it can be set a value P_{s0} from the relationship between the tank burst pressure p_1 and the atmospheric pressure p_0, and the ratio between the sound speed under ambient conditions a_0 and the speed of sound in gas conditions a_1.

The speed of sound $a_0 = 340\ {}^{m}/_{s}$.

The speed of sound a_1 can be calculated by the equation:

$$a_1 = \left(\frac{\gamma p_1}{\rho_1}\right)^{\frac{1}{2}} \qquad [5.8]$$

In **Figure 5.5 -** *Sound Speed and Ratio* $\left({}^{a_1}/_{a_0}\right)^2$ *at Tank Burst Conditions*, the calculation result of the relationship $\left({}^{a_1}/_{a_0}\right)^2$ for Models I to X is listed.

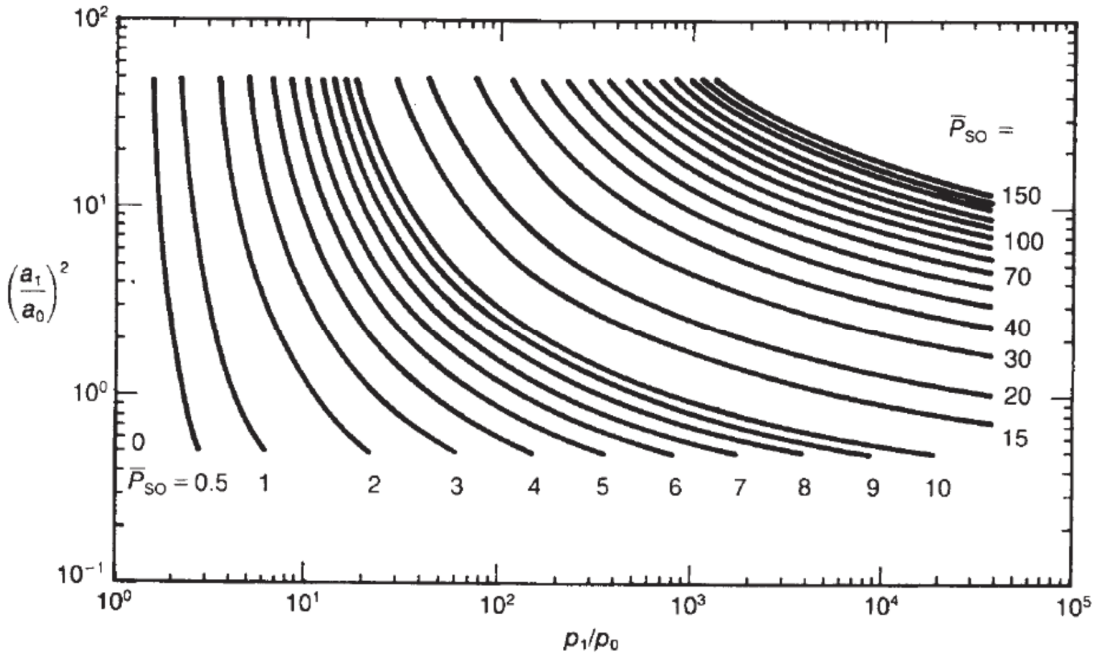

Figure 5.4 - Scaled Peak Overpressure at Short Distance for a Tank Burst $\gamma = 1{,}4$. (Baker et al. 1975)

As indicated above, a correction for the $R \leq 2$ case was performed as indicated by the theory, which looks at Table 5.5 - *Figure 5-1 Curve Associated to Models I to X.*

The range that fits the situation under study will go from curve No. 4 to No. 1, from left to right in Figure 5.1 - This is interpreted as a range of explosion ranges from average to strong type, because the curve "high explosive" is represented by the curve to the right, that is, the curve No. 11.

5.3.2 Multi-Energy Method

Through a lot of explosion experiments, it has been established the explosions curves in Figures 5.5 to 5.7. Known as "TNO blast curves" for explosions

The TNO Multi-Energy method is based on the concept of multi-energy, which is the presentation of a deflagration of gas so that the development of the blast and overpressure obtained only under certain boundary conditions, where only flammable mixture is partially confined or obstructed.

The Mult-energy method does not strictly apply to the case of the explosion of a tank, but it will in the case of a cloud of explosive mixture contained, which approximately is the case under study considering:

- The energy consumed by tank rupture is negligible

- That confinement by the tank is too high

Based on the concept of Multi-Energy, the explosion of gas clouds have been modeled for a number of models of hemispheric loads. The load of each model is characterized by the load size and load stress.

Load size is related to the combustion heat present in the source, while the load stress is related to the explosion overpressure.

Based on these characteristics, scaled blast parameters were calculated (peak overpressure, positive phase duration) as a function of the scaled distance, as it looks in Figures 5.5 to 5.7, as a number between 1 and 10 representing categories from "negligible" to "detonating".

This method is applied here to obtain a set of reference values compare mode with the two other methods already in use.

Again it is assumed that the center of the outbreak corresponds to the center of the opening in the tank caused by the outbreak.

The radius is determined by the equation [5.9] and view:

$$R = r\left(\frac{p_0}{E_{ex}}\right)^{\frac{1}{3}} \qquad [5.9]$$

where

R = scaled distance

r = distance of the person to the center of the explosion [m]

p_0 = atmospheric pressure [Pa]

E_{ex} = explosion energy [J]

For distances r = 1, 2, 3 meters from the center of the explosion should be considered the relations established.

To calculate the explosion energy was considered that in every Model I to X, the amount of flammable mixture that was burned since the flame lit until the tank burst, assuming that the tank burst at the maximum pressure in each of the ten Models considered.

The calorific power of the combustible mixture had already estimated from the calorific power of the heavy naphtha.

$40 \cdot 10^6$ J corresponds to 1 kg of heavy naphtha

1 kg of heavy naphtha corresponds to 16 kg of flammable mixture.

$2{,}5 \cdot 10^6$ J correspond to 1 kg of flammable mixture

$$E_{ex} = m_b 2{,}5.\,10^6 \qquad [5.10]$$

For reference, according to TNO can be estimate the explosion energy as:

$$E_{ex} = 3{,}5.\,10^6 V \qquad [5.11]$$

Where, V is the volume of flammable gas, prior to inflammation.

As the method assumes that the gas is at atmospheric pressure, the volume will be corrected considering the expansion, that is,

$$V_2 = V_1 \left(\frac{p_1}{p_2}\right)^{\frac{1}{\gamma}} \qquad [5.12]$$

Considering only the already inflamed mass, it would be taken into account that in each case a portion of the flammable mass had flowed through the loading port without contributing to the explosion.

This last point is a correction on an aspect cited as a critical to the equation [5.11] in the sense that estimates an amount of energy greater than the actual energy.

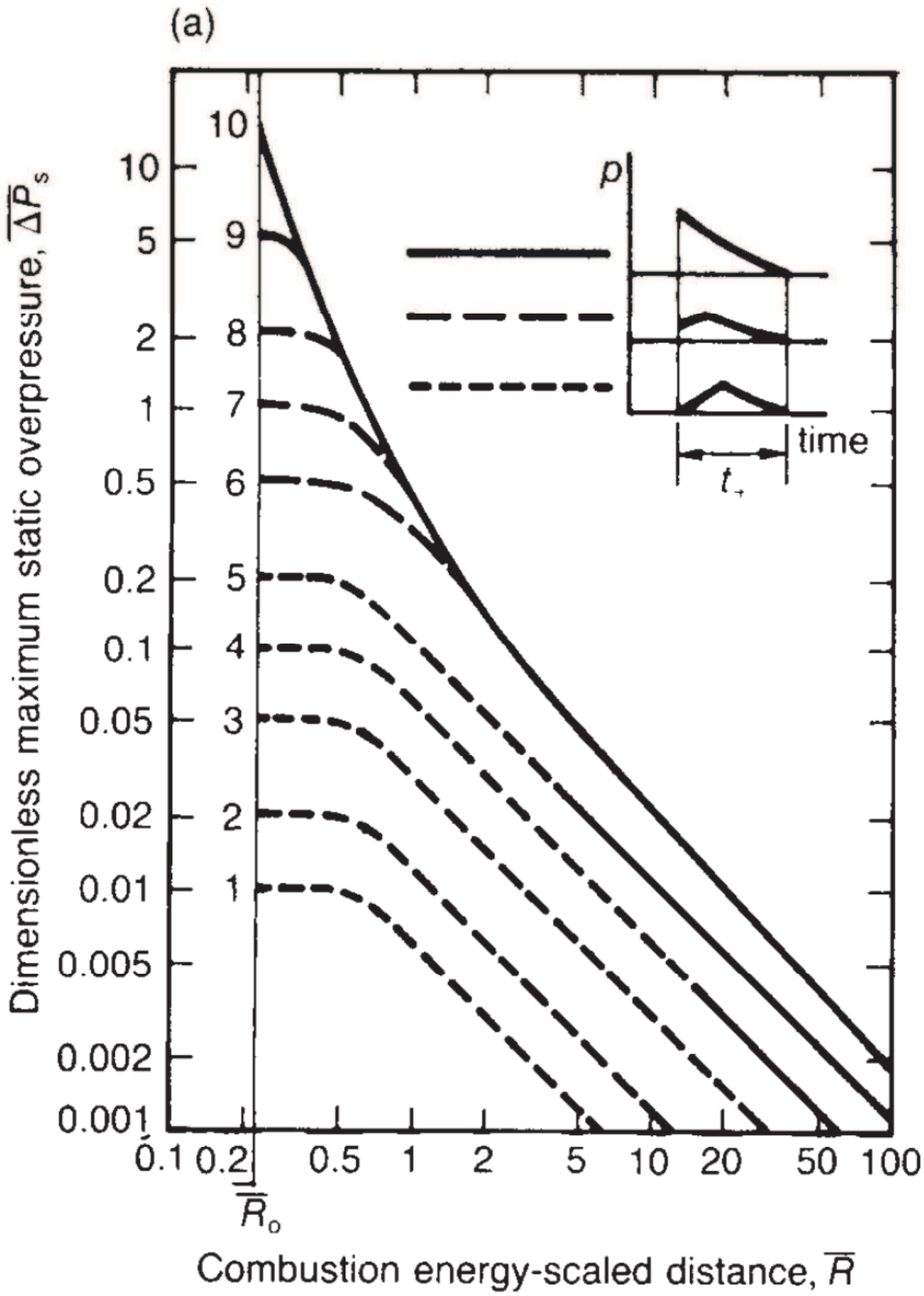

Figure 5.5 - Static Overpressure vs Scaled Distance

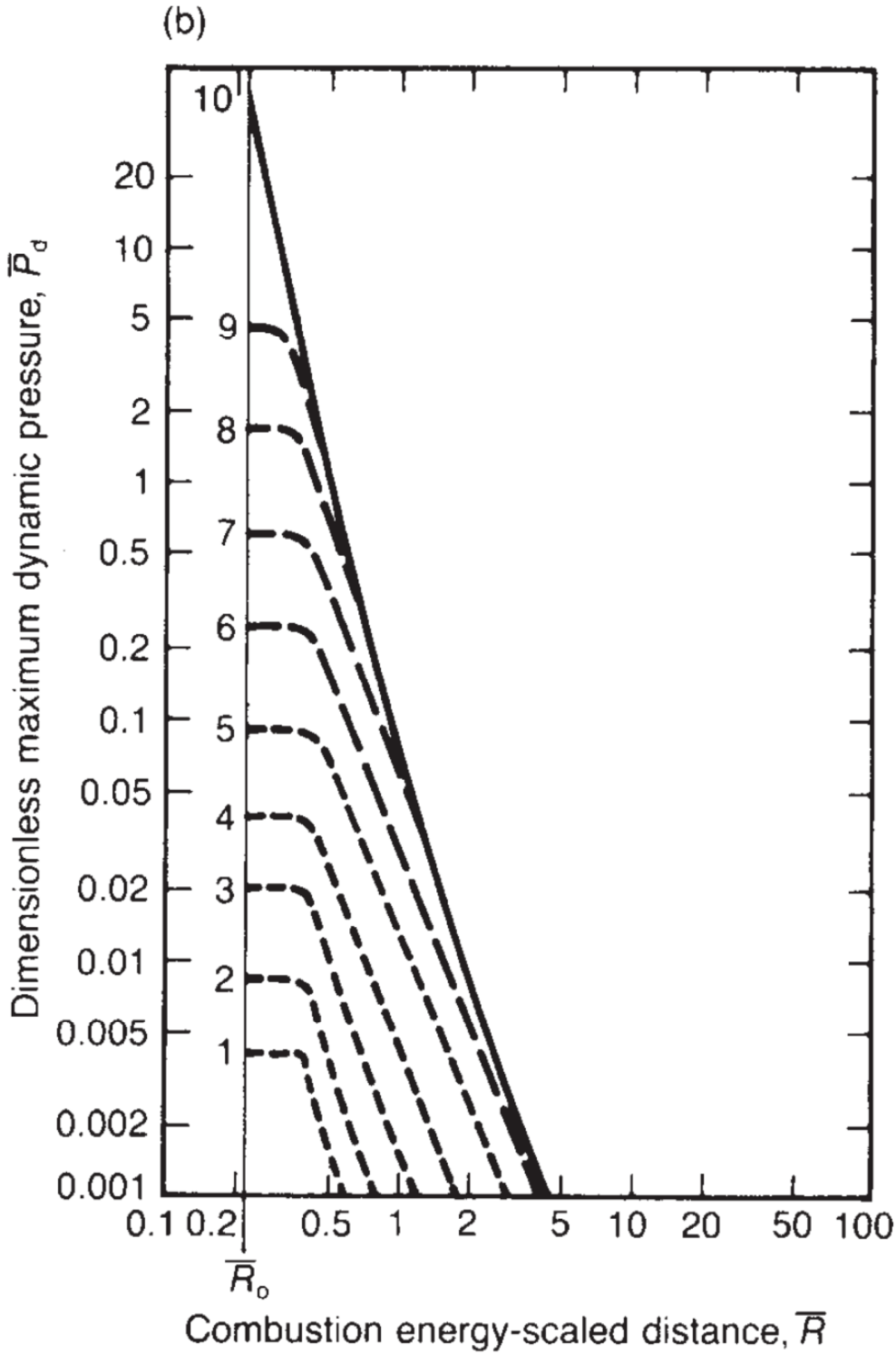

Figure 5.6 - Dynamic Pressure vs. Scaled Distance

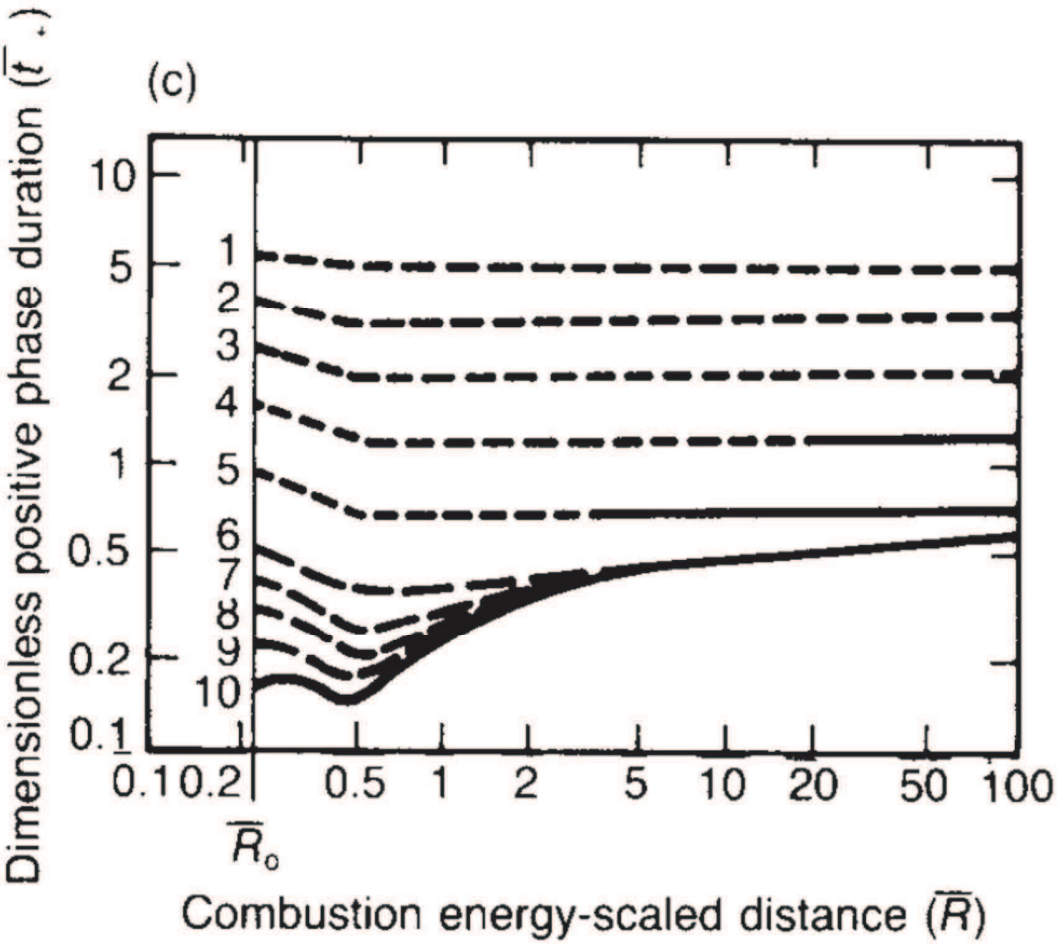

Figure 5.7 – Non-Dimensioned Duration of Positive Phase vs. Scaled Distance

A factor of 2 must be applied by the reflection of the explosion on the ground.

Expressed below looks the explosion energies calculated by equations [5.10] and [5.11] respectively.

It will be applied equation [5.10] for calculate the explosion energy.

Figures 5.5, 5.6, and 5.7 provide the overpressure caused by the explosion, the dynamic pressure of the particles moved by the shock wave and the duration of the pressure pulse as scaled.

Depending on the burst pressure obtained for each Model from I to X the curve that best represents each model was established.

Based on this information Table 5.8 was constructed.

Column 1: Model Identification.

Column No. 2: Distance between a person hypothetically standing on the tank and the center of the explosion.

Column No. 3: Burst energy, calculated according to equation [5.2].

Column No. 4: Incident shock wave pressure.

Column No. 5: Identification of the corresponding curve in Figure

Column No. 6: Dynamic pressure as the corresponding curve from Figure

Column No. 7: Time scaling according to equation, selected from the corresponding curve in Figure.

Column 8: Time calculated from the scaled time of Column No. 7 and Equation.

Column No. 10: Total Impulse calculated according to the equation.

Thus was obtained for each Model from I to X, the values of pressure and impulse that will determine the effects on a person who hypothetically had been standing on the tank 1, 2, 3 meters respectively from the origin point of the explosion, that is, at the center of the surface of tank rupture.

5.3.3 Limitations of Existing Model

Considering the possibility that the tank has been broken by an overpressure, the burst pressure can be assumed that for each model have been those corresponding to the maximum pressure achieved.

In **Table 5.9** - *Maximum Pressures per Model*, maximum pressure values corresponding to each model are listed.

It is important to see that if the accident would have developed as a tank burst at the maximum pressure reached by each Model, as will be discussed in the following chapters, the possibility that a person standing on the damaged tank, as a consequence of the explosion it would have had more than a few meters of displacement is zero.

Moreover, later this thesis will show that a person who had lit a flame on the loading port of the tank, if it had developed the accident as an explosion of the tank to the maximum pressure reached for each model, the person would not had moved beyond a few meters.

Asphalt diluted RC2 liquid spill found nearby tank on the opposite tank end of the outbreak would not have occurred, because the pressure would had been relieved by the opening made by the explosion, and the flow of the gases could have been driven the liquid in the opposite direction.

Nor would have an explanation for splashing in the tank truck.

5.3.4 Substitute Model

All these elements lead to discard the assumption that the tank may be broken by a pressure rise of the characteristics already explained.

At this point, it is necessary to introduce a new assumption that surrogate the above assumption and may be able to respond to the facts that contradict the above assumption.

The new assumption states that in a given moment of the process of inflammation inside the tank, the not inflamed mix of heavy naphtha vapor and air would have entered in self-ignition conditions.

If observed **Table 5.10 -** *Temperatures of Flammable Mixture in the Self-ignition Vicinity*, it may be noted that it would set the conditions for spontaneous ignition in non-inflamed heavy naphtha vapor and air mixture contained in the ends of the tank.

A first question is that if the inflammation inside the tank is being developed in symmetrical way, why self-ignition was generated only at one end of the flammable mixture no inflamed yet.

The answer could be supported on two concepts, first the turbulence factor; it could have been somewhat higher in the side with the vent because the flames could have gone through it at some speed increasing turbulence and thus the speed of propagation of the flame front.

Consistent with the above, if it is observed **Table 5.10 -** *Flammable Mixture Temperature in the Vicinity of the Self-ignition* may be noted that the models with higher turbulence factor are arriving earlier in time to the conditions of self-ignition.

The inflammation started in the loading port should have been closer to the end that exploded and not in the center of the loading port. This observation comes from the experience on the measurement of explosive atmospheres, in which different positions were tested for a person trying to illuminate the inside of the tank with a flame.

As a result of the above-mentioned aspects, self-ignition occurred before at one end.

Development time of self-ignition, causing a detonation is less than 0,01 s, so it is understood that a slight difference in the turbulence factor, and the initial position of the flame would have been sufficient for detonation originated at one end before the other.

Moreover, the gas flow through the loading port detonation once produced and before the tank opening have significantly increased, whereby the pressure inside the tank would have decreased, pulling with it the possibility self-ignition and subsequent detonation at the other end of the tank.

After detonation, the tank is immediately ruptured, even in times of the order of 0,01 s.

It will then analyze what would have happened if there had been self-ignition and detonation thus at the end of the tank that eventually burst.

It will take the same treatment as the previous case, that is:

- Method of Baker et al.
- The Multienergy method

Repeated below are the theoretical concepts already explained for these methods in case the reader goes directly to this point without reading the reference already made to the method above, along with the computation of the scene of tank burst detonation.

5.3.5.1 Baker et al. Model and Basic Method

A method for estimating the parameters of the outbreak of a pressurized tank containing gas is described below.

The method was developed by W.E. Baker et al. (1975), and refers to a spherical tank containing a massless ideal gas.

5.3.5.1.1 Energy Explosion

Explosion energy is calculated by the equation [5.1]:

$$E_{ex} = \frac{2(p_1 - p_0)V}{(\gamma_u - 1)}$$

Where

2 = coefficient for ground reflection of the pressure wave

p_1 = burst pressure

p_0 = atmospheric pressure

V = volume of the self-ignition mixture

γ_u = polytrophic index of air and heavy naphtha vapors mixture not inflamed yet

Therefore the equation [5.1] leads to [5.2]:

$$E_{ex} = \frac{2(p_1 - 101300)V}{(1{,}36 - 1)}$$

In **Table 5.12 -** *Explosion Energy Values for Explosion Models Development*, different values of the explosion energy are set E_{ex} calculated according to equation [5-2].

In Table 5.12 - *Explosion Energy Values for Explosion Development Models Compared to the Energy Released by in Tank Burned Mixture* potential values of chemical energy released E_u as a result of inflammation of the mass m_u in the tank, as a result of the self-ignition.

For the calculation of E_u is considered that for every 1 kg of heavy naphtha inflamed are released 40. 10^6 Joules.

In calculating the total energy of the explosion will be considered:

- The contribution of sudden self-ignition that have caused the outbreak.
- The contribution of the rest of the gases pressurized inside the tank at the time of the blast.

In the first case the equation applied is [5-2] combined with the ideal gas equation.

$$pV = m_u R_g T \qquad [5.13]$$

Where,

p = maximum pressure reached by the detonation

V = volume occupied by uninflamed mixture which self-inflamed at detonation

m_u = uninflamed mass which self-inflamed at detonation

$R_g = 240 \ \frac{J}{kg\ K}$

$T = 2783\ K$

In the second case, the contribution of other gases present in the tank at the time of detonation, is calculated using the equation[5.1].

$$E_{ex} = \frac{2(p_1 _ 101300)V}{(1{,}36 - 1)}$$

Where,

p_1= pressure inside the tank at the previous stage before detonation

V = volume occupied by the gases not self-inflamed at the previous stage before detonation

Now, the first case is explained.

To do this it have extracted the values for V, m_u, from **Table 4.6 -** *Model No. I. Numerical Values of Characteristically Model Variables Properties for Each Time Interval* to **Table 4.15 -** *Model No. X. Numerical Values of Characteristically Model Variables Properties for Each Time Interval* corresponding to the moment at which it would have arrived at the self-ignition temperature listed in **Table 5.10 -** *Temperature of Flammable Mixture in the Self-ignition Vicinity*.

From these values it could be possible build the **Table 5.11 -** *Self-ignited Mass, Self-Ignited Volume, Temperature at Self-ignition Start*. Applying equation [5.1] to the values given in the Table, it have built the **Table 5-12.** *Explosion Energy Values for Explosion Development Models*

Previously it had been determined that there was a 1 kg heavy naphtha in 16 kg of mixture of air and heavy naphtha vapors.

Therefore, for every 1 kg of mass burned m_b of vapor and air mixture is released heavy naphtha 2,5 . 10^6 J

In **Table 5.12 -** *Energy Explosion Values for Explosion Development Models Compared with Energy Released by Flammable Mixture Burned in Tank*, establishing energy values that could potentially release the mixture of air and heavy naphtha vapors ignited inside the tank.

Because this was found to be the power source, in column No. 5 of the Table from Model II to X is observed that is converting more than 100% of the energy supplied by the flammable mixture.

This can be attributed to the ignited fuel and then removed through the loading port of the tank.

It will then proceed to develop the second case.

To do this it have extracted the values for V, p from **Table 4.6 -** *Model No. I. Numerical Values of Characteristically Model Variables Properties for Each Time Interval* to **Table 4.15 -** *Model No. X. Numerical Values of Characteristically Model Variables Properties for Each Time Interval* corresponding to the moment at which it would have arrived at the self-ignition temperature listed in **Table 5.10 -** *Temperature of Flammable Mixture in the Self-ignition Vicinity.*

From these values was build the **Table 5.13 -** *Pressure in the Tank, not Self-ignited Volume, Temperature at Self-ignition Start* . Applying equation [5.1] to the values given in the Table, was build the **Table 5.14 -** *Explosion Energy Values for Explosion Development Models*

To calculate the total energy of the explosion the values obtained in the two cases are added, collecting the results in **Table 5.15 -** *Total Explosion Energy*.

Depending on the values of total explosion energy obtained it will proceed to calculate the performance of the explosion on the method of Baker et. al.

5.3.5.1.2 Pressure and Impulse

It will be assumed that the center of the burst corresponds to the center of the opening in the tank caused by the burst.

The radius is determined by the following equation [5.3]:

$$R = r\left(\frac{p_0}{E_{ex}}\right)^{\frac{1}{3}}$$

where

R = scaled distance

r = distance of the person to the center of the explosion [m]

p_0 = atmospheric pressure [Pa]

E_{ex} = explosion energy [J]

If a person is supposed to be standing on the tank at a distance r from the center of the explosion, a scaled distance R is given by the equation [5.3] for each value of r.

A person standing on the tank at a distance r will receive a maximum pressure pulse where crossed by the pressure wave.

For each value of R found it can be calculated the scaled overpressure, which by means of equation [5.4] can be converted to the value of the pressure pulse received by the said person.

$$P_s = \frac{p_s}{p_0} - 1$$

Where

P_s = lateral pressure scaled

p_s = lateral pressure received by a person standing on the tank

Scaled overpressure is obtained from **Figure 5.1-** *Overpressure Burst of Tank Burst* initially using the "high explosive" curve.

As it will see below, a correction for the case $R \leq 2$ was performed as indicated by the theory, resulting that the range that fits to the situation under study will go from the curve No. 2 to No. 5, from left to right.

This is interpreted as an average explosion, because the curve "high explosive" is represented by the curve to the right, that is, the curve No. 11.

The impulse on the body of a person standing on the tank can be obtained from equation [5.5].

$$I = \frac{i_s a_0}{p_0^{\frac{2}{3}} E_{ex}^{\frac{1}{3}}}$$

Where

I = scaled impulse

i_s = lateral impulse [Pa. s]

a_0 = velocity of sound in the gas

The scaled impulse can be obtained from **Figure 5.2 -** *Scaled Impulse for Pentonite* and **Figure 5.3 -** *Scaled Impulse for Tank Burst*.

Table 5-4. *Lateral Pressure and Lateral Impulse for 1, 2, 3 meters from the Center of the Explosion*, has expressed the result of calculating the lateral pressure p_s and the lateral impulse i_s for a person standing on the tank at three different distances r of 1, 2, 3 meters.

Equations [5.4] to [5.5] should be assigned the following correction when $R \leq 2$ as recorded in this case.

Firstly, an effective radius r_0 is determined for the equivalent hemisphere formed by the initial gas volume, equation [5.5] :

$$r_0 = \left(\frac{3V_1}{2\pi}\right)^{\frac{3}{4}}$$

$r_0 = 1{,}9\ m$ for a volume of 5,0 m³

$r_0 = 2{,}6\ m$ for a volume of 7,5 m³

$r_0 = 3{,}2\ m$ for a volume of 10,0 m³

As a function of r_0 can be calculated R_0 by the equation [5.6].

$$R_0 = r_0 \left(\frac{p_0}{E_x}\right)^{\frac{1}{3}}$$

In the **Figure 5.4 -** *Scaled Peak Overpressure at Short Distance for a Tank Burst $\gamma = 1{,}4$*, it can be set a value P_{s0} from the relationship between the tank burst pressure p_1 and the atmospheric pressure p_0, and the ratio between the sound speed under ambient conditions a_0 and the speed of sound in gas conditions a_1.

The speed of sound $a_0 = 340\ {}^{m}/_{s}$.

The speed of sound a_1 can be calculated by the equation [5.7]:

$$a_1 = \left(\frac{\gamma p_1}{\rho_1}\right)^{\frac{1}{2}}$$

In **Figure 5.5 -** *Sound Speed and Ratio* $\left({}^{a_1}/_{a_0}\right)^2$ *at Tank Burst Conditions*, the calculation result of the relationship $\left({}^{a_1}/_{a_0}\right)^2$ for Models I to X is listed.

From this, it was built Table 5-16. *Speed of Sound and Ratio* $\left({}^{a_1}/_{a_0}\right)^2$ *at Tank Burst Conditions*

With this it could be possible to obtain pressure values and reference distance for each model, from which it was possible to determine the curve of Figure 5-1 for each model. The results were collected in **Table 5-17**. *Figure 5-1 Curve Associated Models I to X.*

As indicated above, a correction was made for the case **R < 2** as indicated by the theory, which looks at **Table 5-15.** *Figure 5-1 Curve Associated Models I to X.*

The range that fits the situation under study will be curve No. 7 to No. 8, from left to right in **Figure 5-1** .

This is interpreted as a relatively severe explosion, because the curve "high explosive" is represented by the curve to the right, that is, the curve No. 11.

5.3.5.2 Multi-Energy Method

Through a lot of experiments, it has been established explosions curves shown in Figures 5.5 to 5.7. Known as "blast TNO curves" for explosions

The TNO Multi-Energy method is based on the concept of multi-energy, which is the presentation of a deflagration of gas so that the development of the blast and overpressure obtained only under certain boundary conditions, where only flammable mixture is partially confined or obstructed.

The Multi-Energy method does not strictly apply to the case of the explosion of a tank, but it does in the case of a cloud of explosive mixture contained, which is approximately the case under study considering:

- The energy consumed by tank rupture is negligible

- That confinement by the tank is too high

Based on the concept of Multi-Energy, the explosion of gas clouds have been modeled for a number of models of hemispheric loads. The load of each model is characterized by a load size and load stress.

Load size is related to the heat of combustion present in the source, while the loading stress is related to the explosion pressure.

Based on these characteristics, we calculated the scaled blast parameters (peak overpressure, positive phase duration) as a function of the scaled distance, as shows Figures 5.5 to 7, as a number between 1 and 10 representing 10 categories from "negligible" to "detonation".

This method is applied here to obtain a set of reference values to compare two other methods already in use. Therefore values of Multi-Energy method should not be used to determine consequences and effects of the explosion.

Again it is assumed that the center of the burst corresponds to the center of the opening in the tank caused by the burst.

The radius is determined by the equation [5.3] already viewed:

$$R = r\left(\frac{p_0}{E_{ex}}\right)^{\frac{1}{3}}$$

where

R = scaled distance

r = distance of the person to the center of the explosion [m]

p_0 = atmospheric pressure [Pa]

E_{ex} = explosion energy [J]

It was already indicated that in tanks burst is considered that a shock wave is generated, not a pressure wave; therefore it will be considered as the case object of study approaches the curve No. 9.

For distances r = 1, 2, 3 meters from the center of the explosion should consider the relations established.

For reference, according to TNO can be estimate the explosion energy, according to equation [5.10] as:

$$E_{ex} = 3{,}5.\,10^6 V$$

Where V is the volume of flammable gas, which in this case is interpreted as the entire self-ignited volume considered in preconditions to the self-ignition and corrected to atmospheric pressure according to the equation [5.11].

$$V_2 = V_1 \left(\frac{p_1}{p_2}\right)^{\frac{1}{\gamma}}$$

To this is added the already inflamed volume in the previous instant to self-ignition also corrected by the equation.

This last point is cited as critical to the equation [5.10] in the sense that estimates an amount greater than the actual energy.

In this case we will consider the energy corresponding to the already inflamed by the equation [5.9] in addition to the amount contributed by the self-detonation, which is estimated from the equation [5.10].

While some authors suggest that this equation tends to over dimensional energy of the explosion (a fact that was discussed earlier in this thesis), it is considered that the mass of gas is pressurized when self-ignition, thus equation [5.10] shows some degree of moderation, and therefore fear to an overestimation of the energy of the explosion is contained.

Therefore apply equation [5.10] to calculate the energy of the explosion, with the corrections that were said above.

Considering the volume at the time self-ignition occurs, and energy gave by the inflamed mixture until that time, it was built the **Table 5-18.** *Burst Energy of Inflamed Gases .*

Figures 5-5, 5-6, and 5-7 provide the overpressure caused by the explosion, the dynamic pressure of the particles flow by the shock wave, and the duration of the pressure pulse as scaled.

Depending on the burst pressure obtained for each model I to X the curve that best represents each model was established.

Based on the information Table 5-21 was constructed.

Column 1: Model Identification.

Column No. 2: Distance between a person hypothetically standing on the tank and the center of the explosion.

Column No. 3: Burst energy, calculated according to equation [5.2].

Column No. 4: Incident shock wave pressure.

Column No. 5: Identification of the corresponding curve in Figure

Column No. 6: Dynamic pressure as the corresponding curve from Figure

Column No. 7: Time scaling according to equation, selected from the corresponding curve in Figure.

Column 8: Time calculated from the scaled time of Column No. 7 and Equation.

Column No. 10: Total Impulse calculated according to the equation.

Thus was obtained for each Model from I to X, the values of pressure and impulse that will determine the effects on a person who hypothetically had been standing on the tank 1, 2, 3 meters respectively from the origin point of the explosion, that is, at the center of the surface of tank rupture.

Chapter 6

Consequences of Explosion Effects on Persons in Accident

6.1 Effects of Burst

The human body can adapt to significant changes in pressure if it is given enough time to compensate for pressure changes in the organs in which air is present.

If this change occurs suddenly, the difference in pressure can damage organs. The most vital organ containing air are the lungs.

In the technical literature it pays more attention to lung damage since lung damage can cause death.

A less vital organ, however more sensitive to pressure changes, it is the ear.

6.1.1 Lung Injury

When a pressure difference between the outside and the inside of the lungs is established, with greater pressure outside, the chest is pressed inward, which can lead to lung damage. [3]

Since this pressed inward process required time besides the value of overpressure, the duration of this situation is important.

Figure 6.1 - *Explosion Damage. Survival Curves for a 70 kg Person Located at Free Flow with Body Axis Perpendicular to Pressure Wave Direction* describes the probability of survival by pulmonary damage depending on the incident overpressure and duration of the pressure pulse.

The curves in **Figure 6.1** applied to a 70 kg person exposed to an atmospheric pressure of 100 kPa.

The correct chart choose is determined by establishing the position of the person relative to the direction of propagation of the pressure wave.

This is necessary, because the pressure exerted by the pressure wave on the person as a result of reflection of it on the person's body and the flow surrounding to the person may be greater than the maximum overpressure incident in pressure wave.

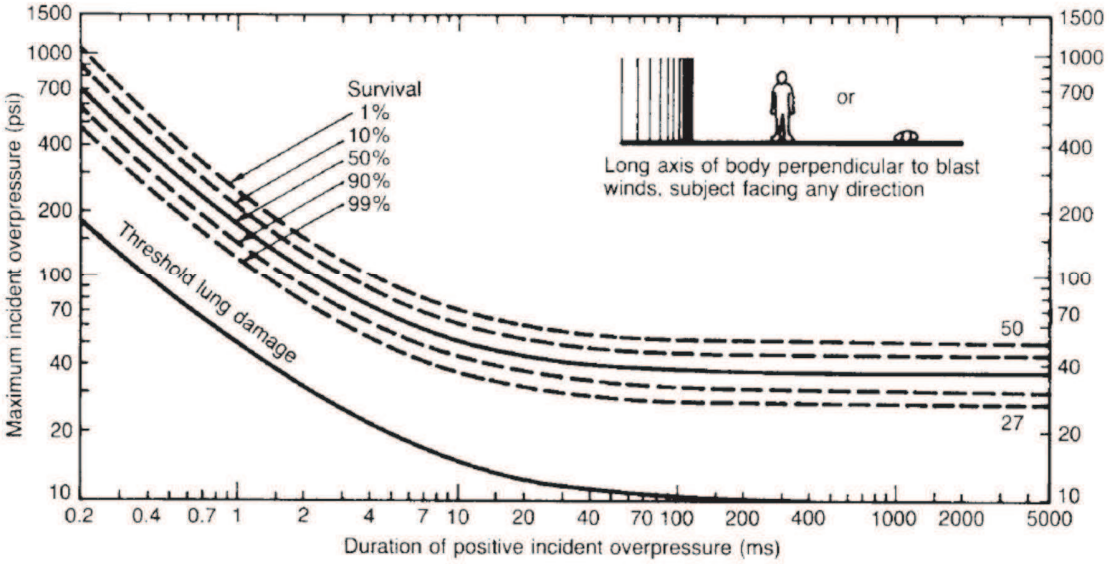

Figure 6.1 - Explosion Damage. Survival Curves for a 70 kg Person at Free Flow Situation with Body Axis Perpendicular to Pressure Wave Direction. (Bowen IG, Fletcher and Richmond, 1968).

The situation of the person in front of the pressure wave is illustrated in **Figure 6.2 -** *Flow Around a Person Standing at Free Flow Situation with Corporal Axis Perpendicular to the Direction of Pressure Wave.*

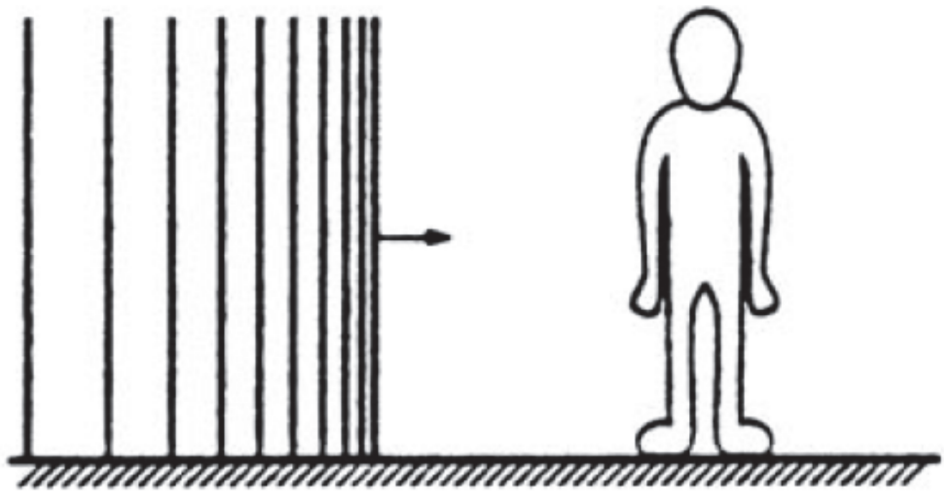

Figure 6.2 - Flow Around a Person Standing at Free Flow Situation with Corporal Axis Perpendicular to the Direction of Pressure Wave

In the case illustrated in **Figure 6.2** - *Flow Around a Person Standing at Free Flow Situation with Corporal Axis Perpendicular to the Direction of Pressure Wave* the flow exerts an additional force on the person, that is, the dynamic pressure q.

The total pressure in this case is:

$$p = p_s + q \qquad [6.1]$$

The dynamic pressure can be determined by the equation:

$$q = \frac{5p_s^2}{2p_s + 14.10^5} \qquad [6.2]$$

p_s, q are expressed Pascals.

In **Figure 6.1** - *Explosion Damage. Survival Curves for a 70 kg Person at Free Flow Situation with Body Axis Perpendicular to Pressure Wave Direction* this calculation was made and entered with the value of incident overpressure p_s.

The result of the load of a pressure wave can also be expressed as a function of impulse pressure.

Similar to Figure 6.1, **Figure 6.3** - *Explosions Damage Effects: Lung Injury. Diagram Pressure – Impulse of Survival Applicable to All Standard Postures and Different Body Weights* shows the relationship between overpressure, impulse and probability of survival for lung injury to a person under the pressure wave for some time but evaluated through scale impulse.

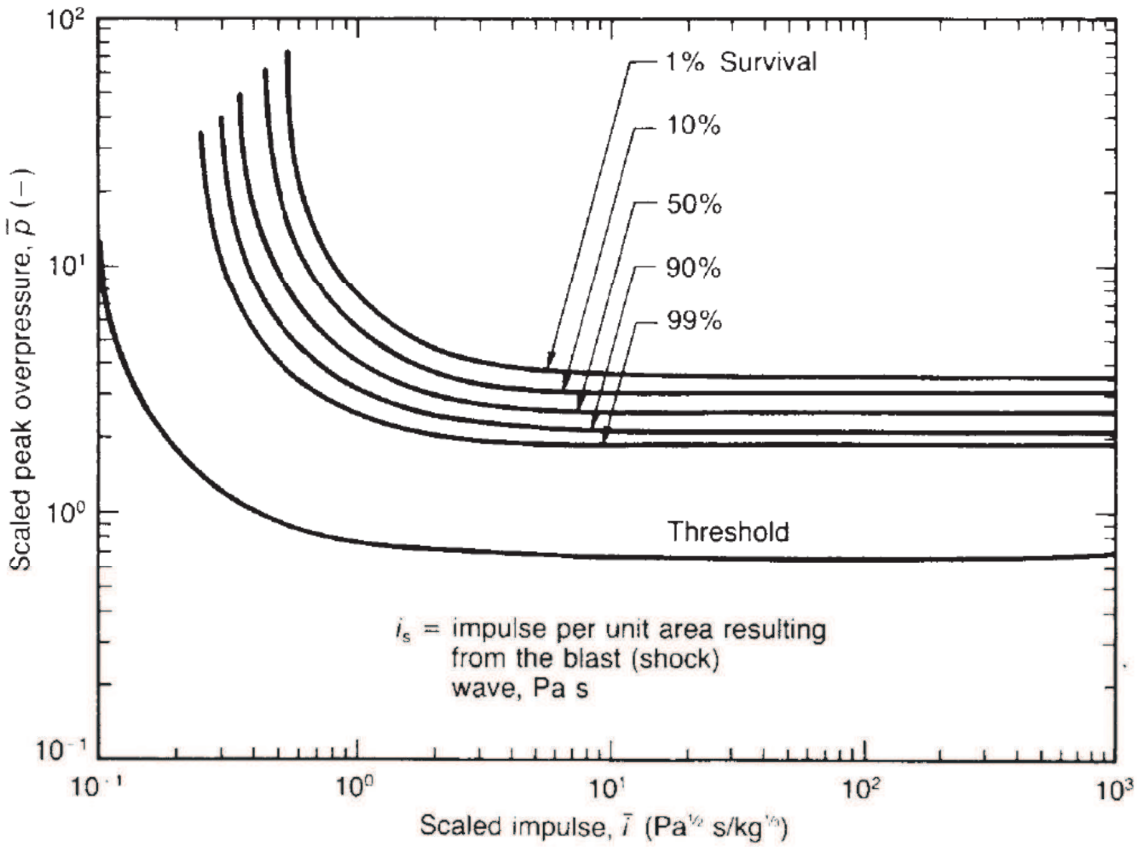

Figure 6.3 - Explosions Damage Effects: Lung Injury. Diagram Pressure – Impulse of Survival Applicable to All Standard Postures and Different Body Weights (W.E. Baker et al 1983.).

Scaled pressure P is calculated by the equation:

$$P = \frac{p}{p_0} \qquad [6.3]$$

Where

p

p_0 = atmospheric pressure

The scaled impulse I is calculated by the equation:

$$I = \frac{i}{p_0^{1/2} m^{1/3}} \qquad [6.4]$$

Where,

m = body mass in kg.

In the **Table 6.1** - *Percentage Survival and Pulmonary Damage of a Person Standing on the Tank at Burst Time by Method of Baker et al.* and **Table 6.2** - *Pulmonary Damage and Survival Percentage of a Person Standing on the Tank Damage at Burst Time by Multi-Energy Method* indicates whether lung damage had occurred and what would have been the percentage of survival in the event that a person had been standing on the tank at the time of burst in different locations established (1, 2, 3 meters from the burst center).

Greenbook indicates that the damage could be reduced if it were a pressure wave, due to the Figure 6-3 is developed to the case of a shock wave.

The tank bursts are treated by the literature as generating shock waves, so it is assumed that as indicated in **Figure 6.3** - *Explosions Damage Effects: Lung Injury. Diagram Pressure – Impulse of Survival Applicable to All Standard Postures and Different Body Weights* is consistent with what happened in the accident under study.

6.1.2 Ear Damage

Figure 6.4 - *Eardrums Rupture Probability for Overpressure*, sets the percentage of probability of ruptured eardrums as a function of the pressure on them.

It should be considered here as the exerted pressure the reflected pressure as set in the Greenbook.

The reflected pressure can be calculated by the equation:

$$p_r = \frac{8p_s^2 + 14.10^5 p_s}{p_s + 7.10^5} \qquad [6.5]$$

In the **Table 6.3** - *Eardrum Rupture Probability by Overpressure for Models I to X According to the Baker et al. Method* and **Table 6.4** - *Eardrum Rupture Probability for Overpressure for Models I to X*, it look the results of calculating the probability of eardrums rupture as **Figure 6-4** *Eardrums Rupture Probability for Overpressure* for the reflected pressure p_r from incident overpressure p_s.

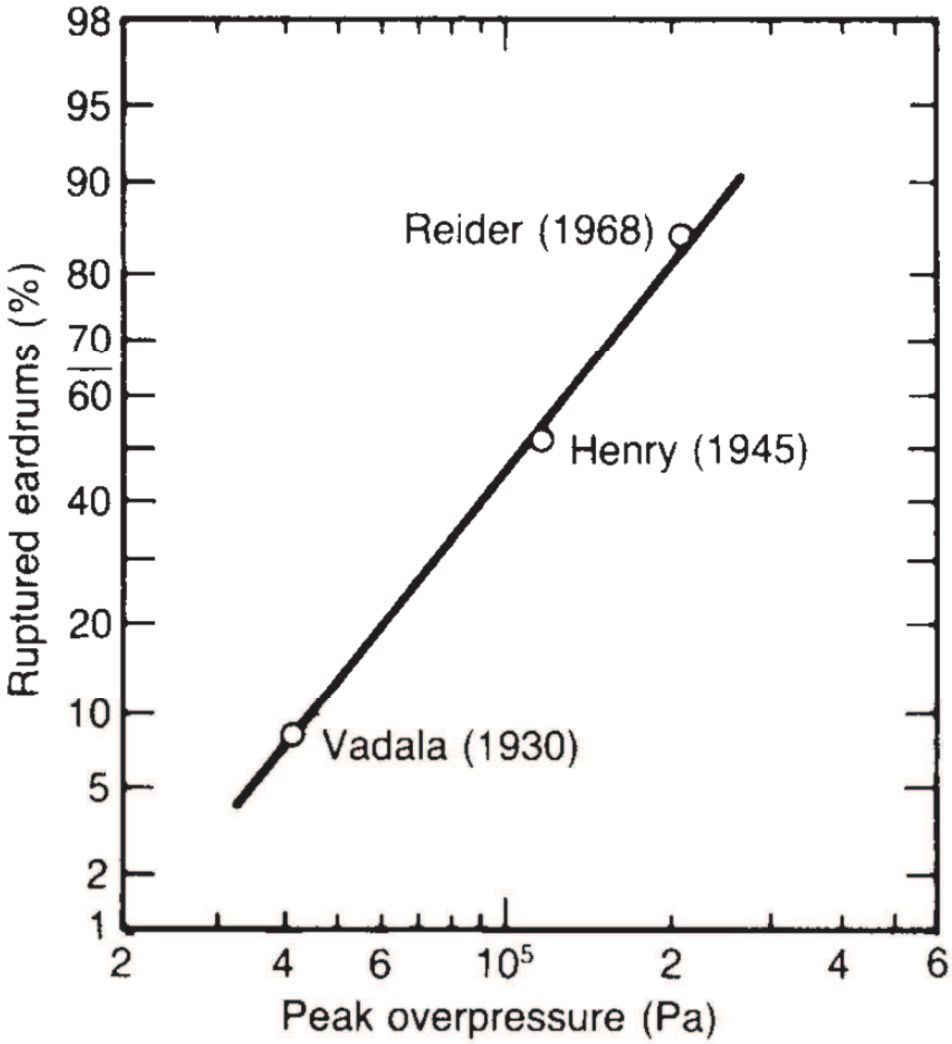

Figure 6.4 - Eardrum Rupture Probability for Overpressure

6.2 Effects of Body Displacement

Air particles behind the shock wave have a specific speed and the direction of the burst. Consequently this called "wind of the explosion," can take a person and move it a particular distance. [3]

Assume for this purpose that the person is in the position of **Figure 6.2 -** *Flow Around a Person Standing at Free Flow Situation with Corporal Axis Perpendicular to the Direction of Pressure Wave*

Displacement creates risks of collision with solid objects with probability of death by impact to the skull or body in general.

The dynamic stress or pressure q exerted by the wind of the explosion on a stationary object or person is:

$$q = \frac{1}{2} C_D A \rho_1 u^2 \qquad [6.6]$$

Where,

C_D = Drag Coefficient

A = perpendicular surface to the propagation of the shock wave

ρ_1 = air density behind the shockwave

u = velocity of particles in the wave

$$mv' = \frac{1}{2} C_D A \rho_1 (u - v_m)^2 \qquad [6.7]$$

Where,

v' = acceleration of the person's body

m = mass of the person's body

v_m = velocity of the person's body

The particle velocity u and density ρ_1 are dependent on the atmospheric pressure p_0 and the density of air ρ_0 in front the shock wave according to the following equation:

$$\rho_1 = \frac{7p_0 + 6p_s(t)}{7p_0 + p_s(t)} p_0 \qquad [6.8]$$

$$u(t) = p_s(t) \left(\frac{5}{\rho_0 (7p_0 + 6p_s(t))} \right)^{\frac{1}{2}} \qquad [6.9]$$

The maximum body displacement can be determined by solving the differential equation [6.7], substituting in this $\rho_1(t)$ and $u(t)$ by equations [6.8] and [6.9].

$$p_s(t) = p_s\left(1 - \frac{t}{t_p}\right) \qquad [6.10]$$

$$i_s = \int_0^{t_p} p_s(t)\, dt \qquad [6.11]$$

$$i_s = 2\frac{i_s}{p_s} \qquad [6.12]$$

To solve the differential equation [6.7] the following procedure was performed:

a) Split the range $[0, t_p]$ in 10 segments.
b) The average value of $p_s(t)$ for each segment was calculated.
c) The average value of $u(t)$ for each segment was calculated.
d) The average value of $\rho_1(t)$ for each segment or calculated.
e) Differential equation [6.7] was solved for each segment.
f) The $v(t_p)$ value of the speed with which the body was expelled from its location on the tank for each position studied (r = 1, 2, 3) and for each Model I to X was obtained.

The differential equation [6.7] now is:

$$v' = 2{,}5.\,10^{-3}\rho_1(u - v_m)^2 \qquad [6.13]$$

Where,

m = 75 kg

C_D = 1

A = 0.382

The solution of the equation [6.13] is:

$$v(t_{p_1}) = u_0 - \left(0{,}191\rho_{10}dt_p + \frac{1}{u_0}\right)^{-1} \qquad [6.14]$$

In general for all the range divided into 10 segments i.

$$v(t_{p_{i+1}}) = u_i - \left(0{,}191\rho_{1i}dt_p + \frac{1}{u_i - v(t_{p_i})}\right)^{-1} \qquad [6.15]$$

Where,

$v(t_{p_{i+1}})$ = velocity of the body at the beginning of interval $i+1$

$v(t_{p_i})$ = velocity of the body at the beginning of interval i

ρ_{1i} = average air density in the range $[i, i+1]$

u_i = average speed articulated in the range $[i, i+1]$

$dt_p = \frac{t_p}{10}$

Figure 6.5 - *Landing Speed of Body Displacement Based on Lateral Pressure and Impulse for a 70 kg Weight Person* assumes a 70 kg weight, a body density of 1000 kg / m^3 and a ratio between length and width of 7.

The frontal area which impacts the person (assuming it as a cylinder) is 0,382 m^2.

Will be assumed throughout the entire body movement that will not change this frontal area.

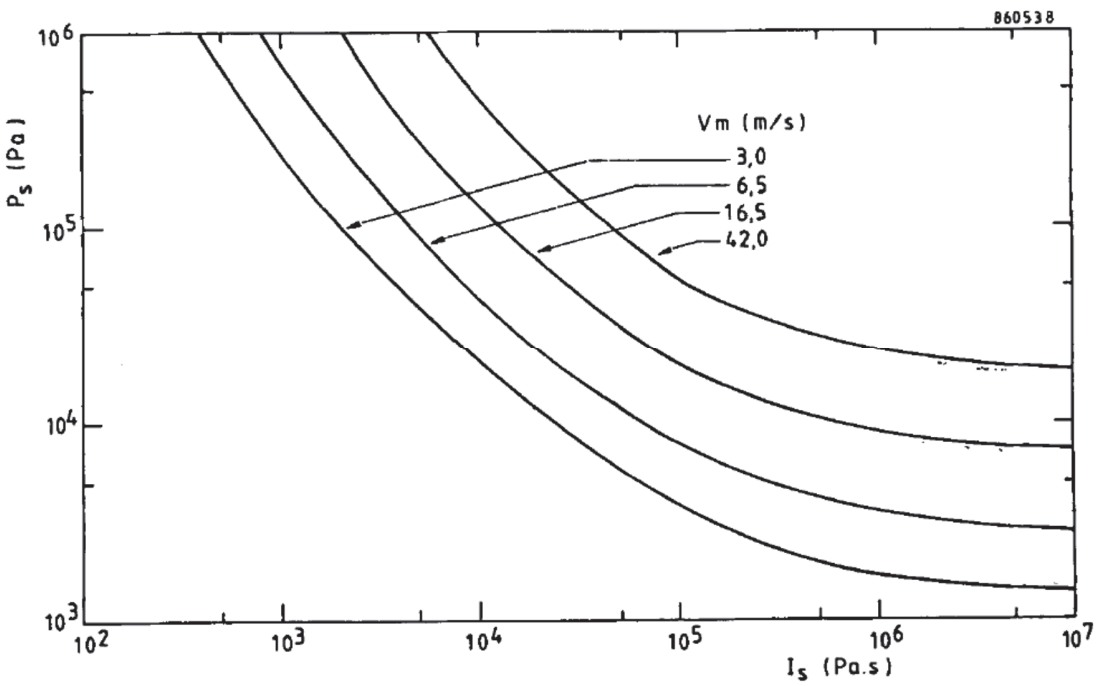

Figure 6-5. Landing Speed of Body Displacement Based on Lateral Pressure and Impulse for a 70 kg Weight Person

Assuming that for the range of speeds obtained (up to 6 m/s) the speed loss by air friction is negligible, we can determine that the landing speed values are similar to the values of the speed at the end of interval t_p.

It can be seen by comparing the values established by Figure 6.5, which are listed in column 7 of **Table 6.15** - *Takeoff Speed for a Person Standing on the Tank at 1, 2, 3 mts of Explosion Center by Baker et. al. Method vs. Arrival Speed by Figure 6.5* and **Table 6.16** - *Takeoff Speed for a Person Standing on the Tank at 1, 2, 3 meters from the Explosion Center by Multienergy Method vs. Arrival Speed by Figure 6.5*, are similar to those obtained by calculation on the **Table 6.9** - *Corporal Speed of a Person Standing on the Tank During Shockwave Action for Each Model I to X According to Baker et al. Method* and **Table 6.14** - *Corporal Speed of a Person Standing on the Tank During Shockwave Action for Each Model I to X According to Multi-Energy Method*, which are listed in column 6 of **Table 6.15** - *Takeoff Speed for a Person Standing on the Tank at 1, 2, 3 mts of Explosion Center by Baker et. al. Method vs. Arrival Speed by Figure 6.5* and **Table 6.16** - *Takeoff Speed for a Person Standing on the Tank at 1, 2, 3 meters from the Explosion Center by Multienergy Method vs. Arrival Speed by Figure 6.5* considering takeoff speeds and arrival of the body are similar.

6. 3 Consequences of Explosion Effects on Persons at the Accident in Case of Tank Burst by Detonation

6. 3.1 Burst Effects in Case of Tank Burst by Detonation

Repeated are below the theoretical concepts already said for the methodologies to calculate blast effects on people in the accident, just in case the reader goes directly to this point without reading the reference already made above in paragraphs 6.1 and 6.2, along with the correspondent calculation in a tank burst by detonation scenario.

The human body can adapt to significant changes in pressure if it is given enough time for it, in order to compensate for pressure changes in the organs containing air.

If this change occurs suddenly, the difference in pressure can damage organs.

The most vital organ containing air are the lungs.

In the technical literature pays more attention to lung damage because lung damage can cause death.

A less vital organ, however not sensitive to pressure changes, it is the ear.

6. 3. 1.1 Lung Injury

When a pressure difference between the outside and the inside of the lungs is established, with greater pressure outside the chest is pressed inward, which can lead to lung damage.

Since this process requires pressed inward time and the value of overpressure, the duration of this situation is important.

Figure 6.1 - *Explosion Damage. Survival curves for a 70 kg person at Location Free Flow Corporal Axis Perpendicular to the Direction of Pressure Wave*, describes the probability of survival for lung damage as a function of incident overpressure and duration of the pressure pulse.

The curves in **Figure 6.1 -** *Explosion Damage. Survival curves for a 70 kg person at Location Free Flow Corporal Axis Perpendicular to the Direction of Pressure Wave*, applied to a 70 kg person weighing about exposed to an atmospheric pressure of 100 kPa.

Choosing the correct chart is determined by establishing the position of the person relative to the direction of propagation of the pressure wave.

This is necessary, because the pressure exerted by the pressure wave of the person as a result of reflection of the same in the flow and surrounding person to person may be greater than the maximum pressure in the incident pressure wave.

The situation of the person in front of the pressure wave is illustrated in **Figure 6.2 -** *Flow Around a save Person at Location Free Flow Corporal Axis Perpendicular to the direction of wave pressure*.

In the case illustrated in **Figure 6.2 -** *Flow Around a save Person at Location Free Flow Corporal Axis Perpendicular to the direction of wave pressure* the flow exerts an additional force on the person, that is, the dynamic pressure q.

The total pressure in this case is according to equation [6.1]:

$$p = p_s + q$$

The dynamic pressure can be determined by the equation [6.2]:

$$q = \frac{5p_s^2}{2p_s + 14.10^5}$$

p_s, q are expressed Pascals.

In **Figure 6.1 -** *Explosion Damage. Survival Curves for a 70 kg Person at Free Flow Situation with Body Axis Perpendicular to Pressure Wave Direction* this calculation was made and entered with the value of incident overpressure p_s.

The result of the load of a pressure wave can also be expressed as a function of impulse pressure.

Similar to Figure 6.1, **Figure 6.3** - *Explosions Damage Effects: Lung Injury. Diagram Pressure – Impulse of Survival Applicable to All Standard Postures and Different Body Weights* shows the relationship between overpressure, impulse and probability of survival for lung injury to a person under the pressure wave for some time but evaluated through scale impulse.

Scaled pressure P is calculated by the equation [6.3]:

$$P = \frac{p}{p_0}$$

Where

p = pressure exerted on the body

p_0 = atmospheric pressure

The scaled impulse I is calculated by the equation:

$$I = \frac{i}{p_0^{1/2} m^{1/3}} \qquad [6.4]$$

Where,

m = body mass in kg.

Table 6.17 - *Lung Damage and Survival Percentage save of a Person Standing on Tank at Burst Moment by Baker et al. Method* and **6.18** - *Lung Damage and Survival Percentage save of a Person Standing on Tank at Burst Moment by Multi-Energy Method indicates whether lung damage had occurred and what would have been the percentage of survival in the case that a person has been standing on the tank at the time of explosion in the different set locations (1, 2, 3 m from the center of the outbreak).*

In Greenbook it is established that the damage could be reduced if it were a pressure wave due to the Figure 6-3 is developed to the case of a shock wave.

The tank bursts are treated by the literature as generating shock waves, so it is assumed that as indicated in **Figure 6.3 -** *Explosions Damage Effects: Lung Injury. Diagram Pressure – Impulse of Survival Applicable to All Standard Postures and Different Body Weights* is consistent with what happened in the accident under study.

6. 3. 1.2 Eardrum Rupture

The **Figure 6.4 -** *Eardrum Rupture Probability by Overpressure*, sets the percentage of probability of eardrums ruptured as a function of the pressure on them.

It should be considered here as the reflected pressure as set in the Greenbook.

The reflected pressure can be calculated by the equation [6.5]:

$$p_r = \frac{8p_s^2 + 14.10^5 p_s}{p_s + 7.10^5}$$

In the **Table 6.19 -** *Eardrum Rupture Probability by Overpressure for Models I to X According to Baker et al. Method* and **6.20 -** *Eardrum Rupture Probability by Overpressure for Models I to X by Multi-Energy Method*, look the results of calculating the probability of rupture eardrums according to **Figure 6-4** *Eardrums Rupture Probability for Overpressure* for the reflected pressure p_r from incident overpressure p_s.

6.3.2 Effects of Body Displacement

Air particles behind the shock wave have a specific speed and the same direction of the burst.

Consequently this called "wind of the explosion," can take a person and move it a particular distance.

Assume for this purpose that the person is in the position of **Figure 6.2 -** *Flow Around a Person Standing at Free Flow Situation with Corporal Axis Perpendicular to the Direction of Pressure Wave*

Displacement creates risks of collision with solid objects with probability of death by impact to the skull or body in general.

The dynamic stress or pressure q exerted by the wind of the explosion on a stationary object or person is:

$$q = \frac{1}{2} C_D A \rho_1 u^2 \qquad [6.6]$$

Where,

C_D = Drag Coefficient

A = perpendicular surface to the propagation of the shock wave

ρ_1 = air density behind the shockwave

u = velocity of particles in the wave

$$mv' = \frac{1}{2} C_d A \rho_1 (u - v_m)^2 \qquad [6.7]$$

Where,

v' = acceleration of the person's body

m = mass of the person's body

v_m = velocity of the person's body

The particle velocity u and density ρ_1 are dependent on the atmospheric pressure p_0 and the density of air ρ_0 in front the shock wave according to the following equation:

$$\rho_1 = \frac{7p_0 + 6p_s(t)}{7p_0 + p_s(t)} p_0 \qquad [6.8]$$

$$u(t) = p_s(t) \left(\frac{5}{\rho_0 (7p_0 + 6p_s(t))} \right)^{\frac{1}{2}} \qquad [6.9]$$

The maximum body displacement can be determined by solving the differential equation [6.7], substituting in this $\rho_1(t)$ and $u(t)$ by equations [6.8] and [6.9].

$$p_s(t) = p_s \left(1 - \frac{t}{t_p} \right) \qquad [6.10]$$

$$i_s = \int_0^{t_p} p_s(t)\, dt \qquad [6.11]$$

$$i_s = 2\frac{i_s}{p_s} \qquad [6.12]$$

To solve the differential equation [6.7] the following procedure was performed:

a) Split the range $[0, t_p]$ in 10 segments.
b) The average value of $p_s(t)$ for each segment was calculated.
c) The average value of $u(t)$ for each segment was calculated.
d) The average value of $\rho_1(t)$ for each segment or calculated.
e) Differential equation [6.7] was solved for each segment.
f) The $v(t_p)$ value of the speed with which the body was expelled from its location on the tank for each position studied (r = 1, 2, 3) and for each Model I to X was obtained.

The differential equation [6.7] now is:

$$v' = 2{,}5.\,10^{-3}\rho_1(u - v_m)^2 \qquad [6.13]$$

Where,

m = 75 kg

C_d = 1

A = 0.382

The solution of the equation [6.13] is:

$$v(t_{p_1}) = u_0 - \left(0{,}191\rho_{10}dt_p + \frac{1}{u_0}\right)^{-1} \qquad [6.14]$$

In general for all the range divided into 10 segments i.

$$v(t_{p_{i+1}}) = u_i - \left(0{,}191\rho_{1i}dt_p + \frac{1}{u_i - v(t_{p_i})}\right)^{-1} \qquad [6.15]$$

Where,

$v(t_{p_{i+1}})$ = velocity of the body at the beginning of interval $i+1$

$v(t_{p_i})$ = velocity of the body at the beginning of interval i

ρ_{1i} = average air density in the range $[i, i+1]$

u_i = average speed articulated in the range $[i, i+1]$

dt_p $= \frac{t_p}{10}$

Figure 6.5 - *Landing Speed of Body Displacement Based on Lateral Pressure and Impulse for a 70 kg Weight Person* assumes a 70 kg weight, a body density of 1000 kg / m^3 and a ratio between length and width of 7.

The frontal area which impacts the person (assuming it as a cylinder) is 0,382 m^2.

Will be assumed throughout the entire body movement that will not change this frontal area.

Assuming that for the range of speeds obtained (up to 6 m/s) the speed loss by air friction is negligible, it can be established that the landing speed values are similar to the values of the speed at the end of interval t_p.

It has made the following comparison between the values established by the **Figure 6.5 -** *Landing Speed of Body Displacement Based on Lateral Pressure and Impulse for a 70 kg Weight Person* and those obtained by calculation in **Table 6.25 -** *Corporal speed of a tank saves Person in Action During Shockwave for each model I to X according to the method of Baker et al*, and **Table 6.30 -** *Corporal speed of a tank saves Person in Action During Shockwave for each model I to X by Method of Multi-Energy*.

The values are listed in **Table 6.31** and **Table 6.32** respectively.

In cases where "Out of Range" is indicated, is because the method reach pressures up to 1.10^6 Pa.

Chapter 7

Displacement of a Body Standing on the Tank

It have been studied all the possible range of volumes of flammable mixture in the tank based on the accident records, considering all turbulence factors expected range.

Respect to the energy released during the explosion, it has been considered the method of Baker et. al. applied to the explosion of a tank and the TNO Multienegy method that, according to expert opinion, overestimate the energy level of the explosion. Thus it has been covered all the released energy range.

Consequently, studied the situation described in the proceedings, and possible changes to inaccuracies in such information, it has been established that for positions 1, 2, 3 meters respectively with respect to the center of the explosion, for Models I to X, the initial velocities of a body standing on the tank would be:

If it had been the case of burst explosion of the tank without detonation, the person on the tank had experienced a slight movement, ending a few meters from its original position.

If it had been the case of burst tank explosion with detonation, the person on the tank had experienced a slight movement, ending a few meters from its original position. Only would had registered a displacement of tens or hundreds of meters if the person had experienced lung damage or death from severe lung damage, in addition to rupture eardrums or high hearing damage.

The person surviving the accident, which suffered a major displacement in the accident, according to medical reports contained in the proceedings had none of the health problems listed above.

Consequently, the presence of the person in any standing position on the tank is discarded.

As will be shown, the only possible position for this person is on the loading port lighting a flame.

Moreover, on the assumption of the case of exploding by detonation, the corresponding explosion energy calculations considering the highest possible values were made, that is, adding all possible inputs of energy and considering the factor 2 for shock wave reflection on the floor.

Another analysis is then performed allowing consider that the explosion energy values for some cases were overestimated. Thus it is certain that it was covered all possible energy range of explosion.

The analysis is as follows:

Energy values for a distance of 17 m from the point of explosion, which was the approximate position of the windshield of the truck, were compared.

Pressure not exceeded truck windshield resistance, according to the proceedings information the truck suffered no break windshield, so the burst pressure did not exceed the value of breakage.

This value is estimated at 10000 Pa, for a distance of 17 m. [3]

This pressure corresponds to the sum of the lateral pressure and the dynamic pressure.

If taken as a reference side windows even not knowing if the windows were down or in fully up position, it is estimated that the burst pressure should not have exceeded the reference value of the windscreen because although they are thinner, area is lower and as a result also its burst pressure is higher than for the windshield.

In the method of Baker et. al Models with the $R_7 < 3.0$ m should be discarded, it also means that should be discarded Multienergy method for the Models with $R_{17} < 2.6$.

Note the total matching in Models discarded by both methods.

The possibility that the person who suffered the greatest displacement, located in several tens of meters from the damaged tank, since that person survived, exclude are the cases in which the person on the tank would have died for lung damage.

Therefore the analysis for the person with the largest displacement is in the following Table by the Baker et. al. Method

Were grayed discarded Models by the fact that if it occurred, it should have broken the windshield of the truck.

On cases available, that is, center distances greater than 1 m, the distances of 2m and 3m have been analyzed.

The results are summarized in the **Table 7.4 -** *Relevance of Speed Displacement by the Baker et. al. Method*

The values that apply are not correspond to significant displacement; v10 takeoff speed should be about 20 m / s for a displacement of the order described in the proceeding, while for a 2 meters distance, the takeoff speed v10 of the various Models are in the order of 1 to 2 m/s.

Then it should be asked if there is an explosion distance point between 1 to 2 m, which allows for a takeoff speed of about 20 m / s and simultaneously register absence of lung damage or eardrums rupture.

In that sense, are discarded Models III and V because for the distance of 2 meters eardrums ruptured would occur, which does not appear in the proceedings as one of the damages suffered by the person who experienced the largest displacement.

The cases that can be considered correspond to Models I, II, and VIII.

Note that in Models I and VIII for 1meter distance takeoff speed is less than 20 m/s, therefore a displacement of the properties listed in the proceedings would not be achieved.

Respect to the Model II, in any speed approximate to 20 m/s it have occur lung damage, which not was experienced by the person who suffered the greatest displacement according to the information of medical treatment.

Therefore it not have been able to find displacements of the order of several tens of meters or more than a hundred meters in the case of a person standing on the tank (except for the vicinity of the loading port lighting a flame) when the explosion occurred.

If it has been possible to find displacements of the order of less than ten meters, which would imply that a person on the tank could have been thrown into the flames that would have formed in the vicinity of the tank due to a liquid outlet.

Making a similar analysis for the Multienergy Method TNO, has arrived at the following analogs results.

Chapter 8

Movement of a Body Initially on the Loading Port Lighting a Flame

Initially, at the time of lighting a flame on the port of the damaged tank loading port, the body position of the person who lit the flame would have been the one illustrated in **Figure 8.1 -** *Starting Position of Flame Ignition on the Loading Port Detail*

Importantly, the area of the body that reacts to the flow of gases that started coming out of the port of loading once the flame is lit is the trunk.

As for the body members, arms have articulated in the shoulders and legs would have done it in the hip, being in a position which would opposite lower reaction.

For the determination of the position would initially take the trunk, when conducting the tests of explosive atmospheres, the different possible positions were tested.

Holding the concentration of flammable gases in air meter by hand, allowed to determine in the vicinity of the tank loading port the location of concentration points of flammable gases that would had generated an explosion.

This can be seen as the positions of a hand that put it in an environment of explosive atmosphere.

According to the test, to have the hand in an environment of atmosphere in the case of asphalt diluted RC2 at around 50 ° C, hands should have been on the loading port or at interior.

Thus it was established the body position that would have allowed a hand in that position, which is illustrated in **Figure 8.1.**

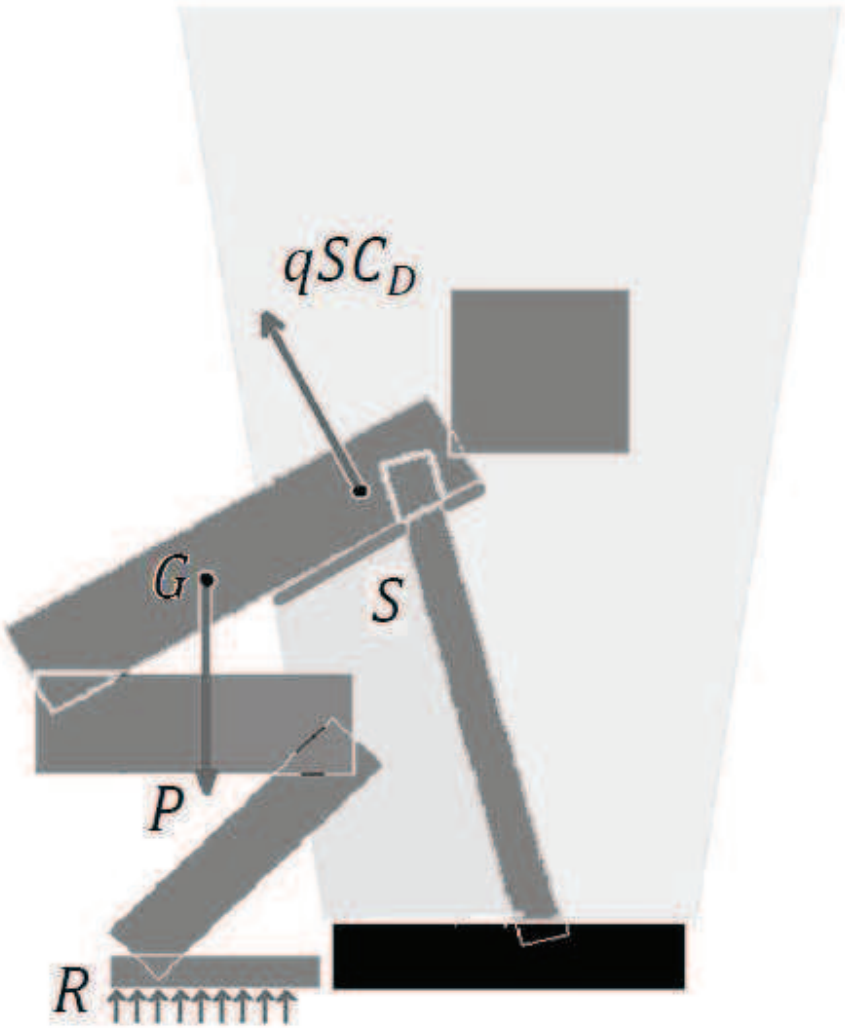

Figure 8.1 Starting Position of Flame Ignition on the Loading Port Detail

From the turn on flame moment, gases begin to flow out of the loading port.

This gas flow raises the body.

The stresses on the body can be calculated by the following equations for the flow of gases exiting the loading port. [2], [12]

$$m'_s(t) = \rho_0 u_0 A C_D \qquad [8.1]$$

$$\rho_x u_x^2 = \frac{\rho_0 u_0^2 d_0^2}{x^2 k_1^2} \qquad [8.2]$$

$$\rho_x u_x^2 = \frac{m'_s(t)^2 d_0^2}{x^2 k_1^2 \rho_0 {C_D}^2 A^2} \qquad [8.3]$$

Where,

ρ_x = density of exhaust gases through loading port at height x of the loading port

u_x = speed of exhaust gases through loading port at a height x of the loading port

$m'_s(t)$ = mass flow rate of exhaust gases through loading port

d_0 = diameter of the loading port

x = height of the body on the loading port

k_1 = $\tan\beta$, value assigned 0.32

ρ_0 = density of gas in the exit condition of the loading port

C_D = discharge coefficient of the loading port, value assigned 0,6

A = loading port section

Loading port diameter is estimated in 0,5 m and section in 0,2 m^2.

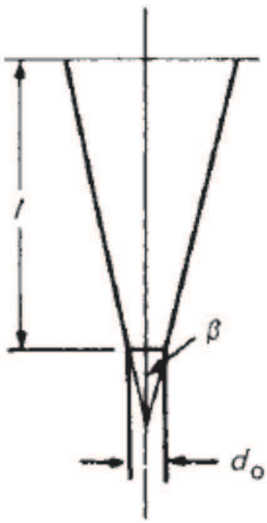

Figure 8.2 - Flow Diagram of Gases Through Loading Port

To evaluate the effect that the gas flow has on the body should apply the first and second cardinal equation, to thereby obtain the equations of motion of the body.

It has done this work for the ten models that cover the range of possible behavior for the damaged tank throughout the process of explosion from the ignition of the gases to tank burst.

The flow of gases exiting the loading port, passes through external vicinity of the body generating efforts of drag and lift.

The application of these stresses on the body allow establish body position from the moment that lit a flame until the outbreak occurred.

Using equation [7-3] has been able to establish the dynamic pressure on the body. It will vary depending on the height x on the loading port as indicated this equation.

The body's reaction to the action of the dynamic pressure generates the following efforts [5], [15], [16], [17]:

$$F_D = C_D A q_x \qquad [8.4]$$

$$F_L = C_L A q_x \qquad [8.5]$$

Where,

F_D = force on the body in and direction of gas flow (drag).

C_D = drag coefficient

A = body surface area that reacts to the flow of gases

q_x = dynamic loading at height x of body over loading port

F_L = force on the body in perpendicular direction to the gas flow (lift) in direction from tank broken end toward tank not broken end.

C_L = lift coefficient

The cardinal equations applied to the body are [13]:

First cardinal equation

$$F = m a_G \qquad [8.6]$$

Where,

F = resultant of external forces applied to the body

m = mass of the body

a_G = acceleration of the body at its centroid

Second cardinal equation

$$M_Q = (G - Q)a_Q + \frac{d(I_Q\omega)}{dt} \quad [8.7]$$

Where,

M_Q = resultant of external forces on the point Q moment

$(G - Q)$ = distance from the centroid of the body Q to the point of application Q

a_Q = acceleration at point Q

I_Q = moment of inertia at the point Q

ω = angular velocity of the body

$\frac{d(I_Q\omega)}{dt}$ = time derivative of $I_Q\omega$

It is understood that can be assumed $\frac{dI_Q}{dt} = 0$ since it is assumed that the trunk would have generated reaction forces to the gas flow.

Thus the equation can be rewritten in this way

$$M_Q = m(G - Q)a_Q + I_Q\frac{d\omega}{dt} \quad [8.8]$$

Taking the subscripts H and V to horizontal and vertical directions respectively can be set to the following equations

$$ma_{GH} = R_H - C_D A q_x \sin\beta - C_L A q_x \cos\beta \quad [8.9]$$

$$ma_{GV} = R_V + C_D A q_x \cos\beta - C_L A q_x \sin\beta - mg \quad [8.10]$$

$R_H \leq f R_V$ non slip condition

$$a_{GH} = \frac{R_H - C_D A q_x \sin\beta - C_L A q_x \cos\beta}{m} \quad [8.11]$$

$$a_{GV} = \frac{R_V + C_D A q_x \cos\beta - C_L A q_x \sin\beta}{m} - g \quad [8.12]$$

$$v_{GH_i} = a_{GH} dt + v_{GH_{i-1}} \quad [8.13]$$

$$v_{GV_i} = a_{GV} dt + v_{GV_{i-1}} \quad [8.14]$$

$$x_{G_i} = \frac{1}{2} a_{GH} dt^2 + v_{GH_i} dt + x_{i-1} \quad [8.15]$$

$$z_{G_i} = \frac{1}{2} a_{GV} dt^2 + v_{GV_i} dt + z_i \quad [8.16]$$

$$\tan\beta = \frac{v_{GV_i}}{v_{GH_i}} \quad [8.17]$$

Where,

v_{GH_i} = centroid velocity in the horizontal direction at time i

v_{GV_i} = velocity of the centroid in the vertical direction at time i

x_{G_i} = vertical displacement of the center of gravity of the body

z_{G_i} = horizontal displacement of the centroid of the body

g = gravitational acceleration

$\omega = \frac{d\beta}{dt}$ angular velocity

The second cardinal equation is calculated in the point G.

$$M_G = I_G \frac{d\omega}{dt} \quad [8.18]$$

Consequently, the equation can be written as follows:

$$\frac{d\omega}{dt} = \frac{-C_D A q_x (Q - G) \sin\alpha - C_L A q_x (Q - G) \cos\alpha}{I_G} \qquad [8.19]$$

θ = is the angle of the trunk with respect to the horizontal plane

α = is the angle of attack

$Q - G = 0{,}25\ m$

$m = 75\ kg$

$I_G = 75 \frac{1{,}25^2}{12}\ kg.m$

$I_G = 12\ kg.m$

$\theta(0) = 30°$

Following it indicates the angle of attack α and efforts lift L and drag D for different possible configurations follows:

$$\alpha = \beta - \theta$$

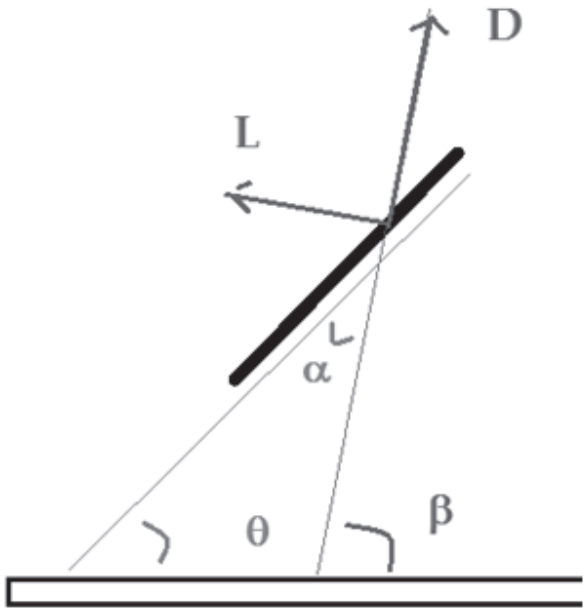

$$\alpha = \pi - (\beta + \theta)$$

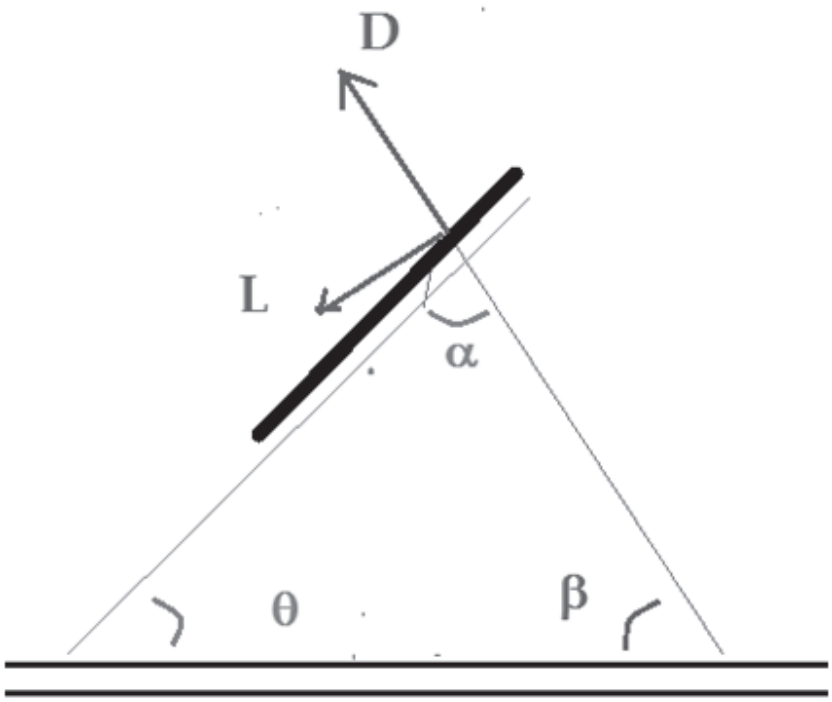

$$\alpha = \beta + \theta$$

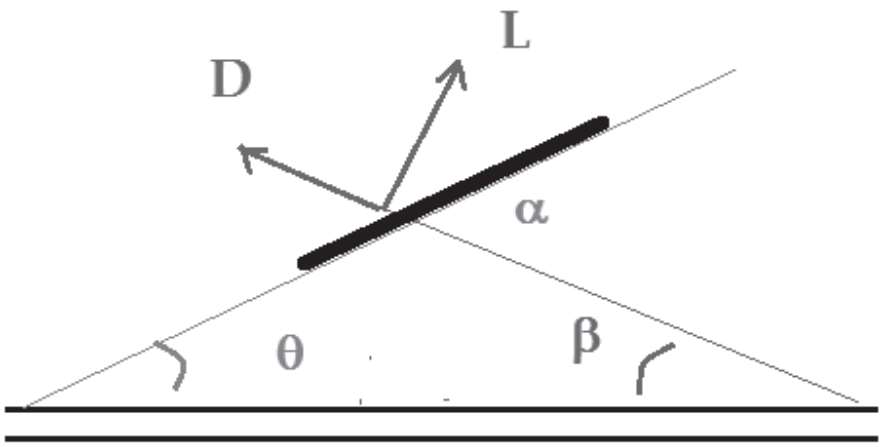

Figure 8.3 - Body Positions, Angles, and Drag and Lift Efforts

The movement is divided into two phases:

In the first phase the trunk would have remained without rotating translating vertically, during this process the legs are extended and finally the trunk is maintained at 30 °.

During this process reaction forces appear in the tank and there is almost no displacement speed .

In the second phase the body loses contact with the surface of the tank and continues to rise, while experiencing a trunk turn and horizontal displacement. Disappear reaction forces.

Applying this chapter equations it has been able to develop body movement on the loading port throughout the whole tank explosion process, since lit the flame until the outbreak of it.

Drag and lift coefficients were obtained from wind tunnel studies and others cited in the bibliographic reference.

Some degree of body symmetry is assumed, that is, the behavior of the human body in terms of the areas of Lift and Drag and the coefficients of Lift and Drag not vary significantly when the human figure is reversed, as the aforementioned values correspond arriving a flow from the head, while in the scene the flow entered from the legs.

Body positions corresponding Models I to X are described below.

In **Tables 8-1** to **8-19** the time t is given in seconds, p in the tank, the temperature T of the noninflamed mixture, body surface area S impacted by the exhaust gases of the loading port opening, the dynamic pressure qx corrected for the height of the body above the loading port, vertical acceleration a_v and vertical velocity v_v, height of centroid above the loading port xi, horizontal acceleration and velocity a_h and v_h, horizontal position of the body from its initial position z_i, body's trunk angular acceleration ω', angular velocity ω, rotation over time ωt, and θ initial position taken values between 20 ° and 40 ° respect to the horizontal, the Lift and Drag coefficients C_L and C_D, and the angle of attack α.

The tables record body by height and horizontal displacement coordinates and body's trunk angle at each hundredth of a second from initial position (determined the explosive atmospheres test already done) up to detonation.

At the time of production of self-ignition, considering that it could have had a duration of 3 milliseconds, the maximum value that q_x could have reached is 200000 Pa, otherwise would have occurred lung damage according to Figure 6-1.

As it couldn't be possible to solve adequately the case under study after detonation, it is understood that the value of q_x may be lower, hence 200000 Pa is taken as a maximum value.

Distances arising calculation also will be used as maximum possible. In the original version of the Phase III Report: Technical Resolution accident, had taken a value of 1800000 Pa as a result of a calculation of detonation inside the tank.

The surviving person didn't registered lung damage, and the deceased had good lung function at hospital admission.

It has been calculated body movement in air from the moment of departure from the loading port opening until landing for I to X Models, show in **Table 8-20** to **Table 8-36**.

Horizontal and vertical acceleration a_h and a_v, speed v_h and v_v, and body position z_i and x_i, with one hundredth of second accuracy respect to initial position, that is, when lit the flame.

In **Table 8-37**_*Height and Displacement Model I to X* summary table of the total displacement would have reached the body of the person who lit the flame on the loading port is listed.

As a general result in some cases the maximum possible distance traveled is in the order of that expressed in the accident records. In most cases the distances have been significantly less.

Horizontal displacement in the air, sliding on the ground, and the total displacement is indicated.

For the movement sliding on the ground was considered a factor of friction between the ground and the person of 0,8, because although it was considered an area of easy slip as it is the grass, accident records indicated that the survivor was found among weeds. The existence of weeds is considered that had a significant effect braking.

As the damaged tank was 2 meters high, it was assumed that the soil was 2 meters below the initial position of the person on the loading port.

Therefore in **Table 8-20** to **Table 8-36** final height is approximately -2.0 m.

Equating the kinetic energy to the friction work:

$$\frac{1}{2}mv^2 = fmgd \qquad [8.20]$$

$$d = \frac{1}{2}\frac{v^2}{fgd} \qquad [8.21]$$

$d = 0{,}063v^2$

Where,

d = displacement

v = landing speed

f = friction coefficient, value 0,8

g = gravitational constant

Experimental verification

Experience scale was performed with a compressed air hose with its end discharging a high velocity stream of compressed air vertically, just as the loading port gases discharged at high speed.

First experience with the hose to low flow was performed by simulating the behavior before detonation, the displacement of the body was maintained by a relatively small fraction of a second at short distance from the hose extreme.

Experience with a second hose strangled at maximum flow is then made to simulate the detonation.

It was found that for an initial position as in **Figure 8.1**, the path had significant horizontal displacement and little height displacement as shown in **Figure 8.4**.

The test was repeated numerous times an always give the same trajectory.

Human scale plastic figure was loaded with extra weight to match the weight of a human according to their size.

Its horizontal displacement in the air was around and above 40 times their body height, equivalent to about 70 meters of horizontal displacement and 17 meters high for a person 1.70 m tall.

This experiment is completely reproducible and repeatable, that is, the result is independent of the person performing.

This experimental verification showed values significantly higher than the range of values obtained by the mathematical model displacement.

The amount and quality of information used in the mathematical model is vastly superior to that of the experiment, so it is considered that although the experiment is reproducible, their values do not reflect the case study.

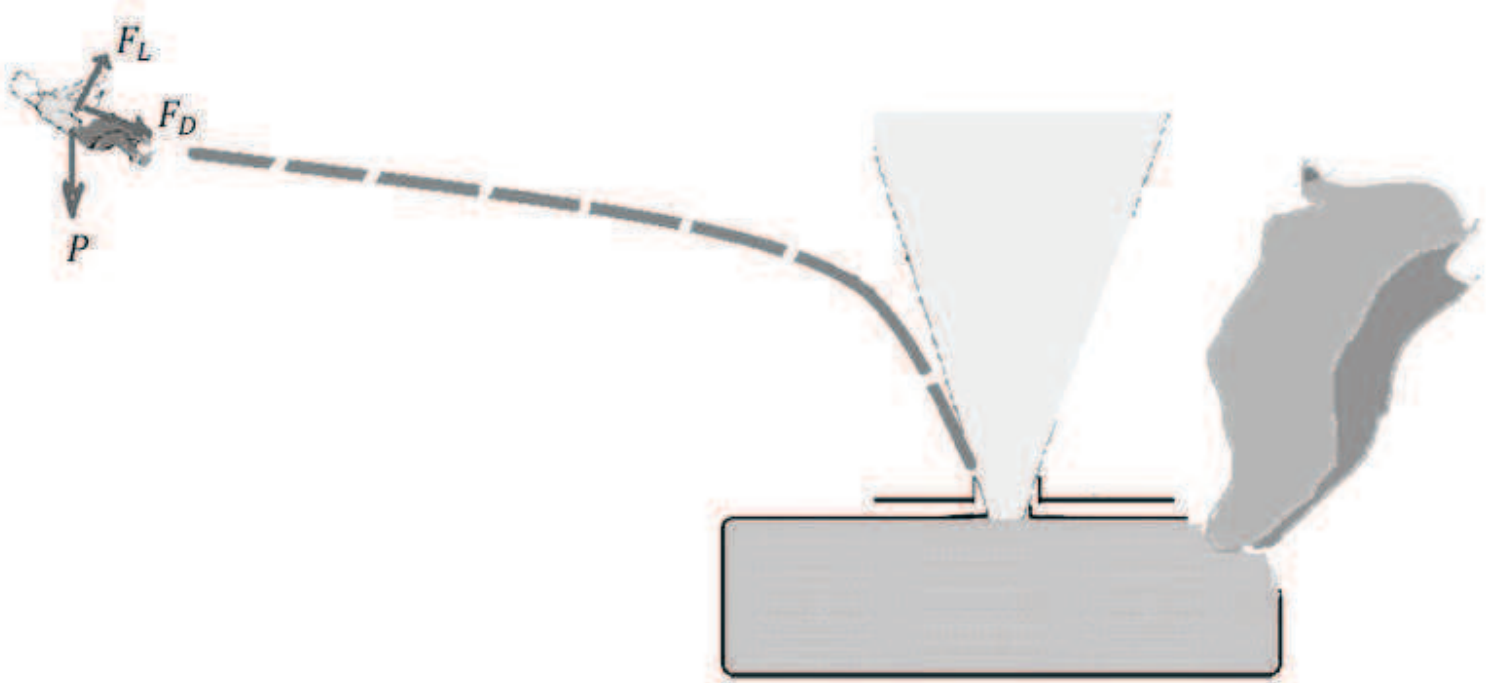

Figure 8.4 - Sequence of Movement.

The following **Chapter 9** – Detonation and Shock Wave Creation and **Chapter 10** – Interaction Between Shock Wave and a Liquid Layer cannot be totally void because they consider a pressure level at the loading port enough to produce lung damage to a person that lit the flame.
Nevertheless they explain well tank deformations and asphalt diluted RC2 spill in the vicinity of damaged tank.

Chapter 9

Detonation and Shock Wave Creation

At the time of detonation occurrence, would have formed a shock wave.

According to Chapman Jouget equations the shockwave characteristics would be [2], [18], [19]:

$$\frac{\gamma}{\gamma - 1}(p_1 v_1 - p_2 v_2) - q = \frac{1}{2}(p_{2-}p_1)(v_1 + v_2) \qquad [9.1]$$

Where,

γ = polytropic index

p_1 = gas pressure entering shockwave

v_1 = specific volume gas entering shockwave

p_2 = gas pressure leaving shockwave

v_2 = specific volume gas living shockwave

q = energy added per mass unit

$$p_2 = 2\frac{(\gamma_2 - 1)}{v_1} \qquad [9.2]$$

$$\frac{\rho_2}{\rho_1} = \frac{(\gamma_1 + 1)}{\gamma_1} \qquad [9.3]$$

$$u_1 = \sqrt[2]{2q(\gamma_2^2 - 1)} \qquad [9.4]$$

Given

$q = 2{,}5.10^6$

$\gamma_2 = 1{,}25$

Then:

$$u_1 = 1677\ \frac{m}{s}$$

Considering ten Models used in this Thesis, a representative density value is

$$\rho_1 = 1{,}8\ \frac{kg}{m^3} \qquad [9.5]$$

Then, the shockwave would generated a dynamic pressure pulse in order of

$$p_d = \frac{1}{2}\rho_1 u_1^2 \qquad [9.6]$$

$$p_d = 2{,}7.10^6\ Pa \qquad [9.7]$$

Approximately this dynamic pressure when pass through the loading port would have a mean velocity v that

$$p_d = 1{,}5\frac{1}{2}\rho_1 v^2 \qquad [9.8]$$

1,5 value is debt to the pressure fall at the loading port, which is 0,5 at the inlet and 1,0 at the outlet approximately of the dynamic pressure with velocity v the loading port

Then:

$v = 1414 \frac{m}{s}$

Thus dynamic pressure at the loading port outlet would be approximately:

$q = 1{,}8.10^6\ Pa$

Based on detonation energies studies already done by the methods of Baker et. al. and Multi-energy, duration of the pressure pulse is in the order of 3 milliseconds.

Therefore, it can be considered that this pulse generate at the loading port outlet a dynamic pressure load of $1{,}8.10^6\ Pa$ for 3 milliseconds.

In the calculations of body movement on the loading port was applied that dynamic pressure load when detonation occurred.

Once the burst begins, the pressure wave sweeps the gases between it and the loading port.

This can be seen through photography (not shown in this Thesis) which can be seen in the tank for signs of overpressure from the end that broke up the charge port.

The rest of the tank didn't shown signs of overpressure.

The amount of mass that went out the loading port is about:

$$m = \rho C_d S v dt \qquad [9.9]$$

Where,

m = mass that flowed through the loading port

ρ = gas density

C_d = discharge coefficient of the loading port used as nozzle

S = loading port surface area

v = gas velocity through the loading port

dt = time period while the gases flowed

Values established are:

$\rho = 1{,}8 \frac{kg}{m^3}$

C_d =0,6

$S = 0{,}2\ m^2$

$v = 1414\ \frac{m}{s}$

$dt = 3.10^{-3}\ s$

Then,

$m = 0{,}92\ kg$

Gas flow through the loading port for 3 msec was 305 m/s.

This flow is of the order of the maximum flow of a large-sized commercial jet airplane turbine. [6]

Therefore the person who lit the flame was in an equivalent situation as to be located immediately at the output of a large-sized commercial jet airplane turbine during this time.

As seen in the ten Models made, this experience made a big contribution to the displacement of about a hundred meters from the person who lit the flame.

The reaction force on the tank, considering that this tank type seems to be UL 142 Standard, for whose size should be built in steel sheet thickness of about 4 mm, it should have bent down the loading port arriving at yield stress value of the material, producing a permanent depression in said zone.

For a dynamic pressure of 1,8. 10^6 Pa and an area of 0,2 m^2 will reach a force of 3,6. 10^5 N, which was evaluated by the following calculations as enough to yield the surrounding material in to the tank.

In the picture in the accident's records (not shown in this Thesis) shown permanent depression that the above-described evidencing this phenomenon.

The force of the loading port of the tank was:

$$\frac{1}{2}\rho_1 v^2 S = 3{,}6.10^5\ N$$

The effort on the section assuming a distance of 0,1 m and considering a differential element x of loading port edge [14],[22]:

For a moment M , and the resistant modulus W the stress σ can be estimated as:

$$\sigma = \frac{M}{W} \qquad [9.10]$$

$$M = 3{,}6.\,10^5 0{,}1 \frac{x}{\pi\phi} \qquad [9.11]$$

$$W = 2e^2 \frac{x}{6} \qquad [9.12]$$

$$s = \frac{3{,}6.\,10^5.\,0{,}1.6x}{2\pi\phi e^2 x} \qquad [9.13]$$

$$s = \frac{3{,}6.\,10^5.\,0{,}1.6}{2\pi\phi e^2}$$

$s = 3.\,10^8\ Pa$ yield value

$s = 4{,}3.\,10^8\ Pa$ stress on the loading port calculated

The burst pressure of the area of the tank that exploded, considering a thickness of 4 mm would be a minimum of 1.6. 106 Pa for a longitudinal rupture rate of 3.2 cylindrical body. 106 Pa for a break of the lid.

In the first case the equation applied is:

$$2\sigma e = p\phi \qquad [9.14]$$

and in second case

$$\sigma\phi\pi = p\phi^2 \frac{\pi}{4} \qquad [9{,}15]$$

Where,

σ = resistencia a la tracción del material

ϕ = diámetro del tanque

p = presión interior de rotura

The tank was composed of a cylindrical body and two caps at the extremes.

The welded joint of the cylindrical body of the tank with the cap can be considered to have a burst pressure of $1.6.\ 10^6$ Pa.

The dynamic pressure generated by the shock wave became static pressure when striking the side wall of the tank.

As said pressure is about $2.7.\ 10^6$ Pa, it overpass the rupture resistance of the weld junction causing the outbreak.

The area of the cylindrical body of the tank between the loading port and the extreme was subjected to a pressure below $1.6.10^6$ Pa because the tank was not opened there.

This is because in this area the static pressure at the time of the burst was less than these values and when the burst occur, dynamic pressure generated only find a restriction at the end that broke.

On the way to the loading port the contact with walls of the tank did not lead to a conversion of dynamic pressure to static enough to break the tank in that area.

Chapter 10

Interaction Betwen Shock Wave and a Liquid Layer

As the flow progressed on the surface, a surface wave of large amplitude have been formed; its size depends on the Mach number. [7], [20],[21], [22]

The equations governing the phenomenon are:

$$d(MU_w) = (P_t - P_{oo})(H - h)w \qquad [10.1]$$

$$P_t - P_{oo} = \frac{1}{2}\rho_{oo}u_{oo}^2 \qquad [10.2]$$

$$U_w = U_{oo}\frac{\rho_{oo}}{\rho_{liq}}\frac{1}{2}\left(\frac{H}{h} - 1\right) \qquad [10.3]$$

Where,

M = wave mass

U_w = wave horizontal velocity

P_t = pressure in wave vicinity

P_{oo} = pressure far from the wave

H = wave height

h = liquid height

w = wave width

ρ_{oo} = gas density far from the wave

ρ_{liq} =liquid density

U_{oo} = shockwave velocity

The following values are known:

$P_{oo} = 2{,}7.10^6\ Pa$

$h = 0{,}32\ m$

$w = 2{,}0\ m$

$\rho_{oo} = 1{,}8\ \frac{kg}{m^3}$

$\rho_{liq} = 1{,}0.10^3\ \frac{kg}{m^3}$

$u_{oo} = 1677\ \frac{m}{s}$

$dt = pulse\ duration, 3\ ms$

After making several trials with different ratios of values, it has been concluded that the values that best fit the phenomenon object of study, according to the equations that govern it, are approximately the following:

M up to 200 kg

$U_w = 50\ \frac{m}{s}$

$H = 1m$

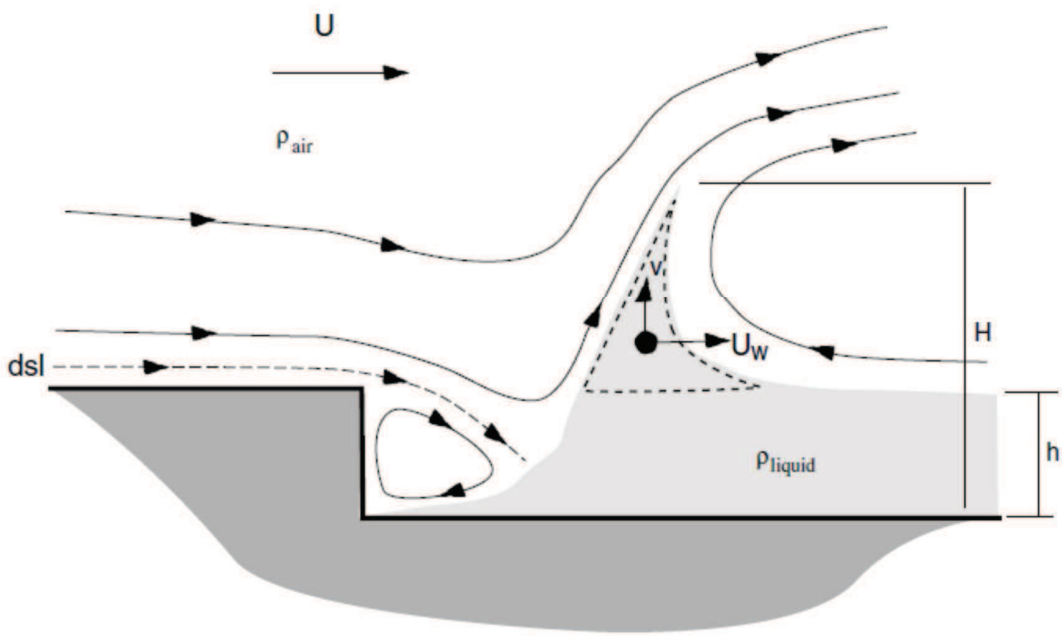

Figure 10.1 Wave Creation Scheme

The wave begins to move towards the loading port getting away from the end of the tank, that, at that time begins to explode.

This wave isolated part of the already burned mixture and the mixture still unburned, so that at burst time and before tank rupture (estimated between 5 and 15 ms after the burst), it had formed this wave and that separation had occurred between the mixture self-inflamed and the rest of the inflamed and non-inflamed mixture in the tank. [9],[10]

The gas trapped between the wave and loading port start compressing as the wave progressed.

The compression of the trapped gas is estimated to could have reached 500,000 Pa at the time the wave reached the loading port.

At the time this pressure govern the vertical movement of the fluid through the loading port.

In this case it would have gone from 100 to 200 kg of asphalt diluted RC2 liquid through loading port. The height corresponding to that pressure, considering pressure loss in the loading port, would be in the order of 30 meters.

This liquid rising with inflamed heavy naphtha could be the 35 meters column of flames described in the accident's records.

In experiments carried out with a plastic bottle of 500 cc simulating the tank with a water level simulating the liquid level, a perforation simulating the loading port and blowing at the free end simulating the detonation was observed that the flow goes vertically occurs then a flow breakdown, descending as rain and the effect of advancing in all directions overlaps with an increase in the wave's advancing direction in the tank.

Modeling with liquid flowing at 27 m/s (corresponding to a height of 35 m) through the loading port, with a value of radial velocity of 1 m/s and a feed velocity in the direction of wave flow of 1,3 m/s.

Values are in **Table 10.1** - *Liquid Flowed Through Loading Port X and Y Axes Velocity as an Angle Function* and the corresponding graph in **Figure 10.2** - *Dispersion Modeling of Liquid Through Loading Port with Table 10-1 X and Y axes Velocity and Vertical Velocity 27 m/s. Tank and Loading Port Represented in Red. The Limits of Asphalt Diluted RC2 in Dots.*

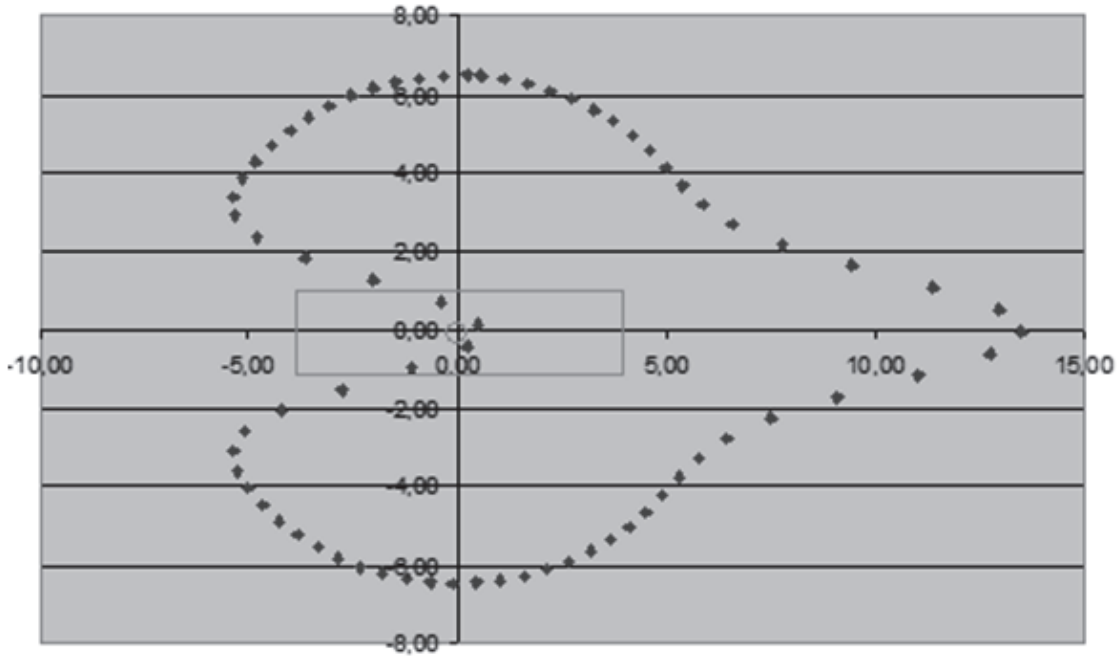

Figure 10.2 - Dispersion Modeling of Liquid Trough Loading Port with Table 10-1 X and Y axes Velocity and Vertical Velocity 27 m/s. Tank and Loading Port Represented in Red. The Limits of Asphalt Diluted RC2 in Dots. (Distances are in meters)

Also it have been calculated the droplet size by the flow breakdown. [11],[23]

$$\frac{SMD}{d_0} = 82{,}23 D_D^{0{,}64} We^{-0{,}07} Re^{-0{,}5} \qquad [10.4]$$

Where,

SMD = droplet size

C_D = drag coefficient

We = Weber number

Re = Reynolds number

$SMD = 0{,}013\ m$

$C_D = 0{,}4$

$We = 4{,}5.10^6$

$Re = 3{,}0.10^5$

It can be seen by the photographs in the accident's records (not shown) that the drops on the tanker truck had a diameter of about 13 mm (0,013 m) as it was calculated.

The angle at which drops fell in the tanker truck demonstrate that advanced horizontally in the order of 1 m / s, if we take in count the height reached and the distance between the tanker and the damaged tank which was given by the length of the hose of 7 to 8 meters according to the accident's records.

This assumption would confirm the previous assumed of the radial flow velocity exiting the loading port, because the droplets that fall on the tanker would be in a perpendicular plane respect to the wave advance and therefore they would not be affected by that advance velocity.

Chapter 11

Conclusions

This thesis concludes that every heavy fuel accident in wich it can be established:

- precisely the kind of heavy fuel involved in the accident
- the fuel temperature at the moment of the accident
- the volume of the tank
- the free volume of the tank
- an explosive atmospheres study in a tank similar or equivalent to the one damaged, including same fuel and temperature
- opening area and shape
- number of people involved in the accident
- final position of people involved in case they appear far from scene
- tank deformation broadly
- spill of fuel configuration in the neighborhood of the tank

it is possible to find an explanation of the accident that fit with everyone of these aspects considered as evidence.

Following the twenty steps algorithm and using the case of study as a guide is possible to solve another case.
This one by one procedure, can contribute significantly to make this statement of "find an explanation of the accident that fit with everyone of these aspects" turn it from sound pretencious, to humbly a scientific and seriously contribution to up to now unsolved or not well resolved accidents involving heavy fuel, tanks, and explosions.
The free volume of tank could be not at accurate as it will be needed.
In this scenario, as is was used in the case of study, is advisable to use several free volumes.
To discard volumes after the simulation, is advisable to seek in the other aspects of this systemic aproach and discard that volumes that don't completely fit in the rest of the aspects.

This work in order to make a real contribution to the scientific community it would have to be seen as a starting point by wich other accidents happened in the past can be faced again.

Each one a single turn per accident studied in a growing spiral process.

In order to enable this growing spiral process, the next steps then would be the diffusion of this work among organizations and relevant persons involved in the scientific community, the petroleum industry, the safety of industrial process, among other, at worldwide level.

Acording to that, an as a wholistic result, the statement of "close approach to the accident's real explanation" can be sustained debt to the multi-matching of crossed information provided by the different perspectives each chapter gives.

Nevertheless each explosion accident involving heavy fuel tanks has its unique circunstances, this work is intended to act as a conducting wire among them from the stand point of view of give a general procedure or approach to tackle the problem.

The case study is at the same time a demonstrative prove of the consistency and power of the procedure and a tool to guide more clearly in the application of the procedure.

This procedure is applicable to other problems of accidents in similar contexts. This methodology is very general and allows to investigate other cases that have fewer variables, thus illustrating the potential of the developed algorithm.

Part IV

ANNEX

Appendix A

ANNEX: Chapter 4 - Tank Behavior Model I to Model X

Model No. I. Tank 7,5 m^3 of Free Volume, Control Volume 5 m^3, Turbulence Factor = 2.

The model was run for these conditions.

The results are in Table 4-6.

If the accident scene had been of this kind would have been possible to reach the tank burst at self-ignition temperature.

A scenario self-ignition of unburned mixture at about 0.52 s was recorded.

As discussed later, if the container had exploded by the maximum pressure reached in the corresponding model 176000 Pa, it was not possible that a person had moved a great distance, and there would have been not damage to the vessel walls as illustrated in the photographs of the proceedings.

Consequently the alternative that the tank had exploded by the internal pressure would not be admissible. By contrast the hypothesis of self-ignition detonation would be valid.

t	r_{i-1}	m_{bi}	m_{ui}	p_i	ρ_{bi}	m_{si}	m_{ui}	V_{bi}	ri	x_i	dm_{sbi}	dm_{sui}	dm_{si}	dm_{bi}	g_{mix}	ρ_{mix}	ρ_{ui}	T_{ui}
0,01	0,01	0,00	**11,20**	101300	0,15	0, 00	**11,17**	0,00	0,01	3,50	0,00	0,00	0,00	0,00	1,36	1,50	1,49	283
0,02	0,01	0,00	**11,18**	101400	0,15	0,02	**11,17**	0,01	0,13	3,50	0,00	0,02	0,02	0,00	1,36	1,49	1,49	283
0,03	0,13	0,00	**11,15**	101400	0,15	0,04	**11,17**	0,01	0,13	3,50	0,00	0,02	0,02	0,00	1,36	1,49	1,49	283
0,04	0,13	0,00	**11,13**	101400	0,15	0,06	**11,14**	0,03	0,19	3,49	0,00	0,02	0,02	0,00	1,36	1,49	1,49	283
0,05	0,19	0,01	**11,10**	101500	0,15	0,09	**11,12**	0,05	0,23	3,48	0,00	0,03	0,03	0,01	1,36	1,48	1,49	283
0,06	0,23	0,01	**11,06**	101500	0,15	0,12	**11,07**	0,08	0,28	3,47	0,00	0,03	0,03	0,01	1,36	1,47	1,49	283
0,07	0,28	0,02	**10,99**	102000	0,15	0,18	**11,03**	0,14	0,32	3,44	0,00	0,05	0,05	0,01	1,36	1,47	1,50	284
0,08	0,32	0,03	**10,92**	102000	0,15	0,23	**10,91**	0,21	0,38	3,41	0,00	0,05	0,05	0,02	1,36	1,45	1,50	284
0,09	0,38	0,05	**10,82**	103000	0,15	0,31	**10,84**	0,31	0,43	3,36	0,00	0,08	0,08	0,02	1,36	1,44	1,51	285
0,1	0,43	0,07	**10,69**	104000	0,16	0,42	**10,72**	0,44	0,48	3,30	0,01	0,10	0,10	0,03	1,36	1,42	1,52	286
0,11	0,48	0,09	**10,54**	105000	0,16	0,54	**10,57**	0,58	0,53	3,23	0,01	0,11	0,12	0,04	1,36	1,39	1,53	286
0,12	0,53	0,12	**10,38**	106000	0,16	0,67	**10,38**	0,75	0,57	3,15	0,02	0,12	0,13	0,05	1,36	1,36	1,54	287
0,13	0,57	0,15	**10,20**	107000	0,16	0,82	**10,15**	0,94	0,62	3,07	0,02	0,12	0,15	0,06	1,36	1,33	1,55	288
0,14	0,62	0,18	**10,00**	109000	0,16	0,98	**9,98**	1,12	0,66	2,98	0,03	0,13	0,17	0,06	1,36	1,30	1,57	290
0,15	0,66	0,22	**9,79**	111000	0,17	1,16	**9,81**	1,31	0,69	2,89	0,04	0,14	0,18	0,07	1,36	1,25	1,58	292
0,16	0,69	0,25	**9,56**	112000	0,17	1,35	**9,56**	1,49	0,72	2,81	0,05	0,14	0,19	0,08	1,36	1,21	1,59	293
0,17	0,72	0,28	**9,34**	113000	0,17	1,54	**9,31**	1,68	0,75	2,72	0,06	0,13	0,19	0,09	1,36	1,17	1,60	294
0,18	0,75	0,32	**9,11**	115000	0,17	1,74	**9,13**	1,85	0,77	2,64	0,07	0,13	0,20	0,10	1,35	1,13	1,62	297
0,19	0,77	0,35	**8,88**	115000	0,17	1,94	**8,82**	2,03	0,80	2,56	0,07	0,12	0,20	0,11	1,35	1,08	1,61	297
0,2	0,80	0,38	**8,64**	117000	0,18	2,14	**8,65**	2,19	0,82	2,48	0,08	0,12	0,20	0,11	1,35	1,04	1,63	299
0,21	0,82	0,41	**8,41**	118000	0,18	2,35	**8,44**	2,34	0,84	2,41	0,09	0,12	0,21	0,12	1,35	0,99	1,63	301
0,22	0,84	0,44	**8,18**	118000	0,18	2,55	**8,15**	2,51	0,86	2,33	0,09	0,11	0,20	0,13	1,35	0,95	1,63	301
0,23	0,86	0,47	**7,94**	120000	0,18	2,75	**7,99**	2,64	0,87	2,27	0,10	0,10	0,21	0,13	1,35	0,91	1,65	304
0,24	0,87	0,50	**7,71**	120000	0,18	2,96	**7,72**	2,80	0,89	2,20	0,11	0,10	0,20	0,14	1,35	0,86	1,64	305
0,25	0,89	0,53	**7,48**	121000	0,18	3,16	**7,49**	2,95	0,90	2,13	0,11	0,09	0,20	0,14	1,35	0,82	1,65	306
0,26	0,90	0,56	**7,25**	122000	0,18	3,36	**7,28**	3,09	0,92	2,06	0,12	0,08	0,20	0,15	1,34	0,78	1,65	308
0,27	0,92	0,59	**7,02**	123000	0,18	3,55	**7,07**	3,22	0,93	2,00	0,12	0,08	0,20	0,15	1,34	0,74	1,65	310

t	r_{i-1}	m_{bi}	m_{ui}	p_i	ρ_{bi}	m_{si}	m_{ui}	V_{bi}	ri	x_i	dm_{sbi}	dm_{sui}	dm_{si}	dm_{bi}	γ_{mix}	ρ_{mix}	ρ_{ui}	T_{ui}
0,28	0,93	0,62	**6,80**	123000	0,18	3,75	**6,77**	3,39	0,95	1,92	0,12	0,07	0,19	0,16	1,34	0,70	1,65	311
0,29	0,95	0,66	**6,57**	125000	0,19	3,94	**6,61**	3,51	0,96	1,86	0,13	0,06	0,19	0,16	1,34	0,66	1,66	315
0,3	0,96	0,69	**6,35**	126000	0,19	4,13	**6,39**	3,64	0,97	1,80	0,13	0,06	0,19	0,17	1,34	0,62	1,66	317
0,31	0,97	0,72	**6,12**	127000	0,19	4,32	**6,15**	3,78	0,98	1,74	0,14	0,05	0,19	0,17	1,33	0,58	1,66	320
0,32	0,98	0,75	**5,90**	128000	0,19	4,51	**5,90**	3,93	0,99	1,67	0,14	0,04	0,19	0,1 8	1,33	0,54	1,65	323
0,33	0,99	0,79	**5,69**	129000	0,19	4,69	**5,63**	4,09	1,01	1,60	0,14	0,04	0,18	0,18	1,33	0,50	1,65	326
0,34	1,01	0,83	**5,47**	131000	0,20	4,87	**5,43**	4,21	1,0 2	1,54	0,15	0,03	0,18	0,18	1,32	0,47	1,65	331
0,35	1,02	0,86	**5,25**	133000	0,20	5,05	**5,23**	4,34	1,03	1,48	0,15	0,03	0,18	0,19	1,32	0,43	1,65	336
0,36	1,03	0,90	**5,04**	135000	0,20	5,22	**5,01**	4,46	1,04	1,42	0,15	0,02	0,17	0,19	1,31	0,40	1,65	341
0,37	1,04	0,94	**4,82**	138000	0,21	5,39	**4,85**	4,56	1,04	1,37	0,15	0,02	0,17	0,20	1,30	0,36	1,65	348
0,38	1,04	0,98	**4,61**	140000	0,21	5,56	**4,60**	4,70	1,05	1,31	0,15	0,01	0,17	0,20	1,30	0,33	1,64	355
0,39	1,05	1,03	**4,40**	143000	0,21	5,72	**4,39**	4,81	1,06	1,26	0,15	0,01	0,16	0,20	1,29	0,30	1,63	365
0,4	1,06	1,08	**4,19**	147000	0,22	5,88	**4,24**	4,90	1,07	1,22	0,15	0,01	0,16	0,20	1,28	0,27	1,63	376
0,41	1,07	1,13	**3,99**	150000	0,22	6,03	**3,99**	5,02	1,08	1,16	0,15	0,00	0,15	0,21	1,26	0,24	1,61	388
0,42	1,08	1,18	**3,78**	154000	0,23	6,18	**3,80**	5,12	1,09	1,11	0,15	0,00	0,15	0,21	1,25	0,22	1,59	402
0,43	1,09	1,24	**3,57**	158000	0,24	6,33	**3,55**	5,23	1,09	1,06	0,15	0,00	0,15	0,21	1,25	0,23	1,57	421
0,44	1,09	1,30	**3,37**	163000	0,24	6,48	**3,35**	5,32	1,10	1,02	0,15	0,00	0,15	0,21	1,25	0,24	1,54	442
0,45	1,10	1,35	**3,16**	167000	0,25	6,64	**3,14**	5,41	1,11	0,98	0,16	0,00	0,16	0,20	1,25	0,24	1,50	464
0,46	1,11	1,40	**2,96**	171000	0,26	6,80	**2,98**	5,47	1,11	0,95	0,16	0,00	0,16	0,20	1,25	0,25	1,47	486
0,47	1,11	1,44	**2,76**	173000	0,26	6,96	**2,74**	5,56	1,12	0,91	0,16	0,00	0,16	0,20	1,25	0,26	1,41	510
0,48	1,12	1,48	**2,57**	175000	0,26	7,13	**2,56**	5,63	1,12	0,87	0,17	0,00	0,17	0,19	1,25	0,26	1,37	533
0,49	1,12	1,50	**2,38**	176000	0,26	7,30	**2,38**	5,70	1,13	0,84	0,17	0,00	0,17	0,19	1,25	0,26	1,32	555
0,5	1,13	1,52	**2,20**	176000	0,26	7,47	**2,18**	5,78	1,13	0,81	0,17	0,00	0,17	0,18	1,25	0,26	1,27	578
0,51	1,13	1,54	**2,02**	176000	0,26	7,64	**2,05**	5,83	1,13	0,78	0,17	0,00	0,17	0,18	1,25	0,26	1,23	598
0,52	1,13	1,54	**1,84**	174000	0,26	7,81	**1,82**	5,93	1,14	0,73	0,17	0,00	0,17	0,17	1,25	0,26	1,16	626
0,53	1,14	1,55	**1,68**	173000	0,26	7,98	**1,70**	5,98	1,14	0,71	0,17	0,00	0,17	0,17	1,25	0,26	1,12	644
0,54	1,14	1,55	**1,52**	170000	0,25	8,14	**1,50**	6,07	1,15	0,67	0,17	0,00	0,17	0,16	1,25	0,26	1,05	673

t	r_{i-1}	m_{bi}	m_{ui}	p_i	ρ_{bi}	m_{si}	m_{ui}	V_{bi}	ri	x_i	dm_{sbi}	dm_{sui}	dm_{si}	dm_{bi}	γ_{mix}	ρ_{mix}	ρ_{ui}	T_{ui}
0,55	1,15	1,54	**1,36**	167000	0,25	8,31	**1,32**	6,16	1,16	0,62	0,16	0,00	0,16	0,15	1,25	0,25	0,99	706
0,56	1,16	1,53	**1,22**	165000	0,25	8,47	**1,26**	6,20	1,16	0,61	0,16	0,00	0,16	0,14	1,25	0,25	0,97	709
0,57	1,16	1,51	**1,08**	161000	0,24	8,62	**1,11**	6,28	1,16	0,57	0,16	0,00	0,16	0,14	1,25	0,25	0,91	735
0,58	1,16	1,50	**0,94**	158000	0,24	8,78	**1,01**	6,34	1,17	0,54	0,15	0,00	0,15	0,14	1,25	0,24	0,87	754
0,59	1,17	1,48	**0,81**	153000	0,23	8,92	**0,79**	6,47	1,17	0,48	0,15	0,00	0,15	0,13	1,25	0,24	0,77	828
0,6	1,17	1,47	**0,69**	150000	0,22	9,07	**0,72**	6,53	1,18	0,45	0,14	0,00	0,14	0,12	1,25	0,23	0,74	847
0,61	1,18	1,44	**0,58**	145000	0,22	9,29	**0,58**	6,63	1,18	0,41	0,22	0,00	0,22	0,11	1,25	0,22	0,67	906

Table 4.6 - Model No. I. Numerical Values of Model Variables Properties for Each Time Interval

Model No. II. Tank 7,5 m^3 of Free Volume, Control Volume 5 m^3, Turbulence Factor = 3.

The model was run for these conditions.

The results are in Table 4-7.

If the accident scene it had been of this kind, it would have been possible to reach the self-ignition temperature leading to tank burst.

Self-ignition of unburned mixture was recorded at about the 0,31 s stage.

As discussed later, if the container had exploded by the maximum pressure reached in the corresponding model 200000 Pa, it was not possible that a person had moved a great distance, and there would not have been damage to the vessel walls as the illustrated in the photographs of the proceedings.

Consequently the alternative that the tank had exploded by the internal pressure would not be admissible. By contrast the hypothesis of self-ignition detonation would be valid.

t	r_{i-1}	m_{bi}	m_{ui}	p_i	ρ_{bi}	m_{si}	m_{ui}	V_{bi}	r_i	x_i	dm_{sbi}	dm_{sui}	dm_{si}	dm_{bi}	γ_{mix}	ρ_{mix}	ρ_{ui}	T_{ui}
0,01	0,01	0,00	**11,17**	101400	0,15	0,02	**11,18**	0,00	0,01	3,50	0,00	0,02	0,02	0,00	1,36	1,50	1,49	283
0,02	0,01	0,00	**11,15**	101400	0,15	0,04	**11,14**	0,03	0,20	3,49	0,00	0,02	0,02	0,00	1,36	1,49	1,49	283
0,03	0,20	0,00	**11,12**	101400	0,15	0,06	**11, 14**	0,03	0,20	3,49	0,00	0,02	0,02	0,01	1,36	1,49	1,49	283
0,04	0,20	0,01	**11,09**	101400	0,15	0,08	**11,04**	0,09	0,29	3,46	0,00	0,02	0,02	0,01	1,36	1,48	1,49	283
0,05	0,29	0,02	**11,02**	102000	0,15	0,10	**10,99**	0,16	0,34	3,43	0,00	0,05	0,05	0,02	1,36	1,48	1,50	284
0,06	0,34	0,04	**10,91**	103000	0,15	0,16	**10,88**	0,28	0,41	3,37	0,00	0,08	0,08	0,03	1,36	1,46	1,51	285
0,07	0,41	0,07	**10,75**	105000	0,16	0,24	**10,77**	0,45	0,48	3,29	0,01	0,12	0,12	0,04	1,36	1,44	1,53	286
0,08	0,48	0,11	**10,56**	106000	0,16	0,37	**10,49**	0,68	0,55	3,19	0,01	0,12	0,14	0,06	1,36	1,40	1,54	287
0,09	0,55	0,16	**10,33**	110000	0,16	0,50	**10,33**	0,95	0,62	3,06	0,02	0,15	0,18	0,08	1,36	1,37	1,58	291
0,1	0,62	0,21	**10,06**	113000	0,17	0,68	**10,02**	1,25	0,68	2,92	0,04	0,16	0,20	0,10	1,36	1,31	1,60	294
0,11	0,68	0,28	**9,77**	117000	0,18	0,88	**9,71**	1,57	0,73	2,77	0,06	0,17	0,22	0,13	1,36	1,25	1,64	298
0,12	0,73	0,35	**9,45**	122000	0,18	1,11	**9,42**	1,89	0,78	2,62	0,08	0,17	0,25	0,15	1,35	1,19	1,68	303
0,13	0,78	0,42	**9,11**	127000	0,19	1,35	**9,11**	2,19	0,82	2,48	0,10	0,16	0,26	0,17	1,35	1,12	1,72	308
0,14	0,82	0,49	**8,76**	132000	0,20	1,62	**8,78**	2,49	0,85	2,34	0,12	0,15	0,27	0,20	1,35	1,05	1,75	314
0,15	0,85	0,57	**8,41**	137000	0,21	1,89	**8,42**	2,77	0,88	2,21	0,14	0,14	0,28	0,22	1,35	0,98	1,78	321
0,16	0,88	0,65	**8,05**	142000	0,21	2,17	**8,04**	3,04	0,91	2,08	0,16	0,13	0,28	0,24	1,35	0,91	1,80	328
0,17	0,91	0,73	**7,68**	147000	0,22	2,45	**7,63**	3,31	0,94	1,96	0,17	0,11	0,28	0,26	1,34	0,84	1,82	336
0,18	0,94	0,81	**7,31**	154000	0,23	2,73	**7,35**	3,53	0,96	1,86	0,19	0,10	0,28	0,27	1,34	0,77	1,85	347
0,19	0,96	0,90	**6,94**	160000	0,24	3,01	**6,96**	3,75	0,98	1,75	0,20	0,08	0,28	0,29	1,33	0,70	1,86	358
0,2	0,98	0,99	**6,57**	166000	0,25	3,29	**6,53**	3,99	1,00	1,64	0,21	0,07	0,27	0,30	1,33	0,64	1,86	372
0,21	1,00	1,09	**6,20**	174000	0,26	3,56	**6,18**	4,18	1,02	1,55	0,21	0,05	0,27	0,32	1,32	0,58	1,86	389
0,22	1,02	1,19	**5,83**	182000	0,27	3,83	**5,80**	4,37	1,03	1,46	0,22	0,04	0,26	0,33	1,31	0,53	1,85	409
0,23	1,03	1,30	**5,45**	190000	0,28	4,09	**5,37**	4,56	1,04	1,37	0,31	0,05	0,36	0,33	1,30	0,48	1,83	433
0,24	1,04	1,32	**5,08**	190000	0,28	4,45	**5,18**	4,63	1,05	1,34	0,31	0,03	0,34	0,34	1,29	0,44	1,81	438
0,25	1,05	1,34	**4,72**	187000	0,28	4,79	**4,70**	4,80	1,06	1,26	0,30	0,02	0,32	0,34	1,29	0,38	1,74	447
0,26	1,06	1,38	**4,37**	188000	0,28	5,12	**4,41**	4,91	1,07	1,21	0,29	0,01	0,30	0,33	1,25	0,34	1,70	460
0,27	1,07	1,43	**4,04**	189000	0,28	5,42	**4,04**	5,05	1,08	1,14	0,28	0,00	0,28	0,33	1,25	0,28	1,65	477

t	r_{i-1}	m_{bi}	m_{ui}	p_i	ρ_{bi}	m_{si}	m_{ui}	V_{bi}	r_i	x_i	dm_{sbi}	dm_{sui}	dm_{si}	dm_{bi}	γ_{mix}	ρ_{mix}	ρ_{ui}	T_{ui}
0,31	1,11	1,65	**2,78**	200000	0,30	6,49	**2 77**	5,50	1,11	0,93	0,27	0,00	0,27	0,30	1,25	0,30	1,39	602
,28	1,08	1,48	**3,71**	191000	0,29	5,70	**3,73**	5,17	1,09	1,09	0,26	0,00	0,26	0,33	1,25	0,29	1,60	498
,29	1,09	1,54	**3,39**	195000	0,29	5,96	**3,38**	5,29	1,10	1,03	0,26	0, 00	0,26	0,32	1,25	0,29	1,53	531
0,3	1,10	1,60	**3,08**	198000	0,30	6,23	**3,05**	5,41	1,11	0,98	0,27	0,00	0,27	0,31	1,25	0,30	1,46	567
0,32	1,11	1,68	**2,49**	200000	0,30	6,77	**2,48**	5,60	1,12	0,89	0,27	0,00	0,27	0,29	1,25	0,30	1,31	637
0,33	1,12	1,69	**2,21**	198000	0,30	7,04	**2,17**	5,72	1,13	0,83	0,27	0,00	0,27	0,28	1,25	0,30	1,22	678
0,34	1,13	1,70	**1,94**	196000	0,29	7,31	**1,97**	5,80	1,13	0,80	0,27	0,00	0,27	0,26	1,25	0,29	1,15	707
0,35	1,13	1,69	**1,69**	191000	0,29	7,58	**1,67**	5,92	1,14	0,74	0,26	0,00	0,26	0,25	1,25	0,29	1,06	754
0,36	1,14	1,68	**1,46**	186000	0,28	7,85	**1,42**	6,03	1,15	0,69	0,26	0,00	0,26	0,23	1,25	0,28	0,97	799
0,37	1,15	1,66	**1,24**	180000	0,27	8,11	**1,21**	6,14	1,15	0,63	0,25	0,00	0,25	0,22	1,25	0,27	0,89	842
0,38	1,15	1,62	**1,04**	173000	0,26	8,36	**1,00**	6,26	1,16	0,58	0,24	0,00	0,24	0,20	1,25	0,26	0,81	892
0,39	1,16	1,58	**0,86**	166000	0,25	8,60	**0,85**	6,37	1,17	0,53	0,16	0,00	0,16	0,19	1,25	0,25	0,75	927
0,4	1,17	1,60	**0,68**	166000	0,25	8,76	**0,63**	6,46	1,17	0,49	0,16	0,00	0,16	0,17	1,25	0,25	0,60	1144
0,41	1,17	1,62	**0,54**	166000	0,25	8,92	**0,50**	6,51	1,18	0,46	0,16	0,00	0,16	0,14	1,25	0,25	0,51	1364
0,42	1,18	1,60	**0,42**	162000	0,24	9,08	**0,37**	6,60	1,18	0,42	0,16	0,00	0,16	0,12	1,25	0,24	0,40	1667
0,43	1,18	1,56	**0,33**	157000	0,24	9,24	**0,34**	6,65	1,18	0,40	0,15	0,00	0,15	0,10	1,25	0,24	0,40	1655
0,44	1,18	1,51	**0,23**	149000	0,22	9,39	**0,24**	6,76	1,19	0,35	0,14	0,00	0,14	0,09	1,25	0,22	0,32	1927
0,45	1,19	1,46	**0,15**	142000	0,21	9,53	**0,15**	6,86	1,20	0,30	0,13	0,00	0,13	0,08	1,25	0,21	0,23	2584
0,46	1,20	1,40	**0,10**	135000	0,20	9,66	**0,11**	6,95	1,20	0,26	0,12	0,00	0,12	0,06	1,25	0,20	0,19	2920

Table 4-7. Model No. II. Numerical Values of Model Variables Properties for Each Time Interval

Model No. III. Tank 7,5 m^3 of Free Volume, Control Volume 5 m^3, Turbulence Factor = 4.

The model was run for these conditions.

The results are in Table 4-8.

If the accident scene had been of this kind it would have been possible to reach the self-ignition temperature leading tank to burst.

Self-ignition of unburned mixture at about the 0,21 s stage was recorded.

As discussed later, if the container had exploded by the maximum pressure reached in the corresponding model to 245 000 Pa, it was not possible that a person had moved a great distance, and there would not have been damage to the vessel walls as illustrated in the photographs of the proceedings.

Consequently the alternative that the tank had exploded by the internal pressure in would not be admissible. By contrary or the hypothesis of self-ignition detonation would be valid.

t	r_{i-1}	m_{bi}	m_{ui}	p_i	ρ_{bi}	m_{si}	m_{ui}	V_{bi}	r_i	x_i	dm_{sbi}	dm_{sui}	dm_{si}	dm_{bi}	γ_{mix}	ρ_{mix}	ρ_{ui}	T_{ui}
0,01	0,02	0,00	**11,19**	101300	0,15	0,00	**11,17**	0,00	0,02	3,50	0,00	0,00	0,00	0,01	1,36	1, 50	1,49	283
0,02	0,02	0,01	**11,18**	102000	0,15	0,00	**11,12**	0,07	0,26	3,47	0,00	0,05	0,05	0,00	1,36	1,49	1,50	284
0,03	0,26	0,01	**11,12**	102000	0,15	0,05	**11,12**	0,07	0,26	3,47	0,00	0,05	0,05	0,02	1,36	1,49	1,50	284
0,04	0,26	0,03	**11,05**	102000	0,15	0,11	**10,90**	0,22	0,38	3,40	0,00	0,05	0,05	0,02	1,36	1,48	1,50	284
0,05	0,38	0,06	**10,97**	105000	0,16	0,16	**10,91**	0,36	0,45	3,34	0,01	0,12	0,12	0,05	1,36	1,47	1,53	286
0,06	0,45	0,10	**10,80**	107000	0,16	0,29	**10,63**	0,63	0,54	3,21	0,01	0,14	0,15	0,07	1,36	1,44	1,55	288
0,07	0,54	0,16	**10,59**	113000	0,17	0,44	**10,52**	0,95	0,62	3,06	0,03	0,18	0,21	0,10	1,36	1,41	1,61	293
0,08	0,62	0,24	**10,30**	120000	0,18	0,65	**10,31**	1,33	0,69	2,88	0,05	0,20	0,25	0,14	1,36	1,35	1,67	299
0,09	0,69	0,33	**9,96**	127000	0,19	0,90	**9,94**	1,75	0,76	2,69	0,07	0,20	0,28	0,18	1,36	1,27	1,73	306
0,10	0,76	0,44	**9,57**	136000	0,20	1,18	**9,56**	2,18	0,82	2,49	0,11	0,20	0,30	0,23	1,35	1,19	1,80	316
0,11	0,82	0,57	**9,14**	146000	0,22	1,48	**9,13**	2,59	0,87	2,29	0,14	0,18	0,32	0,28	1,35	1,10	1,86	327
0,12	0,87	0,70	**8,69**	157000	0,24	1,80	**8,64**	2,99	0,91	2,11	0,17	0,16	0,33	0,32	1,35	1,01	1,92	342
0,13	0,91	0,85	**8,21**	170000	0,25	2,13	**8,17**	3,35	0,94	1,94	0,20	0,13	0,33	0,36	1,34	0,92	1,97	360
0,14	0,94	1,01	**7,71**	185000	0,28	2,46	**7,71**	3,66	0,97	1,79	0,22	0,11	0,33	0,40	1,34	0,83	2,01	384
0,15	0,97	1,19	**7,20**	201000	0,30	2,80	**7,17**	3,96	1,00	1,65	0,34	0,13	0,47	0,44	1,33	0,74	2,03	413
0,16	1,00	1,29	**6,64**	207000	0,31	3,26	**6,71**	4,15	1,01	1,57	0,35	0,09	0,45	0,46	1,32	0,67	2,00	431
0,17	1,01	1,39	**6,08**	213000	0,32	3,71	**6,11**	4,37	1,03	1,46	0,36	0,07	0,43	0,47	1,31	0,58	1,95	455
0,18	1,03	1,51	**5,54**	220000	0,33	4,14	**5,51**	4,58	1,05	1,36	0,36	0,05	0,41	0,48	1,30	0,52	1,89	485
0,19	1,05	1,63	**5,01**	229000	0,34	4,55	**5,01**	4,75	1,06	1,29	0,36	0,03	0,39	0,48	1,29	0,47	1,82	523
0,20	1,06	1,74	**4,50**	237000	0,35	4,94	**4,47**	4,92	1,07	1,21	0,36	0,02	0,38	0,47	1,27	0,42	1,73	570
0,21	1,07	1,86	**4,01**	245000	0,37	5,32	**3,96**	5,07	1,08	1,14	0,36	0,00	0,36	0,46	1,25	0,37	1,63	628
0,22	1,08	1,96	**3,56**	252000	0,38	5,68	**3,53**	5,18	1,09	1,08	0,34	0,00	0,34	0,32	1,25	0,38	1,52	690
0,23	1,09	1,94	**3,23**	245000	0,37	6,02	**3,20**	5,29	1,10	1,03	0,34	0,00	0,34	0,31	1,25	0,37	1,45	706
0,24	1,10	1,91	**2,93**	236000	0,35	6,36	**2,88**	5,40	1,10	0,98	0,33	0,00	0,33	0,30	1,25	0,35	1,37	718
0,25	1,10	1,87	**2,63**	227000	0,34	6,69	**2,56**	5,51	1,11	0,93	0,32	0,00	0,32	0,28	1,25	0,34	1,29	734
0,26	1,11	1,84	**2,35**	220000	0,33	7,00	**2,37**	5,59	1,12	0,89	0,31	0,00	0,31	0,27	1,25	0,33	1,24	738

t	r_{i-1}	m_{bi}	m_{ui}	p_i	ρ_{bi}	m_{if}	m_{ui}	V_{bi}	r_i	x_i	dm_{sbi}	dm_{sui}	dm_{if}	dm_{bi}	γ_{mix}	ρ_{mix}	ρ_{ui}	T_{ui}
0,27	1,12	1,81	**2,07**	211000	0,32	7,31	**2,06**	5,72	1,13	0,83	0,29	0,00	0,29	0,26	1,25	0,32	1,15	762
0,28	1,13	1,78	**1,81**	203000	0,30	7,60	**1,77**	5,84	1,13	0,77	0,28	0,00	0,28	0,25	1,25	0,30	1,07	792
0,29	1,13	1,74	**1,56**	195000	0,29	7,89	**1,51**	5,96	1,14	0,72	0,27	0,00	0,27	0,23	1,2 5	0,29	0,98	826
0,30	1,14	1,70	**1,33**	187000	0,28	8,16	**1,29**	6,08	1,15	0,66	0,26	0,00	0,26	0,22	1,25	0,28	0,91	859
0,31	1,15	1,66	**1,11**	179000	0,27	8,42	**1,10**	6,19	1,16	0,61	0,18	0,00	0,18	0,20	1,25	0,27	0,84	887
0,32	1,16	1,69	**0,91**	179000	0,27	8,60	**0,84**	6,29	1,16	0,57	0,17	0,00	0,17	0,19	1,25	0,27	0,70	1069
0,33	1,16	1,70	**0,71**	179000	0,27	8,77	**0,67**	6,36	1,17	0,53	0,17	0,00	0,17	0,16	1,25	0,27	0,59	1268
0,34	1,17	1,69	**0,55**	176000	0,26	8,94	**0,57**	6,42	1,17	0,51	0,17	0,00	0,17	0,14	1,25	0,26	0,52	1400
0,35	1,17	1,66	**0,42**	170000	0,25	9,12	**0,45**	6,50	1,18	0,47	0,17	0,00	0,17	0,12	1,25	0,25	0,45	1573
0,36	1,18	1,61	**0,30**	163000	0,24	9,28	**0,34**	6,60	1,18	0,42	0,16	0,00	0,16	0,11	1,25	0,24	0,38	1806

Table 4.8 - Model No. III. Numerical Values of Model Variables Properties for Each Time Interval

Model No. IV. Tank 7,5 m^3 of Free Volume, Volume Control 5 m^3, Turbulence Factor = 5.

The model was run for these conditions.

The results are in Table 4-9.

If the accident scene had been of this kind would have been possible to reach the tank to burst self-ignition temperature.

Self-ignition stage of unburned mixture at about 0.16 s was recorded.

As discussed later, if the container had exploded by the maximum pressure reached in the corresponding model 316000 Pa, it was not possible that a person had moved a great distance, and there would have been damage to the vessel walls as illustrated in the photographs of the proceedings.

Consequently the alternative that the tank had exploded by the internal pressure in the same would not be admissible. By contrast the hypothesis of spontaneous ignition detonation would be valid.

t	r_{i-1}	m_{bi}	m_{ui}	p_i	ρ_{bi}	m_{if}	m_{ui}	V_{bi}	r_i	x_i	dm_{sbi}	dm_{sui}	dm_{if}	dm_{bi}	γ_{mix}	ρ_{mix}	ρ_{ui}	T_{ui}
0,01	0,02	0,00	**11,18**	101300	0,15	0,00	**11,17**	0,00	0,02	3,50	0,00	0,00	0,00	0,02	1,36	1,50	1,49	283
0,02	0,02	0,02	**11,16**	102000	0,15	0,00	**11,02**	0,14	0,33	3,44	0,00	0,05	0,05	0,00	1,36	1,49	1,50	284
0,03	0,33	0,02	**11,10**	103000	0,15	0,05	**11,10**	0,14	0,33	3,44	0,00	0,08	0,08	0,04	1,36	1,49	1,51	285
0,04	0,33	0,06	**10,98**	106000	0,16	0,14	**10,92**	0,40	0,47	3,32	0,00	0,13	0,14	0,05	1,36	1,47	1,54	287
0,05	0,47	0,11	**10,80**	109000	0,16	0,28	**10,75**	0,64	0,54	3,20	0,01	0,16	0,17	0,09	1,36	1,44	1,57	290
0,06	0,54	0,18	**10,54**	116000	0,17	0,45	**10,53**	1,06	0,64	3,01	0,03	0,20	0,23	0,13	1,36	1,40	1,64	296
0,07	0,64	0,28	**10,21**	124000	0,19	0,68	**10,17**	1,53	0,73	2,79	0,06	0,21	0,27	0,19	1,36	1,33	1,71	303
0,08	0,73	0,42	**9,81**	136000	0,20	0,95	**9,82**	2,05	0,80	2,55	0,09	0,21	0,31	0,25	1,35	1,25	1,80	315
0,09	0,80	0,57	**9,34**	150000	0,22	1,26	**9,36**	2,55	0,86	2,31	0,14	0,20	0,34	0,32	1,35	1,15	1,89	330
0,1	0,86	0,76	**8,82**	166000	0,25	1,60	**8,77**	3,05	0,91	2,08	0,18	0,17	0,35	0,39	1,35	1,04	1,97	351
0,11	0,91	0,97	**8,26**	187000	0,28	1,95	**8,25**	3,47	0,95	1,88	0,22	0,14	0,36	0,46	1,34	0,93	2,05	380
0,12	0,95	1,22	**7,66**	211000	0,32	2,31	**7,66**	3,85	0,99	1,71	0,35	0,16	0,51	0,52	1,33	0,82	2,10	419
0,13	0,99	1,38	**6,98**	224000	0,34	2,81	**6,96**	4,13	1,01	1,58	0,38	0,11	0,49	0,57	1,32	0,73	2,07	452
0,14	1,01	1,58	**6,30**	241000	0,36	3,30	**6,31**	4,37	1,03	1,46	0,39	0,08	0,48	0,59	1,31	0,64	2,02	497
0,15	1,03	1,77	**5,62**	257000	0,38	3,78	**5,56**	4,61	1,05	1,35	0,40	0,06	0,46	0,60	1,30	0,57	1,93	556
0,16	1,05	1,97	**4,96**	275000	0,41	4,24	**4,94**	4,79	1,06	1,27	0,41	0,03	0,45	0,59	1,28	0,52	1,82	630
0,17	1,06	2,15	**4,34**	291000	0,44	4,69	**4,32**	4,94	1,07	1,20	0,42	0,02	0,44	0,57	1,27	0,48	1,69	719
0,18	1,07	2,31	**3,74**	304000	0,46	5,13	**3,73**	5,07	1,08	1,14	0,43	0,00	0,43	0,54	1,25	0,45	1,53	826
0,19	1,08	2,42	**3,20**	312000	0,47	5,56	**3,19**	5,18	1,09	1,08	0,42	0,00	0,42	0,50	1,25	0,44	1,38	944
0,2	1,09	2,50	**2,70**	316000	0,47	5,98	**2,70**	5,29	1,10	1,03	0,42	0,00	0,42	0,46	1,25	0,44	1,22	1079
0,21	1,10	2,54	**2,24**	314000	0,47	6,40	**2,20**	5,41	1,11	0,98	0,41	0,00	0,41	0,41	1,25	0,43	1,05	1244
0,22	1,11	2,54	**1,83**	308000	0,46	6,81	**1,83**	5,51	1,11	0,93	0,41	0,00	0,41	0,36	1,25	0,43	0,92	1399
0,23	1,11	2,49	**1,47**	296000	0,44	7,22	**1,47**	5,63	1,12	0,87	0,40	0,00	0,40	0,32	1,25	0,41	0,79	1570
0,24	1,12	2,41	**1,15**	280000	0,42	7,62	**1,16**	5,76	1,13	0,82	0,38	0,00	0,38	0,28	1,25	0,40	0,66	1755
0,25	1,13	2,31	**0,87**	261000	0,39	8,00	**0,85**	5,91	1,14	0,75	0,36	0,00	0,36	0,24	1,25	0,38	0,53	2039

t	r_{i-1}	m_{bi}	m_{ui}	p_i	ρ_{bi}	m_{if}	m_{ui}	V_{bi}	r_i	x_i	dm_{sbi}	dm_{sui}	dm_{if}	dm_{bi}	γ_{mix}	ρ_{mix}	ρ_{ui}	T_{ui}
0,26	1,14	2,18	**0,64**	241000	0,36	8,36	**0,63**	6,05	1,15	0,68	0,34	0,00	0,34	0,19	1,25	0,37	0,43	2320
0,27	1,15	2,04	**0,44**	219000	0,33	8,70	**0,43**	6,22	1,16	0,60	0,32	0,00	0,32	0,16	1,25	0,35	0,34	2709

Table 4.9 - Model No. IV. Numerical Values of Model Variables Properties for Each Time Interval

Model No. V. Tank 7,5 m^3 of Free Volume, Control Volume 1 m^3, Turbulence Factor = 3.

The model was run for these conditions.

The results are shown in Table 4-10.

If the accident scene had been of this kind would have been possible to reach the tank to burst self-ignition temperature.

Self-ignition stage of unburned mixture at about 0, 41 s was recorded.

As discussed later, if the container had exploded by the maximum pressure reached in the corresponding model to 219 000 Pa, it was not possible that a person had moved a great distance, and there would have been damage to the vessel walls as illustrated in the photographs of the proceedings.

Consequently the alternative that the tank had exploded by the internal pressure would not be admissible. By contrast the hypothesis of self-ignition detonation would be valid.

t	r_{i-1}	m_{bi}	m_{ui}	p_i	ρ_{bi}	m_{if}	m_{ui}	V_{bi}	r_i	x_i	dm_{sbi}	dm_{sui}	dm_{if}	dm_{bi}	γ_{mix}	ρ_{mix}	ρ_{ui}	T_{ui}
0,01	0,01	0,00	**11,20**	101300	0,15	0,00	**11,17**	0,00	0,01	3,50	0,00	0,00	0,00	0,00	1,36	1,52	1,49	283
0,02	0,01	0,00	**11,19**	101300	0,15	0,00	**11,17**	0,00	0,05	3,50	0,00	0,00	0,00	0,00	1,36	1,51	1,49	283
0,03	0,05	0,00	**11,19**	101300	0,15	0,00	**11,17**	0,00	0,10	3,50	0,00	0,00	0,00	0,00	1,36	1,51	1,49	283
0,04	0,10	0,00	**11,19**	101300	0,15	0,00	**11,14**	0,02	0,17	3,49	0,00	0,00	0,00	0,00	1,36	1,51	1,49	283
0,05	0,17	0,01	**11,19**	102000	0,15	0,00	**11,14**	0,06	0,25	3,48	0,00	0,05	0,05	0,01	1,36	1,51	1,50	284
0,06	0,25	0,02	**11,13**	103000	0,15	0,05	**11,11**	0,13	0,32	3,44	0,01	0,08	0,09	0,02	1,36	1,46	1,51	285
0,07	0,32	0,03	**11,03**	104000	0,16	0,14	**11,07**	0,21	0,37	3,41	0,01	0,09	0,11	0,03	1,36	1,34	1,52	285
0,08	0,37	0,05	**10,91**	104000	0,16	0,25	**10,92**	0,31	0,42	3,36	0,02	0,08	0,10	0,04	1,36	1,19	1,52	285
0,09	0,42	0,07	**10,80**	104000	0,16	0,35	**10,75**	0,42	0,47	3,31	0,03	0,07	0,10	0,05	1,36	1,09	1,52	286
0,1	0,47	0,08	**10,68**	105000	0,16	0,44	**10,70**	0,50	0,50	3,27	0,04	0,06	0,11	0,06	1,35	1,00	1,53	286
0,11	0,50	0,09	**10,57**	105000	0,16	0,55	**10,56**	0,59	0,53	3,23	0,05	0,05	0,10	0,06	1,35	0,83	1,53	286
0,12	0,53	0,11	**10,45**	105000	0,16	0,65	**10,38**	0,70	0,56	3,18	0,05	0,04	0,09	0,07	1,35	0,73	1,53	287
0,13	0,56	0,12	**10,34**	106000	0,16	0,74	**10,33**	0,78	0,58	3,14	0,07	0,03	0,10	0,08	1,34	0,63	1,54	287
0,14	0,58	0,14	**10,23**	106000	0,16	0,84	**10,16**	0,89	0,61	3,09	0,07	0,02	0,09	0,09	1,33	0,47	1,54	287
0,15	0,61	0,15	**10,12**	107000	0,16	0,93	**10,14**	0,94	0,62	3,06	0,09	0,00	0,09	0,10	1,31	0,38	1,55	288
0,16	0,62	0,17	**10,03**	108000	0,16	1,01	**10,05**	1,04	0,64	3,02	0,08	0,00	0,08	0,10	1,25	0,16	1,56	289
0,17	0,64	0,21	**9,93**	112000	0,17	1,10	**9,97**	1,25	0,68	2,92	0,07	0,00	0,07	0,11	1,25	0,17	1,59	293
0,18	0,68	0,26	**9,82**	116000	0,17	1,16	**9,82**	1,48	0,72	2,82	0,08	0,00	0,08	0,12	1,25	0,17	1,63	296
0,19	0,72	0,31	**9,69**	121000	0,18	1,24	**9,70**	1,71	0,75	2,71	0,09	0,00	0,09	0,14	1,25	0,18	1,67	301
0,2	0,75	0,37	**9,55**	127000	0,19	1,33	**9,58**	1,94	0,79	2,60	0,10	0,00	0,10	0,16	1,25	0,19	1,72	307
0,21	0,79	0,44	**9,39**	133000	0,20	1,43	**9,37**	2,20	0,82	2,47	0,11	0,00	0,11	0,18	1,25	0,20	1,77	313
0,22	0,82	0,52	**9,21**	141000	0,21	1,54	**9,22**	2,45	0,85	2,36	0,12	0,00	0,12	0,20	1,25	0,21	1,83	322
0,23	0,85	0,61	**9,01**	149000	0,22	1,67	**8,96**	2,72	0,88	2,23	0,13	0,00	0,13	0,22	1,25	0,22	1,88	331
0,24	0,88	0,71	**8,78**	159000	0,24	1,80	**8,75**	2,97	0,91	2,12	0,15	0,00	0,15	0,25	1,25	0,24	1,93	343
0,25	0,91	0,82	**8,53**	170000	0,25	1,95	**8,50**	3,21	0,93	2,00	0,16	0,00	0,16	0,27	1,25	0,25	1,98	357
0,26	0,93	0,94	**8,27**	182000	0,27	2,11	**8,23**	3,44	0,95	1,90	0,17	0,00	0,17	0,29	1,25	0,27	2,03	374
0,27	0,95	1,00	**7,98**	187000	0,28	2,28	**8,02**	3,56	0,96	1,84	0,25	0,00	0,25	0,31	1,25	0,28	2,04	383

t	r_{i-1}	m_{bi}	m_{ui}	p_i	ρ_{bi}	m_{if}	m_{ui}	V_{bi}	r_i	x_i	dm_{sbi}	dm_{sui}	dm_{if}	dm_{bi}	γ_{mix}	ρ_{mix}	ρ_{ui}	T_{ui}
0,28	0,96	1,06	**7,66**	191000	0,29	2,53	**7,72**	3,70	0,97	1,78	0,26	0,00	0,26	0,32	1,25	0,29	2,03	391
0, 29	0,97	1,12	**7,34**	195000	0,29	2,79	**7,40**	3,84	0,99	1,71	0,26	0,00	0,26	0,33	1,25	0,29	2,02	401
0,3	0,99	1,19	**7,01**	199000	0,30	3,05	**7,06**	3,99	1,00	1,64	0,27	0,00	0,27	0, 34	1,25	0,30	2,01	412
0,31	1,00	1,25	**6,68**	203000	0,30	3,32	**6,72**	4,13	1,01	1,58	0,28	0,00	0,28	0,34	1,25	0,30	1,99	425
0,32	1,01	1,32	**6,34**	207000	0,31	3,60	**6,39**	4,26	1,02	1,52	0,28	0,00	0,28	0,35	1,25	0,31	1,97	438
0,33	1,02	1,38	**5,99**	210000	0,31	3,88	**6,00**	4,40	1,03	1,45	0,29	0,00	0,29	0,35	1,25	0,31	1,93	452
0,34	1,03	1,44	**5,64**	213000	0,32	4,16	**5,64**	4,53	1,04	1,39	0,29	0,00	0,29	0,35	1,25	0,32	1,90	468
0,35	1,04	1,50	**5,29**	216000	0,32	4,45	**5,32**	4,64	1,05	1,34	0,29	0,00	0,29	0,35	1,25	0,32	1,86	485
0,36	1,05	1,55	**4,94**	219000	0,33	4,75	**5,05**	4,73	1,06	1,30	0,30	0,00	0,30	0,35	1,25	0,33	1,82	501
0,37	1,06	1,60	**4,60**	219000	0,33	5,05	**4,61**	4,87	1,07	1,23	0,30	0,00	0,30	0,35	1,25	0,33	1,75	521
0,38	1,07	1,64	**4,25**	219000	0,33	5,35	**4,23**	4,99	1,08	1,17	0,30	0,00	0,30	0,34	1,25	0,33	1,69	541
0,39	1,08	1,67	**3,91**	219000	0,33	5,64	**3,92**	5,09	1,08	1,13	0,30	0,00	0,30	0,33	1,25	0,33	1,63	560
0,4	1,08	1,70	**3,58**	218000	0,33	5,94	**3,61**	5,19	1,09	1,08	0,30	0,00	0,30	0,33	1,25	0,33	1,56	581
0,41	1,09	1,72	**3,25**	215000	0,32	6,24	**3,20**	5,33	1,10	1,01	0,30	0,00	0,30	0,32	1,25	0,32	1,48	607
0,42	1,10	1,73	**2,94**	213000	0,32	6,54	**2,96**	5,41	1,11	0,97	0,29	0,00	0,29	0,30	1,25	0,32	1,42	626
0,43	1,11	1,73	**2,63**	209000	0,31	6,83	**2,61**	5,54	1,11	0,92	0,29	0,00	0,29	0,29	1,25	0,31	1,33	654
0,44	1,11	1,73	**2,34**	205000	0,31	7,12	**2,35**	5,64	1,12	0,87	0,28	0,00	0,28	0,28	1,25	0,31	1,26	678
0,45	1,12	1,72	**2,06**	200000	0,30	7,41	**2,06**	5,75	1,13	0,82	0,28	0,00	0,28	0,27	1,25	0,30	1,18	708
0,46	1,13	1,71	**1,79**	194000	0,29	7,68	**1,76**	5,88	1,14	0,76	0, 27	0,00	0,27	0,25	1,25	0,29	1,08	745
0,47	1,14	1,68	**1,53**	188000	0,28	7,95	**1,54**	5,98	1,14	0,71	0,26	0,00	0,26	0,24	1,25	0,28	1,01	774
0,48	1,14	1,66	**1,29**	181000	0,27	8,21	**1,27**	6,11	1,15	0,65	0,25	0,00	0,25	0,23	1,25	0,27	0,92	821
0,49	1,15	1,62	**1,07**	174000	0,26	8,47	**1,09**	6,22	1,16	0,60	0,24	0,00	0,24	0,21	1,25	0,26	0,85	853
0,5	1,16	1,58	**0,86**	166000	0,25	8,71	**0,84**	6,37	1,17	0,53	0,23	0,00	0,23	0,19	1,25	0,25	0,75	928
0,51	1,17	1,53	**0,67**	157000	0,24	8,94	**0,61**	6,53	1,18	0,45	0,22	0,00	0,22	0,17	1,25	0,24	0,63	1043

t	r_{i-1}	m_{bi}	m_{ui}	p_i	ρ_{bi}	m_{if}	m_{ui}	V_{bi}	r_i	x_i	dm_{sbi}	dm_{sui}	dm_{if}	dm_{bi}	γ_{mix}	ρ_{mix}	ρ_{ui}	T_{ui}
0,52	1,18	1,47	**0,49**	148000	0,22	9,16	**0,49**	6,65	1,18	0,40	0,21	0,00	0,21	0,15	1,25	0,22	0,57	1073
0,53	1,18	1,41	**0,35**	139000	0,21	9,37	**0,34**	6,79	1,19	0,33	0,20	0,00	0,20	0,14	1,25	0,21	0,49	1194

Table 4.10 - Model No. V. Numerical Values of Model Variables Properties for Each Time Interval

Model No. VI. Tank 7,5m^3 Free Volume, Control Volume 1 m^3, Turbulence Factor = 4

The model was run for these conditions.

The results are in Table 4-11.

If the accident scene had been of this kind would have been possible to reach the tank to burst self-ignition temperature.

Self-ignition stage of unburned mixture at about 0.24 s was recorded.

As discussed later, if the container had exploded by the maximum pressure reached in the corresponding model 293000 Pa, it was not possible that a person had moved a great distance, and there would not have been damage to the vessel walls as illustrated in the photographs of the proceedings.

Consequently the alternative that the tank had exploded by the internal pressure would not be admissible. By contrast the hypothesis of self-ignition detonation would be valid.

.

t	r_{i-1}	m_{bi}	m_{ui}	p_i	ρ_{bi}	m_{if}	m_{ui}	V_{bi}	r_i	x_i	dm_{sbi}	dm_{sui}	dm_{if}	dm_{bi}	γ_{mix}	ρ_{mix}	ρ_{ui}	T_{ui}
0,01	0,02	0,00	**11,19**	101300	0,15	0,00	**11,17**	0,00	0,02	3,50	0,00	0,00	0,00	0,01	1,36	1,52	1,49	283
0,02	0,02	0,00	**11,19**	101300	0,15	0,00	**11,17**	0,00	0,06	3,50	0,00	0,00	0,00	0,00	1,36	1,50	1,49	283
0,03	0,06	0,00	**11,19**	101300	0,15	0,00	**11,16**	0,01	0,13	3,50	0,00	0,00	0,00	0,00	1,36	1,50	1,49	283
0,04	0,13	0,01	**11,18**	101300	0,15	0,00	**11,10**	0,05	0,23	3,48	0,00	0,00	0,00	0,01	1,36	1,50	1,49	283
0,05	0,23	0,02	**11,08**	103000	0,15	0,00	**11,09**	0,14	0,33	3,44	0,00	0,08	0,09	0,02	1,36	1,50	1,51	285
0,06	0,33	0,04	**10,94**	105000	0,16	0,09	**11,06**	0,27	0,40	3,38	0,02	0,11	0,12	0,04	1,36	1,30	1,53	286
0,07	0,40	0,07	**10,80**	105000	0,16	0,21	**10,79**	0,44	0,48	3,30	0,03	0,08	0,12	0,06	1,36	1,04	1,53	286
0,08	0,48	0,10	**10,65**	106000	0,16	0,33	**10,58**	0,62	0,54	3,22	0,05	0,07	0,12	0,08	1,35	0,93	1,54	287
0,09	0,54	0,12	**10,50**	108000	0,16	0,44	**10,53**	0,74	0,57	3,16	0,08	0,05	0,13	0,10	1,34	0,75	1,56	289
0,1	0,57	0,14	**10,35**	109000	0,16	0,57	**10,37**	0,88	0,60	3,09	0,09	0,03	0,12	0,12	1,33	0,49	1,57	290
0,11	0,60	0,18	**10,21**	111000	0,17	0,70	**10,20**	1,07	0,64	3,01	0,10	0,01	0,11	0,13	1,31	0,17	1,59	292
0,12	0,64	0,25	**10,05**	117000	0,18	0,81	**9,98**	1,42	0,71	2,84	0,08	0,00	0,08	0,15	1,25	0,18	1,64	297
0,13	0,71	0,34	**9,86**	126000	0,19	0,89	**9,79**	1,80	0,77	2,66	0,10	0,00	0,10	0,19	1,25	0,19	1,72	306
0,14	0,77	0,45	**9,63**	138000	0,21	0,98	**9,60**	2,20	0,82	2,48	0,12	0,00	0,12	0,23	1,25	0,21	1,81	317
0,15	0,82	0,60	**9,35**	153000	0,23	1,10	**9,35**	2,61	0,87	2,29	0,14	0,00	0,14	0,28	1,25	0,23	1,91	333
0,16	0,87	0,77	**9,02**	171000	0,26	1,24	**9,01**	3,02	0,91	2,10	0,16	0,00	0,16	0,33	1,25	0,26	2,01	355
0,17	0,91	0,98	**8,64**	193000	0,29	1,39	**8,62**	3,39	0,95	1,92	0,18	0,00	0,18	0,38	1,25	0,29	2,10	384
0,18	0,95	1,14	**8,21**	208000	0,31	1,57	**8,18**	3,65	0,97	1,80	0,27	0,00	0,27	0,43	1,25	0,31	2,13	408
0,19	0,97	1,30	**7,75**	224000	0,34	1,84	**7,74**	3,88	0,99	1,69	0,30	0,00	0,30	0,46	1,25	0,34	2,14	436
0,2	0,99	1,47	**7,26**	240000	0,36	2,14	**7,29**	4,08	1,01	1,60	0,32	0,00	0,32	0,48	1,25	0,36	2,13	469
0,21	1,01	1,63	**6,77**	254000	0,38	2,46	**6,74**	4,28	1,02	1,51	0,34	0,00	0,34	0,50	1,25	0,38	2,09	506
0,22	1,02	1,77	**6,26**	267000	0,40	2,80	**6,24**	4,44	1,04	1,43	0,36	0,00	0,36	0,50	1,25	0,40	2,04	546
0,23	1,04	1,90	**5,76**	278000	0,42	3,15	**5,77**	4,57	1,05	1,37	0,37	0,00	0,37	0,50	1,2 5	0,42	1,97	588
0,24	1,05	2,01	**5,27**	286000	0,43	3,52	**5,28**	4,70	1,06	1,31	0,39	0,00	0,39	0,50	1,25	0,43	1,89	632
0,25	1,06	2,10	**4,78**	291000	0,44	3,91	**4,79**	4,82	1,06	1,25	0,39	0,00	0,39	0,48	1,25	0,44	1,79	678

t	r_{i-1}	m_{bi}	m_{ui}	p_i	ρ_{bi}	m_{if}	m_{ui}	V_{bi}	r_i	x_i	dm_{sbi}	dm_{sui}	dm_{if}	dm_{bi}	γ_{mix}	ρ_{mix}	ρ_{ui}	T_{ui}
0,26	1,06	2,17	**4,32**	293000	0,44	4,31	**4,31**	4,94	1,07	1,20	0,40	0,00	0,40	0,47	1,25	0,44	1,68	726
0,27	1,07	2,21	**3,87**	292000	0,44	4,71	**3,83**	5,06	1,08	1,14	0,40	0,00	0,40	0,45	1,25	0,44	1,57	776
0,28	1,08	2,23	**3, 45**	290000	0,43	5,11	**3,48**	5,15	1,09	1,10	0,40	0,00	0,40	0,42	1,25	0,43	1,48	817
0,29	1,09	2,24	**3,05**	285000	0,43	5,50	**3,07**	5,26	1,10	1,05	0,39	0,00	0,39	0,40	1,25	0,43	1,37	868
0,3	1,10	2,24	**2,67**	278000	0,42	5,90	**2,67**	5,37	1,10	0,99	0,39	0,00	0,39	0,38	1,25	0,42	1,26	923
0,31	1,10	2,21	**2,32**	269000	0,40	6,28	**2,28**	5,49	1,11	0,94	0,37	0,00	0,37	0,35	1,25	0,40	1,14	986
0,32	1,11	2,17	**2,00**	260000	0,39	6,66	**2,03**	5,58	1,12	0,90	0,36	0,00	0,36	0,32	1,25	0,39	1,06	1021
0,33	1,12	2,13	**1,69**	249000	0,37	7,02	**1,68**	5,71	1,13	0,83	0,35	0,00	0,35	0,30	1,25	0,37	0,94	1100
0,34	1,13	2,07	**1,42**	237000	0,35	7,37	**1,39**	5,84	1,13	0,77	0,33	0,00	0,33	0,28	1,25	0,35	0,84	1180
0,35	1,13	2,00	**1,17**	225000	0,34	7,70	**1,18**	5,95	1,14	0,72	0,32	0,00	0,32	0,25	1,25	0,34	0,76	1227
0,36	1,14	1,93	**0,94**	212000	0,32	8,02	**0,91**	6,10	1,15	0,66	0,30	0,00	0,30	0,23	1,25	0,32	0,65	1360
0,37	1,15	1,85	**0,74**	199000	0,30	8,32	**0,75**	6,21	1,16	0,60	0,28	0,00	0,28	0,20	1,25	0,30	0,59	1413
0,38	1,16	1,77	**0,56**	186000	0,28	8,60	**0,57**	6,35	1,17	0,54	0,26	0,00	0,26	0,18	1,25	0,28	0,50	1550
0,39	1,17	1,68	**0,40**	172000	0,26	8,86	**0,36**	6,53	1,18	0,45	0,24	0,00	0,24	0,16	1,25	0,26	0,37	1946

Table 4.11 - Model No. VI. Numerical Values of Model Variables Properties for Each Time Interval

Model No. VII. Tank 7,5m^3 Free Volume, Control Volume 1 m^3, Turbulence Factor = 5

The model was run for these conditions.

The results are shown in Table 4-12.

If the accident scene had been of this kind would have been possible to reach the tank to burst self-ignition temperature.

Self-ignition stage of unburned mixture at about 0.16 s was recorded.

As discussed later, if the container had exploded by the maximum pressure reached in the corresponding model 343000 Pa, it was not possible that a person had moved a great distance, and there would have been damage to the vessel walls as illustrated in the photographs of the actuac ions.

Consequently the alternative that the tank had exploded by the internal pressure in the same would not be admissible. By contrast the hypothesis of spontaneous ignition detonation would be valid.

t	r_{i-1}	m_{bi}	m_{ui}	p_i	ρ_{bi}	m_{if}	m_{ui}	V_{bi}	r_i	x_i	dm_{sbi}	dm_{sui}	dm_{if}	dm_{bi}	γ_{mix}	ρ_{mix}	ρ_{ui}	T_{ui}
0,01	0,02	0,00	**11,19**	101300	0,15	0,00	**11,17**	0,00	0,01	3,50	0,00	0,00	0,00	0,01	1,36	11,20	1,49	283
0,02	0,01	0,01	**10,96**	103000	0,15	0,00	**11,26**	0,04	0,21	3,49	0,00	0,23	0,23	0,00	1,36	1,51	1,51	285
0,03	0,21	0 02	**10,86**	103000	0,15	0,23	**11,10**	0,14	0,32	3,44	0,00	0,08	0,09	0,02	1,36	1,16	1,51	285
0,04	0,32	0,06	**10,75**	103000	0,15	0,32	**10,77**	0,36	0,45	3,34	0,01	0,06	0,07	0,04	1,36	1,08	1,51	285
0,05	0,45	0,10	**10,59**	106000	0,16	0,39	**10,59**	0,61	0,53	3,22	0,04	0,08	0,12	0,08	1,35	1,01	1,54	287
0,06	0,53	0,13	**10,41**	109000	0,16	0,51	**10,49**	0,81	0,59	3,13	0,09	0,06	0,14	0,12	1,34	0,69	1,57	290
0,07	0,59	0,18	**10,24**	111000	0,17	0,65	**10,21**	1,06	0,64	3,01	0,11	0,03	0,13	0,15	1,25	0,17	1,59	292
0,08	0,64	0,27	**10,05**	121000	0,18	0,79	**10,06**	1,50	0,72	2,80	0,09	0,00	0,09	0,18	1,25	0,18	1,68	301
0,09	0,72	0,41	**9,81**	134000	0,20	0,87	**9,77**	2,02	0,80	2,56	0,11	0,00	0,11	0,24	1,25	0,20	1,78	313
0,10	0,80	0,59	**9,49**	153000	0,23	0,99	**9,44**	2,57	0,86	2,30	0,13	0,00	0,13	0,32	1,25	0,23	1,91	333
0,11	0,86	0,83	**9,09**	179000	0,27	1,12	**9,06**	3,09	0,92	2,06	0,16	0,00	0,16	0,40	1,25	0,27	2,05	363
0,12	0,92	1,05	**8,61**	203000	0,30	1,28	**8,66**	3,46	0,95	1,89	0,26	0,00	0,26	0,48	1,25	0,30	2,14	395
0,13	0,95	1,30	**8,07**	228000	0,34	1,54	**8,04**	3,81	0,98	1,73	0,29	0,00	0,29	0,54	1,25	0,34	2,18	436
0,14	0,98	1,56	**7,48**	255000	0,38	1,84	**7,44**	4,08	1,01	1,60	0,33	0,00	0,33	0,59	1,25	0,38	2,18	488
0,15	1,01	1,81	**6,86**	282000	0,42	2,17	**6,89**	4,29	1,02	1,50	0,37	0,00	0,37	0,62	1,25	0,42	2,15	548
0,16	1,02	2,04	**6,23**	305000	0,46	2,53	**6,28**	4,46	1,04	1,42	0,40	0,00	0,40	0,63	1,25	0,46	2,07	615
0,17	1,04	2,23	**5,60**	322000	0,48	2,93	**5,58**	4,63	1,05	1,34	0,43	0,00	0,43	0,62	1,25	0,48	1,94	690
0,18	1,05	2,38	**5,00**	335000	0,50	3,36	**5,02**	4,75	1,06	1,28	0,45	0,00	0,45	0,60	1,25	0,50	1,83	765
0,19	1,06	2,49	**4,43**	342000	0,51	3,81	**4,45**	4,87	1,07	1,23	0,46	0,00	0,46	0,57	1,25	0,51	1,69	843
0,20	1,07	2,56	**3,89**	343000	0,51	4,28	**3,86**	4,99	1,08	1,17	0,47	0,00	0,47	0,54	1,25	0,51	1,54	928
0,21	1,08	2,60	**3,39**	340000	0,51	4,74	**3,37**	5,10	1,08	1,12	0,47	0,00	0,47	0,50	1,25	0,51	1,41	1008
0,22	1,08	2,60	**2,93**	333000	0,50	5,21	**2,91**	5,21	1,09	1,07	0,46	0,00	0,46	0,46	1,25	0,50	1,27	1092

m_{ui}	p_i	ρ_{bi}	m_{if}	m_{ui}	V_{bi}	r_i	x_i	dm_{sbi}	dm_{sui}	dm_{if}	dm_{bi}	γ_{mix}	ρ_{mix}	ρ_{ui}	T_{ui}
2,50	323000	0,48	5,67	**2,49**	5,32	1,10	1,02	0,45	0,00	0,45	0,42	1,25	0,48	1,14	1176
2,12	311000	0,47	6,12	**2,14**	5,43	1,11	0,97	0,43	0,00	0,43	0,39	1,25	0,47	1, 03	1254
1,76	297000	0,44	6,56	**1,79**	5,55	1,12	0,91	0,42	0,00	0,42	0,35	1,25	0,44	0,92	1351
1,44	281000	0,42	6,97	**1,43**	5,68	1,12	0,85	0,40	0,00	0,40	0,32	1,25	0,42	0,79	1485
1,16	264000	0,40	7,37	**1,16**	5,81	1,13	0,79	0,37	0,00	0,37	0,28	1,25	0,40	0,69	1604
0,92	247000	0,37	7,74	**0,95**	5,93	1,14	0,73	0,35	0,00	0,35	0,25	1,25	0,37	0,61	1691
0,70	230000	0,34	8,09	**0,75**	6,07	1,15	0,67	0,33	0,00	0,33	0,22	1,25	0,34	0,52	1842
0,50	212000	0,32	8,42	**0,50**	6,23	1,16	0,59	0,30	0,00	0,30	0,19	1,25	0,32	0,39	2254

ɔ. VII. Numerical Values of Variables Model properties for each time interval.

Model No. VIII. Tank Volume 5 m^3, Control Volume 1 m^3 Turbulence Factor = 5

The model was run for these conditions.

The results are shown in Table 4-13.

If the accident scene had been of this kind would have been possible to reach the tank to burst self-ignition temperature.

Self-ignition stage of unburned mixture at about 0.19 s was recorded.

As discussed later, if the container had exploded by the maximum pressure reached in the corresponding model 268000 Pa, it was not possible that a person had moved a great distance, and there would have been damage to the vessel walls as illustrated in the photographs of the proceedings.

Consequently the alternative d and that the tank had exploded by the internal pressure in the same would not be admissible. By contrast the hypothesis of spontaneous ignition detonation would be valid.

t	r_{i-1}	m_{bi}	m_{ui}	p_i	ρ_{bi}	m_{if}	m_{ui}	V_{bi}	r_i	x_i	dm_{sbi}	dm_{sui}	dm_{if}	dm_{bi}	γ_{mix}	ρ_{mix}	ρ_{ui}	T_{ui}
0,01	0,02	0,00	**7,47**	101300	0,15	0,00	**7,45**	0,00	0,02	3,50	0,00	0,00	0,00	0,02	1,36	1,51	1,49	283
0,02	0,02	0,00	**7,47**	101300	0,15	0,00	**7,45**	0,00	0,08	3,50	0,00	0,00	0,00	0,00	1,36	1,51	1,49	283
0,03	0,08	0,00	**7,41**	102000	0,15	0,00	**7,46**	0 02	0,16	3,48	0,00	0,05	0,06	0,00	1,36	1,51	1,50	284
0,04	0,16	0,01	**7,35**	102000	0,15	0,06	**7,36**	0,08	0,28	3,44	0,00	0,05	0,06	0,01	1,36	1,43	1,50	284
0,05	0,28	0,04	**7,22**	104000	0,16	0,11	**7,24**	0,23	0,39	3,33	0,01	0,10	0,10	0,03	1,36	1,37	1,52	285
0,06	0,39	0,07	**7,05**	106000	0,16	0,21	**7,02**	0,43	0,48	3,19	0,03	0,10	0,13	0,06	1,36	1,18	1,54	287
0,07	0,48	0,10	**6,87**	109000	0,16	0,35	**6,88**	0,61	0,53	3,07	0,07	0,09	0,16	0,10	1,35	0,97	1,57	290
0,08	0,53	0,13	**6,68**	111000	0,17	0,50	**6,70**	0,78	0,58	2,95	0,10	0,06	0,16	0,13	1,34	0,70	1,58	292
0,09	0,58	0,16	**6,50**	114000	0,17	0,66	**6,54**	0,94	0,62	2,84	0,12	0,03	0,15	0,15	1,33	0,47	1,61	295
0,10	0,62	0,20	**6,33**	117000	0,18	0,81	**6,33**	1,14	0,66	2,70	0,13	0,00	0,13	0,17	1,25	0,18	1,64	298
0,11	0,66	0,29	**6,13**	131000	0,20	0,94	**6,15**	1,49	0,72	2,46	0,10	0,00	0,10	0,20	1,25	0,20	1,75	312
0,12	0,72	0,42	**5,88**	149000	0,22	1,05	**5,87**	1,86	0,77	2,19	0,13	0,00	0,13	0,25	1,25	0,22	1,87	332
0,13	0,77	0,57	**5,56**	174000	0,26	1,18	**5,58**	2,20	0,82	1,95	0,16	0,00	0,16	0,31	1,25	0,26	2,00	363
0,14	0,82	0,70	**5,18**	191000	0,29	1,34	**5,20**	2,45	0,85	1,78	0,25	0,00	0,25	0,38	1,25	0,29	2,04	391
0,15	0,85	0,84	**4,77**	210000	0,31	1,58	**4,79**	2,67	0,87	1,63	0,27	0,00	0,27	0,41	1,25	0,31	2,05	426
0,16	0,87	0,98	**4,33**	228000	0,34	1,86	**4,32**	2,86	0,89	1,50	0,30	0,00	0,30	0,44	1,25	0,34	2,02	470
0,17	0,89	1,11	**3,88**	245000	0,37	2,16	**3,89**	3,02	0,91	1,39	0,32	0,00	0,32	0,45	1,25	0,37	1,96	521
0,18	0,91	1,22	**3,43**	258000	0,39	2,48	**3,45**	3,15	0,92	1,30	0,34	0,00	0,34	0,45	1,25	0,39	1,86	578
0,19	0,92	1,30	**2,98**	266000	0,40	2,83	**3,01**	3,27	0,93	1,21	0,36	0,00	0,36	0,44	1,25	0,40	1,74	638
0,20	0,93	1,36	**2,56**	268000	0,40	3,18	**2,54**	3,39	0,95	1,13	0,37	0,00	0,37	0,42	1,25	0,40	1,58	706
0,21	0,95	1,39	**2,16**	266000	0,40	3,55	**2,16**	3,49	0,96	1,05	0,37	0,00	0,37	0,40	1,25	0,40	1,44	771
0,22	0,96	1,40	**1,79**	259000	0,39	3,92	**1,77**	3,61	0,97	0,97	0,36	0,00	0,36	0,37	1,25	0,39	1,27	848
0,23	0,97	1,39	**1,46**	249000	0,37	4,27	**1,45**	3,72	0,98	0,90	0,35	0,00	0,35	0,33	1,25	0,37	1,13	919
0,24	0,98	1,35	**1,16**	236000	0,35	4,62	**1,14**	3,83	0,99	0,82	0,33	0,00	0,33	0,30	1,25	0,35	0,97	1009
0,25	0,99	1,31	**0,90**	221000	0,33	4,95	**0,88**	3,95	1,00	0,73	0,31	0,00	0,31	0,27	1,25	0,33	0,83	1103

t	r_{i-1}	m_{bi}	m_{ui}	p_i	ρ_{bi}	m_{if}	m_{ui}	V_{bi}	r_i	x_i	dm_{sbi}	dm_{sui}	dm_{if}	dm_{bi}	γ_{mix}	ρ_{mix}	ρ_{ui}	T_{ui}
0,26	1,00	1,25	**0,66**	205000	0,31	5,27	**0,67**	4,06	1,01	0,65	0,29	0,00	0,29	0,23	1,25	0,31	0,72	1191
0,27	1,01	1,18	**0,46**	188000	0,28	5,56	**0,46**	4,20	1,02	0,56	0,27	0,00	0,27	0,20	1,25	0,28	0,57	1363

Table 4.13 - Model No. VIII. Numerical Values of Variables Model properties for each Time Interval

Model No. IX. Tank volume 10 m^3 of Royalty, Volume Control 1 m^3 Turbulence Factor = 3

The model was run for these conditions.

The results are shown in Table 4-14.

If the accident scene had been of this kind would have been possible to reach the tank to burst self-ignition temperature.

Self-ignition stage of unburned mixture at about 0.34 s was recorded.

As discussed later, if the container had exploded by the maximum pressure reached in the corresponding model 266000 Pa, it was not possible that a person had moved a great distance, and there would have been damage to the vessel walls as illustrated in the photographs of the proceedings.

Consequently the alternative that the tank had exploded by the internal pressure in the same would not be admissible. By contrast the hypothesis of spontaneous ignition detonation would be valid.

t	r_{i-1}	m_{bi}	m_{ui}	p_i	ρ_{bi}	m_{if}	m_{ui}	V_{bi}	r_i	x_i	dm_{sbi}	dm_{sui}	dm_{if}	dm_{bi}	γ_{mix}	ρ_{mix}	ρ_{ui}	T_{ui}
0,01	0,01	0,00	**14,90**	101300	0,15	0,00	**14,90**	0,00	0,01	3,50	0,00	0,00	0,00	0,00	1,36	1,49	1,49	283
0,02	0,01	0,00	**14,87**	101500	0,15	0,03	**14,88**	0,03	0,20	3,49	0,00	0,03	0,03	0,00	1,36	1,49	1,49	283
0,03	0,20	0,01	**14,83**	101500	0,15	0,06	**14,79**	0,09	0,28	3,47	0,00	0,03	0,03	0,01	1,36	1,44	1,49	283
0,04	0,28	0,03	**14,76**	102000	0,15	0,11	**14,69**	0,19	0,36	3,43	0,00	0,05	0,05	0,02	1,36	1,41	1,50	284
0,05	0,36	0,05	**14,66**	103000	0,15	0,19	**14,62**	0,30	0,42	3,39	0,02	0,07	0,08	0,03	1,36	1,31	1,51	285
0,06	0,42	0,06	**14,54**	104000	0,16	0,29	**14,58**	0,40	0,46	3,36	0,03	0,07	0,10	0,05	1,36	1,14	1,52	285
0,07	0,46	0,08	**14,43**	104000	0,16	0,39	**14,39**	0,52	0,51	3,32	0,04	0,06	0,09	0,06	1,35	0,94	1,52	286
0,08	0,51	0,10	**14,32**	105000	0,16	0,49	**14,35**	0,61	0,53	3,28	0,05	0,05	0,10	0,07	1,35	0,85	1,53	286
0,09	0,53	0,11	**14,21**	105000	0,16	0,58	**14,18**	0,72	0,56	3,25	0,06	0,04	0,09	0,07	1,34	0,66	1,53	286
0,10	0,56	0,13	**14,10**	106000	0,16	0,67	**14,13**	0,81	0,59	3,21	0,07	0,03	0,09	0,08	1,34	0,57	1,54	287
0,11	0,59	0,15	**13,99**	106000	0,16	0,76	**13,92**	0,94	0,62	3,17	0,07	0,02	0,09	0,09	1,33	0,39	1,54	287
0,12	0,62	0,17	**13,89**	108000	0,16	0,84	**13,93**	1,05	0,64	3,13	0,08	0,00	0,08	0,10	1,25	0,28	1,56	289
0,13	0,64	0,20	**13,78**	109000	0,16	0,92	**13,75**	1,23	0,67	3,07	0,08	0,00	0,08	0,11	1,25	0,16	1,57	290
0,14	0,67	0,25	**13,66**	113000	0,17	0,99	**13,67**	1,49	0,72	2,98	0,07	0,00	0,07	0,12	1,25	0,17	1,61	293
0,15	0,72	0,31	**13,52**	117000	0,18	1,07	**13,49**	1,78	0,76	2,87	0,08	0,00	0,08	0,14	1,25	0,18	1,64	297
0,16	0,76	0,38	**13,35**	122000	0,18	1,16	**13,32**	2,10	0,81	2,76	0,09	0,00	0,09	0,16	1,25	0,18	1,69	302
0,17	0,81	0,47	**13,17**	128000	0,19	1,26	**13,13**	2,44	0,85	2,64	0,10	0,00	0,10	0,19	1,25	0,19	1,74	307
0,18	0,85	0,56	**12,96**	136000	0,20	1,38	**13,01**	2,77	0,88	2,53	0,12	0,00	0,12	0,21	1,25	0,20	1,80	315
0,19	0,88	0,67	**12,72**	144000	0,22	1,51	**12,75**	3,13	0,92	2,40	0,13	0,00	0,13	0,24	1,25	0,22	1,86	323
0,20	0,92	0,80	**12,45**	153000	0,23	1,64	**12,42**	3,50	0,96	2,27	0,14	0,00	0,14	0,27	1,25	0,23	1,91	334
0,21	0,96	0,95	**12,15**	165000	0,25	1,80	**12,21**	3,83	0,99	2,16	0,15	0,00	0,15	0,30	1,25	0,25	1,98	347
0,22	0,99	1,11	**11,82**	177000	0,27	1,96	**11,83**	4,19	1,02	2,03	0,17	0,00	0,17	0,33	1,25	0,27	2,03	362
0,23	1,02	1,29	**11,47**	191000	0,29	2,14	**11,47**	4,50	1,04	1,92	0,18	0,00	0,18	0,36	1,25	0,29	2,09	381
0,24	1,04	1,41	**11,08**	199000	0,30	2,41	**11,12**	4,72	1,06	1,85	0,27	0,00	0,27	0,38	1,25	0,30	2,10	394
0,25	1,06	1,53	**10,68**	207000	0,31	2,68	**10,72**	4,93	1,07	1,77	0,28	0,00	0,28	0,40	1,25	0,31	2,11	408
0,26	1,07	1,65	**10,27**	215000	0,32	2,97	**10,30**	5,13	1,09	1,70	0,29	0,00	0,29	0,41	1,25	0,32	2,11	424
0,27	1,09	1,77	**9,85**	223000	0,33	3,27	**9,87**	5,32	1,10	1,64	0,30	0,00	0,30	0,42	1,25	0,33	2,11	441

t	r_{i-1}	m_{bi}	m_{ui}	p_i	ρ_{bi}	m_{si}	m_{ui}	V_{bi}	ri	x_i	dm_{sbi}	dm_{sui}	dm_{si}	dm_{bi}	γ_{mix}	ρ_{mix}	ρ_{ui}	T_{ui}
0,28	1,10	1,90	**9,41**	231000	0,35	3,58	**9,45**	5,48	1,11	1,58	0,31	0,00	0,31	0,43	1,25	0,35	2,09	460
0,29	1,11	2,02	**8,98**	238000	0,36	3,91	**8,98**	5,66	1,12	1,52	0,32	0,00	0,32	0,44	1,25	0,36	2,07	480
0,30	1,12	2,13	**8,53**	244000	0,37	4,23	**8,47**	5,83	1,13	1,46	0,33	0,00	0,33	0,44	1,25	0,37	2,03	501
0,31	1,13	2,23	**8,09**	250000	0,37	4,57	**8,03**	5,97	1,14	1,41	0,34	0,00	0,34	0,44	1,25	0,37	1,99	523
0,32	1,14	2,33	**7,65**	256000	0,38	4,92	**7,68**	6,07	1,15	1,37	0,35	0,00	0,35	0,44	1,25	0,38	1,96	545
0,33	1,15	2,41	**7,21**	260000	0,39	5,27	**7,23**	6,20	1,16	1,33	0,35	0,00	0,35	0,44	1,25	0,39	1,90	569
0,34	1,16	2,49	**6,77**	263000	0,39	5,63	**6,79**	6,32	1,17	1,28	0,36	0,00	0,36	0,43	1,25	0,39	1,85	593
0,35	1,17	2,56	**6,35**	265000	0,40	5,99	**6,36**	6,44	1,17	1,24	0,36	0,00	0,36	0,43	1,25	0,40	1,79	617
0,36	1,17	2,61	**5,93**	266000	0,40	6,36	**5,95**	6,55	1,18	1,21	0,36	0,00	0,36	0,42	1,25	0,40	1,73	642
0,37	1,18	2,65	**5,52**	266000	0,40	6,72	**5,54**	6,66	1,19	1,17	0,36	0,00	0,36	0,41	1,25	0,40	1,66	668
0,38	1,19	2,69	**5,13**	265000	0,40	7,08	**5,14**	6,77	1,19	1,13	0,36	0,00	0,36	0,40	1,25	0,40	1,59	693
0,39	1,19	2,71	**4,74**	263000	0,39	7,44	**4,74**	6,88	1,20	1,09	0,36	0,00	0,36	0,38	1,25	0,39	1,52	720
0,40	1,20	2,72	**4,37**	260000	0,39	7,80	**4,35**	7,00	1,20	1,05	0,36	0,00	0,36	0,37	1,25	0,39	1,45	749
0,41	1,20	2,73	**4,01**	256000	0,38	8,16	**3,95**	7,12	1,21	1,01	0,35	0,00	0,35	0,36	1,25	0,38	1,37	779
0,42	1,21	2,72	**3,67**	252000	0,38	8,50	**3,64**	7,21	1,22	0,97	0,35	0,00	0,35	0,34	1,25	0,38	1,31	804
0,43	1,22	2,71	**3,34**	247000	0,37	8,84	**3,30**	7,32	1,22	0,94	0,34	0,00	0,34	0,33	1,25	0,37	1,23	835
0,44	1,22	2,69	**3,03**	242000	0,36	9,18	**3,03**	7,42	1,23	0,90	0,33	0,00	0,33	0,31	1,25	0,36	1,17	858
0,45	1,23	2,66	**2,73**	236000	0,35	9,51	**2,72**	7,53	1,23	0,86	0,33	0,00	0,33	0,30	1,25	0,35	1,10	893
0,46	1,23	2,63	**2,44**	230000	0,34	9,83	**2,47**	7,63	1,24	0,83	0,32	0,00	0,32	0,29	1,25	0,34	1,04	919
0,47	1,24	2,59	**2,17**	223000	0,33	10,14	**2,16**	7,76	1,25	0,78	0,31	0,00	0,31	0,27	1,25	0,33	0,96	964
0,48	1,25	2,55	**1,91**	216000	0,32	10,44	**1,92**	7,87	1,25	0,74	0,30	0,00	0,30	0,26	1,25	0,32	0,90	997
0,49	1,25	2,50	**1,67**	208000	0,31	10,73	**1,62**	8,02	1,26	0,69	0,29	0,00	0,29	0,24	1,25	0,31	0,82	1063
0,50	1,26	2,44	**1,45**	200000	0,30	11,00	**1,40**	8,14	1,27	0,65	0,28	0,00	0,28	0,22	1,25	0,30	0,75	1109
0,51	1,27	2,37	**1,25**	192000	0,29	11,27	**1,21**	8,26	1,27	0,61	0,27	0,00	0,27	0,21	1,25	0,29	0,70	1150
0,52	1,27	2,31	**1,06**	184000	0,28	11,53	**1,04**	8,38	1,28	0,57	0,26	0,00	0,26	0,19	1,25	0,28	0,64	1194

t	r_{i-1}	m_{bi}	m_{ui}	p_i	ρ_{bi}	m_{si}	m_{ui}	V_{bi}	ri	x_i	dm_{sbi}	dm_{sui}	dm_{si}	dm_{bi}	γ_{mix}	ρ_{mix}	ρ_{ui}	T_{ui}
0,53	1,28	2,24	**0,88**	176000	0,26	11,78	**0,88**	8,51	1,29	0,52	0,25	0,00	0,25	0,18	1,25	0,26	0,59	1245
0,54	1,29	2,24	**0,71**	174000	0,26	11,95	**0,71**	8,59	1,29	0,49	0,17	0,00	0,17	0,17	1,25	0,26	0,50	1439

Table 4.14 - Model No. IX. Numerical Values of Variables Model properties for each time interval.

Model No. X. Tank Volume 10 m^3, Control Volume 1 m^3, Turbulence Factor = 5

The model was run for these conditions.

The results are in Table 4-15.

If the accident scene had been of this kind would have been possible to reach the tank to burst self-ignition temperature.

Self-ignition stage of unburned mixture at about 0, 16 s was recorded.

As discussed later, if the container had exploded by the maximum pressure reached in the corresponding model 40 2000 Pa, it was not possible that a person had moved a great distance, and there would have been damage to the vessel walls as illustrated in the photographs of the proceedings.

Consequently the alternative that e l tank had exploded by the internal pressure in the same would not be admissible. By contrast the hypothesis of spontaneous ignition detonation would be valid.

t	r_{i-1}	m_{bi}	m_{ui}	p_i	ρ_{bi}	m_{si}	m_{ui}	V_{bi}	ri	x_i	dm_{sbi}	dm_{sui}	dm_{si}	dm_{bi}	γ_{mix}	ρ_{mix}	ρ_{ui}	T_{ui}
0,01	0,02	0,00	**14,90**	101300	0,15	0,00	**14,90**	0,00	0,02	3,50	0,00	0,00	0,00	0,02	1,36	1,49	1,49	283
0,02	0,02	0,02	**14,88**	103000	0,15	0,00	**14,87**	0,14	0,33	3,45	0,00	0,08	0,08	0,00	1,36	1,49	1,51	285
0,03	0,33	0,05	**14,74**	104000	0,16	0,11	**14,68**	0, 33	0,44	3,38	0,01	0,09	0,11	0,04	1,36	1,32	1,52	285
0,04	0,44	0,09	**14,57**	106000	0,16	0,24	**14,52**	0,56	0,52	3,30	0,04	0,09	0,13	0,08	1,35	1,12	1,54	287
0,05	0,52	0,13	**14,40**	108000	0,16	0,38	**14,38**	0,78	0,58	3,23	0,08	0,06	0,14	0,12	1,35	0,80	1,56	289
0,06	0,58	0,17	**14,22**	110000	0,16	0,51	**14,18**	1,01	0,63	3,14	0,10	0,03	0,14	0,15	1,33	0,46	1,58	290
0,07	0,63	0,23	**14,04**	113000	0,17	0,63	**13,92**	1,33	0,69	3,03	0,12	0,00	0,12	0,18	1,25	0,17	1,61	293
0,08	0,69	0,35	**13,83**	123000	0,18	0,72	**13,75**	1,90	0,78	2,83	0,09	0,00	0,09	0,22	1,25	0,18	1,70	302
0,09	0,78	0,53	**13,54**	137000	0,21	0,84	**13,49**	2,56	0,86	2,60	0,11	0,00	0,11	0,29	1,25	0,21	1,81	315
0,10	0,86	0,76	**13,16**	157000	0,24	0,98	**13,20**	3,25	0,93	2,36	0,14	0,00	0,14	0,38	1,25	0,24	1,95	335
0,11	0,93	1,08	**12,68**	182000	0,27	1,14	**12,64**	3,95	1,00	2,12	0,16	0,00	0,16	0,48	1,25	0,27	2,09	363
0,12	1,00	1,39	**12,10**	208000	0,31	1,41	**12,12**	4,46	1,04	1,94	0,27	0,00	0,27	0,58	1,25	0,31	2,19	396
0,13	1,04	1,74	**11,44**	237000	0,35	1,71	**11,45**	4,91	1,07	1,78	0,30	0,00	0,30	0,66	1,25	0,35	2,25	439
0,14	1,07	2,12	**10,72**	269000	0,40	2,06	**10,78**	5,26	1,10	1,66	0,35	0,00	0,35	0,72	1,25	0,40	2,28	492
0,15	1,10	2,50	**9,96**	300000	0,45	2,45	**9,98**	5,56	1,12	1,55	0,39	0,00	0,39	0,77	1,25	0,45	2,25	556
0,16	1,12	2,85	**9,17**	329000	0,49	2,88	**9,19**	5,79	1,13	1,47	0,43	0,00	0,43	0,78	1,25	0,49	2,18	629
0,17	1,13	3,17	**8,39**	354000	0,53	3,34	**8,39**	5,97	1,14	1,41	0,47	0,00	0,47	0,78	1,25	0,53	2,08	708
0,18	1,14	3,43	**7,63**	374000	0,56	3,84	**7,63**	6,12	1,15	1,36	0,50	0,00	0,50	0,76	1,25	0,56	1,97	792
0,19	1,15	3,64	**6,90**	389000	0,58	4,36	**6,94**	6,25	1,16	1,31	0,52	0,00	0,52	0,73	1,25	0,58	1,85	876
0,20	1,16	3,80	**6,20**	398000	0,60	4,90	**6,23**	6,37	1,17	1,27	0,54	0,00	0,54	0,70	1,25	0,60	1,72	966
0,21	1,17	3,91	**5,54**	402000	0,60	5,45	**5,57**	6,49	1,18	1,23	0,55	0,00	0,55	0,66	1,25	0,60	1,59	1056
0,22	1,18	3,97	**4,93**	401000	0,60	6,00	**4,91**	6,61	1,18	1,18	0,55	0,00	0,55	0,61	1,25	0,60	1,45	1153
0,23	1,18	3,99	**4,36**	396000	0,59	6,54	**4,31**	6,73	1,19	1,14	0,55	0,00	0,55	0,57	1,25	0,59	1,32	1252
0,24	1,19	3,98	**3,84**	389000	0,5 8	7,08	**3,88**	6,83	1,19	1,11	0,54	0,00	0,54	0,52	1,25	0,58	1,22	1327

t	r_{i-1}	m_{bi}	m_{ui}	p_i	ρ_{bi}	m_{si}	m_{ui}	V_{bi}	ri	x_i	dm_{sbi}	dm_{sui}	dm_{si}	dm_{bi}	γ_{mix}	ρ_{mix}	ρ_{ui}	T_{ui}
0,25	1,19	3,94	**3,35**	378000	0,57	7,61	**3,31**	6,96	1,20	1,06	0,52	0,00	0,52	0,49	1,25	0,57	1,09	14 48
0,26	1,20	3,87	**2,91**	366000	0,55	8,12	**2,94**	7,06	1,21	1,03	0,51	0,00	0,51	0,44	1,25	0,55	1,00	1524
0,27	1,21	3,79	**2,50**	352000	0,53	8,61	**2,52**	7,19	1,22	0,98	0,49	0,00	0,49	0,41	1,25	0,53	0,90	1638
0,28	1,22	3,69	**2,13**	336000	0,50	9,08	**2,08**	7,33	1,22	0,93	0,47	0,00	0,47	0,37	1,25	0,50	0,78	1795
0,29	1,22	3,57	**1,81**	320000	0,48	9,53	**1,83**	7,44	1,23	0,89	0,45	0,00	0,45	0,33	1,25	0,48	0,72	1863
0,30	1,23	3,44	**1,50**	303000	0,45	9,95	**1,49**	7,59	1,24	0,84	0,43	0,00	0,43	0,30	1,25	0,45	0,62	2047

Table 4.15 - Model No. X. Numerical Values of Variables Model properties for each time interval.

Appendix B

ANNEX: Chapter 5 Tables

Model	$p_{i\ max.}$	Volume	E_{ex}
I	176000	7,5	3112500
II	200000	7,5	4112500
III	252000	7,5	6279167
IV	316000	7,5	8945833
V	219000	7,5	4904167
VI	293000	7,5	7987500
VII	343000	7,5	10070833
VIII	268000	5	4630556
IX	266000	10	9150000
X	402000	10	16705556

Table 5.1- Explosion Energy Values for the Explosion Development Models

Model	E_{ex}	m_b	E_b	E_{ex} / E_b
I	3112500	1,50	3750000	0,83
II	4112500	1,68	4200000	0,98
III	6279167	1,96	4900000	1,28
IV	8945833	1,09	2725000	3,28
V	4904167	1,64	4100000	1,20
VI	7987500	2,17	5425000	1,47
VII	10070833	2,56	6400000	1,57
VIII	4630556	1,36	3400000	1,36
IX	9150000	2,61	6525000	1,40
X	16705556	3,91	9775000	1,71

Table 5.2 - Explosion Energy Values for the Explosion Energy Models for Explosion Compared with the Energy Released by the Flammable Mixture Burned in the Tank.

Model	E_{ex}	m_0	E_0	E_{ex} / E_0
I	3112500	11,2	28000000	0,11
II	4112500	11,2	28000000	0,15
III	6279167	11,2	28000000	0,22
IV	8945833	11,2	28000000	0,32
V	4904167	11,2	28000000	0,18
VI	7987500	11,2	28000000	0,29
VII	10070833	11,2	28000000	0,36
VIII	4630556	7,5	18750000	0,25
IX	9150000	14,9	37250000	0,25
X	16705556	14,9	37250000	0,45

Table 5-3. Explosion Energy Values for Explosion Development Models Energy Compared with the Releasable Energy by the Flammable Mixture Initially Contained in the Tank.

Model	p_1	ρ_1	a_1	$(a_1/a_0)^2$
I	176000	0,26	920	7,3
II	200000	0,30	913	7,2
III	252000	0,38	910	7,2
IV	316000	0,47	917	7,3
V	219000	0,33	911	7,2
VI	293000	0,44	912	7,2
VII	343000	0,51	917	7,3
VIII	268000	0,40	915	7,2
IX	266000	0,40	912	7,2
X	402000	0,60	915	7,2

Table 5.4 - Sound Speed and Ratio $(a_1 / a_0)^2$ at Tank Burst Conditions.

Model	r	R	r_0	R_0	$(a_1/ a_0)^2$	p_1/p_0	P_{s0}	Associated Curve
I	1	0,32	2,6	0,84	7,3	1,7	0,5	Curve No. 4
	2	0,65	2,6	0,84	7,3	1,7	0,5	Curve No. 4
	3	0,97	2,6	0,84	7,3	1,7	0,5	Curve No. 4
II	1	0,29	2,6	0,77	7,2	2,0	0,6	Curve No. 5
	2	0,59	2,6	0,77	7,2	2,0	0,6	Curve No. 5
	3	0,88	2,6	0,77	7,2	2,0	0,6	Curve No. 5
III	1	0,26	2,6	0,67	7,2	2,5	1,0	Curve No. 6
	2	0,51	2,6	0,67	7,2	2,5	1,0	Curve No. 6
	3	0,77	2,6	0,67	7,2	2,5	1,0	Curve No. 6
IV	1	0,23	2,6	0,59	7,3	3,2	1,3	Curve No. 6
	2	0,46	2,6	0,59	7,3	3,2	1,3	Curve No. 6
	3	0,68	2,6	0,59	7,3	3,2	1,3	Curve No. 6
V	1	0,28	2,6	0,72	7,2	2,2	0,7	Curve No. 4
	2	0,56	2,6	0,72	7,2	2,2	0,7	Curve No. 4
	3	0,83	2,6	0,72	7,2	2,2	0,7	Curve No. 4
VI	1	0,24	2,6	0,62	7,3	2,9	1,1	Curve No. 6
	2	0,47	2,6	0,62	7,3	2,9	1,1	Curve No. 6
	3	0,71	2,6	0,62	7,3	2,9	1,1	Curve No. 6
VII	1	0,22	2,6	0,57	7,2	3,4	1,6	Curve No. 8
	2	0,44	2,6	0,57	7,2	3,4	1,6	Curve No. 8
	3	0,66	2,6	0,57	7,2	3,4	1,6	Curve No. 8
VIII	1	0,28	1,9	0,54	7,2	2,7	1,1	Curve No. 5
	2	0,57	1,9	0,54	7,2	2,7	1,1	Curve No. 5
	3	0,85	1,9	0,54	7,2	2,7	1,1	Curve No. 5
IX	1	0,23	3,2	0,72	7,2	2,7	1,1	Curve No. 11
	2	0,45	3,2	0,72	7,2	2,7	1,1	Curve No. 11
	3	0,68	3,2	0,72	7,2	2,7	1,1	Curve No. 11
X	1	0,19	3,2	0,59	7,2	4,0	1,8	Curve No. 11
	2	0,37	3,2	0,59	7,2	4,0	1,8	Curve No. 11
	3	0,56	3,2	0,59	7,2	4,0	1,8	Curve No. 11

Table 5.5 - Figure 5.1 Curve Associated to Models I to X.

Model	Associated Curve	r	R	P'_s	Factor	P_s	p'_s	p_1	p_s
I	Curve No. 4	1	0,32	1,70	1,6	2,72	275536	176000	**176000**
	Curve No. 4	2	0,65	0,75	1,6	1,20	121560	176000	**121560**
	Curve No. 4	3	0,97	0,40	1,6	0,64	64832	176000	**64832**
II	Curve No. 5	1	0,29	2,10	4,0	8,40	850920	200000	**200000**
	Curve No. 5	2	0,59	0,95	1,6	1,52	153976	200000	**153976**
	Curve No. 5	3	0,88	0,60	1,6	0,96	97248	200000	**97248**
III	Curve No. 6	1	0,26	2,80	4,0	11,20	1134560	252000	**252000**
	Curve No. 6	2	0,51	1,40	1,6	2,24	226912	252000	**226912**
	Curve No. 6	3	0,77	0,75	1,6	1,20	121560	252000	**121560**
IV	Curve No. 6	1	0,23	3,20	4,0	12,80	1296640	316000	**316000**
	Curve No. 6	2	0,46	1,70	1,6	2,72	275536	316000	**275536**
	Curve No. 6	3	0,68	0,95	1,6	1,52	153976	316000	**153976**
V	Curve No. 4	1	0,28	1,80	4,0	7,20	729 360	219000	**219000**
	Curve No. 4	2	0,56	0,90	1,6	1,44	145872	219000	**145872**
	Curve No. 4	3	0,83	0,50	1,6	0,80	81040	219000	**81040**
VI	Curve No. 6	1	0,24	3,10	4,0	12,40	1256120	293000	**293000**
	Curve No. 6	2	0,47	1,70	1,6	2,72	275536	293000	**275536**
	Curve No. 6	3	0,71	0,90	1,6	1,44	145872	293000	**145872**
VII	Curve No. 8	1	0,22	9,00	4,0	36,00	3646800	343000	**343000**
	Curve No. 8	2	0,44	2,50	1,6	4,00	405200	343000	**343000**
	Curve No. 8	3	0,66	1,00	1,6	1,60	162080	343000	**162080**
VIII	Curve No. 5	1	0,28	2,20	4,0	8,80	891440	268000	**268000**
	Curve No. 5	2	0,57	1,00	1,6	1,60	162080	268000	**162080**
	Curve No. 5	3	0,85	0,60	1,6	0,96	97248	268000	**97248**

Model	Associated Curve	r	R	P'_s	Factor	P_s	p'_s	p_1	p_s
IX	Curve No. 11	1	0,23	13,00	4,0	52,00	5267600	266000	**266000**
	Curve No. 11	2	0,45	2,40	1,6	3,84	388992	266000	**266000**
	Curve No. 11	3	0,68	1,00	1,6	1,60	162080	266000	**162080**
X	Curve No. 11	1	0,19	17,00	4,0	68,00	6888400	402000	**402000**
	Curve No. 11	2	0,37	4,00	1,6	6,40	648 320	402000	**402000**
	Curve No. 11	3	0,56	1,70	1,6	2,72	275536	402000	**275536**

Table 5.7 - Lateral Impulse Determination i_s by the Figure 5-3 Curve, Cylindrical Form Factor, and Tank Burst Pressure

Model	r	E	R	p_{s1}	Curve No.	P_d	t+	t	i_s	i_{tot}
I	1	7000000	0,25	176000	6,5	40000	0,4	0,0046	405	497
	2	7000000	0,49	170000	6,5	40000	0,3	0,0034	289	357
	3	7000000	0,74	160000	6,5	10000	0,35	0,004	320	340
II	1	7840000	0,24	200000	7	60000	0,35	0,0045	450	585
	2	7840000	0,48	190000	7	40000	0,25	0,0032	304	368
	3	7840000	0,71	170000	7	10000	0,3	0,0039	332	351
III	1	9146667	0,23	252000	7,5	100000	0,35	0,0049	617	862
	2	9146667	0,45	240000	7,5	50000	0,25	0,0035	420	508
	3	9146667	0,68	200000	7,5	20000	0,25	0,0035	350	385
IV	1	11666667	0,21	316000	8	170000	0,3	0,0044	695	1069
	2	11666667	0,42	290000	8	150000	0,25	0,0037	537	814
	3	11666667	0,63	240000	8	40000	0,2	0,0029	348	406
V	1	7653333	0,24	219000	7	60000	0,4	0,0056	613	781
	2	7653333	0,48	190000	7	40000	0,3	0,0042	399	483
	3	7653333	0,72	180000	7	10000	0,25	0,0035	315	333
VI	1	10126667	0,22	293000	8	170000	0,3	0,0043	630	995
	2	10126667	0,44	290000	8	150000	0,25	0,0036	522	792
	3	10126667	0,66	240000	8	40000	0,2	0,0029	348	406
VII	1	11946667	0,21	343000	8,3	200000	0,25	0,0038	652	1032
	2	11946667	0,41	300000	8,3	100000	0,2	0,003	450	600
	3	11946667	0,62	240000	8,3	40000	0,2	0,003	360	420
VIII	1	6346667	0,26	268000	7,7	140000	0,35	0,0042	563	857
	2	6346667	0,51	250000	7,7	70000	0,25	0,003	375	480
	3	6346667	0,77	190000	7,7	30000	0,25	0,003	285	330
IX	1	12180000	0,21	266000	7,7	140000	0,35	0,0056	745	1137
	2	12180000	0,41	250000	7,7	70000	0,25	0,004	500	640
	3	12180000	0,62	220000	7,7	30000	0,25	0,004	440	500
X	1	18246667	0,18	402000	8,5	300000	0,25	0,0043	864	1509
	2	18246667	0,36	320000	8,5	150000	0,2	0,0035	560	823
	3	18246667	0,54	260000	8,5	70000	0,2	0,0035	455	578

Table 5.8 - Pressure and Impulse Values for Multienergy method

Model	Duration	Maximum Pressure	$(Dp/dt)_{max}$	$T_{ui\ max}$
I	0,61	176000	4	> 900
II	0,46	200000	8	> 2000
III	0,36	252000	9	> 1800
IV	0,27	316000	18	> 2700
V	0,53	219000	12	> 1200
VI	0,39	293000	22	> 2000
VII	0,30	343000	27	> 2000
VIII	0,27	268000	19	> 1300
IX	0,54	266000	12	> 1400
X	0,30	402000	32	> 2000

Table 5.9 - Maximum Pressures per Model

Model	Duration	Pressure	T_{ui}
I	0,50	176000	578
II	0,31	200000	602
III	0,21	245000	628
IV	0,16	275000	630
V	0,40	218000	581
VI	0,23	278000	588
VII	0,16	305000	615
VIII	0,18	258000	578
IX	0,39	263000	593
X	0,16	329000	629

Table 5.10 - Flammable Mixture Temperatures in the Vicinity of Self-ignition

Model	m_{ui}	V_{bi}	V_{ui}	T_{ui}
I	2,20	5,78	0,86	578
II	2,77	5,50	1,00	602
III	3,96	5,07	1,22	628
IV	4,94	4,79	1,36	630
V	3,61	5,19	1,15	581
VI	5,77	4,57	1,46	588
VII	6,28	4,46	1,52	615
VIII	3,45	3,15	2,18	578
IX	6,79	6,32	0,59	593
X	9,19	5,79	0,86	629

Table 5.11 - Self-ignited Mass, Self-Ignited Volume, Temperature at Self-ignition Start

Model	p	V	E_x
I	1701812	0,86	7661109
II	1850138	1,00	9715769
III	2176924	1,22	14010465
IV	2435074	1,36	17568129
V	2089460	1,15	12730371
VI	2632155	1,46	20586253
VII	2761592	1,52	22432251
VIII	1057627	2,18	11561617
IX	7721971	0,59	24874472
X	7168296	0,86	33606503

Table 5.12 - Explosion Energy Values for Explosion Development Models

Model	E_{ex}	m_b	E_b	E_{ex}/E_b
I	3112500	1,50	3750000	0,83
II	4112500	1,68	4200000	0,98
III	6279167	1,96	4900000	1,28
IV	8945833	1,09	2725000	3,28
V	4904167	1,64	4100000	1,20
VI	7987500	2,17	5425000	1,47
VII	10070833	2,56	6400000	1,57
VIII	4630556	1,36	3400000	1,36
IX	9150000	2,61	6525000	1,40
X	16705556	3,91	9775000	1,71

Table 5.12 - Energy Explosion Values for Explosion Development Models Compared with Energy Released by Flammable Mixture Burned in Tank

Model	p	$V_{bi} + V_{ui} / 2$	T_{ui}
I	176000	5,78	578
II	200000	5,50	602
III	245000	5,07	628
IV	275000	4,79	630
V	218000	5,19	581
VI	278000	4,57	588
VII	305000	4,46	615
VIII	258000	3,15	578
IX	263000	6,32	593
X	329000	5,79	629

Table 5.13 - Pressure in the Tank, not Self-ignited Volume, Temperature at Self-ignition Start

Model	p	V	E_x
I	176000	5,78	2397373
II	200000	5,50	3015833
III	245000	5,07	4047550
IV	275000	4,79	4622350
V	218000	5,19	3368018
VI	278000	4,57	4487905
VII	305000	4,46	5052201
VIII	258000	3,15	2740284
IX	263000	6,32	5681897
X	329000	5,79	7321884

Table 5.14 - Explosion Energy Values for Explosion Development Models

Model	E_{ex1}	E_{ex2}	$E_{ex\ TOTAL}$
I	2397373	7661109	10058481
II	3015833	9715769	12731602
III	4047550	14010465	18058015
IV	4622350	17568129	22190479
V	3368018	12730371	16098390
VI	4487905	20586253	25074158
VII	5052201	22432251	27484452
VIII	2740284	11561617	14301901
IX	5681897	24874472	30556369
X	7321884	33606503	40928386

Table 5.15 - Total Explosion Energy

Model	p_1	m_u	V	ρ_1	a_1	$(a_1/a_0)^2$
I	1701812	2,20	0,86	0,38	2366	48
II	1850138	2,77	1,00	0,50	2143	40
III	2176924	3,96	1,22	0,78	1867	30
IV	2435074	4,94	1,36	1,03	1718	26
V	2089460	3,61	1,15	0,69	1940	33
VI	2632155	5,77	1,46	1,26	1615	23
VII	2761592	6,28	1,52	1,41	15 67	21
VIII	1057627	3,45	2,18	1,09	1099	10
IX	7721971	6,79	0,59	1,07	2998	78
X	7168296	9,19	0,86	1,59	2376	49

Table 5.16 - Speed of Sound and Ratio $(a_1/a_0)^2$ at Tank Burst Conditions

Model	r	R	r_0	R_0	$(a_1/a_0)^2$	p_1/p_0	P_{s0}	Associated Curve
I	1	0,22	0,51	0,11	48	17	9,5	Curve No. 7
	2	0,44	0,51	0,11	48	17	9,5	Curve No. 7
	3	0,66	0,51	0,11	48	17	9,5	Curve No. 7
II	1	0,20	0,57	0,12	40	22	12,0	Curve No. 7
	2	0,40	0,57	0,12	40	22	12,0	Curve No. 7
	3	0,60	0,57	0,12	40	22	12,0	Curve No. 7
III	1	0,18	0,66	0,12	30	19	9,5	Curve No. 7
	2	0,36	0,66	0,12	30	19	9,5	Curve No. 7
	3	0,54	0,66	0,12	30	19	9,5	Curve No. 7
IV	1	0,17	0,72	0,12	26	24	12,0	Curve No. 7
	2	0,34	0,72	0,12	26	24	12,0	Curve No. 7
	3	0,51	0,72	0,12	26	24	12,0	Curve No. 7
V	1	0,19	0,64	0,12	33	21	10,0	Curve No. 7
	2	0,38	0,64	0,12	33	21	10,0	Curve No. 7
	3	0,57	0,64	0,12	33	21	10,0	Curve No. 7
VI	1	0,16	0,76	0,12	23	26	11,0	Curve No. 7
	2	0,32	0,76	0,12	23	26	11,0	Curve No. 7
	3	0,48	0,76	0,12	23	26	11,0	Curve No. 7
VII	1	0,16	0,79	0,12	21	28	12,0	Curve No. 7
	2	0,32	0,79	0,12	21	28	12,0	Curve No. 7
	3	0,48	0,79	0,12	21	28	12,0	Curve No. 7
VIII	1	0,20	1,03	0,20	10	11	5,0	Curve No. 7
	2	0,40	1,03	0,20	10	11	5,0	Curve No. 7
	3	0,60	1,03	0,20	10	11	5,0	Curve No. 7
IX	1	0,15	0,39	0,06	78	77	35,0	Curve No. 8
	2	0,30	0,39	0,06	78	77	35,0	Curve No. 8
	3	0,45	0,39	0,06	78	77	35,0	Curve No. 8
X	1	0,14	0,51	0,07	49	72	30,0	Curve No. 8
	2	0,28	0,51	0,07	49	72	30,0	Curve No. 8
	3	0,42	0,51	0,07	49	72	30,0	Curve No. 8

Table 5.17 - Figure 5-1 Curve Associated Models I to X.

Model	Associated Curve	r	R	P'_s	Factor	P_s	p'_s	p_1	p_s
I	Curve No. 7	1	0,22	5,50	4,0	22,00	2228600	1701812	1701812
	Curve No. 7	2	0,44	2,20	1,6	3,52	356576	1701812	356576
	Curve No. 7	3	0,66	1,00	1,6	1,60	162080	1701812	162080
II	Curve No. 7	1	0,20	6,50	4,0	26,00	2633800	1850138	1850138
	Curve No. 7	2	0,40	2,60	1,6	4,16	421408	1850138	421408
	Curve No. 7	3	0,60	1,30	1,6	2,08	210704	1850138	210704
III	Curve No. 7	1	0,18	7,50	4,0	30,00	3039000	2176924	2176924
	Curve No. 7	2	0,36	3,00	1,6	4,80	486240	2176924	486240
	Curve No. 7	3	0,54	1,60	1,6	2,56	259328	2176924	259328
IV	Curve No. 7	1	0,17	8,00	4,0	32,00	3241600	2435074	2435074
	Curve No. 7	2	0,34	3,20	1,6	5,12	518656	2435074	518656
	Curve No. 7	3	0,51	1,90	1,6	3,04	307952	2435074	307952
V	Curve No. 7	1	0,19	7,00	4,0	28,00	2836400	2089460	2089460
	Curve No. 7	2	0,38	2,80	1,6	4,48	453824	2089460	453824
	Curve No. 7	3	0,57	1,40	1,6	2,24	226912	2089460	226912
VI	Curve No. 7	1	0,16	8,50	4,0	34,00	3444200	2632155	2632155
	Curve No. 7	2	0,32	2,50	1,6	4,00	405200	2632155	405200
	Curve No. 7	3	0,48	2,10	1,6	3,36	340368	2632155	340368
VII	Curve No. 7	1	0,16	8,50	4,0	34,00	3444200	2761592	2761592
	Curve No. 7	2	0,32	2,50	1,6	4,00	405200	2761592	405200
	Curve No. 7	3	0,48	2,10	1,6	3,36	340368	2761592	340368
VIII	Curve No. 7	1	0,20	6,50	4,0	26,00	2633800	1057627	1057627
	Curve No. 7	2	0,40	2,00	1,6	3,20	324160	1057627	324160
	Curve No. 7	3	0,60	1,30	1,6	2,08	210704	1057627	210704
IX	Curve No. 8	1	0,15	15,50	4,0	62,00	6280600	7721971	6280600
	Curve No. 8	2	0,30	5,20	1,6	8,32	842 816	7721971	842 816
	Curve No. 8	3	0,45	2,20	1,6	3,52	356576	7721971	356576
X	Curve No. 8	1	0,14	16,50	4,0	66,00	6685800	7168296	6685800
	Curve No. 8	2	0,28	6,00	4,0	24,00	2431200	7168296	2431200
	Curve No. 8	3	0,42	2,40	1,6	3,84	388992	7168296	388992

Table 5.18 - Lateral Overpressure Set p_s by the Figure 5-1 Curve, the Cylindrical Form Factor, and Tank Burst Pressure

Model	Associated Curve	r	R	I'	Factor	I	a_0	E_{ex}	i_s	p_s
I	Curve No. 7	1	0,22	0,22	2,00	0,44	340	10058481	**598**	1701812
	Curve No. 7	2	0,44	0,09	1,11	0,10	340	10058481	**136**	356576
	Curve No. 7	3	0,66	0,07	1,11	0,08	340	10058481	**109**	162080
II	Curve No. 7	1	0,20	0,26	2,00	0,52	340	12731602	**764**	1850138
	Curve No. 7	2	0,40	0,11	1,11	0,12	340	12731602	**176**	421408
	Curve No. 7	3	0,60	0,08	1,11	0,09	340	12731602	**132**	210704
III	Curve No. 7	1	0,18	0,32	2,00	0,64	340	18058015	**1055**	2176924
	Curve No. 7	2	0,36	0,12	1,11	0,13	340	18058015	**214**	486240
	Curve No. 7	3	0,54	0,08	1,11	0,09	340	18058015	**148**	259328
IV	Curve No. 7	1	0,17	0,36	2,00	0,72	340	22190479	**1270**	2435074
	Curve No. 7	2	0,34	0,13	1,11	0,14	340	22190479	**247**	518656
	Curve No. 7	3	0,51	0,09	1,11	0,10	340	22190479	**176**	307952
V	Curve No. 7	1	0,19	0,28	2,00	0,56	340	16098390	**889**	2089460
	Curve No. 7	2	0,38	0,11	1,11	0,12	340	16098390	**190**	453824
	Curve No. 7	3	0,57	0,08	1,11	0,09	340	16098390	**143**	226912
VI	Curve No. 7	1	0,16	0,40	2,00	0,80	340	25074158	**1469**	2632155
	Curve No. 7	2	0,32	0,14	1,11	0,16	340	25074158	**294**	405200
	Curve No. 7	3	0,48	0,09	1,11	0,10	340	25074158	**184**	340368
VII	Curve No. 7	1	0,16	0,40	2,00	0,80	340	27484452	**1514**	2761592
	Curve No. 7	2	0,32	0,14	1,11	0,16	340	27484452	**303**	405200
	Curve No. 7	3	0,48	0,09	1,11	0,10	340	27484452	**189**	340368
VIII	Curve No. 7	1	0,20	0,26	2,00	0,52	340	14301901	**794**	1057627
	Curve No. 7	2	0,40	0,11	1,11	0,12	340	14301901	**183**	324160
	Curve No. 7	3	0,60	0,08	1,11	0,09	340	14301901	**137**	210704
IX	Curve No. 8	1	0,15	0,42	2,00	0,84	340	30556369	**1647**	6280600
	Curve No. 8	2	0,30	0,15	2,00	0,30	340	30556369	**588**	842 816
	Curve No. 8	3	0,45	0,09	1,11	0,10	340	30556369	**196**	356576
X	Curve No. 8	1	0,14	0,50	2,00	1,00	340	40928386	**2159**	6685800
	Curve No. 8	2	0,28	0,16	2,00	0,32	340	40928386	**691**	2431200
	Curve No. 8	3	0,42	0,10	1,11	0,11	340	40928386	**237**	388992

Table 5.19 - Lateral Impulse Set i_s by Figure 5-3 Curve, Cylindrical Form Factor and Tank Burst Pressure

Model	p	m_{ui}	ρ_u	V_b	E_{ex1}
I	176000	1,52	1,49	1,02	7140940
II	200000	1,65	1,49	1,11	7751678
III	245000	1,86	1,49	1,25	873 8255
IV	275000	1,97	1,49	1,32	9255034
V	218000	1,70	1,49	1,14	7986577
VI	278000	1,90	1,49	1,28	8926174
VII	305000	2,04	1,49	1,37	9583893
VIII	258000	1,22	1,49	0,82	5731544
IX	263000	2,49	1,49	1,67	11697987
X	329000	2,85	1,49	1,91	13389262

Table 5.20 - Burst Energy of Inflamed Gases

Model	p	m_{ui}	ρ_u	V_b	E_{ex2}
I	176000	2,20	1,49	1,47	10313453
II	200000	2,77	1,49	1,86	13013423
III	245000	3,96	1,49	2,66	18604027
IV	275000	4,94	1,49	3,32	23208054
V	218000	3,61	1,49	2,42	16938838
VI	278000	5,77	1,49	3,87	27106993
VII	305000	6,28	1,49	4,21	29482403
VIII	258000	3,45	1,49	2,31	16188422
IX	263000	6,79	1,49	4,56	31911606
X	329000	9,19	1,49	6,17	43158290

Table 5.21 - Explosion Energy of Self-Ignited Gases

Model	E_{ex1}	E_{ex2}	$E_{ex\ TOTAL}$
I	7140940	10313453	17454393
II	7751678	13013423	20765101
III	8738255	18604027	27342282
IV	9255034	23208054	32463087
V	7986577	16938838	24925415
VI	8926174	27106993	36033167
VII	9583893	29482403	39066296
VIII	5731544	16188422	21919966
IX	11697987	31911606	43609592
X	13389262	43158290	56547552

Table 5.22 - Total Explosion Energy

Model	r	E	R	p_{s1}	Curve No.	P_d	t +	t	i_s	i_{tot}
I	1	17454393	0.18	1745399	10	4432360	0.15	0.0024	2106	7454
	2	17454393	0.37	400000	10	506500	0.15	0.0024	483	1094
	3	17454393	0.55	150000	10	75405	0.15	0.0024	181	272
II	1	20765101	0.17	1745399	10	4432360	0.15	0.0026	2230	7894
	2	20765101	0.35	470000	10	810400	0.15	0.0026	601	1636
	3	20765101	0.52	170000	10	113996	0.15	0.0026	217	363
III	1	27342282	0.16	1745399	10	4432360	0.15	0.0028	2442	8644
	2	27342282	0.32	550000	10	1624567	0.15	0.0028	770	3043
	3	27342282	0.47	200000	10	202600	0.15	0.0028	280	563
IV	1	32463087	0.15	1745399	10	4432360	0.15	0.0030	2585	9148
	2	32463087	0.3	580000	10	1723370	0.15	0.0030	859	3411
	3	32463087	0.45	220000	10	234960	0.15	0.0030	326	674
V	1	24925415	0.16	1745399	10	4432360	0.15	0.0027	2369	8384
	2	24925415	0.33	530000	10	848567	0.15	0.0027	719	1871
	3	24925415	0.49	180000	10	150899	0.15	0.0027	244	449
VI	1	36033167	0.14	1745399	10	4432360	0.15	0.0031	2675	9468
	2	36033167	0.29	590000	10	1508990	0.15	0.0031	904	3217
	3	36033167	0.43	240000	10	245598	0.15	0.0031	368	744
VII	1	39066296	0.14	1745399	10	4432360	0.15	0.0031	2747	9724
	2	39066296	0.28	600000	10	2026000	0.15	0.0031	944	4134
	3	39066296	0.42	250000	10	293189	0.15	0.0031	394	855

Model	r	E	R	p_{s1}	Curve No.	P_d	t +	t	i_s	i_{tot}
VIII	1	21919966	0.17	1057627	10	4432360	0.15	0.0026	1376	7141
	2	21919966	0.34	510000	10	829483	0.15	0.0026	663	1742
	3	21919966	0.51	180000	10	138109	0.15	0.0026	234	414
IX	1	43609592	0.14	1745399	10	4432360	0.15	0.0033	2849	10084
	2	43609592	0.27	620000	10	2150465	0.15	0.0033	1012	4522
	3	43609592	0.41	260000	10	303900	0.15	0.00 33	424	920
X	1	56547552	0.12	1745399	10	4432360	0.15	0.0036	3104	10986
	2	56547552	0.25	670000	10	2349600	0.15	0.0036	1192	5370
	3	56547552	0.37	400000	10	506500	0.15	0.0036	711	1612

Table 5.23 - Pressure and Impulse Values for the Multienergy Method

Appendix C

ANNEX: Chapter 6 Tables

Associated Curve	r	p_s	q	p	i_s	i_{tot}	P	I	S	Lung Injury	Survival
Curve No. 4	1	176000	88402	264402	148	222	2,6	0,17	9,3	Not	
Curve No. 4	2	121560	44966	166526	74	101	1,7	0,08	19,4	Not	
Curve No. 4	3	64832	13739	78571	55	67	0,8	0,05	31,0	Not	
Curve No. 5	1	200000	111111	311111	303	471	3,1	0,36	5,0	If	> 99%
Curve No. 5	2	153976	69407	223383	91	132	2,2	0,10	14,8	Not	
Curve No. 5	3	97248	29656	126904	71	93	1,3	0,07	21,8	Not	
Curve No. 6	1	252000	166765	418 765	442	735	4,2	0,56	3,3	If	99%
Curve No. 6	2	226912	138873	365785	116	187	3,7	0,14	10,3	Not	
Curve No. 6	3	121560	44966	166526	81	111	1,7	0,08	17,9	Not	
Curve No. 6	1	316000	245709	561 709	549	976	5,6	0,74	2,5	If	50%
Curve No. 6	2	275536	194560	470096	131	224	4,7	0,17	8,5	Not	
Curve No. 6	3	153976	69407	223383	105	152	2,2	0,12	13,1	Not	
Curve No. 4	1	219000	130471	349471	322	514	3,5	0,39	4,5	If	> 99%
Curve No. 4	2	145872	62890	208762	96	137	2,1	0,10	14,5	Not	
Curve No. 4	3	81040	21022	102062	64	81	1,0	0,06	25,3	Not	
Curve No. 6	1	293000	216135	509135	504	876	5,1	0,67	2,8	If	70%
Curve No. 6	2	275536	194560	470096	126	215	4,7	0,16	8,8	Not	
Curve No. 6	3	145872	62890	208762	101	145	2,1	0,11	13,8	Not	
Curve No. 8	1	343000	281 997	624 997	625	1139	6,2	0,87	2,2	If	20%
Curve No. 8	2	343000	281 997	624 997	150	273	6,2	0,21	6,9	Not	
Curve No. 8	3	162080	76182	238262	109	160	2,4	0,12	12,4	Not	
Curve No. 5	1	268000	185496	453496	316	535	4,5	0,41	4,1	If	> 99%
Curve No. 5	2	162080	76182	238262	95	140	2,4	0,11	14,0	Not	
Curve No. 5	3	97248	29656	126904	74	97	1,3	0,07	21,0	Not	
Curve No. 11	1	266000	183116	449116	553	934	4,5	0,71	2,8	If	90%
Curve No. 11	2	266000	183116	449116	145	245	4,5	0,19	7,9	Not	
Curve No. 11	3	162080	76182	238262	105	154	2,4	0,12	12,8	Not	
Curve No. 11	1	402000	366615	768 615	900	1721	7,7	1,31	1,5	If	<1%
Curve No. 11	2	402000	366615	768 615	209	400	7,7	0,30	4,8	Not	
Curve No. 11	3	275536	194560	470096	145	247	4,7	0,19	7,8	Not	

Table 6.1 - Percentage Survival and Pulmonary Damage of a Person Standing on the Tank at Burst Time by Method of Baker et al.

Curve No.	r	p_{s1}	P_d	p_{tot}	i_s	i_{tot}	P	I	S	Lung Injury	Survival
6.5	1	176000	40000	216000	405	497	2,2	0,38	5,4	Not	> 99%
6.5	2	170000	40000	210000	289	357	2,1	0,27	6,8	Not	> 99%
6.5	3	160000	10000	170000	320	340	1,7	0,26	7,5	Not	
7	1	200000	60000	260000	450	585	2,6	0,45	4,5	If	> 99%
7	2	190000	40000	230000	304	368	2,3	0,28	6,5	If	> 99%
7	3	170000	10000	180000	332	351	1,8	0,27	7,2	If	> 99%
7.5	1	252000	100000	352000	617	862	3,5	0,66	3,2	If	99%
7.5	2	240000	50000	290000	420	508	2,9	0,39	4,8	If	> 99%
7.5	3	200000	20000	220000	350	385	2,2	0,29	6,3	If	> 99%
8	1	316000	170000	486000	695	1069	4,9	0,81	2,5	If	50%
8	2	290000	150000	440000	537	814	4,4	0,62	3,1	If	95%
8	3	240000	40000	280000	348	406	2,8	0,31	5,7	If	> 99%
7	1	219000	60000	279000	613	781	2,8	0,59	3,7	If	> 99%
7	2	190000	40000	230000	399	483	2,3	0,37	5,4	If	> 99%
7	3	180000	10000	190000	315	333	1,9	0,25	7,3	If	> 99%
8	1	293000	170000	463000	630	995	4,6	0,76	2,6	If	70%
8	2	290000	150000	440000	522	792	4,4	0,60	3,1	If	90%
8	3	240000	40000	280000	348	406	2,8	0,31	5,7	If	> 99%
8.3	1	343000	200000	543000	652	1032	5,4	0,79	2,4	If	40%
8.3	2	300000	100000	400000	450	600	4,0	0,46	3,9	If	99%
8.3	3	240000	40000	280000	360	420	2,8	0,32	5,6	If	> 99%
7.7	1	268000	140000	408000	563	857	4,1	0,65	3,0	If	90%
7.7	2	250000	70000	320000	375	480	3,2	0,37	4,9	If	> 99%
7.7	3	190000	30000	220000	285	330	2,2	0,25	7,1	If	> 99%
7.7	1	266000	140000	406000	745	1137	4,1	0,86	2,5	If	70%
7.7	2	250000	70000	320000	500	640	3,2	0,49	4,0	If	99%
7.7	3	220000	30000	250000	440	500	2,5	0,38	5,1	If	> 99%
8.5	1	402000	300000	702000	864	1509	7,0	1,15	1,7	If	<1%
8.5	2	320000	150000	470000	560	823	4,7	0,63	3,0	If	90%
8.5	3	260000	70000	330000	455	578	3,3	0,44	4,2	If	> 99%

Table 6.2 - Pulmonary Damage and Survival Percentage of a Person Standing on the Tank Damage at Burst Time by Multi-Energy Method

Model	Associated Curve	r	p_s	Eardrum Rupture Probability
I	Curve No. 4	1	176000	80
	Curve No. 4	2	121560	50
	Curve No. 4	3	64832	20
II	Curve No. 5	1	200000	85
	Curve No. 5	2	153976	70
	Curve No. 5	3	97248	50
III	Curve No. 6	1	252000	90
	Curve No. 6	2	226912	85
	Curve No. 6	3	121560	50
IV	Curve No. 6	1	316000	95
	Curve No. 6	2	275536	90
	Curve No. 6	3	153976	70
V	Curve No. 4	1	219000	85
	Curve No. 4	2	145872	70
	Curve No. 4	3	81040	30
VI	Curve No. 6	1	293000	90
	Curve No. 6	2	275536	90
	Curve No. 6	3	145872	70
VII	Curve No. 8	1	343000	95
	Curve No. 8	2	343000	95
	Curve No. 8	3	162080	70
VIII	Curve No. 5	1	268000	90
	Curve No. 5	2	162080	70
	Curve No. 5	3	97248	50
IX	Curve No. 11	1	266000	90
	Curve No. 11	2	266000	90
	Curve No. 11	3	162080	70
X	Curve No. 11	1	402000	98
	Curve No. 11	2	402000	95
	Curve No. 11	3	275536	90

Table 6.3 - Eardrum Rupture Probability by Overpressure for Models I to X According to the Baker et al. Method

Model	Curve No.	r	p_{s1}	Break Chance Timpani
I	6.5	1	176000	80
	6.5	2	170000	80
	6.5	3	160000	70
II	7	1	200000	85
	7	2	190000	85
	7	3	170000	80
III	7.5	1	252000	90
	7.5	2	240000	85
	7.5	3	200000	85
IV	8	1	316000	95
	8	2	290000	90
	8	3	240000	85
V	7	1	219000	85
	7	2	190000	85
	7	3	180000	80
VI	8	1	293000	90
	8	2	290000	90
	8	3	240000	85
VII	8.3	1	343000	95
	8.3	2	300000	95
	8.3	3	240000	85
VIII	7.7	1	268000	90
	7.7	2	250000	90
	7.7	3	190000	85
IX	7.7	1	266000	90
	7.7	2	250000	90
	7.7	3	220000	85
X	8.5	1	402000	98
	8.5	2	320000	95
	8.5	3	260000	90

Table 6 .4 - Eardrum Rupture Probability by Overpressure for Models I to X According to the Multi-Energy Method

Model	Associated Curve	r [m]	p_s [Pa]	i_s [Pa.s]	t_p [10^{-3} s]	dt_p
I	Curve No, 4	1	176000	148	1,68	0,17
	Curve No, 4	2	121560	74	1,22	0,12
	Curve No, 4	3	64832	55	1,70	0,17
II	Curve No, 5	1	200000	303	3,03	0,30
	Curve No, 5	2	153976	91	1,18	0,12
	Curve No, 5	3	97248	71	1,46	0,15
III	Curve No, 6	1	252000	442	3,51	0,35
	Curve No, 6	2	226912	116	1,02	0,10
	Curve No, 6	3	121560	81	1,33	0,13
IV	Curve No, 6	1	316000	549	3,47	0,35
	Curve No, 6	2	275536	131	0,95	0,10
	Curve No, 6	3	153976	105	1,36	0,14
V	Curve No, 4	1	219000	322	2,94	0,29
	Curve No, 4	2	145872	96	1,32	0,13
	Curve No, 4	3	81040	64	1,58	0,16
VI	Curve No, 6	1	293000	504	3,44	0,34
	Curve No, 6	2	275536	126	0,91	0,09
	Curve No, 6	3	145872	101	1,38	0,14
VII	Curve No, 8	1	343000	625	3,64	0,36
	Curve No, 8	2	343000	150	0,87	0,09
	Curve No, 8	3	162080	109	1,35	0,13
VIII	Curve No, 5	1	268000	316	2,36	0,24
	Curve No, 5	2	162080	95	1,17	0,12
	Curve No, 5	3	97248	74	1,52	0,15
IX	Curve No, 11	1	266000	553	4,16	0,42
	Curve No, 11	2	266000	145	1,09	0,11
	Curve No, 11	3	162080	105	1,30	0,13
X	Curve No, 11	1	402000	900	4,48	0,45
	Curve No, 11	2	402000	209	1,04	0,10
	Curve No, 11	3	275536	145	1,05	0,11

Table 6.5 - Lateral Pressure, Lateral Impulse, Scaled Time, Pulse Duration, for Each Model I to X According to the Baker et al. Method

Model	Associated Curve	r [m]	p_{s0}	p_{s1}	p_{s2}	p_{s3}	p_{s4}	p_{s5}	p_{s6}	p_{s7}	p_{s8}	p_{s9}
I	Curve No. 4	1	167200	149600	132000	114400	96800	79200	61600	44000	26400	8800
	Curve No. 4	2	115482	103326	91170	79014	66858	54702	42546	30390	18234	6078
	Curve No. 4	3	61590	55107	48624	42141	35658	29174	22691	16208	9725	3242
II	Curve No. 5	1	190000	170000	150000	130000	110000	90000	70000	50000	30000	10000
	Curve No. 5	2	146277	130880	115482	100084	84687	69289	53892	38494	23096	7699
	Curve No. 5	3	92386	82661	72936	63211	53486	43762	34037	24312	14587	4862
III	Curve No. 6	1	239400	214200	189000	163800	138600	113400	88200	63000	37800	12600
	Curve No. 6	2	215 566	192875	170184	147493	124802	102110	79419	56728	34037	11346
	Curve No. 6	3	115482	103326	91170	79014	66858	54702	42546	30390	18234	6078
IV	Curve No. 6	1	300200	268600	237000	205400	173800	142200	110600	79000	47400	15800
	Curve No. 6	2	261759	234206	206652	179098	151545	123991	96438	68884	41330	13777
	Curve No. 6	3	146277	130880	115482	100084	84687	69289	53892	38494	23096	7699
V	Curve No. 4	1	208050	186150	164250	142350	120450	98550	76650	54750	32850	10950
	Curve No. 4	2	138578	123991	109404	94817	80230	65642	51055	36468	21881	7294
	Curve No. 4	3	76988	68884	60780	52676	44572	36468	28364	20260	12156	4052
VI	Curve No. 6	1	278350	249050	219750	190450	161150	131850	102550	73250	43950	14650
	Curve No. 6	2	261759	234206	206652	179098	151545	123991	96438	68884	41330	13777
	Curve No. 6	3	138578	123991	109404	94817	80230	65642	51055	36468	21881	7294
VII	Curve No. 8	1	325 850	291550	257250	222950	188650	154350	120050	85750	51450	17150
	Curve No. 8	2	325 850	291550	257250	222950	188650	154350	120050	85750	51450	17150
	Curve No. 8	3	153976	137768	121560	105352	89144	72936	56728	40520	24312	8104
VIII	Curve No. 5	1	254600	227800	201000	174200	147400	120600	93800	67000	40200	13400
	Curve No. 5	2	153976	137768	121560	105352	89144	72936	56728	40520	24312	8104
	Curve No. 5	3	92386	82661	72936	63211	53486	43762	34037	24312	14587	4862
IX	Curve No. 11	1	252700	226100	199500	172900	146300	119700	93100	66500	39900	13300
	Curve No. 11	2	252700	226100	199500	172900	146300	119700	93100	66500	39900	13300
	Curve No. 11	3	153976	137768	121560	105352	89144	72936	56728	40520	24312	8104
X	Curve No. 11	1	381900	341700	301500	261300	221100	180900	140700	100500	60300	20100
	Curve No. 11	2	381900	341700	301500	261300	221100	180900	140700	100500	60300	20100
	Curve No. 11	3	261759	234206	206652	179098	151545	123991	96438	68884	41330	13777

Table 6 .6 - Lateral Pressure During Shockwave for Each Model I to X by Baker et al. Method

Model	Associated Curve	r [m]	u_0	u_1	u_2	u_3	u_4	u_5	u_6	u_7	u_8	u_9
I	Curve No. 4	1	366	331	295	259	221	183	144	104	63	21
	Curve No. 4	2	261	235	209	183	156	129	101	73	44	15
	Curve No. 4	3	144	129	115	100	85	70	54	39	24	8
II	Curve No. 5	1	411	372	332	291	249	207	163	118	72	24
	Curve No. 5	2	325	293	261	228	195	161	127	91	55	19
	Curve No. 5	3	212	191	169	148	126	104	81	58	35	12
III	Curve No. 6	1	504	457	409	360	309	257	203	147	90	30
	Curve No. 6	2	460	417	372	327	281	233	184	133	81	27
	Curve No. 6	3	261	235	209	183	156	129	101	73	44	15
IV	Curve No. 6	1	613	557	500	441	380	316	251	183	112	38
	Curve No. 6	2	545	495	443	390	335	279	221	160	98	33
	Curve No. 6	3	325	293	261	228	195	161	127	91	55	19
V	Curve No. 4	1	446	404	361	317	271	225	178	129	78	27
	Curve No. 4	2	309	279	248	217	185	153	120	87	53	18
	Curve No. 4	3	178	160	142	124	105	87	68	49	29	10
VI	Curve No. 6	1	574	522	468	412	354	295	234	170	104	35
	Curve No. 6	2	545	495	443	390	335	279	221	160	98	33
	Curve No. 6	3	309	279	248	217	185	153	120	87	53	18
VII	Curve No. 8	1	657	598	537	474	408	341	271	197	121	41
	Curve No. 8	2	657	598	537	474	408	341	271	197	121	41
	Curve No. 8	3	340	307	274	240	205	169	133	96	58	20
VIII	Curve No. 5	1	532	483	432	380	327	272	215	156	95	32
	Curve No. 5	2	340	307	274	240	205	169	133	96	58	20
	Curve No. 5	3	212	191	169	148	126	104	81	58	35	12
IX	Curve No. 11	1	528	480	429	378	325	270	213	155	95	32
	Curve No. 11	2	528	480	429	378	325	270	213	155	95	32
	Curve No. 11	3	340	307	274	240	205	169	133	96	58	20
X	Curve No. 11	1	749	683	615	544	470	393	313	229	141	48
	Curve No. 11	2	749	683	615	544	470	393	313	229	141	48
	Curve No. 11	3	545	495	443	390	335	279	221	160	98	33

Table 6.7 - Speed of Particles Moved by Shockwave, During this Action for Each Model I to X According to Baker et al. Method

Model	Associated Curve	r [m]	ρ_{10}	ρ_{11}	ρ_{12}	ρ_{13}	ρ_{14}	ρ_{15}	ρ_{16}	ρ_{17}	ρ_{18}	ρ_{19}
I	Curve No. 4	1	2,4	2,3	2,2	2,0	1,9	1,8	1,7	1,6	1,4	1,3
	Curve No. 4	2	2,0	2,0	1,9	1,8	1,7	1,6	1,5	1,4	1,4	1,3
	Curve No. 4	3	1,7	1,6	1,6	1,5	1,5	1,4	1,4	1,3	1,3	1,2
II	Curve No. 5	1	2,5	2,4	2,3	2,1	2,0	1,9	1,7	1,6	1,4	1,3
	Curve No. 5	2	2,2	2,1	2,0	2,0	1,8	1,7	1,6	1,5	1,4	1,3
	Curve No. 5	3	1,9	1,8	1,8	1,7	1,6	1,6	1,5	1,4	1,3	1,2
III	Curve No. 6	1	2,7	2,6	2,5	2,3	2,2	2,0	1,9	1,7	1,5	1,3
	Curve No. 6	2	2,6	2,5	2,4	2,2	2,1	2,0	1,8	1,6	1,5	1,3
	Curve No. 6	3	2,0	2,0	1,9	1,8	1,7	1,6	1,5	1,4	1,4	1,3
IV	Curve No. 6	1	3,0	2,9	2,7	2,6	2,4	2,2	2,0	1,8	1,6	1,3
	Curve No. 6	2	2,8	2,7	2,6	2,4	2,3	2,1	1,9	1,7	1,5	1,3
	Curve No. 6	3	2,2	2,1	2,0	2,0	1,8	1,7	1,6	1,5	1,4	1,3
V	Curve No. 4	1	2,6	2,5	2,3	2,2	2,1	1,9	1,8	1,6	1,5	1,3
	Curve No. 4	2	2,2	2,1	2,0	1,9	1,8	1,7	1,6	1,5	1,4	1,3
	Curve No. 4	3	1,8	1,7	1,7	1,6	1,6	1,5	1,4	1,4	1,3	1,2
VI	Curve No. 6	1	2,9	2,8	2,6	2,5	2,3	2,2	2,0	1,8	1,6	1,3
	Curve No. 6	2	2,8	2,7	2,6	2,4	2,3	2,1	1,9	1,7	1,5	1,3
	Curve No. 6	3	2,2	2,1	2,0	1,9	1,8	1,7	1,6	1,5	1,4	1,3
VII	Curve No. 8	1	3,1	3,0	2,8	2,6	2,5	2,3	2,1	1,9	1,6	1,3
	Curve No. 8	2	3,1	3,0	2,8	2,6	2,5	2,3	2,1	1,9	1,6	1,3
	Curve No. 8	3	2,3	2,2	2,1	2,0	1,9	1,8	1,6	1,5	1,4	1,3
VIII	Curve No. 5	1	2,8	2,7	2,5	2,4	2,2	2,1	1,9	1,7	1,5	1,3
	Curve No. 5	2	2,3	2,2	2,1	2,0	1,9	1,8	1,6	1,5	1,4	1,3
	Curve No. 5	3	1,9	1,8	1,8	1,7	1,6	1,6	1,5	1,4	1,3	1,2
IX	Curve No. 11	1	2,8	2,7	2,5	2,4	2,2	2,1	1,9	1,7	1,5	1,3
	Curve No. 11	2	2,8	2,7	2,5	2,4	2,2	2,1	1,9	1,7	1,5	1,3
	Curve No. 11	3	2,3	2,2	2,1	2,0	1,9	1,8	1,6	1,5	1,4	1,3
X	Curve No. 11	1	3,3	3,2	3,0	2,8	2,6	2,4	2,2	2,0	1,7	1,4
	Curve No. 11	2	3,3	3,2	3,0	2,8	2,6	2,4	2,2	2,0	1,7	1,4
	Curve No. 11	3	2,8	2,7	2,6	2,4	2,3	2,1	1,9	1,7	1,5	1,3

Table 6.8 - Air Density During Shockwave Action for Each Model I to X by Baker et al. Method

Model	Associated Curve	r [m]	v_1	v_2	v_3	v_4	v_5	v_6	v_7	v_8	v_9	v_{10}
I	Curve No. 4	1	0,1	0,2	0,3	0,4	0,4	0,4	0,5	0,5	0,5	**0,5**
	Curve No. 4	2	0,0	0,1	0,1	0,1	0,1	0,1	0,1	0,1	0,1	**0,1**
	Curve No. 4	3	0,0	0,0	0,0	0,0	0,0	0,0	0,1	0,1	0,1	**0,1**
II	Curve No. 5	1	0,3	0,6	0,8	0,9	1,0	1,0	1,1	1,1	1,1	**1,1**
	Curve No. 5	2	0,1	0,1	0,2	0,2	0,2	0,2	0,2	0,2	0,2	**0,2**
	Curve No. 5	3	0,0	0,1	0,1	0,1	0,1	0,1	0,1	0,1	0,1	**0,1**
III	Curve No. 6	1	0,6	1,1	1,4	1,7	1,9	2,0	2,1	2,1	2,1	**2,1**
	Curve No. 6	2	0,1	0,3	0,3	0,4	0,4	0,5	0,5	0,5	0,5	**0,5**
	Curve No. 6	3	0,0	0,1	0,1	0,1	0,1	0,2	0,2	0,2	0,2	**0,2**
IV	Curve No. 6	1	1,0	1,7	2,3	2,8	3,1	3,2	3,3	3,4	3,4	**3,4**
	Curve No. 6	2	0,2	0,4	0,5	0,6	0,6	0,7	0,7	0,7	0,7	**0,7**
	Curve No. 6	3	0,1	0,1	0,2	0,2	0,2	0,3	0,3	0,3	0,3	**0,3**
V	Curve No. 4	1	0,4	0,7	0,9	1,1	1,2	1,2	1,3	1,3	1,3	**1,3**
	Curve No. 4	2	0,1	0,1	0,2	0,2	0,2	0,2	0,2	0,2	0,2	**0,2**
	Curve No. 4	3	0,0	0,0	0,1	0,1	0,1	0,1	0,1	0,1	0,1	**0,1**
VI	Curve No. 6	1	0,8	1,5	2,0	2,3	2,6	2,7	2,8	2,9	2,9	**2,9**
	Curve No. 6	2	0,2	0,3	0,5	0,5	0,6	0,6	0,7	0,7	0,7	**0,7**
	Curve No. 6	3	0,1	0,1	0,2	0,2	0,2	0,2	0,2	0,3	0,3	**0,3**
VII	Curve No. 8	1	1,2	2,2	2,9	3,4	3,8	4,0	4,2	4,2	4,3	**4,3**
	Curve No. 8	2	0,3	0,5	0,7	0,8	0,9	1,0	1,0	1,0	1,0	**1,0**
	Curve No. 8	3	0,1	0,2	0,2	0,2	0,3	0,3	0,3	0,3	0,3	**0,3**
VIII	Curve No. 5	1	0,5	0,8	1,1	1,3	1,5	1,5	1,6	1,6	1,6	**1,6**
	Curve No. 5	2	0,1	0,1	0,2	0,2	0,2	0,3	0,3	0,3	0,3	**0,3**
	Curve No. 5	3	0,0	0,1	0,1	0,1	0,1	0,1	0,1	0,1	0,1	**0,1**
IX	Curve No. 11	1	0,8	1,4	1,9	2,3	2,5	2,7	2,8	2,8	2,8	**2,8**
	Curve No. 11	2	0,2	0,4	0,5	0,6	0,7	0,7	0,7	0,7	0,7	**0,7**
	Curve No. 11	3	0,1	0,2	0,2	0,2	0,3	0,3	0,3	0,3	0,3	**0,3**
X	Curve No. 11	1	2,1	3,7	5,0	5,9	6,5	6,9	7,2	7,3	7,3	**7,3**
	Curve No. 11	2	0,5	0,9	1,2	1,4	1,5	1,6	1,7	1,7	1,7	**1,7**
	Curve No. 11	3	0,2	0,4	0,5	0,6	0,7	0,7	0,8	0,8	0,8	**0,8**

Table 6.9 - Corporal Speed of a Person Standing on the Tank During Shockwave Action for Each Model I to X According to Baker et al. Method

Model	Associated Curve	r [m]	p_s [Pa]	i_s [Pa.s]	t_p [10^{-3} s]	dt_p
I	6,5	1	176000	405	4,60	0,46
	6,5	2	170000	289	3,40	0,34
	6,5	3	160000	320	4,00	0,40
II	7	1	200000	450	4,50	0,45
	7	2	190000	304	3,20	0,32
	7	3	170000	332	3,91	0,39
III	7,5	1	252000	617	4,90	0,49
	7,5	2	240000	420	3,50	0,35
	7,5	3	200000	350	3,50	0,35
IV	8	1	316000	695	4,40	0,44
	8	2	290000	537	3,70	0,37
	8	3	240000	348	2,90	0,29
V	7	1	219000	613	5,60	0,56
	7	2	190000	399	4,20	0,42
	7	3	180000	315	3,50	0,35
VI	8	1	293000	630	4,30	0,43
	8	2	290000	522	3,60	0,36
	8	3	240000	348	2,90	0,29
VII	8,3	1	343000	652	3,80	0,38
	8,3	2	300000	450	3,00	0,30
	8,3	3	240000	360	3,00	0,30
VIII	7,7	1	268000	563	4,20	0,42
	7,7	2	250000	375	3,00	0,30
	7,7	3	190000	285	3,00	0,30
IX	7,7	1	266000	745	5,60	0,56
	7,7	2	250000	500	4,00	0,40
	7,7	3	220000	440	4,00	0,40
X	8,5	1	402000	864	4,30	0,43
	8,5	2	320000	560	3,50	0,35
	8,5	3	260000	455	3,50	0,35

Table 6.10 - Lateral Pressure, Lateral Impulse, Scaled Time, Pulse Duration for Each Model I to X by Multi-Energy Method

Model	Associated Curve	r [m]	p_{s0}	p_{s1}	p_{s2}	p_{s3}	p_{s4}	p_{s5}	p_{s6}	p_{s7}	p_{s8}	p_{s9}
I	6,5	1	167200	149600	132000	114400	96800	79200	61600	44000	26400	8800
	6,5	2	161500	144500	127500	110500	93500	76500	59500	42500	25500	8500
	6,5	3	152000	136000	120000	104000	88000	72000	56000	40000	24000	8000
II	7	1	190000	170000	150000	130000	110000	90000	70000	50000	30000	10000
	7	2	180500	161500	142500	123500	104500	85500	66500	47500	28500	9500
	7	3	161500	144500	127500	110500	93500	76500	59500	42500	25500	8500
III	7,5	1	239400	214200	189000	163800	138600	113400	88200	63000	37800	12600
	7,5	2	228000	204000	180000	156000	132000	108000	84000	60000	36000	12000
	7,5	3	190000	170000	150000	130000	110000	90000	70000	50000	30000	10000
IV	8	1	300200	268600	237000	205400	173800	142200	110600	79000	47400	15800
	8	2	275500	246500	217500	188500	159500	130500	101500	72500	43500	14500
	8	3	228000	204000	180000	156000	132000	108000	84000	60000	36000	12000
V	7	1	208050	186150	164250	142350	120450	98550	76650	54750	32850	10950
	7	2	180500	161500	142500	123500	104500	85500	66500	47500	28500	9500
	7	3	171000	153000	135000	117000	99000	81000	63000	45000	27000	9000
VI	8	1	278350	249050	219750	190450	161150	131850	102550	73250	43950	14650
	8	2	275500	246500	217500	188500	159500	130500	101500	72500	43500	14500
	8	3	228000	204000	180000	156000	132000	108000	84000	60000	36000	12000
VII	8,3	1	325 850	291550	257250	222950	188650	154350	120050	85750	51450	17150
	8,3	2	285000	255000	225000	195000	165000	135000	105000	75000	45000	15000
	8,3	3	228000	204000	180000	156000	132000	108000	84000	60000	36000	12000
VIII	7,7	1	254600	227800	201000	174200	147400	120600	93800	67000	40200	13400
	7,7	2	237500	212500	187500	162500	137500	112500	87500	62500	37500	12500
	7,7	3	180500	161500	142500	123500	104500	85500	66500	47500	28500	9500
IX	7,7	1	252700	226100	199500	172900	146300	119700	93100	66500	39900	13300
	7,7	2	237500	212500	187500	162500	137500	112500	87500	62500	37500	12500
	7,7	3	209000	187000	165000	143000	121000	99000	77000	55000	33000	11000
X	8,5	1	381900	341700	301500	261300	221100	180900	140700	100500	60300	20100
	8,5	2	304000	272000	240000	208000	176000	144000	112000	80000	48000	16000
	8,5	3	247000	221000	195000	169000	143000	117000	91000	65000	39000	13000

Table 6.11 - Lateral Pressure During Shockwave for Each Model I to X by Multi-Energy Method

Model	Associated Curve	r [m]	u_0	u_1	u_2	u_3	u_4	u_5	u_6	u_7	u_8	u_9
I	6,5	1	366	331	295	259	221	183	144	104	63	21
	6,5	2	355	321	286	251	214	177	139	101	61	21
	6,5	3	336	304	271	237	202	167	131	95	58	19
II	7	1	411	372	332	291	249	207	163	118	72	24
	7	2	393	355	317	278	238	197	155	112	68	23
	7	3	355	321	286	251	214	177	139	101	61	21
III	7,5	1	504	457	409	360	309	257	203	147	90	30
	7,5	2	483	438	392	344	295	245	194	140	86	29
	7,5	3	411	372	332	291	249	207	163	118	72	24
IV	8	1	613	557	500	441	380	316	251	183	112	38
	8	2	569	517	464	408	351	292	231	168	103	35
	8	3	483	438	392	344	295	245	194	140	86	29
V	7	1	446	404	361	317	271	225	178	129	78	27
	7	2	393	355	317	278	238	197	155	112	68	23
	7	3	374	338	302	264	226	187	147	106	65	22
VI	8	1	574	522	468	412	354	295	234	170	104	35
	8	2	569	517	464	408	351	292	231	168	103	35
	8	3	483	438	392	344	295	245	194	140	86	29
VII	8,3	1	657	598	537	474	408	341	271	197	121	41
	8,3	2	586	533	478	421	362	302	239	174	106	36
	8,3	3	483	438	392	344	295	245	194	140	86	29
VIII	7,7	1	532	483	432	380	327	272	215	156	95	32
	7,7	2	501	454	406	357	307	255	201	146	89	30
	7,7	3	393	355	317	278	238	197	155	112	68	23
IX	7,7	1	528	480	429	378	325	270	213	155	95	32
	7,7	2	501	454	406	357	307	255	201	146	89	30
	7,7	3	447	405	362	318	273	226	178	129	79	27
X	8,5	1	749	683	615	544	470	393	313	229	141	48
	8,5	2	619	563	505	446	384	320	254	185	113	39
	8,5	3	518	470	421	370	318	264	209	152	93	31

Table 6.12 - Speed of Particles Moved by Shockwave, During this Action for Each Model I to X According to Multi-Energy Method

Model	Associated Curve	r [m]	ρ_{10}	ρ_{11}	ρ_{12}	ρ_{13}	ρ_{14}	ρ_{15}	ρ_{16}	ρ_{17}	ρ_{18}	ρ_{19}
I	6,5	1	2,4	2,3	2,2	2,0	1,9	1,8	1,7	1,6	1,4	1,3
	6,5	2	2,3	2,2	2,1	2,0	1,9	1,8	1,7	1,5	1,4	1,3
	6,5	3	2,3	2,2	2,1	2,0	1,9	1,8	1,6	1,5	1, 4	1,3
II	7	1	2,5	2,4	2,3	2,1	2,0	1,9	1,7	1,6	1,4	1,3
	7	2	2,4	2,3	2,2	2,1	2,0	1,9	1,7	1,6	1,4	1,3
	7	3	2,3	2,2	2,1	2,0	1,9	1,8	1,7	1,5	1,4	1,3
III	7,5	1	2,7	2,6	2,5	2,3	2,2	2,0	1,9	1,7	1,5	1,3
	7,5	2	2,7	2,6	2,4	2,3	2,2	2,0	1,8	1,7	1,5	1,3
	7,5	3	2,5	2,4	2,3	2,1	2,0	1,9	1,7	1,6	1,4	1,3
IV	8	1	3,0	2,9	2,7	2,6	2,4	2,2	2,0	1,8	1,6	1,3
	8	2	2,9	2,8	2,6	2,5	2,3	2,1	2,0	1,8	1,6	1,3
	8	3	2,7	2,6	2,4	2,3	2,2	2,0	1,8	1,7	1,5	1,3
V	7	1	2,6	2,5	2,3	2,2	2,1	1,9	1,8	1,6	1,5	1,3
	7	2	2,4	2,3	2,2	2,1	2,0	1,9	1,7	1,6	1,4	1,3
	7	3	2,4	2,3	2,2	2,1	1,9	1,8	1,7	1,6	1,4	1,3
VI	8	1	2,9	2,8	2,6	2,5	2,3	2,2	2,0	1,8	1,6	1,3
	8	2	2,9	2,8	2,6	2,5	2,3	2,1	2,0	1,8	1,6	1,3
	8	3	2,7	2,6	2,4	2,3	2,2	2,0	1,8	1,7	1,5	1,3
VII	8,3	1	3,1	3,0	2,8	2,6	2,5	2,3	2,1	1,9	1,6	1,3
	8,3	2	2,9	2,8	2,7	2,5	2,3	2,2	2,0	1,8	1,6	1,3
	8,3	3	2,7	2,6	2,4	2,3	2,2	2,0	1,8	1,7	1,5	1,3
VIII	7,7	1	2,8	2,7	2,5	2,4	2,2	2,1	1,9	1,7	1,5	1,3
	7,7	2	2,7	2,6	2,5	2,3	2,2	2,0	1,9	1,7	1,5	1,3
	7,7	3	2,4	2,3	2,2	2,1	2,0	1,9	1,7	1,6	1,4	1,3
IX	7,7	1	2,8	2,7	2,5	2,4	2,2	2,1	1,9	1,7	1,5	1,3
	7,7	2	2,7	2,6	2,5	2,3	2,2	2,0	1,9	1,7	1,5	1,3
	7,7	3	2,6	2,5	2,3	2,2	2,1	1,9	1,8	1,6	1,5	1,3
X	8,5	1	3,3	3,2	3,0	2,8	2,6	2,4	2,2	2,0	1,7	1,4
	8,5	2	3,0	2,9	2,7	2,6	2,4	2,2	2,0	1,8	1,6	1,3
	8,5	3	2,8	2,6	2,5	2,4	2,2	2,1	1,9	1,7	1,5	1,3

Table 6.13 - Air Density During Shockwave Action for Each Model I to X by Multi-Energy Method

Model	Associated Curve	r [m]	v_1	v_2	v_3	v_4	v_5	v_6	v_7	v_8	v_9	v_{10}
I	6,5	1	0,4	0,6	0,9	1,0	1,1	1,2	1,2	1,3	1,3	**1,3**
	6,5	2	0,2	0,4	0,6	0,7	0,8	0,8	0,8	0,9	0,9	**0,9**
	6,5	3	0,3	0,5	0,6	0,7	0,8	0,8	0,9	0,9	0,9	**0,9**
II	7	1	0,5	0,8	1,1	1,3	1,5	1,5	1,6	1,6	1,6	**1,6**
	7	2	0,3	0,5	0,7	0,8	0,9	1,0	1,0	1,0	1,0	**1,0**
	7	3	0,3	0,5	0,7	0,8	0,9	0,9	1,0	1,0	1,0	**1,0**
III	7,5	1	0,8	1,5	2,0	2,4	2,6	2,8	2,9	2,9	2,9	**2,9**
	7,5	2	0,5	1,0	1,3	1,5	1,7	1,8	1,9	1,9	1,9	**1,9**
	7,5	3	0,4	0,7	0,9	1,0	1,1	1,2	1,2	1,3	1,3	**1,3**
IV	8	1	1,2	2,2	2,9	3,5	3,9	4,1	4,2	4,3	4,3	**4,3**
	8	2	0,9	1,5	2,1	2,4	2,7	2,9	3,0	3,0	3,0	**3,0**
	8	3	0,5	0,8	1,1	1,3	1,4	1,5	1,5	1,6	1,6	**1,6**
V	7	1	0,7	1,3	1,7	2,0	2,2	2,3	2,4	2,5	2,5	**2,5**
	7	2	0,4	0,7	0,9	1,1	1,2	1,3	1,3	1,4	1,4	**1,4**
	7	3	0,3	0,5	0,7	0,8	0,9	1,0	1,0	1,0	1,0	**1,0**
VI	8	1	1,0	1,8	2,5	2,9	3,2	3,4	3,5	3,6	3,6	**3,6**
	8	2	0,8	1,5	2,0	2,4	2,6	2,8	2,9	2,9	2,9	**2,9**
	8	3	0,5	0,8	1,1	1,3	1,4	1,5	1,5	1,6	1,6	**1,6**
VII	8,3	1	1,3	2,3	3,0	3,6	4,0	4,2	4,4	4,4	4,4	**4,5**
	8,3	2	0,8	1,3	1,8	2,1	2,4	2,5	2,6	2,6	2,6	**2,6**
	8,3	3	0,5	0,8	1,1	1,3	1,5	1,5	1,6	1,6	1,6	**1,6**
VIII	7,7	1	0,8	1,5	2,0	2,3	2,6	2,7	2,8	2,9	2,9	**2,9**
	7,7	2	0,5	0,9	1,2	1,4	1,6	1,7	1,7	1,8	1,8	**1,8**
	7,7	3	0,3	0,5	0,7	0,8	0,9	0,9	1,0	1,0	1,0	**1,0**
IX	7,7	1	1,1	1,9	2,6	3,1	3,4	3,6	3,7	3,8	3,8	**3,8**
	7,7	2	0,7	1,2	1,6	1,9	2,1	2,2	2,3	2,4	2,4	**2,4**
	7,7	3	0,5	0,9	1,2	1,4	1,6	1,7	1,8	1,8	1,8	**1,8**
X	8,5	1	2,0	3,6	4,8	5,7	6,3	6,7	6,9	7,0	7,0	**7,0**
	8,5	2	1,0	1,8	2,4	2,9	3,2	3,4	3,5	3,5	3,5	**3,5**
	8,5	3	0,6	1,2	1,5	1,8	2,0	2,1	2,2	2,2	2,3	**2,3**

Table 6.14 - Corporal Speed of a Person Standing on the Tank During Shockwave Action for Each Model I to X According to Multi-Energy Method

Model	Associated Curve	r [m]	p_s [Pa]	i_s [Pa.s]	V_{10}	V landing
I	Curve No. 4	1	176000	148	**0,5**	<3
	Curve No. 4	2	121560	74	**0,1**	<3
	Curve No. 4	3	64832	55	**0,1**	<3
II	Curve No. 5	1	200000	303	**1,1**	<3
	Curve No. 5	2	153976	91	**0,2**	<3
	Curve No. 5	3	97248	71	**0,1**	<3
III	Curve No. 6	1	252000	442	**2,1**	close 3
	Curve No. 6	2	226912	116	**0,5**	<3
	Curve No. 6	3	121560	81	**0,2**	<3
IV	Curve No. 6	1	316000	549	**3,4**	close 3
	Curve No. 6	2	275536	131	**0,7**	<3
	Curve No. 6	3	153976	105	**0,3**	<3
V	Curve No. 4	1	219000	322	**1,3**	<3
	Curve No. 4	2	145872	96	**0,2**	<3
	Curve No. 4	3	81040	64	**0,1**	<3
VI	Curve No. 6	1	293000	504	**2,9**	close 3
	Curve No. 6	2	275536	126	**0,7**	<3
	Curve No. 6	3	145872	101	**0,3**	<3
VII	Curve No. 8	1	343000	625	**4,3**	3.0
	Curve No. 8	2	343000	150	**1,0**	<3
	Curve No. 8	3	162080	109	**0,3**	<3
VIII	Curve No. 5	1	268000	316	**1,6**	<3
	Curve No. 5	2	162080	95	**0,3**	<3
	Curve No. 5	3	97248	74	**0,1**	<3
IX	Curve No. 11	1	266000	553	**2,8**	close 3
	Curve No. 11	2	266000	145	**0,7**	<3
	Curve No. 11	3	162080	105	**0,3**	<3
X	Curve No. 11	1	402000	900	**7,3**	5.0
	Curve No. 11	2	402000	209	**1,7**	<3
	Curve No. 11	3	275536	145	**0,8**	<3

Table 6.15 - Takeoff Speed for a Person Standing on the Tank at 1, 2, 3 mts of Explosion Center by Baker et. al. Method vs. Arrival Speed by Figure 6-5.

Model	Associated Curve	r [m]	p_s [Pa]	i_s [Pa. S]	v_{10}	$v_{landing}$
I	6,5	1	176000	405	**1,3**	<3
	6,5	2	170000	289	**0,9**	<3
	6,5	3	160000	320	**0,9**	<3
II	7	1	200000	450	**1,6**	<3
	7	2	190000	304	**1,0**	<3
	7	3	170000	332	**1,0**	<3
III	7,5	1	252000	617	**2,9**	close 3
	7,5	2	240000	420	**1,9**	<3
	7,5	3	200000	350	**1,3**	<3
IV	8	1	316000	695	**4,3**	3,0
	8	2	290000	537	**3,0**	close 3
	8	3	240000	348	**1,6**	<3
V	7	1	219000	613	**2,5**	close 3
	7	2	190000	399	**1,4**	<3
	7	3	180000	315	**1,0**	<3
VI	8	1	293000	630	**3,6**	close 3
	8	2	290000	522	**2,9**	close 3
	8	3	240000	348	**1,6**	<3
VII	8,3	1	343000	652	**4,5**	3,0
	8,3	2	300000	450	**2,6**	<3
	8,3	3	240000	360	**1,6**	<3
VIII	7,7	1	268000	563	**2,9**	close 3
	7,7	2	250000	375	**1,8**	<3
	7,7	3	190000	285	**1,0**	<3
IX	7,7	1	266000	745	**3,8**	3,0
	7,7	2	250000	500	**2,4**	<3
	7,7	3	220000	440	**1,8**	<3
X	8,5	1	402000	864	**7,0**	5,0
	8,5	2	320000	560	**3,5**	<3
	8,5	3	260000	455	**2,3**	<3

Table 6.16 - Takeoff Speed for a Person Standing on the Tank at 1, 2, 3 meters from the Explosion Center by Multienergy Method vs. Arrival Speed by Figure 6-5.

Associated Curve	r	p_s	q	p	i_s	i_{tot}	P	I	S	Lung Injury	Survival
Curve No, 7	1	1701812	3014562	4716374	598	1657	46,6	1,25	1,13	Yes	Null
Curve No, 7	2	356576	300845	657 421	136	251	6,5	0,19	7,52	Yes	> 99%
Curve No, 7	3	162080	76182	238262	109	160	2,4	0,12	12,56	No	
Curve No, 7	1	1850138	3355711	5205849	764	2150	51,4	1,62	0,88	Yes	Null
Curve No, 7	2	421408	395897	817305	176	341	8,1	0,26	5,57	Yes	> 99%
Curve No, 7	3	210704	121873	332577	132	208	3,3	0,16	9,56	No	
Curve No, 7	1	2176924	4118112	6295036	1055	3051	62,1	2,31	0,63	Yes	Null
Curve No, 7	2	486240	498 275	984 515	214	433	9,7	0,33	4,41	Yes	99%
Curve No, 7	3	259328	175256	434584	148	248	4,3	0,19	7,94	No	
Curve No, 7	1	2435074	4728425	7163499	1270	3736	70,7	2,82	0,52	Yes	Null
Curve No, 7	2	518656	551846	1070502	247	510	10,6	0,39	3,78	Yes	90%
Curve No, 7	3	307952	235216	543168	176	310	5,4	0,23	6,34	No	
Curve No, 7	1	2089460	3912803	6002263	889	2554	59,3	1,93	0,75	Yes	Null
Curve No, 7	2	453824	446247	900071	190	377	8,9	0,28	5,05	Yes	99%
Curve No, 7	3	226912	138873	365785	143	231	3,6	0,17	8,65	No	
Curve No, 7	1	2632155	5198017	7830172	1469	4370	77,3	3,30	0,45	Yes	Null
Curve No, 7	2	405200	371397	776597	294	563	7,7	0,43	3,61	Yes	90%
Curve No, 7	3	340368	278388	618756	184	334	6,1	0,25	5,85	No	
Curve No, 7	1	2761592	5507863	8269455	1514	4534	81,6	3,43	0,43	Yes	Null
Curve No, 7	2	405200	371397	776597	303	581	7,7	0,44	3,52	Yes	90%
Curve No, 7	3	340368	278388	618756	189	344	6,1	0,26	5,71	No	
Curve No, 7	1	1057627	1591030	2648657	794	1988	26,1	1,50	1,03	Yes	Null
Curve No, 7	2	324160	256502	580662	183	328	5,7	0,25	6,00	No	
Curve No, 7	3	210704	121873	332577	137	216	3,3	0,16	9,26	No	
Curve No, 8	1	6280600	14126986	20407586	1647	5352	201,5	4,04	0,34	Yes	Null
Curve No, 8	2	842 816	1151043	1993859	588	1391	19,7	1,05	1,45	Yes	Null
Curve No, 8	3	356576	300845	657 421	196	361	6,5	0,27	5,42	Yes	> 99%
Curve No, 8	1	6685800	15130359	21816159	2159	7045	215,4	5,32	0,26	Yes	Null
Curve No, 8	2	2431200	4719224	7150424	691	2032	70,6	1,54	0,91	Yes	Null
Curve No, 8	3	388992	347 373	736 365	237	449	7,3	0,34	4,43	Yes	99%

Table 6.17 - Lung Damage and Survival Percentage save of a Person Standing on Tank at Burst Moment by Baker et al. Method

Curve No.	r	p_{s1}	P_d	p_{tot}	i_s	i_{tot}	P	I	S	Lung Injury	Survival
10	1	1745399	4432360	6177759	2106	7454	61,0	5,63	0,3	If	Nula
10	2	400000	506500	906500	483	1094	8,9	0,83	2,1	If	5%
10	3	150000	75405	225405	181	272	2,2	0,21	8,3	If	> 99%
10	1	1745399	4432360	6177759	2230	7894	61,0	5,97	0,3	If	Nula
10	2	470000	810400	1280400	601	1636	12,6	1,24	1,4	If	Nula
10	3	170000	113996	283996	217	363	2,8	0,27	6,3	If	> 99%
10	1	1745399	4432360	6177759	2442	8644	61,0	6,53	0,3	If	Nula
10	2	550000	1624567	2174567	770	3043	21,5	2,30	0,8	If	Nula
10	3	200000	202600	402600	280	563	4,0	0,43	4,1	If	> 99%
10	1	1745399	4432360	6177759	2585	9148	61,0	6,91	0,3	If	Nula
10	2	580000	1723370	2303370	859	3411	22,7	2,58	0,7	If	Nula
10	3	220000	234960	454960	326	674	4,5	0,51	3,5	If	> 99%
10	1	1745399	4432360	6177759	2369	8384	61,0	6,34	0,3	If	Nula
10	2	530000	848567	1378567	719	1871	13,6	1,41	1,2	If	Nula
10	3	180000	150899	330899	244	449	3,3	0,34	5,1	If	> 99%
10	1	1745399	4432360	6177759	2675	9468	61,0	7,16	0,3	If	Nula
10	2	590000	1508990	2098990	904	3217	20,7	2,43	0,7	If	Nula
10	3	240000	245598	485 598	368	744	4,8	0,56	3,2	If	99%
10	1	1745399	4432360	6177759	2747	9724	61,0	7,35	0,2	If	Nula
10	2	600000	2026000	2626000	944	4134	25,9	3,12	0,6	If	Nula
10	3	250000	293189	543189	394	855	5,4	0,65	2,8	If	70%
10	1	1057627	4432360	5489987	1376	7141	54,2	5,40	0,3	If	Nula
10	2	510000	829483	1339483	663	1742	13,2	1,32	1,3	If	Nula
10	3	180000	138109	318109	234	414	3,1	0,31	5,5	If	> 99%
10	1	1745399	4432360	6177759	2849	10084	61,0	7,62	0,2	If	Nula
10	2	620000	2150465	2770465	1012	4522	27,3	3,42	0,5	If	Nula
10	3	260000	303900	563900	424	920	5,6	0,70	2,6	If	50%
10	1	1745399	4432360	6177759	3104	10986	61,0	8,30	0,2	If	Nula
10	2	670000	2349600	3019600	1192	5370	29,8	4,06	0,5	If	Nula
10	3	400000	506500	906500	711	1612	8,9	1,22	1,5	If	Nula

Table 6.18 - Lung Damage and Survival Percentage save of a Person Standing on Tank at Burst Moment by Multi-Energy Method

Model	Associated Curve	r	p_s	Eardrum Rupture Probability
I	Curve No. 7	1	1701812	100
	Curve No. 7	2	356576	97
	Curve No. 7	3	162080	70
II	Curve No. 7	1	1850138	100
	Curve No. 7	2	421408	99
	Curve No. 7	3	210704	85
III	Curve No. 7	1	2176924	100
	Curve No. 7	2	486240	100
	Curve No. 7	3	259328	85
IV	Curve No. 7	1	2435074	100
	Curve No. 7	2	518656	100
	Curve No. 7	3	307952	95
V	Curve No. 7	1	2089460	100
	Curve No. 7	2	453824	100
	Curve No. 7	3	226912	85
VI	Curve No. 7	1	2632155	100
	Curve No. 7	2	405200	99
	Curve No. 7	3	340368	95
VII	Curve No. 7	1	2761592	100
	Curve No. 7	2	405200	99
	Curve No. 7	3	340368	95
VIII	Curve No. 7	1	1057627	100
	Curve No. 7	2	324160	95
	Curve No. 7	3	210704	85
IX	Curve No. 8	1	6280600	100
	Curve No. 8	2	842 816	100
	Curve No. 8	3	356576	95
X	Curve No. 8	1	6685800	100
	Curve No. 8	2	2431200	100
	Curve No. 8	3	388992	90

Table 6.19 - Eardrum Rupture Probability by Overpressure for Models I to X According to Baker et al. Method

Model	Curve No.	r	p_{s1}	Eardrum Rupture Probability
I	10	1	1745399	100
	10	2	400000	98
	10	3	150000	65
II	10	1	1745399	100
	10	2	470000	100
	10	3	170000	70
III	10	1	1745399	100
	10	2	550000	100
	10	3	200000	85
IV	10	1	1745399	100
	10	2	580000	100
	10	3	220000	85
V	10	1	1745399	100
	10	2	530000	100
	10	3	180000	75
VI	10	1	1745399	100
	10	2	590000	100
	10	3	240000	90
VII	10	1	1745399	100
	10	2	600000	100
	10	3	250000	75
VIII	10	1	1057627	100
	10	2	510000	100
	10	3	180000	75
IX	10	1	1745399	100
	10	2	620000	100
	10	3	260000	90
X	10	1	1745399	100
	10	2	670000	100
	10	3	400000	98

Table 6.20 - Eardrum Rupture Probability by Overpressure for Models I to X by Multi-Energy Method

Model	Associated Curve	r [m]	p_s [Pa]	i_s [Pa. S]	t_p [10^{-3} s]	dt_p
I	Curve No, 7	1	1701812	598	0,7028	0,07
	Curve No, 7	2	356576	136	0,7628	0,08
	Curve No, 7	3	162080	109	1,3450	0,13
II	Curve No, 7	1	1850138	764	0,8259	0,08
	Curve No, 7	2	421408	176	0,8353	0,08
	Curve No, 7	3	210704	132	1,2529	0,13
III	Curve No, 7	1	2176924	1055	0,9693	0,10
	Curve No, 7	2	486240	214	0,8802	0,09
	Curve No, 7	3	259328	148	1,1414	0,11
IV	Curve No, 7	1	2435074	1270	1,0431	0,10
	Curve No, 7	2	518656	247	0,9525	0,10
	Curve No, 7	3	307952	176	1,1430	0,11
V	Curve No, 7	1	2089460	889	0,8509	0,09
	Curve No, 7	2	453824	190	0,8373	0,08
	Curve No, 7	3	226912	143	1,2604	0,13
VI	Curve No, 7	1	2632155	1469	1,1162	0,11
	Curve No, 7	2	405200	294	1,4511	0,15
	Curve No, 7	3	340368	184	1,0812	0,11
VII	Curve No, 7	1	2761592	1514	1,0965	0,11
	Curve No, 7	2	405200	303	1,4956	0,15
	Curve No, 7	3	340368	189	1,1106	0,11
VIII	Curve No, 7	1	1057627	794	1,5015	0,15
	Curve No, 7	2	324160	183	1,1291	0,11
	Curve No, 7	3	210704	137	1,3004	0,13
IX	Curve No, 8	1	6280600	1647	0,5245	0,05
	Curve No, 8	2	842 816	588	1,3953	0,14
	Curve No, 8	3	356576	196	1,0993	0,11
X	Curve No, 8	1	6685800	2159	0,6458	0,06
	Curve No, 8	2	2431200	691	0,5684	0,06
	Curve No, 8	3	388992	237	1,2185	0,12

Table 6.21 - Lateral Pressure, Lateral Impulse, Scaled Time, Pulse Duration for each model I to X according to the method of Baker et al.

Model	Associated Curve	r [m]	p_{s0}	p_{s1}	p_{s2}	p_{s3}	p_{s4}	p_{s5}	p_{s6}	p_{s7}	p_{s8}	p_{s9}
I	Curve No. 7	1	1616721	1446540	1276359	1106178	935 997	765 815	595634	425453	255272	85091
	Curve No. 7	2	338747	303090	267432	231774	196117	160459	124802	89144	53486	17829
	Curve No. 7	3	153976	137768	121560	105352	89144	72936	56728	40520	24312	8104
II	Curve No. 7	1	1757631	1572617	1387604	1202590	1017576	832 562	647 548	462535	277521	92507
	Curve No. 7	2	400338	358197	316056	273915	231774	189634	147493	105352	63211	21070
	Curve No. 7	3	200169	179098	158028	136958	115887	94817	73746	52676	31606	10535
III	Curve No. 7	1	2068078	1850385	1632693	1415001	1197308	979 616	761923	544231	326539	108846
	Curve No. 7	2	461928	413304	364680	316056	267432	218808	170184	121560	72936	24312
	Curve No. 7	3	246362	220429	194496	168563	142630	116698	90765	64832	38899	12966
IV	Curve No. 7	1	2313320	2069813	1826306	1582798	1339291	1095783	852276	608 769	365261	121754
	Curve No. 7	2	492723	440858	388992	337126	285261	233395	181530	129664	77798	25933
	Curve No. 7	3	292554	261759	230964	200169	169374	138578	107783	76988	46193	15398
V	Curve No. 7	1	1984987	1776041	1567095	1358149	1149203	940 257	731311	522365	313419	104473
	Curve No. 7	2	431133	385 750	340368	294986	249603	204221	158838	113456	68074	22691
	Curve No. 7	3	215 566	192875	170184	147493	124802	102110	79419	56728	34037	11346
VI	Curve No. 7	1	2500547	2237332	1974116	1710901	1447685	1184470	921 254	658 039	394823	131608
	Curve No. 7	2	384940	344 420	303900	263380	222860	182340	141820	101300	60780	20260
	Curve No. 7	3	323350	289313	255276	221239	187202	153166	119129	85092	51055	17018
VII	Curve No. 7	1	2623512	2347353	2071194	1795035	1518876	1242716	966557	690 398	414 239	138080
	Curve No. 7	2	384940	344 420	303900	263380	222860	182340	141820	101300	60780	20260
	Curve No. 7	3	323350	289313	255276	221239	187202	153166	119129	85092	51055	17018
VIII	Curve No. 7	1	1004746	898983	793 220	687 458	581 695	475 932	370169	264407	158644	52881
	Curve No. 7	2	307952	275536	243120	210704	178288	145872	113456	81040	48624	16208
	Curve No. 7	3	200169	179098	158028	136958	115887	94817	73746	52676	31606	10535
IX	Curve No. 8	1	5966570	5338510	4710450	4082390	3454330	2826270	2198210	1570150	942090	314030
	Curve No. 8	2	800675	716 394	632 112	547830	463549	379267	294986	210704	126422	42141
	Curve No. 8	3	338747	303090	267432	231774	196117	160459	124802	89144	53486	17829
X	Curve No. 8	1	6351510	5682930	5014350	4345770	3677190	3008610	2340030	1671450	1002870	334290
	Curve No. 8	2	2309640	2066520	1823400	1580280	1337160	1094040	850920	607800	364680	121560
	Curve No. 8	3	369542	330 643	291744	252845	213946	175046	136147	97248	58349	19450

Table 6.22 - Lateral During Shockwave for each model I to X by Method of Pressure Baker et al.

Model	Associated Curve	r [m]	u_0	u_1	u_2	u_3	u_4	u_5	u_6	u_7	u_8	u_9
I	Curve No. 7	1	2168	2015	1853	1680	1494	1291	1068	819	533	196
	Curve No. 7	2	678	618	555	490	423	353	281	205	126	43
	Curve No. 7	3	340	307	274	240	205	169	133	96	58	20
II	Curve No. 7	1	2289	2129	1960	1780	1585	1373	1139	876	573	212
	Curve No. 7	2	779	711	640	567	490	410	327	240	148	51
	Curve No. 7	3	431	390	348	306	262	217	171	124	75	26
III	Curve No. 7	1	2537	2365	2182	1986	1774	1543	1286	996	658	247
	Curve No. 7	2	875	800	721	640	555	466	372	274	169	58
	Curve No. 7	3	517	469	420	369	317	264	208	151	92	31
IV	Curve No. 7	1	2720	2539	2345	2138	1914	1669	1396	1086	722	274
	Curve No. 7	2	921	843	761	676	587	493	395	291	180	62
	Curve No. 7	3	599	545	489	431	371	309	245	178	109	37
V	Curve No. 7	1	2473	2304	2124	1932	1725	1499	1248	964	636	238
	Curve No. 7	2	827	756	681	604	523	438	350	257	159	54
	Curve No. 7	3	460	417	372	327	281	233	184	133	81	27
VI	Curve No. 7	1	2853	2665	2464	2249	2016	1761	1477	1153	770	295
	Curve No. 7	2	754	688	619	548	474	396	316	231	142	49
	Curve No. 7	3	652	594	533	471	406	338	269	196	120	41
VII	Curve No. 7	1	2938	2745	2540	2320	2081	1820	1528	1195	801	308
	Curve No. 7	2	754	688	619	548	474	396	316	231	142	49
	Curve No. 7	3	652	594	533	471	406	338	269	196	120	41
VIII	Curve No. 7	1	1571	1451	1325	1191	1049	896	730	550	349	124
	Curve No. 7	2	626	569	511	451	388	324	257	187	115	39
	Curve No. 7	3	431	390	348	306	262	217	171	124	75	26
IX	Curve No. 8	1	4717	4435	4134	3811	3459	3072	2636	2127	1501	637
	Curve No. 8	2	1334	1229	1118	1001	877	745	604	451	284	100
	Curve No. 8	3	678	618	555	490	423	353	281	205	126	43
X	Curve No. 8	1	4882	4592	4282	3949	3588	3189	2740	2216	1569	671
	Curve No. 8	2	2718	2536	2343	2136	1912	1667	1395	1085	721	274
	Curve No. 8	3	729	665	598	529	457	382	304	222	137	47

Table 6.23 - Particle speed Carried by Shockwave, During this action for each model I to X as the Method of Baker et al.

Model	Associated Curve	r [m]	ρ_{10}	ρ_{11}	ρ_{12}	ρ_{13}	ρ_{14}	ρ_{15}	ρ_{16}	ρ_{17}	ρ_{18}	ρ_{19}
I	Curve No, 7	1	5,4	5,2	5,1	4,9	4,6	4,3	4,0	3,5	2,8	1,9
	Curve No, 7	2	3,2	3,0	2,9	2,7	2,5	2,3	2,1	1,9	1,6	1,3
	Curve No, 7	3	2,3	2,2	2,1	2,0	1,9	1,8	1,6	1,5	1,4	1,3
II	Curve No, 7	1	5,5	5,4	5,2	5,0	4,8	4,5	4,1	3,6	2,9	1,9
	Curve No, 7	2	3,4	3,2	3,1	2,9	2,7	2,5	2,2	2,0	1,7	1,4
	Curve No, 7	3	2,5	2,4	2,3	2,2	2,1	1,9	1,8	1,6	1,5	1,3
III	Curve No, 7	1	5,7	5,6	5,4	5,2	5,0	4,7	4,3	3,8	3,1	2,0
	Curve No, 7	2	3,6	3,4	3,3	3,1	2,9	2,6	2,4	2,1	1,8	1,4
	Curve No, 7	3	2,8	2,6	2,5	2,4	2,2	2,1	1,9	1,7	1,5	1,3
IV	Curve No, 7	1	5,8	5,7	5,5	5,4	5,1	4,9	4,5	4,0	3,3	2,1
	Curve No, 7	2	3,7	3,5	3,3	3,2	2,9	2,7	2,4	2,1	1,8	1,4
	Curve No, 7	3	3,0	2,8	2,7	2,5	2,4	2,2	2,0	1,8	1,6	1,3
V	Curve No, 7	1	5,6	5,5	5,3	5,2	4,9	4,6	4,3	3,8	3,1	2,0
	Curve No, 7	2	3,5	3,3	3,2	3,0	2,8	2,6	2,3	2,0	1,7	1,4
	Curve No, 7	3	2,6	2,5	2,4	2,2	2,1	2,0	1,8	1,6	1,5	1,3
VI	Curve No, 7	1	5,9	5,8	5,6	5,5	5,2	5,0	4,6	4,1	3,4	2,1
	Curve No, 7	2	3,3	3,2	3,0	2,8	2,6	2,4	2,2	2,0	1,7	1,4
	Curve No, 7	3	3,1	3,0	2,8	2,6	2,5	2,3	2,1	1,9	1,6	1,3
VII	Curve No, 7	1	5,9	5,8	5,7	5,5	5,3	5,0	4,7	4,2	3,4	2,2
	Curve No, 7	2	3,3	3,2	3,0	2,8	2,6	2,4	2,2	2,0	1,7	1,4
	Curve No, 7	3	3,1	3,0	2,8	2,6	2,5	2,3	2,1	1,9	1,6	1,3
VIII	Curve No, 7	1	4,7	4,6	4,4	4,2	3,9	3,6	3,3	2,8	2,3	1,6
	Curve No, 7	2	3,0	2,9	2,7	2,6	2,4	2,2	2,0	1,8	1,6	1,3
	Curve No, 7	3	2,5	2,4	2,3	2,2	2,1	1,9	1,8	1,6	1,5	1,3
IX	Curve No, 8	1	6,6	6,5	6,4	6,3	6,2	6,0	5,8	5,3	4,6	3,1
	Curve No, 8	2	4,4	4,2	4,0	3,8	3,6	3,3	3,0	2,6	2,1	1,5
	Curve No, 8	3	3,2	3,0	2,9	2,7	2,5	2,3	2,1	1,9	1,6	1,3
X	Curve No, 8	1	6,6	6,5	6,5	6,4	6,2	6,1	5,8	5,4	4,7	3,1
	Curve No, 8	2	5,8	5,7	5,5	5,4	5,1	4,9	4,5	4,0	3,3	2,1
	Curve No, 8	3	3,3	3,1	3,0	2,8	2,6	2,4	2,2	1,9	1,7	1,4

Table 6.24 - Air Density During Action Shockwave for each model I to X by Method of Baker et al.

Model	Associated Curve	r [m]	v_1	v_2	v_3	v_4	v_5	v_6	v_7	v_8	v_9	v_{10}
I	Curve No. 7	1	4,4	8,2	11,2	13,6	15,4	16,6	17,4	17,8	17,9	**17,9**
	Curve No. 7	2	0,3	0,5	0,7	0,8	0,9	0,9	1,0	1,0	1,0	**1,0**
	Curve No. 7	3	0,1	0,2	0,2	0,2	0,3	0,3	0,3	0,3	0,3	**0,3**
II	Curve No. 7	1	5,9	10,9	15,0	18,2	20,6	22,2	23,3	23,8	24,0	**24,0**
	Curve No. 7	2	0,4	0,8	1,0	1,2	1,4	1,4	1,5	1,5	1,5	**1,5**
	Curve No. 7	3	0,1	0,3	0,3	0,4	0,5	0,5	0,5	0,5	0,5	**0,5**
III	Curve No. 7	1	8,8	16,3	22,4	27,3	30,9	33,5	35,2	36,0	36,3	**36,4**
	Curve No. 7	2	0,6	1,1	1,5	1,7	1,9	2,0	2,1	2,2	2,2	**2,2**
	Curve No. 7	3	0,2	0,4	0,5	0,6	0,7	0,7	0,7	0,7	0,7	**0,7**
IV	Curve No. 7	1	11,2	20,6	28,4	34,6	39,3	42,7	44,8	45,9	46,3	**46,3**
	Curve No. 7	2	0,7	1,3	1,8	2,1	2,4	2,5	2,6	2,7	2,7	**2,7**
	Curve No. 7	3	0,3	0,5	0,7	0,9	1,0	1,0	1,0	1,1	1,1	**1,1**
V	Curve No. 7	1	7,3	13,5	18,5	22,5	25,6	27,7	29,1	29,8	30,0	**30,0**
	Curve No. 7	2	0,5	0,9	1,2	1,4	1,6	1,7	1,7	1,8	1,8	**1,8**
	Curve No. 7	3	0,2	0,3	0,4	0,5	0,5	0,6	0,6	0,6	0,6	**0,6**
VI	Curve No. 7	1	13,3	24,6	33,9	41,3	47,0	51,1	53,7	55,1	55,6	**55,6**
	Curve No. 7	2	0,7	1,2	1,6	2,0	2,2	2,3	2,4	2,4	2,4	**2,4**
	Curve No. 7	3	0,4	0,6	0,9	1,0	1,1	1,2	1,2	1,2	1,3	**1,3**
VII	Curve No. 7	1	14,0	25,8	35,6	43,5	49,5	53,8	56,6	58,1	58,6	**58,7**
	Curve No. 7	2	0,7	1,3	1,7	2,0	2,2	2,4	2,5	2,5	2,5	**2,5**
	Curve No. 7	3	0,4	0,7	0,9	1,0	1,1	1,2	1,3	1,3	1,3	**1,3**
VIII	Curve No. 7	1	4,4	8,0	10,8	13,0	14,6	15,6	16,3	16,6	16,6	**16,7**
	Curve No. 7	2	0,3	0,6	0,8	0,9	1,1	1,1	1,2	1,2	1,2	**1,2**
	Curve No. 7	3	0,2	0,3	0,4	0,4	0,5	0,5	0,5	0,5	0,5	**0,5**
IX	Curve No. 8	1	19,1	35,7	49,8	61,4	70,8	77,9	82,8	85,7	86,9	**87,1**
	Curve No. 8	2	2,7	4,9	6,7	8,0	9,0	9,6	9,9	10,1	10,2	**10,2**
	Curve No. 8	3	0,4	0,7	1,0	1,1	1,3	1,3	1,4	1,4	1,4	**1,4**
X	Curve No. 8	1	25,3	47,2	65,8	81,3	93,6	103,0	109,5	113,4	115,0	**115,2**
	Curve No. 8	2	6,1	11,2	15,5	18,9	21,5	23,4	24,6	25,2	25,5	**25,5**
	Curve No. 8	3	0,5	0,9	1,3	1,5	1,7	1,8	1,8	1,9	1,9	**1,9**

Table 6.25 - Corporal speed of a tank saves Person in Action During Shockwave for each model I to X according to the method of Baker et al.

Model	Associated Curve	r [m]	p_s [Pa]	i_s [Pa. S]	t_p [10^{-3} s]	dt_p
I	10	1	1745399	2106	2,41	0,24
	10	2	400000	483	2,42	0,24
	10	3	150000	181	2,41	0,24
II	10	1	1745399	2230	2,56	0,26
	10	2	470000	601	2,56	0,26
	10	3	170000	217	2,55	0,26
III	10	1	1745399	2442	2,80	0,28
	10	2	550000	770	2,80	0,28
	10	3	200000	280	2,80	0,28
IV	10	1	1745399	2585	2,96	0,30
	10	2	580000	859	2,96	0,30
	10	3	220000	326	2,96	0,30
V	10	1	1745399	2369	2,71	0,27
	10	2	530000	719	2,71	0,27
	10	3	180000	244	2,71	0,27
VI	10	1	1745399	2675	3,07	0,31
	10	2	590000	904	3,06	0,31
	10	3	240000	368	3,07	0,31
VII	10	1	1745399	2747	3,15	0,31
	10	2	600000	944	3,15	0,31
	10	3	250000	394	3,15	0,32
VIII	10	1	1057627	1376	2,60	0,26
	10	2	510000	663	2,60	0,26
	10	3	180000	234	2,60	0,26
IX	10	1	1745399	2849	3,26	0,33
	10	2	620000	1012	3,26	0,33
	10	3	260000	424	3,26	0,33
X	10	1	1745399	3104	3,56	0,36
	10	2	670000	1192	3,56	0,36
	10	3	400000	711	3,56	0,36

Table 6.26 - Lateral pressure Lateral Impulse, Time Scaling, Pulse Duration for each model I to X by Method of Multi-Energy

Model	Associated Curve	r [m]	p_{s0}	p_{s1}	p_{s2}	p_{s3}	p_{s4}	p_{s5}	p_{s6}	p_{s7}	p_{s8}	p_{s9}
I	10	1	1658129	1483589	1309049	1134509	959 969	785430	610890	436 350	261810	87270
	10	2	380000	340000	300000	260000	220000	180000	140000	100000	60000	20000
	10	3	142500	127500	112500	97500	82500	67500	52500	37500	22500	7500
II	10	1	1658129	1483589	1309049	1134509	959 969	785430	610890	436 350	261810	87270
	10	2	446500	399500	352500	305500	258500	211500	164500	117500	70500	23500
	10	3	161500	144500	127500	110500	93500	76500	59500	42500	25500	8500
III	10	1	1658129	1483589	1309049	1134509	959 969	785430	610890	436 350	261810	87270
	10	2	522500	467500	412500	357500	302500	247500	192500	137500	82500	27500
	10	3	190000	170000	150000	130000	110000	90000	70000	50000	30000	10000
IV	10	1	1658129	1483589	1309049	1134509	959 969	785430	610890	436 350	261810	87270
	10	2	551000	493000	435000	377000	319000	261000	203000	145000	87000	29000
	10	3	209000	187000	165000	143000	121000	99000	77000	55000	33000	11000
V	10	1	1658129	1483589	1309049	1134509	959 969	785430	610890	436 350	261810	87270
	10	2	503500	450500	397500	344500	291500	238500	185500	132500	79500	26500
	10	3	171000	153000	135000	117000	99000	81000	63000	45000	27000	9000
VI	10	1	1658129	1483589	1309049	1134509	959 969	785430	610890	436 350	261810	87270
	10	2	560500	501500	442500	383500	324500	265500	206500	147500	88500	29500
	10	3	228000	204000	180000	156000	132000	108000	84000	60000	36000	12000
VII	10	1	1658129	1483589	1309049	1134509	959 969	785430	610890	436 350	261810	87270
	10	2	570000	510000	450000	390000	330000	270000	210000	150000	90000	30000
	10	3	237500	212500	187500	162500	137500	112500	87500	62500	37500	12500
VIII	10	1	1004746	898983	793 220	687 458	581 695	475 932	370169	264407	158644	52881
	10	2	484500	433500	382500	331500	280500	229500	178500	127500	76500	25500
	10	3	171000	153000	135000	117000	99000	81000	63000	45000	27000	9000
IX	10	1	1658129	1483589	1309049	1134509	959 969	785430	610890	436 350	261810	87270
	10	2	589000	527000	465000	403000	341000	279000	217000	155000	93000	31000
	10	3	247000	221000	195000	169000	143000	117000	91000	65000	39000	13000
X	10	1	1658129	1483589	1309049	1134509	959 969	785430	610890	436 350	261810	87270
	10	2	636500	569500	502500	435500	368500	301500	234500	167500	100500	33500
	10	3	380000	340000	300000	260000	220000	180000	140000	100000	60000	20000

Table 6.27 - Lateral Pressure during Shockwave for each model I to X as the Multi-Energy Method

Model	Associated Curve	r [m]	u_0	u_1	u_2	u_3	u_4	u_5	u_6	u_7	u_8	u_9
I	10	1	2204	2049	1885	1710	1521	1315	1089	836	545	201
	10	2	746	681	612	542	468	392	312	228	140	48
	10	3	317	286	255	223	190	157	124	89	54	18
II	10	1	2204	2049	1885	1710	1521	1315	1089	836	545	201
	10	2	851	778	701	622	539	452	361	265	164	56
	10	3	355	321	286	251	214	177	139	101	61	21
III	10	1	2204	2049	1885	1710	1521	1315	1089	836	545	201
	10	2	965	883	798	710	617	519	416	307	190	66
	10	3	411	372	332	291	249	207	163	118	72	24
IV	10	1	2204	2049	1885	1710	1521	1315	1089	836	545	201
	10	2	1006	921	833	742	645	543	436	322	200	69
	10	3	447	405	362	318	273	226	178	129	79	27
V	10	1	2204	2049	1885	1710	1521	1315	1089	836	545	201
	10	2	937	857	775	688	598	503	402	296	184	63
	10	3	374	338	302	264	226	187	147	106	65	22
VI	10	1	2204	2049	1885	1710	1521	1315	1089	836	545	201
	10	2	1019	934	845	752	654	552	443	327	203	71
	10	3	483	438	392	344	295	245	194	140	86	29
VII	10	1	2204	2049	1885	1710	1521	1315	1089	836	545	201
	10	2	1032	946	857	763	664	560	449	332	207	72
	10	3	501	454	406	357	307	255	201	146	89	30
VIII	10	1	1571	1451	1325	1191	1049	896	730	550	349	124
	10	2	909	831	750	666	578	486	389	286	177	61
	10	3	374	338	302	264	226	187	147	106	65	22
IX	10	1	2204	2049	1885	1710	1521	1315	1089	836	545	201
	10	2	1059	971	879	783	682	576	463	342	213	74
	10	3	518	470	421	370	318	264	209	152	93	31
X	10	1	2204	2049	1885	1710	1521	1315	1089	836	545	201
	10	2	1124	1032	935	834	728	615	495	367	229	80
	10	3	746	681	612	542	468	392	312	228	140	48

Table 6.28 - Particle speed Carried by Shockwave, during this action for each model I to X by Method of Multi-Energy

Model	Associated Curve	r [m]	ρ_{10}	ρ_{11}	ρ_{12}	ρ_{13}	ρ_{14}	ρ_{15}	ρ_{16}	ρ_{17}	ρ_{18}	ρ_{19}
I	10	1	5,4	5,3	5,1	4,9	4,7	4,4	4,0	3,5	2,8	1,9
	10	2	3,3	3,2	3,0	2,8	2,6	2,4	2,2	2,0	1,7	1,4
	10	3	2,2	2,1	2,0	1,9	1,8	1,7	1,6	1,5	1,4	1,3
II	10	1	5,4	5,3	5,1	4,9	4,7	4,4	4,0	3,5	2,8	1,9
	10	2	3,5	3,4	3,2	3,0	2,8	2,6	2,3	2,1	1, 7	1,4
	10	3	2,3	2,2	2,1	2,0	1,9	1,8	1,7	1,5	1,4	1,3
III	10	1	5,4	5,3	5,1	4,9	4,7	4,4	4,0	3,5	2,8	1,9
	10	2	3,8	3,6	3,4	3,2	3,0	2,8	2,5	2,2	1,8	1,4
	10	3	2,5	2,4	2,3	2,1	2,0	1,9	1,7	1,6	1,4	1,3
IV	10	1	5,4	5,3	5,1	4,9	4,7	4,4	4,0	3,5	2,8	1,9
	10	2	3,8	3,7	3,5	3,3	3,1	2,8	2,5	2,2	1,9	1,4
	10	3	2,6	2,5	2,3	2,2	2,1	1,9	1,8	1,6	1,5	1,3
V	10	1	5,4	5,3	5,1	4,9	4,7	4,4	4,0	3,5	2,8	1,9
	10	2	3,7	3,5	3,4	3,2	3,0	2,7	2,5	2,2	1,8	1,4
	10	3	2,4	2,3	2,2	2,1	1,9	1,8	1,7	1,6	1,4	1,3
VI	10	1	5,4	5,3	5,1	4,9	4,7	4,4	4,0	3,5	2,8	1,9
	10	2	3,9	3,7	3,5	3,3	3,1	2,8	2,6	2,2	1,9	1,4
	10	3	2,7	2,6	2,4	2,3	2,2	2,0	1,8	1,7	1,5	1,3
VII	10	1	5,4	5,3	5,1	4,9	4,7	4,4	4,0	3,5	2,8	1,9
	10	2	3,9	3,7	3,5	3,3	3,1	2,9	2,6	2,3	1,9	1,4
	10	3	2,7	2,6	2,5	2,3	2,2	2,0	1,9	1,7	1,5	1,3
VIII	10	1	4,7	4,6	4,4	4,2	3,9	3,6	3,3	2,8	2,3	1,6
	10	2	3,7	3,5	3,3	3,1	2,9	2,7	2,4	2,1	1,8	1,4
	10	3	2,4	2,3	2,2	2,1	1,9	1,8	1,7	1,6	1,4	1,3
IX	10	1	5,4	5,3	5,1	4,9	4,7	4,4	4,0	3,5	2,8	1,9
	10	2	3,9	3,8	3,6	3,4	3,2	2,9	2,6	2,3	1,9	1,5
	10	3	2,8	2,6	2,5	2,4	2,2	2,1	1,9	1,7	1,5	1,3
X	10	1	5,4	5,3	5,1	4,9	4,7	4,4	4,0	3,5	2,8	1,9
	10	2	4,1	3,9	3,7	3,5	3,3	3,0	2,7	2,4	2,0	1,5
	10	3	3,3	3,2	3,0	2,8	2,6	2,4	2,2	2,0	1,7	1,4

Table 6.29 - Air Density during Action Shockwave for each model I to X by Method of Multi-Energy

Model	Associated Curve	r [m]	v_1	v_2	v_3	v_4	v_5	v_6	v_7	v_8	v_9	v_{10}
I	10	1	15,8	28,8	39,4	47,6	53,7	57,9	60,5	61,7	62,1	**62,2**
	10	2	1,1	2,0	2,7	3,2	3,5	3,7	3,9	3,9	3,9	**3,9**
	10	3	0,1	0,2	0,3	0,4	0,4	0,4	0,5	0,5	0,5	**0,5**
II	10	1	16,7	30,5	41,7	50,4	56,8	61,2	63,9	65,2	65,6	**65,7**
	10	2	1,6	2,9	3,9	4,7	5,2	5,5	5,7	5,8	5,8	**5,8**
	10	3	0,2	0,3	0,4	0,5	0,6	0,6	0,6	0,6	0,6	**0,6**
III	10	1	18,3	33,4	45,6	55,0	62,0	66,8	69,7	71,1	71,6	**71,6**
	10	2	2,4	4,4	5,9	7,0	7,8	8,3	8,6	8,7	8,8	**8,8**
	10	3	0,3	0,5	0,7	0,8	0,9	1,0	1,0	1,0	1,0	**1,0**
IV	10	1	19,3	35,3	48,2	58,1	65,5	70,5	73,6	75,1	75,6	**75,6**
	10	2	2,9	5,2	6,9	8,3	9,2	9,8	10,1	10,3	10,3	**10,3**
	10	3	0,4	0,7	0,9	1,1	1,2	1,3	1,3	1,3	1,3	**1,3**
V	10	1	17,7	32,4	44,2	53,4	60,2	64,9	67,7	69,1	69,5	**69,6**
	10	2	2,2	4,0	5,3	6,3	7,0	7,5	7,7	7,9	7,9	**7,9**
	10	3	0,2	0,4	0,5	0,6	0,7	0,7	0,8	0,8	0,8	**0,8**
VI	10	1	20,0	36,5	49,8	60,1	67,7	72,9	76,0	77,6	78,1	**78,1**
	10	2	3,1	5,5	7,4	8,8	9,8	10,5	10,8	11,0	11,0	**11,1**
	10	3	0,5	0,9	1,1	1,3	1,5	1,6	1,6	1,7	1,7	**1,7**
VII	10	1	20,5	37,5	51,1	61,7	69,4	74,8	78,0	79,6	80,1	**80,1**
	10	2	3,3	5,9	7,9	9,4	10,4	11,1	11,5	11,7	11,7	**11,7**
	10	3	0,5	1,0	1,3	1,5	1,7	1,8	1,8	1,9	1,9	**1,9**
VIII	10	1	7,6	13,7	18,6	22,3	25,0	26,8	27,9	28,4	28,5	**28,5**
	10	2	2,0	3,5	4,7	5,6	6,2	6,6	6,9	7,0	7,0	**7,0**
	10	3	0,2	0,4	0,5	0,6	0,7	0,7	0,7	0,7	0,8	**0,8**
IX	10	1	21,3	38,8	52,9	63,9	71,9	77,4	80,7	82,4	82,9	**82,9**
	10	2	3,6	6,5	8,7	10,4	11,5	12,3	12,7	12,9	13,0	**13,0**
	10	3	0,6	1,1	1,4	1,7	1,9	2,0	2,1	2,1	2,1	**2,1**
X	10	1	23,2	42,2	57,5	69,4	78,1	84,0	87,6	89,3	89,8	**89,9**
	10	2	4,5	8,2	11,0	13,1	14,6	15,6	16,1	16,4	16,4	**16,5**
	10	3	1,6	2,9	3,9	4,6	5,1	5,5	5,7	5,7	5,8	**5,8**

Table 6.30 - Corporal speed of a tank saves Person in Action during Shockwave for each model I to X by Method of Multi-Energy

Model	Associated Curve	r [m]	p_s [Pa]	i_s [Pa.s]	v_{10}	$v_{landing}$
I	Curve No, 7	1	1701812	598	**17,9**	Out of range
	Curve No, 7	2	356576	136	**1,0**	<3
	Curve No, 7	3	162080	109	**0,3**	<3
II	Curve No, 7	1	1850138	764	**24,0**	Out of range
	Curve No, 7	2	421408	176	**1,5**	<3
	Curve No, 7	3	210704	132	**0,5**	<3
III	Curve No, 7	1	2176924	1055	**36,4**	Out of range
	Curve No, 7	2	486240	214	**2,2**	<3
	Curve No, 7	3	259328	148	**0,7**	<3
IV	Curve No, 7	1	2435074	1270	**46,3**	Out of range
	Curve No, 7	2	518656	247	**2,7**	<3
	Curve No, 7	3	307952	176	**1,1**	<3
V	Curve No, 7	1	2089460	889	**30,0**	Out of range
	Curve No, 7	2	453824	190	**1,8**	<3
	Curve No, 7	3	226912	143	**0,6**	<3
VI	Curve No, 7	1	2632155	1469	**55,6**	Out of range
	Curve No, 7	2	405200	294	**2,4**	<3
	Curve No, 7	3	340368	184	**1,3**	<3
VII	Curve No, 7	1	2761592	1514	**58,7**	Out of range
	Curve No, 7	2	405200	303	**2,5**	<3
	Curve No, 7	3	340368	189	**1,3**	<3
VIII	Curve No, 7	1	1057627	794	**16,7**	6,5
	Curve No, 7	2	324160	183	**1,2**	<3
	Curve No, 7	3	210704	137	**0,5**	<3
IX	Curve No, 8	1	6280600	1647	**87,1**	Out of range
	Curve No, 8	2	842 816	588	**10,2**	6
	Curve No, 8	3	356576	196	**1,4**	<3
X	Curve No, 8	1	6685800	2159	**115,2**	Out of range
	Curve No, 8	2	2431200	691	**25,5**	Out of range
	Curve No, 8	3	388992	237	**1,9**	<3

Table 6.31 - Takeoff speed for a person standing on the tank to 1, 2, 3 mts Center Explosion by Method of Baker et. al vs. Arrival by Speed Figure 6-5.

Model	Associated Curve	r [m]	p_s [Pa]	i_s [Pa.s]	v_{10}	$v_{landing}$
I	10	1	1745399	2106	**62,2**	Out of range
	10	2	400000	483	**3,9**	3
	10	3	150000	181	**0,5**	<3
II	10	1	1745399	2230	**65,7**	Out of range
	10	2	470000	601	**5,8**	4
	10	3	170000	217	**0,6**	<3
III	10	1	1745399	2442	**71,6**	Out of range
	10	2	550000	770	**8,8**	6
	10	3	200000	280	**1,0**	<3
IV	10	1	1745399	2585	**75,6**	close 3
	10	2	580000	859	**10,3**	6
	10	3	220000	326	**1,3**	<3
V	10	1	1745399	2369	**69,6**	Out of range
	10	2	530000	719	**7,9**	5
	10	3	180000	244	**0,8**	<3
VI	10	1	1745399	2675	**78,1**	Out of range
	10	2	590000	904	**11,1**	6
	10	3	240000	368	**1,7**	<3
VII	10	1	1745399	2747	**80,1**	Out of range
	10	2	600000	944	**11,7**	6,5
	10	3	250000	394	**1,9**	<3
VIII	10	1	1057627	1376	**28,5**	Out of range
	10	2	510000	663	**7,0**	4
	10	3	180000	234	**0,8**	<3
IX	10	1	1745399	2849	**82,9**	Out of range
	10	2	620000	1012	**13,0**	6,5
	10	3	260000	424	**2,1**	<3
X	10	1	1745399	3104	**89,9**	Out of range
	10	2	670000	1192	**16,5**	8,5
	10	3	400000	711	**5,8**	3

Table 6.32 - Takeoff speed for a person standing on the tank to 1, 2, and 3 meters from the center of explosion by Method The multi vs. Arrival by Speed Figure 6-5.

Appendix D

ANNEX: Chapter 7 Tables

Model	Associated Curve	r	R_{17}	Relevance
I	Curve No, 7	0,22	3,74	
II	Curve No, 7	0,2	3,4	
III	Curve No, 7	0,18	3,06	
IV	Curve No, 7	0,17	2,89	Not applicable
V	Curve No, 7	0,19	3,23	
VI	Curve No, 7	0,16	2,72	Not applicable
VII	Curve No, 7	0,16	2,72	Not applicable
VIII	Curve No, 7	0,2	3,4	
IX	Curve No, 8	0,15	2,55	Not applicable
X	Curve No, 8	0,14	2,38	Not applicable

Table 7.1 - Energy values for Detonation that not apply for Overcome Truck Windshield Break at 17 m Distance Approximately of Center Explosion - method of Baker et al

Model	Curve No,	r	R_{17}	Relevance
I	10	0,18	3,06	
II	10	0,17	2,89	
III	10	0,16	2,72	
IV	10	0,15	2,55	Not applicable
V	10	0,16	2,72	
VI	10	0,14	2,38	Not applicable
VII	10	0,14	2,38	Not applicable
VIII	10	0,17	2,89	
IX	10	0,14	2,38	Not applicable
X	10	0,12	2,04	Not applicable

Table 7.2 - Energy values for Detonation that not apply for Overcome Truck Windshield Break at 17 m Distance Approximately of Center Explosion - The multi method

Associated Curve	r	Lung Injury	Survival	Relevance
Curve No, 7	1	If	Nula	Not applicable
Curve No, 7	2	If	> 99%	
Curve No, 7	3	Not		
Curve No, 7	1	If	Nula	Not applicable
Curve No, 7	2	If	> 99%	
Curve No, 7	3	Not		
Curve No, 7	1	If	Nula	Not applicable
Curve No, 7	2	If	99%	
Curve No, 7	3	Not		
Curve No, 7	1	If	Nula	Not applicable
Curve No, 7	2	If	90%	
Curve No, 7	3	Not		
Curve No, 7	1	If	Nula	Not applicable
Curve No, 7	2	If	99%	
Curve No, 7	3	Not		
Curve No, 7	1	If	Nula	Not applicable
Curve No, 7	2	If	90%	
Curve No, 7	3	Not		
Curve No, 7	1	If	Nula	Not applicable
Curve No, 7	2	If	90%	3,52
Curve No, 7	3	Not		5,71
Curve No, 7	1	If	Nula	Not applicable
Curve No, 7	2	Not		
Curve No, 7	3	Not		
Curve No, 8	1	If	Nula	Not applicable
Curve No, 8	2	If	Nula	Not applicable
Curve No, 8	3	If	> 99%	
Curve No, 8	1	If	Nula	Not applicable
Curve No, 8	2	If	Nula	Not applicable
Curve No, 8	3	If	99%	

Table 7.3 - Relevance of Lung Injury by the Baker et. al. Method

Model	Associated Curve	r [m]	v_{10}	$v_{landing}$
I	Curve No, 7	1	**17,9**	Out of range
	Curve No, 7	2	**1,0**	<3
	Curve No, 7	3	**0,3**	<3
II	Curve No, 7	1	**24,0**	Out of range
	Curve No, 7	2	**1,5**	<3
	Curve No, 7	3	**0,5**	<3
III	Curve No, 7	1	**36,4**	Out of range
	Curve No, 7	2	**2,2**	<3
	Curve No, 7	3	**0,7**	<3
IV	Curve No, 7	1	**46,3**	Out of range
	Curve No, 7	2	**2,7**	<3
	Curve No, 7	3	**1,1**	<3
V	Curve No, 7	1	**30,0**	Out of range
	Curve No, 7	2	**1,8**	<3
	Curve No, 7	3	**0,6**	<3
VI	Curve No, 7	1	**55,6**	Out of range
	Curve No, 7	2	**2,4**	<3
	Curve No, 7	3	**1,3**	<3
VII	Curve No, 7	1	**58,7**	Out of range
	Curve No, 7	2	**2,5**	<3
	Curve No, 7	3	**1,3**	<3
VIII	Curve No, 7	1	**16,7**	6,5
	Curve No, 7	2	**1,2**	<3
	Curve No, 7	3	**0,5**	<3
IX	Curve No, 8	1	**87,1**	Out of range
	Curve No, 8	2	**10,2**	6
	Curve No, 8	3	**1,4**	<3
X	Curve No, 8	1	**115,2**	Out of range
	Curve No, 8	2	**25,5**	Out of range
	Curve No, 8	3	**1,9**	<3

Table 7.4 - Relevance of Speed Displacement by the Baker et. al. Method

Model	Associated Curve	r	p_s	Eardrum Rupture Probability
I	Curve No. 7	1	1701812	100
	Curve No. 7	2	356576	97
	Curve No. 7	3	162080	70
II	Curve No. 7	1	1850138	100
	Curve No. 7	2	421408	99
	Curve No. 7	3	210704	85
III	Curve No. 7	1	2176924	100
	Curve No. 7	2	486240	100
	Curve No. 7	3	259328	85
IV	Curve No. 7	1	2435074	100
	Curve No. 7	2	518656	100
	Curve No. 7	3	307952	95
V	Curve No. 7	1	2089460	100
	Curve No. 7	2	453824	100
	Curve No. 7	3	226912	85
VI	Curve No. 7	1	2632155	100
	Curve No. 7	2	405200	99
	Curve No. 7	3	340368	95
VII	Curve No. 7	1	2761592	100
	Curve No. 7	2	405200	99
	Curve No. 7	3	340368	95
VIII	Curve No. 7	1	1057627	100
	Curve No. 7	2	324160	95
	Curve No. 7	3	210704	85
IX	Curve No. 8	1	6280600	100
	Curve No. 8	2	842 816	100
	Curve No. 8	3	356576	95
X	Curve No. 8	1	6685800	100
	Curve No. 8	2	2431200	100
	Curve No. 8	3	388992	90

Table 7.5 - Eardrum Damage by Baker et. al. Method

Curve No.	r	Lung Injury	Survival	Relevance
10	1	If	Null	Not applicable
10	2	If	5%	
10	3	If	> 99%	
10	1	If	Null	Not applicable
10	2	If	Null	Not applicable
10	3	If	> 99%	
10	1	If	Null	Not applicable
10	2	If	Null	Not applicable
10	3	If	> 99%	
10	1	If	Null	Not applicable
10	2	If	Null	Not applicable
10	3	If	> 99%	
10	1	If	Null	Not applicable
10	2	If	Null	Not applicable
10	3	If	> 99%	
10	1	If	Null	Not applicable
10	2	If	Null	Not applicable
10	3	If	99%	
10	1	If	Null	Not applicable
10	2	If	Null	Not applicable
10	3	If	70%	
10	1	If	Null	Not applicable
10	2	If	Null	Not applicable
10	3	If	> 99%	
10	1	If	Null	Not applicable
10	2	If	Null	Not applicable
10	3	If	50%	
10	1	If	Null	Not applicable
10	2	If	Null	Not applicable
10	3	If	Null	Not applicable

Table 7.6 - Relevance of Lung Damage Multienergy Method

Model	Associated Curve	r [m]	v_{10}	v landing
I	10	1	**62,2**	Out of range
	10	2	**3,9**	3
	10	3	**0,5**	<3
II	10	1	**65,7**	Out of range
	10	2	**5,8**	4
	10	3	**0,6**	<3
III	10	1	**71,6**	Out of range
	10	2	**8,8**	6
	10	3	**1,0**	<3
IV	10	1	**75,6**	close 3
	10	2	**10,3**	6
	10	3	**1,3**	<3
V	10	1	**69,6**	Out of range
	10	2	**7,9**	5
	10	3	**0,8**	<3
VI	10	1	**78,1**	Out of range
	10	2	**11,1**	6
	10	3	**1,7**	<3
VII	10	1	**80,1**	Out of range
	10	2	**11,7**	6,5
	10	3	**1,9**	<3
VIII	10	1	**28,5**	Out of range
	10	2	**7,0**	4
	10	3	**0,8**	<3
IX	10	1	**82,9**	Out of range
	10	2	**13,0**	6,5
	10	3	**2,1**	<3
X	10	1	**89,9**	Out of range
	10	2	**16,5**	8,5
	10	3	**5,8**	3

Table 7.7 - Relevance for Speed Displacement Multienergy Method

Model	Curve No.	r	p_{s1}	Eardrum Rupture Probability
I	10	1	1745399	100
	10	2	400000	98
	10	3	150000	65
II	10	1	1745399	100
	10	2	470000	100
	10	3	170000	70
III	10	1	1745399	100
	10	2	550000	100
	10	3	200000	85
IV	10	1	1745399	100
	10	2	580000	100
	10	3	220000	85
V	10	1	1745399	100
	10	2	530000	100
	10	3	180000	75
VI	10	1	1745399	100
	10	2	590000	100
	10	3	240000	90
VII	10	1	1745399	100
	10	2	600000	100
	10	3	250000	75
VIII	10	1	1057627	100
	10	2	510000	100
	10	3	180000	75
IX	10	1	1745399	100
	10	2	620000	100
	10	3	260000	90
X	10	1	1745399	100
	10	2	670000	100
	10	3	400000	98

Table 7. 8 - Eardrum Damage by Multienergy Method

Appendix E

ANNEX: Chapter 8 Tables

t	p_i	T_{ui}	S	q_x	a_v	v_v	x_i	a_h	v_h	z_i	ω'	ω	ω . t	θ	C_L	C_D	β	α
0,01	101300	283	0,37	0	-10			0							0,50	0,60	90	90
0,02	101400	283	0,31	64	-10	0,00	0,00	0	0		0,00	0,00	0,00	30	0,50	0,60	90	60
0,03	101400	283	0,31	65	-10	0,00	0,00	0	0	0,00	-0,32	0,00	0,00	30	0,50	0,60	90	60
0,04	101400	283	0,31	65	-10	0,00	0,00	0	0	0,00	-0,32	-0,01	0,00	30	0,50	0,60	90	60
0,05	101500	283	0,31	129	-10	0,00	0,00	0	0,00	0,00	-0,32	-0,01	0,00	30	0,50	0,60	90	60
0,06	101500	283	0,31	129	-10	0,00	0,00	0	0,00	0,00	-0,64	-0,02	0,00	30	0,50	0,60	90	60
0,07	102000	284	0,31	451	-9	0,00	0,00	-1	0,00	0,00	-0,64	-0,02	0,00	30	0,50	0,60	90	60
0,08	102000	284	0,31	453	-9	0,00	0,00	-1	0,00	0,00	-2,23	-0,04	0,00	30	0,50	0,60	90	60
0,09	103000	285	0,31	1088	-7	0,00	0,00	-2	0,00	0,00	-2,24	-0,07	0,00	30	0,50	0,60	90	60
0,1	104000	286	0,31	1723	-6	0,00	0,00	-4	0,00	0,00	-5,38	-0,12	0,00	30	0,50	0,60	90	60
0,11	105000	286	0,31	2345	-4	0,00	0,00	-5	0,00	0,00	-8,52	-0,21	0,00	30	0,50	0,60	90	60
0,12	106000	287	0,31	2956	-3	0,00	0,00	-6	0,00	0,00	-11,59	-0,32	-0,01	30	0,20	0,30	90	60
0,13	107000	288	0,31	3556	-6	0,00	0,00	-3	0,00	0,00	-6,84	-0,39	-0,01	30	0,20	0,30	90	60
0,14	109000	290	0,31	4717	-4	0,00	0,00	-4	0,00	0,00	-8,22	-0,47	-0,01	31	0,30	0,30	90	59
0,15	111000	292	0,31	5868	-3	0,00	0,00	-7	0,00	0,00	-12,43	-0,60	-0,02	31	0,30	0,30	90	59
0,16	112000	293	0,31	6431	-2	-0,02	-0,01	-8	-0,08	0,00	-15,49	-0,75	-0,03	31	0,20	0,30	15	0
0,17	113000	294	0,31	6949	-2	-0,04	-0,01	7	-0,01	0,00	-8,27	-0,83	-0,03	31	0,20	0,30	74	43
0,18	115000	297	0,31	7995	1	-0,03	-0,01	-4	-0,05	0,00	-15,67	-0,99	-0,04	32	0,40	0,50	33	1
0,19	115000	297	0,31	8054	10	0,07	-0,01	6	0,02	0,00	-21,13	-1,20	-0,05	32	0,20	0,30	77	44
0,2	117000	299	0,31	8986	2	0,09	0,00	-5	-0,03	0,00	-18,25	-1,38	-0,07	33	0,40	0,50	71	76
0,21	118000	301	0,31	9562	3	0,13	0,00	-21	-0,24	0,00	-33,42	-1,72	-0,08	34	0,20	0,70	27	61
0,22	118000	301	0,31	9534	9	0,22	0,00	-21	-0,45	-0,01	-43,77	-2,16	-0,10	35	0,50	0,60	26	61
0,23	120000	304	0,31	10418	20	0,42	0,00	-13	-0,58	-0,01	-47,39	-2,63	-0,12	36	0,50	0,60	36	72
0,24	120000	305	0,30	10505	22	0,64	0,01	-8	-0,66	-0,02	-49,30	-3,12	-0,15	37	0,30	0,70	44	81

t	p_i	T_{ui}	S	q_x	a_v	v_v	x_i	a_h	v_h	z_i	ω'	ω	ω . t	θ	C_L	C_D	β	α
0,25	121000	306	0,30	10820	21	0,85	0,01	-13	-0,79	-0,03	-50,83	-3,63	-0,19	39	0,10	0,80	47	86
0,26	122000	308	0,30	11248	19	1,05	0,02	21	-0,58	-0,03	-57,72	-4,21	-0,23	41	0,10	0,90	61	79
0,27	123000	310	0,30	11597	24	1,29	0,04	-24	-0,82	-0,04	-67,87	-4,89	-0,27	43	0,10	0,80	57	80
0,28	123000	311	0,30	11487	19	1,47	0,05	-24	-1,06	-0,05	-63,18	-5,52	-0,32	45	0,10	0,80	54	81
0,29	125000	315	0,30	12092	19	1,66	0,06	-27	-1,32	-0,06	-63,74	-6,16	-0,38	48	0,10	0,80	51	80
0,3	126000	317	0,30	12466	18	1,84	0,08	-29	-1,61	-0,08	-68,49	-6,84	-0,45	52	0,10	0,80	49	80
0,31	127000	320	0,30	12602	17	2,01	0,10	-30	-1,91	-0,09	-72,21	-7,56	-0,52	55	0,10	0,80	46	78
0,32	128000	323	0,30	12754	16	2,17	0,12	-31	-2,23	-0,11	-74,72	-8,31	-0,60	59	0,10	0,80	44	77
0,33	129000	326	0,29	12868	14	2,31	0,14	-32	-2,55	-0,14	-77,39	-9,09	-0,68	64	0,10	0,80	42	74
0,34	131000	331	0,29	13279	14	2,45	0,17	-34	-2,89	-0,17	-79,74	-9,88	-0,78	69	0,20	0,70	40	71
0,35	133000	336	0,28	13748	6	2,50	0,19	-34	-3,23	-0,20	-77,05	-10,65	-0,88	74	0,30	0,70	38	68
0,36	135000	341	0,28	14082	0	2,50	0,22	-38	-3,61	-0,23	-85,68	-11,51	-0,99	80	0,30	0,70	35	65
0,37	138000	348	0,27	14629	-2	2,48	0,24	-39	-4,00	-0,27	-89,88	-12,41	-1,11	87	0,40	0,60	32	62
0,38	140000	355	0,26	15002	-11	2,37	0,27	-37	-4,37	-0,31	-89,73	-13,31	-1,24	93	0,50	0,60	28	58
0,39	143000	365	0,24	15248	-18	2,19	0,29	-38	-4,75	-0,36	-100,47	-14,31	-1,38	101	0,50	0,60	25	55
0,4	147000	376	0,23	15944	-20	1,99	0,31	-37	-5,12	-0,41	-103,47	-15,35	-1,53	108	0,40	0,50	21	50
0,41	150000	388	0,21	16460	-19	1,80	0,33	-29	-5,40	-0,46	-88,52	-16,23	-1,68	117	0,40	0,50	18	45
0,42	154000	402	0,19	15972	-19	1,61	0,35	-25	-5,65	-0,51	-88,98	-17,12	-1,85	126	0,40	0,40	16	38
0,43	158000	421	0,17	14898	-19	1,42	0,36	-17	-5,82	-0,57	-73,31	-17,85	-2,03	135	0,40	0,40	14	31
0,44	163000	442	0,15	15432	-19	1,23	0,38	-15	-5,97	-0,63	-62,82	-18,48	-2,21	145	0,30	0,30	12	23
0,45	167000	464	0,12	15679	-16	1,07	0,39	-9	-6,06	-0,69	-42,63	-18,91	-2,40	156	0,20	0,30	10	14
0,46	171000	486	0,10	16105	-13	0,93	0,40	-7	-6,13	-0,75	-25,94	-19,17	-2,59	167	0,20	0,30	9	5
0,47	173000	510	0,07	16200	-12	0,81	0,41	-5	-6,18	-0,81	-18,62	-19,35	-2,78	177	0,20	0,30	7	5
0,48	175000	533	0,04	16492	-8	0,73	0,41	-3	-6,21	-0,87	-14,39	-19,50	-2,97	188	0,20	0,30	7	15
0,49	176000	555	0,02	200000	0	0,74	0,42	-12	-6,33	-0,94	-11,48	-19,61	-3,17	200	0,20	0,30	7	26

Table 8.1 - Control Volume 5 m³ – Turbulence Factor 2 – Initial Angle 30° - Free Volume 7,5 m³

t	p_i	T_{ui}	S	q_x	a_v	v_v	x_i	a_h	v_h	z_i	ω'	ω	ω . t	θ	C_L	C_D	β	α
0,01	101400	283	0,37	128	-10	0	0,00	0	0	0,00	0,00	0,00	0,00	30	0,5	0,6	90	60
0,02	101400	283	0,31	129	-10	0	0,00	0	0	0,00	-0,76	-0,01	0,00	30	0,5	0,6	90	60
0,03	101400	283	0,31	129	-10	0	0,00	0	0	0,00	-0,64	-0,01	0,00	30	0,5	0,6	90	60
0,04	101400	283	0,31	129	-10	0	0,00	0	0	0,00	-0,64	-0,02	0,00	30	0,5	0,6	90	60
0,05	102000	284	0,31	898	-8	0	0,00	-2	0,00	0,00	-0,64	-0,03	0,00	30	0,5	0,6	90	60
0,06	103000	285	0,31	2175	-5	0	0,00	-4	0,00	0,00	-4,45	-0,07	0,00	30	0,5	0,6	90	60
0,07	105000	286	0,31	4657	2	0	-0,05	-10	-0,10	0,00	-10,79	-0,18	0,00	30	0,5	0,6	48	18
0,08	106000	287	0,29	6199	9	0	-0,03	1	-0,08	0,00	-19,93	-0,38	-0,01	30	0,2	0,3	12	0
0,09	110000	291	0,30	10811	1	0	-0,03	11	0,03	0,00	-7,64	-0,45	-0,01	30	0,2	0,3	14	44
0,1	113000	294	0,30	14366	5	0	-0,03	-22	-0,20	0,00	-23,87	-0,69	-0,01	31	0,4	0,5	13	43
0,11	117000	298	0,30	18556	27	0	-0,03	-29	-0,49	-0,01	-57,19	-1,27	-0,02	31	0,4	0,5	33	63
0,12	122000	303	0,30	23495	47	1	-0,02	-27	-0,76	-0,01	-73,20	-2,00	-0,04	31	0,4	0,6	46	77
0,13	127000	308	0,30	27975	68	1	-0,01	-30	-1,06	-0,02	-100,57	-3,00	-0,07	32	0,3	0,7	54	86
0,14	132000	314	0,30	31774	83	2	0,01	-49	-1,55	-0,03	-129,18	-4,29	-0,10	34	0,1	0,8	56	89
0,15	137000	321	0,29	34893	89	3	0,04	-58	-2,12	-0,05	-167,33	-5,97	-0,15	36	0,1	0,9	56	88
0,16	142000	328	0,29	37279	91	4	0,07	-85	-2,98	-0,08	-213,89	-8,11	-0,22	39	0,1	0,9	54	88
0,17	147000	336	0,29	38916	92	5	0,12	-93	-3,91	-0,11	-238,93	-10,50	-0,32	43	0,1	0,9	52	85
0,18	154000	347	0,29	40767	93	6	0,17	-100	-4,91	-0,16	-263,95	-13,14	-0,44	48	0,1	0,9	50	82
0,19	160000	358	0,29	41756	91	7	0,24	-104	-5,95	-0,21	-294,33	-16,08	-0,58	55	0,1	0,9	49	76
0,2	166000	372	0,28	41394	86	8	0,31	-94	-6,89	-0,28	-320,28	-19,28	-0,76	63	0,1	0,8	48	69
0,21	174000	389	0,28	41055	70	8	0,39	-93	-7,82	-0,35	-296,56	-22,25	-0,97	73	0,2	0,7	47	60
0,22	182000	409	0,27	40575	45	9	0,48	-113	-8,95	-0,43	-284,49	-25,09	-1,20	85	0,5	0,6	45	50
0,23	190000	433	0,26	78194	8	9	0,57	-174	-10,69	-0,53	-332,99	-28,42	-1,47	99	0,4	0,5	40	42
0,24	190000	438	0,25	71850	-7	9	0,65	-134	-12,03	-0,64	-555,35	-33,98	-1,78	114	0,4	0,4	36	30
0,25	187000	447	0,23	69286	-28	8,61	0,74	-105	-13,08	-0,77	-464,89	-38,62	-2,15	132	0,3	0,4	33	15

t	p_i	T_{ui}	S	q_x	a_v	v_v	x_i	a_h	v_h	z_i	ω'	ω	ω . t	θ	C_L	C_D	β	α
0,26	188000	460	0,20	62069	-15	8,46	0,83	-61	-13,69	-0,90	-330,65	-41,93	-2,55	152	0,2	0,3	32	4
0,27	189000	477	0,17	62706	38	8,83	0,91	-22	-13,91	-1,04	162,52	-40,31	-2,96	175	0,2	0,3	32	27
0,28	191000	498	0,14	48890	21	9,04	1,00	-14	-14,04	-1,18	221,40	-38,09	-3,35	199	0,2	0,3	33	51
0,29	195000	531	0,12	46461	14	9,18	1,09	-15	-14,19	-1,32	177,39	-36,32	-3,72	221	0,4	0,5	33	74
0,3	198000	567	0,09	200000	135	9,59	1,12	-102	-14,50	-1,37	242,08	-33,90	-4,07	242	0,3	0,7	33	

Table 8.2 - Control Volume 5 m³ – Turbulence Factor 3 – Initial Angle 30° - Free Volume 7,5 m³

t	p_i	T_{ui}	S	q_x	a_v	v_v	x_i	a_h	v_h	z_i	$\omega' = M/I$	ω	$\omega . t$	θ	C_L	C_D	β	α
0,01	101300	283	0,37	0	-10			0			0,00			30	0,5	0,6	90	60
0,02	102000	284	0,31	896	-8			-2	0		0,00	0,00	0,00	30	0,5	0,6	90	60
0,03	102000	284	0,31	897	-8	0	0,00	-2	0,00	0,00	-4,45	-0,04	0,00	30	0,5	0,6	90	60
0,04	102000	284	0,31	902	-8	0	0,00	-2	0,00	0,00	-4,45	-0,09	0,00	30	0,5	0,6	90	60
0,05	105000	286	0,31	4623	2	0	0,00	-9	0,00	0,00	-4,47	-0,13	0,00	30	0,5	0,6	90	60
0,06	107000	288	0,31	7063	8	0	0,00	-14	-0,14	0,00	-22,92	-0,36	0,00	30	0,5	0,6	24	0
0,07	113000	293	0,31	13741	7	0	0,00	19	0,05	0,00	-22,75	-0,59	-0,01	30	0,2	0,3	9	0
0,08	120000	299	0,31	20939	11	0	0,00	23	0,28	0,00	-17,68	-0,77	-0,02	31	0,2	0,3	23	0
0,09	127000	306	0,31	27336	24	0	0,00	22	0,50	0,00	-26,82	-1,04	-0,03	31	0,2	0,3	35	4
0,10	136000	316	0,31	34345	38	1	0,00	19	0,69	0,01	-38,49	-1,42	-0,04	31	0,2	0,3	47	15
0,11	146000	327	0,32	41137	52	1	0,01	10	0,79	0,02	-59,32	-2,01	-0,05	32	0,2	0,3	57	25
0,12	157000	342	0,32	47122	63	2	0,03	-2	0,77	0,02	-80,82	-2,82	-0,08	33	0,2	0,3	67	34
0,13	170000	360	0,33	52553	81	3	0,05	-16	0,61	0,03	-100,63	-3,83	-0,11	34	0,3	0,3	77	42
0,14	185000	384	0,34	57175	109	4	0,08	-59	0,02	0,03	-144,05	-5,27	-0,16	36	0,3	0,4	89	53
0,15	201000	413	0,35	120840	277	7	0,14	-170	-1,68	0,03	-189,61	-7,16	-0,22	39	0,4	0,5	75	66
0,16	207000	431	0,37	117320	252	9	0,21	-294	-4,63	-0,01	-522,81	-12,39	-0,32	43	0,5	0,6	63	75
0,17	213000	455	0,38	114241	193	11	0,31	-414	-8,77	-0,07	-641,77	-18,81	-0,47	48	0,4	0,6	51	81
0,18	220000	485	0,38	105954	184	13	0,43	-370	-12,46	-0,18	-674,24	-25,55	-0,70	57	0,3	0,7	46	77
0,19	229000	523	0,37	98213	99	14	0,57	-343	-15,89	-0,32	-852,39	-34,08	-0,99	70	0,4	0,7	41	70
0,20	237000	570	0,35	200000	-129	13,44	0,61	-747	-18,13	-0,37	-993,49	-44,01	-1,38	87	0,5	0,6	36	57

Table 8.3 - Control Volume 5 m³ – Turbulence Factor 4 – Initial Angle 30° - Free Volume 7,5 m³

t	p_i	T_{ui}	q_x	S	a_v	v_v	x_i	a_h	v_h	z_i	ω'	ω	ω . t	θ	C_L	C_D	β	α
0,01	101300	283	0	0,31	-10		0,00	0		0,00	0,00	0,00	0,00	30	0,5	0,6	90	60
0,02	102000	284	0	0,31	-10		0,00	0		0,00	0,00	0,00	0,00	30	0,5	0,6	90	60
0,03	103000	285	29	0,31	-10		0,00	0		0,00	0,00	0,00	0,00	30	0,5	0,6	90	60
0,04	106000	287	78	0,31	-10		0,00	0		0,00	-0,23	0,00	0,00	30	0,5	0,6	90	60
0,05	109000	290	491	0,31	-9		0,00	-1		0,00	-0,60	-0,01	0,00	30	0,5	0,6	90	60
0,06	116000	296	1569	0,31	-6	0,0	0,00	-3	0,0	0,00	-3,77	-0,05	0,00	30	0,5	0,6	90	60
0,07	124000	303	4073	0,31	0	0,0	0,00	-8	-0,1	0,00	-12,06	-0,17	0,00	30	0,5	0,6	0	0
0,08	136000	315	8362	0,31	-3	0,0	0,00	21	0,1	0,00	-15,73	-0,32	0,00	30	0,2	0,3	14	44
0,09	150000	330	13706	0,31	12	0,1	0,00	-14	0,0	0,00	-21,91	-0,54	-0,01	30	0,3	0,4	80	69
0,1	166000	351	19032	0,31	40	0,5	0,00	-28	-0,3	0,00	-70,87	-1,25	-0,02	30	0,3	0,7	59	89
0,11	187000	380	24169	0,31	62	1,1	0,01	-62	-0,9	-0,01	-80,10	-2,05	-0,03	31	0,1	0,9	50	81
0,12	211000	419	55846	0,31	117	2,3	0,03	-149	-2,4	-0,02	-157,29	-3,63	-0,06	32	0,1	0,8	43	75
0,13	224000	452	58684	0,31	105	3,3	0,05	-155	-4,0	-0,06	-360,38	-7,23	-0,12	34	0,1	0,8	40	73
0,14	241000	497	62586	0,30	80	4,1	0,09	-169	-5,6	-0,10	-400,30	-11,23	-0,21	37	0,2	0,8	36	73
0,15	257000	556	65660	0,29	68	4,8	0,14	-192	-7,6	-0,17	-449,00	-15,72	-0,34	42	0,2	0,8	32	74
0,16	275000	630	200000	0,27	419	6,1	0,15	-407	-8,8	-0,19	-487,12	-20,59	-0,53	50	0,2	0,8	35	96

Table 8.4 - Control Volume 5 m³ – Turbulence Factor 5 – Initial Angle 30° - Free Volume 7,5 m³

t	p_i	T_{ui}	q_x	S	a_v	v_v	x_i	a_h	v_h	z_i	ω'	ω	ω . t	θ	C_L	C_D	β	α
0,01	101300	283	0	0,31	-10	0,00	0,00	0	0,00	0,00	0,00	0,00	0	20	0,3	0,7	90	70
0,02	101300	283	0	0,31	-10	0,00	0,00	0	0,00	0,00	0,00	0,00	0	20	0,3	0,7	90	70
0,03	101300	283	0	0,31	-10	0,00	0,00	0	0,00	0,00	0,00	0,00	0	20	0,3	0,7	90	70
0,04	101300	283	0	0,31	-10	0,00	0,00	0	0,00	0,00	0,00	0,00	0	20	0,3	0,7	90	70
0,05	102000	284	447	0,31	-9	0,00	0,00	-1	0,00	0,00	0,00	0,00	0	20	0,3	0,7	90	70
0,06	103000	285	1108	0,31	-7	0,00	0,00	-1	0,00	0,00	-2,19	-0,02	0,00	20	0,3	0,7	90	70
0,07	104000	285	1840	0,31	-5	0,00	0,00	-2	0,00	0,00	-5,43	-0,08	0,00	20	0,3	0,7	90	70
0,08	104000	285	1905	0,31	-5	0,00	0,00	-2	0,00	0,00	-9,02	-0,17	0,00	20	0,3	0,7	90	70
0,09	104000	286	1847	0,31	-5	0,00	0,00	-2	0,00	0,00	-9,33	-0,26	0,00	20	0,3	0,7	90	70
0,1	105000	286	2511	0,31	-3	0,00	0,00	-3	0,00	0,00	-9,05	-0,35	-0,01	20	0,3	0,7	90	70
0,11	105000	286	2748	0,31	-2	-0,02	0,00	-3	-0,03	0,00	-12,32	-0,47	-0,01	21	0,3	0,7	31	10
0,12	105000	287	2611	0,31	-3	-0,05	0,00	5	0,01	0,00	-7,45	-0,55	-0,02	21	0,2	0,3	76	83
0,13	106000	287	3308	0,31	-5	-0,11	0,00	2	0,03	0,00	-5,40	-0,60	-0,02	21	0,1	0,8	74	85
0,14	106000	287	3869	0,31	3	-0,08	0,00	-2	0,01	0,00	-17,17	-0,77	-0,03	22	0,1	0,9	82	77
0,15	107000	288	4265	0,31	6	-0,02	0,00	0	0,01	0,00	-22,41	-1,00	-0,04	22	0,2	0,8	72	86
0,16	108000	289	9544	0,31	22	0,20	0,00	-2	-0,01	0,00	-22,27	-1,22	-0,05	23	0	0,9	86	71
0,17	112000	293	5902	0,31	12	0,32	0,00	-1	-0,03	0,00	-52,44	-1,74	-0,06	24	0,3	0,7	85	72
0,18	116000	296	7760	0,31	13	0,45	0,00	8	0,05	0,00	-28,83	-2,03	-0,08	25	0,3	0,7	83	58
0,19	121000	301	9772	0,31	20	0,65	0,01	-9	-0,04	0,00	-37,76	-2,41	-0,10	26	0,4	0,6	86	68
0,2	127000	307	11879	0,31	21	0,86	0,02	18	0,14	0,00	-44,68	-2,86	-0,13	27	0,3	0,7	80	53
0,21	133000	313	13775	0,32	33	1,18	0,03	-11	0,04	0,00	-57,18	-3,43	-0,16	29	0,4	0,5	88	58
0,22	141000	322	15702	0,32	24	1,43	0,04	-26	-0,22	0,00	-57,31	-4,00	-0,20	31	0,4	0,6	81	68
0,23	149000	331	17455	0,32	39	1,82	0,06	23	0,01	0,00	-73,60	-4,74	-0,24	34	0,3	0,7	89	55
0,24	159000	343	18989	0,33	48	2,30	0,08	-25	-0,24	0,00	-87,83	-5,62	-0,30	37	0,4	0,5	84	60
0,25	170000	357	20351	0,33	39	2,69	0,10	31	0,08	0,00	-82,35	-6,44	-0,36	40	0,4	0,6	88	48
0,26	182000	374	21403	0,34	50	3,18	0,13	-37	-0,30	0,00	-101,44	-7,45	-0,42	44	0,4	0,5	84	52
0,27	187000	383	44544	0,35	102	4,20	0,17	73	0,44	0,00	-98,21	-8,44	-0,50	49	0,4	0,5	84	35

t	p_i	T_{ui}	q_x	S	a_v	v_v	x_i	a_h	v_h	z_i	ω'	ω	ω . t	θ	C_L	C_D	β	α
0,28	191000	391	44187	0,36	105	5,25	0,22	-74	-0,31	0,00	-201,27	-10,45	-0,60	54	0,3	0,3	86	40
0,29	195000	401	43184	0,37	58	5,83	0,27	60	0,29	0,00	-142,11	-11,87	-0,71	60	0,4	0,4	87	26
0,3	199000	412	41917	0,37	77	6,60	0,33	-78	-0,49	0,00	-179,12	-13,66	-0,84	68	0,3	0,3	85	27
0,31	203000	425	40481	0,37	54	7,14	0,40	55	0,06	-0,01	-131,22	-14,97	-0,98	76	0,3	0,3	89	13
0,32	207000	438	38918	0,37	48	7,62	0,48	-57	-0,51	-0,01	-113,65	-16,11	-1,14	85	0,2	0,3	86	9
0,33	210000	452	37308	0,37	48	8,09	0,55	33	-0,18	-0,01	-75,15	-16,86	-1,30	94	0,2	0,3	88	-2
0,34	213000	468	35511	0,37	42	8,51	0,64	34	0,16	-0,01	54,88	-16,31	-1,47	104	0,2	0,3	88	15
0,35	216000	485	33744	0,37	39	8,91	0,72	34	0,50	-0,01	76,07	-15,55	-1,63	113	0,2	0,3	86	26
0,36	219000	501	32028	0,37	36	9,26	0,82	34	0,85	0,00	80,18	-14,75	-1,78	121	0,3	0,3	84	37
0,37	219000	521	30374	0,37	31	9,57	0,91	49	1,34	0,01	103,60	-13,71	-1,92	129	0,3	0,3	89	41
0,38	219000	541	28408	0,37	32	9,88	1,01	43	1,76	0,03	101,06	-12,70	-2,05	137	0,4	0,4	88	49
0,39	219000	560	26570	0,37	41	10,29	1,11	54	2,30	0,05	129,86	-11,41	-2,17	144	0,4	0,5	87	57
0,4	218000	581	24845	0,37	49	10,79	1,21	52	2,81	0,07	142,47	-9,98	-2,28	150	0,4	0,5	86	64

Table 8.5 - Control Volume 1 m³ – Turbulence Factor 3 – Initial Angle 20° - Free Volume 7,5 m³

t	p_i	T_{ui}	q_x	S	a_v	v_v	x_i	a_h	v_h	z_i	ω'	ω	ω . t	θ	C_L	C_D	β	α
0,01	101300	283	0	0,31	-10	0,00	0,00	0	0,00	0,00	0,00	0,00	0	20	0,3	0,7	90	70
0,02	101300	283	0	0,31	-10	0,00	0,00	0	0,00	0,00	0,00	0,00	0	20	0,3	0,7	90	70
0,03	101300	283	0	0,31	-10	0,00	0,00	0	0,00	0,00	0,00	0,00	0	20	0,3	0,7	90	70
0,04	101300	283	0	0,31	-10	0,00	0,00	0	0,00	0,00	0,00	0,00	0	20	0,3	0,7	90	70
0,05	102000	284	447	0,31	-9	0,00	0,00	-1	0,00	0,00	0,00	0,00	0	20	0,3	0,7	90	70
0,06	103000	285	1108	0,31	-7	0,00	0,00	-1	0,00	0,00	-0,88	-0,01	0,00	20	0,3	0,7	90	70
0,07	104000	285	1840	0,31	-5	0,00	0,00	-2	0,00	0,00	-2,17	-0,03	0,00	20	0,3	0,7	90	70
0,08	104000	285	1905	0,31	-5	0,00	0,00	-2	0,00	0,00	-3,61	-0,07	0,00	20	0,3	0,7	90	70
0,09	104000	286	1847	0,31	-5	0,00	0,00	-2	0,00	0,00	-3,73	-0,10	0,00	20	0,3	0,7	90	70
0,1	105000	286	2511	0,31	-3	0,00	0,00	-3	0,00	0,00	-3,62	-0,14	0,00	20	0,3	0,7	90	70
0,11	105000	286	2748	0,31	-2	-0,02	0,00	-3	-0,03	0,00	-4,93	-0,19	0,00	20	0,3	0,7	31	11
0,12	105000	287	2611	0,31	-3	-0,05	0,00	5	0,01	0,00	-3,01	-0,22	-0,01	20	0,2	0,3	76	84
0,13	106000	287	3308	0,31	-7	-0,12	0,00	-4	-0,02	0,00	-2,15	-0,24	-0,01	21	0,1	0,8	79	58
0,14	106000	287	3869	0,31	3	-0,09	0,00	1	-0,01	0,00	-6,28	-0,30	-0,01	21	0,4	0,6	80	60
0,15	107000	288	4266	0,31	2	-0,08	0,00	-5	-0,07	0,00	-7,19	-0,38	-0,01	21	0,4	0,6	49	28
0,16	108000	289	9550	0,31	18	0,10	0,00	4	-0,03	0,00	-7,00	-0,45	-0,02	21	0,3	0,3	73	86
0,17	112000	293	5910	0,31	-5	0,05	0,00	-9	-0,12	0,00	-7,82	-0,52	-0,02	21	0	0,9	23	44
0,18	116000	296	7785	0,31	1	0,06	0,00	-27	-0,39	0,00	-9,61	-0,62	-0,03	22	0,4	0,5	9	31
0,19	121000	301	9837	0,31	9	0,15	0,00	-17	-0,56	-0,01	-12,26	-0,74	-0,04	22	0,3	0,3	15	37
0,2	127000	307	12012	0,30	8	0,23	0,00	-10	-0,66	-0,02	-11,07	-0,85	-0,04	23	0,3	0,3	19	42
0,21	133000	313	14008	0,30	12	0,35	0,00	-10	-0,77	-0,02	-13,93	-0,99	-0,05	23	0,4	0,4	24	47
0,22	141000	322	16086	0,30	24	0,59	0,01	-13	-0,89	-0,03	-22,20	-1,21	-0,06	24	0,4	0,5	33	57
0,23	149000	331	18032	0,30	33	0,92	0,02	-14	-1,04	-0,04	-29,55	-1,51	-0,08	24	0,4	0,6	41	66
0,24	159000	343	19784	0,29	44	1,37	0,03	-14	-1,18	-0,05	-38,13	-1,89	-0,10	25	0,4	0,6	49	74
0,25	170000	357	21392	0,29	50	1,86	0,04	-7	-1,25	-0,06	-41,79	-2,31	-0,12	27	0,3	0,7	56	82
0,26	182000	374	22682	0,29	56	2,42	0,07	12	-1,13	-0,08	-50,36	-2,81	-0,14	28	0,1	0,8	65	87

t	p_i	T_{ui}	q_x	S	a_v	v_v	x_i	a_h	v_h	z_i	ω'	ω	ω . t	θ	C_L	C_D	β	α
0,27	187000	383	47540	0,29	117	3,59	0,10	-79	-1,92	-0,09	-61,08	-3,42	-0,17	30	0	0,9	62	89
0,28	191000	391	47421	0,29	138	4,97	0,14	-79	-2,71	-0,11	-151,83	-4,94	-0,21	32	0	0,9	61	87
0,29	195000	401	46470	0,30	136	6,33	0,19	-80	-3,51	-0,15	-164,58	-6,59	-0,27	36	0	0,9	61	84
0,3	199000	412	44978	0,30	132	7,65	0,26	-79	-4,30	-0,18	-178,19	-8,37	-0,35	40	0	0,9	60	80
0,31	203000	425	43050	0,31	128	8,93	0,35	-78	-5,07	-0,23	-192,56	-10,30	-0,44	45	0,1	0,8	60	75
0,32	207000	438	40804	0,29	92	9,85	0,44	-76	-5,83	-0,29	-169,10	-11,99	-0,55	51	0,2	0,8	59	69
0,33	210000	452	38404	0,29	78	10,63	0,54	-87	-6,70	-0,35	-173,37	-13,72	-0,68	59	0,3	0,7	57	64
0,34	213000	468	35827	0,30	51	11,14	0,65	-89	-7,59	-0,42	-170,77	-15,43	-0,83	67	0,4	0,6	55	57
0,35	216000	485	33363	0,30	26	11,40	0,77	-89	-8,47	-0,50	-143,88	-16,87	-0,99	76	0,4	0,5	53	51
0,36	219000	501	31083	0,25	7	11,47	0,88	-64	-9,11	-0,59	-132,56	-18,19	-1,16	86	0,4	0,5	51	42
0,37	219000	521	29020	0,24	3	11,50	0,99	-57	-9,69	-0,68	-112,39	-19,32	-1,35	97	0,4	0,4	55	28
0,38	219000	541	26801	0,23	-2	11,48	1,11	-45	-10,13	-0,78	-73,45	-20,05	-1,55	108	0,3	0,3	55	17
0,39	219000	560	24826	0,13	-7	11,41	1,22	-18	-10,32	-0,88	-48,45	-20,53	-1,75	120	0,2	0,3	54	6
0,4	218000	581	200000	0,11	27	11,49	1,26	-98	-10,61	-0,91	34,72	-20,19	-1,95	131	0,2	0,3	54	-5

Table 8.6 - Control Volume 1 m³ – Turbulence Factor 3 – Initial Angle 20° - Free Volume 7,5 m³ - Distance Pressure Center to Centroid 0,1m

t	p_i	T_{ui}	q_x	S	a_v	v_v	x_i	a_h	v_h	z_i	ω'	ω	ω . t	θ	C_L	C_D	β	α
0,01	101300	283	0	0,31	-10	0,00	0,00	0	0,00	0,00	0,00	0,00	0	40	0,4	0,5	90	50
0,02	101300	283	0	0,31	-10	0,00	0,00	0	0,00	0,00	0,00	0,00	0	40	0,4	0,5	90	50
0,03	101300	283	0	0,31	-10	0,00	0,00	0	0,00	0,00	0,00	0,00	0	40	0,4	0,5	90	50
0,04	101300	283	0	0,31	-10	0,00	0,00	0	0,00	0,00	0,00	0,00	0	40	0,4	0,5	90	50
0,05	102000	284	447	0,31	-9	0,00	0,00	-1	0,00	0,00	0,00	0,00	0	40	0,4	0,5	90	50
0,06	103000	285	1108	0,31	-8	0,00	0,00	-2	0,00	0,00	-1,85	-0,02	0,00	40	0,4	0,5	90	50
0,07	104000	285	1841	0,31	-6	0,00	0,00	-3	0,00	0,00	-4,58	-0,06	0,00	40	0,4	0,5	90	50
0,08	104000	285	1905	0,31	-6	0,00	0,00	-3	0,00	0,00	-7,60	-0,14	0,00	40	0,4	0,5	90	50
0,09	104000	286	1847	0,31	-6	0,00	0,00	-3	0,00	0,00	-7,86	-0,22	0,00	40	0,4	0,5	90	50
0,1	105000	286	2511	0,31	-5	0,00	0,00	-4	0,00	0,00	-7,62	-0,29	-0,01	40	0,4	0,5	90	50
0,11	105000	286	2748	0,31	-4	-0,04	0,00	-5	-0,05	0,00	-10,37	-0,40	-0,01	41	0,4	0,5	43	3
0,12	105000	287	2611	0,31	-3	-0,08	0,00	1	-0,04	0,00	-7,53	-0,47	-0,01	41	0,2	0,3	64	23
0,13	106000	287	3309	0,31	-5	-0,13	0,00	-1	-0,04	0,00	-5,09	-0,52	-0,02	41	0,3	0,3	71	30
0,14	106000	287	3871	0,31	-4	-0,17	0,00	-3	-0,07	0,00	-8,74	-0,61	-0,02	41	0,3	0,3	66	25
0,15	107000	288	4270	0,31	-3	-0,20	-0,01	-3	-0,10	0,00	-9,93	-0,71	-0,03	42	0,3	0,3	63	21
0,16	108000	289	9567	0,31	6	-0,14	-0,01	-5	-0,15	0,00	-10,67	-0,82	-0,04	42	0,3	0,3	42	0
0,17	112000	293	5932	0,31	0	-0,14	-0,01	0	-0,15	-0,01	-18,48	-1,00	-0,05	43	0,2	0,3	43	0
0,18	116000	296	7832	0,30	1	-0,12	-0,01	3	-0,12	-0,01	-7,63	-1,08	-0,06	43	0,2	0,3	46	3
0,19	121000	301	9915	0,30	4	-0,08	-0,01	3	-0,09	-0,01	-10,72	-1,19	-0,07	44	0,2	0,3	41	0
0,2	127000	307	12133	0,30	7	-0,01	-0,01	5	-0,05	-0,01	-12,72	-1,31	-0,08	45	0,2	0,3	14	0
0,21	133000	313	14184	0,30	5	0,04	-0,01	14	0,09	-0,01	-15,55	-1,47	-0,10	45	0,2	0,3	24	0
0,22	141000	322	16335	0,30	10	0,14	-0,01	12	0,21	-0,01	-18,14	-1,65	-0,11	46	0,2	0,3	33	0
0,23	149000	331	18381	0,30	15	0,29	-0,01	10	0,32	0,00	-20,83	-1,86	-0,13	47	0,2	0,3	42	0
0,24	159000	343	20278	0,31	19	0,48	0,00	7	0,39	0,00	-23,40	-2,09	-0,15	48	0,2	0,3	51	2
0,25	170000	357	22094	0,31	23	0,70	0,00	3	0,42	0,00	-27,23	-2,37	-0,17	50	0,2	0,3	59	9
0,26	182000	374	23667	0,31	25	0,96	0,01	-2	0,40	0,01	-34,53	-2,71	-0,20	51	0,2	0,3	67	16
0,27	187000	383	50246	0,32	65	1,61	0,02	-14	0,26	0,01	-41,50	-3,13	-0,23	53	0,3	0,3	80	28

t	p_i	T_{ui}	q_x	S	a_v	v_v	x_i	a_h	v_h	z_i	ω'	ω	ω . t	θ	C_L	C_D	β	α
0,28	191000	391	50957	0,32	65	2,26	0,04	-55	-0,29	0,01	-131,39	-4,44	-0,26	55	0,3	0,3	82	43
0,29	195000	401	51040	0,33	65	2,91	0,07	58	0,29	0,01	-141,98	-5,86	-0,32	58	0,4	0,5	84	26
0,3	199000	412	50782	0,34	113	4,04	0,10	-79	-0,50	0,01	-197,79	-7,84	-0,38	62	0,3	0,3	83	36
0,31	203000	425	50084	0,35	68	4,72	0,15	61	0,11	0,01	-146,38	-9,30	-0,47	67	0,3	0,3	88	22
0,32	207000	438	48979	0,36	62	5,34	0,20	-69	-0,59	0,01	-139,16	-10,69	-0,57	72	0,3	0,3	83	24
0,33	210000	452	47632	0,37	68	6,02	0,25	62	0,04	0,00	-144,93	-12,14	-0,68	79	0,3	0,3	89	10
0,34	213000	468	45864	0,37	58	6,60	0,32	-67	-0,64	0,00	-127,37	-13,42	-0,81	86	0,2	0,3	84	10
0,35	216000	485	43966	0,37	59	7,19	0,39	37	-0,27	0,00	-87,74	-14,29	-0,95	94	0,2	0,3	87	0
0,36	219000	501	41992	0,37	51	7,70	0,46	-44	-0,71	-0,01	-68,44	-14,98	-1,10	**102**	0,2	0,3	84	
0,37	219000	521	39986	0,37	53	8,22	0,54	-34	-1,04	-0,02	-65,99	-15,64	-1,25	**111**	0,5	0,8	-88	
0,38	219000	541	37471	0,00	-10	8,12	0,62	0	-1,04	-0,03	-159,80	-17,24	-1,41	**121**	0,5	0,8	-87	
0,39	219000	560	35127	0,00	-10	8,02	0,70	0	-1,04	-0,04	0,00	-17,24	-1,59	**130**	0,5	0,8	-86	
0,4	218000	581	33022	0,00	-10	7,92	0,78	0	-1,04	-0,05	0,00	-17,24	-1,76	**140**	0,3	0,4	-86	

Table 8.7 - Control Volume 1 m³ – Turbulence Factor 3 – Initial Angle 40° - Free Volume 7,5 m³

t	p_i	T_{ui}	q_x	S	a_v	v_v	x_i	a_h	v_h	z_i	ω'	ω	ω . t	θ	C_L	C_D	β	α
0,01	101300	283	0	0,31	-10	0,00	0,00	0			0,00	0,00	0,00	20	0,3	0,7	90	70
0,02	101300	283	0	0,31	-10	0,00	0,00	0	0		0,00	0,00	0,00	20	0,3	0,7	90	70
0,03	101300	283	0	0,31	-10	0,00	0,00	0	0	0,00	0,00	0,00	0,00	20	0,3	0,7	90	70
0,04	101300	283	0	0,31	-10	0,00	0,00	0	0	0,00	0,00	0,00	0,00	20	0,3	0,7	90	70
0,05	103000	285	1075	0,31	-7	-0,07	0,00	-1	-0,01	0,00	0,00	0,00	0,00	20	0,3	0,7	90	70
0,06	105000	286	2648	0,31	-2	-0,09	0,00	-3	-0,05	0,00	-5,27	-0,05	0,00	20	0,3	0,7	90	70
0,07	105000	286	2866	0,31	-2	-0,11	0,00	-4	-0,08	0,00	-12,99	-0,18	0,00	20	0,3	0,7	64	44
0,08	106000	287	3230	0,31	0	-0,11	0,00	-2	-0,10	0,00	-13,04	-0,31	0,00	20	0,4	0,5	59	39
0,09	108000	289	4990	0,31	3	-0,08	0,00	-2	-0,12	0,00	-13,03	-0,44	-0,01	20	0,4	0,5	54	33
0,10	109000	290	7006	0,31	8	0,00	0,00	-3	-0,15	0,00	-19,60	-0,64	-0,01	21	0,4	0,4	46	25
0,11	111000	292	16812	0,31	29	0,29	0,00	-1	-0,15	-0,01	-24,06	-0,88	-0,02	21	0,4	0,4	28	49
0,12	117000	297	8158	0,31	8	0,37	0,00	10	-0,06	-0,01	-61,17	-1,49	-0,03	22	0,5	0,6	2	23
0,13	126000	306	11349	0,31	9	0,46	0,00	-23	-0,28	-0,01	-36,78	-1,86	-0,05	23	0,4	0,5	27	50
0,14	138000	317	14774	0,31	25	0,72	0,01	-16	-0,44	-0,01	-47,14	-2,33	-0,07	24	0,4	0,5	40	64
0,15	153000	333	18003	0,31	41	1,12	0,02	-15	-0,59	-0,02	-60,40	-2,93	-0,10	26	0,4	0,6	48	73
0,16	171000	355	20786	0,31	51	1,64	0,03	-21	-0,80	-0,02	-81,88	-3,75	-0,13	27	0,3	0,7	53	81
0,17	193000	384	22965	0,31	56	2,20	0,05	-37	-1,17	-0,03	-102,81	-4,78	-0,17	30	0,1	0,8	62	88
0,18	208000	408	51063	0,31	154	3,74	0,08	-102	-2,19	-0,05	-126,23	-6,04	-0,23	33	0	0,9	59	88
0,19	224000	436	53433	0,31	157	5,31	0,13	-109	-3,28	-0,08	-326,15	-9,31	-0,30	37	0	0,9	58	85
0,20	240000	469	55062	0,31	154	6,85	0,19	-125	-4,54	-0,12	-358,63	-12,89	-0,41	44	0	0,9	56	80
0,21	254000	506	55688	0,31	108	7,93	0,26	-145	-5,99	-0,17	-392,36	-16,82	-0,56	52	0,1	0,8	53	75
0,22	267000	546	55066	0,31	52	8,44	0,34	-160	-7,58	-0,24	-389,35	-20,71	-0,75	63	0,2	0,7	48	69
0,23	278000	588	200000	0,31	30	8,54	0,37	-588	-9,35	-0,26	-384,44	-24,55	-0,98	76	0,3	0,7	42	62

Table 8.8 - Control Volume 1 m³ – Turbulence Factor 4 – Initial Angle 20° - Free Volume 7,5 m³

p_i	T_{ui}	q_x	S	a_v	v_v	x_i	a_h	v_h	z_i	ω'	ω	ω . t	θ	C_L	C_D	β	α
101300	283	0	0,31	-10	0,00	0,00	0			0,00	0,00	0,00	20	0,3	0,7	90	70
101300	283	0	0,31	-10	0,00	0,00	0	0		0,00	0,00	0,00	20	0,3	0,7	90	70
101300	283	0	0,31	-10	0,00	0,00	0	0	0,00	0,00	0,00	0,00	20	0,3	0,7	90	70
101300	283	0	0,31	-10	0,00	0,00	0	0	0,00	0,00	0,00	0,00	20	0,3	0,7	90	70
103000	285	1075	0,31	-7	-0,07	0,00	-1	-0,01	0,00	0,00	0,00	0,00	20	0,3	0,7	90	70
105000	286	2648	0,31	-2	-0,09	0,00	-3	-0,05	0,00	-5,27	-0,05	0,00	20	0,3	0,7	90	70
105000	286	2866	0,31	-2	-0,11	0,00	-4	-0,08	0,00	-12,99	-0,18	0,00	20	0,3	0,7	64	44
106000	287	3230	0,31	0	-0,11	0,00	-2	-0,10	0,00	-13,04	-0,31	0,00	20	0,4	0,5	59	39
108000	289	4990	0,31	3	-0,08	0,00	-2	-0,12	0,00	-13,03	-0,44	-0,01	20	0,4	0,5	54	33
109000	290	7006	0,31	8	0,00	0,00	-3	-0,15	0,00	-19,60	-0,64	-0,01	21	0,4	0,4	46	25
111000	292	16812	0,31	29	0,29	0,00	-1	-0,15	-0,01	-24,06	-0,88	-0,02	21	0,4	0,4	28	49
117000	297	8158	0,31	8	0,37	0,00	10	-0,06	-0,01	-61,17	-1,49	-0,03	22	0,5	0,6	2	23
126000	306	11349	0,31	9	0,46	0,00	-23	-0,28	-0,01	-36,78	-1,86	-0,05	23	0,4	0,5	27	50
138000	317	14774	0,31	25	0,72	0,01	-16	-0,44	-0,01	-47,14	-2,33	-0,07	24	0,4	0,5	40	64
153000	333	18003	0,31	41	1,12	0,02	-15	-0,59	-0,02	-60,40	-2,93	-0,10	26	0,4	0,6	48	73
171000	355	20786	0,31	51	1,64	0,03	-21	-0,80	-0,02	-81,88	-3,75	-0,13	27	0,3	0,7	53	81
193000	384	22965	0,31	56	2,20	0,05	-37	-1,17	-0,03	-102,81	-4,78	-0,17	30	0,1	0,8	62	88
208000	408	51063	0,31	154	3,74	0,08	-102	-2,19	-0,05	-126,23	-6,04	-0,23	33	0	0,9	59	88
224000	436	53433	0,31	157	5,31	0,13	-109	-3,28	-0,08	-326,15	-9,31	-0,30	37	0	0,9	58	85
240000	469	55062	0,31	154	6,85	0,19	-125	-4,54	-0,12	-358,63	-12,89	-0,41	44	0	0,9	56	80
254000	506	55688	0,31	108	7,93	0,26	-145	-5,99	-0,17	-392,36	-16,82	-0,56	52	0,1	0,8	53	75
267000	546	55066	0,31	52	8,44	0,34	-160	-7,58	-0,24	-389,35	-20,71	-0,75	63	0,2	0,7	48	69
278000	588	53827	0,31	1	8,45	0,43	-158	-9,16	-0,32	-384,44	-24,55	-0,98	76	0,3	0,7	42	62
286000	632	200000	0,30	66	8,65	0,45	-599	-10,96	-0,35	-431,79	-28,87	-1,24	91	0,1	0,8	38	51

Table 8.9 - Control Volume 1 m³ – Turbulence Factor 4 – Initial Angle 20° - Free Volume 7,5 m³ - Detonation 632 °K -

t	p_i	T_{ui}	q_x	S	a_v	v_v	x_i	a_h	v_h	z_i	ω'	ω	ω . t	θ	C_L	C_D	β	α
0,01	101300	283	0	0,37	-10	0,00	0,00	0			0,00	0,00	0,00	40	0,4	0,5	90	50
0,02	101300	283	0	0,37	-10	0,00	0,00	0	0		0,00	0,00	0,00	40	0,4	0,5	90	50
0,03	101300	283	0	0,37	-10	0,00	0,00	0	0	0,00	0,00	0,00	0,00	40	0,4	0,5	90	50
0,04	101300	283	0	0,37	-10	0,00	0,00	0	0	0,00	0,00	0,00	0,00	40	0,4	0,5	90	50
0,05	103000	285	1075	0,37	-7	0,00	0,00	-2	0,00	0,00	0,00	0,00	0,00	40	0,4	0,5	90	50
0,06	105000	286	2647	0,37	-4	0,00	0,00	-5	0,00	0,00	-5,31	-0,05	0,00	40	0,4	0,5	90	50
0,07	105000	286	2863	0,37	-3	0,00	0,00	-6	0,00	0,00	-13,07	-0,18	0,00	40	0,4	0,5	90	50
0,08	106000	287	3223	0,37	-2	-0,02	0,00	-6	-0,06	0,00	-14,14	-0,33	0,00	40	0,4	0,5	18	0
0,09	108000	289	4974	0,37	3	0,01	0,00	5	-0,01	0,00	-9,96	-0,42	-0,01	40	0,2	0,3	7	0
0,10	109000	290	6977	0,37	-2	-0,01	0,00	9	0,08	0,00	-7,69	-0,50	-0,01	41	0,2	0,3	9	0
0,11	111000	292	16735	0,37	10	0,09	0,00	22	0,30	0,00	-10,78	-0,61	-0,02	41	0,2	0,3	15	0
0,12	117000	297	8129	0,37	1	0,10	0,00	12	0,43	0,00	-25,75	-0,87	-0,03	41	0,3	0,4	15	0
0,13	126000	306	11337	0,37	5	0,15	0,00	13	0,56	0,01	-18,62	-1,05	-0,03	42	0,2	0,3	15	0
0,14	138000	317	14803	0,37	10	0,25	0,00	18	0,74	0,02	-17,14	-1,22	-0,05	43	0,2	0,3	16	0
0,15	153000	333	18109	0,37	14	0,39	0,01	21	0,95	0,02	-22,09	-1,45	-0,06	43	0,2	0,3	17	0
0,16	171000	355	21036	0,37	19	0,58	0,01	23	1,18	0,04	-26,55	-1,71	-0,08	44	0,2	0,3	20	0
0,17	193000	384	23451	0,37	24	0,82	0,02	25	1,43	0,05	-30,15	-2,01	-0,09	45	0,2	0,3	30	0
0,18	208000	408	52780	0,37	74	1,56	0,03	42	1,85	0,06	-32,67	-2,34	-0,12	47	0,2	0,3	40	0
0,19	224000	436	56201	0,37	86	2,42	0,05	28	2,13	0,08	-70,87	-3,05	-0,14	48	0,2	0,3	48	0
0,20	240000	469	59327	0,37	5	2,47	0,08	-105	1,08	0,10	-72,64	-3,77	-0,18	50	0,2	0,3	66	16
0,21	254000	506	62040	0,37	1	2,48	0,10	-110	-0,02	0,11	-100,49	-4,78	-0,22	53	0,2	0,3	89	38
0,22	267000	546	64085	0,37	93	3,41	0,13	-114	-1,16	0,10	-129,48	-6,07	-0,27	56	0,2	0,8	71	53
0,23	278000	588	200000	0,37	351	4,46	0,14	-764	-3,45	0,09	-301,82	-9,09	-0,35	60	0,1	0,8	52	68

Table 8.10 - Control Volume 1 m³ – Turbulence Factor 4 – Initial Angle 40° - Free Volume 7,5 m³

t	p_i	T_{ui}	q_x	S	a_v	v_v	x_i	a_h	v_h	z_i	ω'	ω	ω . t	θ	C_L	C_D	β	α
0,01	101300	283	0	0,31	-10	0,00	0,00	0			0,00	0,00	0,00	40	0,4	0,5	90	50
0,02	101300	283	0	0,31	-10	0,00	0,00	0	0		0,00	0,00	0,00	40	0,4	0,5	90	50
0,03	101300	283	0	0,31	-10	0,00	0,00	0	0	0,00	0,00	0,00	0,00	40	0,4	0,5	90	50
0,04	101300	283	0	0,31	-10	0,00	0,00	0	0	0,00	0,00	0,00	0,00	40	0,4	0,5	90	50
0,05	103000	285	1075	0,31	-8	0,00	0,00	-2	0,00	0,00	0,00	0,00	0,00	40	0,4	0,5	90	50
0,06	105000	286	2647	0,31	-5	0,00	0,00	-4	0,00	0,00	-4,44	-0,04	0,00	40	0,4	0,5	90	50
0,07	105000	286	2863	0,31	-4	0,00	0,00	-5	0,00	0,00	-10,94	-0,15	0,00	40	0,4	0,5	90	50
0,08	106000	287	3223	0,31	-3	-0,03	0,00	-5	-0,05	0,00	-11,83	-0,27	0,00	40	0,4	0,5	32	0
0,09	108000	289	4974	0,31	2	-0,01	0,00	3	-0,02	0,00	-8,32	-0,36	-0,01	40	0,2	0,3	18	0
0,10	109000	290	6979	0,31	-2	-0,03	0,00	6	0,04	0,00	-6,42	-0,42	-0,01	41	0,2	0,3	27	0
0,11	111000	292	16742	0,31	12	0,09	0,00	12	0,16	0,00	-9,00	-0,51	-0,01	41	0,2	0,3	68	27
0,12	117000	297	8134	0,31	2	0,11	0,00	-4	0,12	0,00	-33,91	-0,85	-0,02	41	0,3	0,4	29	0
0,13	126000	306	11343	0,31	5	0,16	0,00	8	0,20	0,00	-15,69	-1,01	-0,03	42	0,2	0,3	35	0
0,14	138000	317	14810	0,31	11	0,27	0,00	8	0,27	0,01	-14,59	-1,15	-0,04	42	0,2	0,3	38	0
0,15	153000	333	18116	0,31	16	0,43	0,01	8	0,36	0,01	-19,03	-1,34	-0,05	43	0,2	0,3	42	0
0,16	171000	355	21038	0,32	21	0,64	0,01	8	0,43	0,01	-23,27	-1,57	-0,07	44	0,2	0,3	46	2
0,17	193000	384	23444	0,32	26	0,89	0,02	6	0,50	0,02	-28,60	-1,86	-0,09	45	0,2	0,3	61	16
0,18	208000	408	52732	0,32	83	1,72	0,03	-27	0,23	0,02	-41,34	-2,27	-0,11	46	0,3	0,3	82	36
0,19	224000	436	56084	0,33	73	2,46	0,05	-64	-0,41	0,02	-143,29	-3,71	-0,14	48	0,3	0,3	80	32
0,20	240000	469	59146	0,34	-16	2,30	0,08	-113	-1,53	0,01	-153,73	-5,24	-0,18	50	0,3	0,3	56	74
0,21	254000	506	61895	0,34	71	3,01	0,10	-118	-2,72	-0,01	-150,88	-6,75	-0,24	54	0,2	0,7	48	79
0,22	267000	546	63826	0,34	79	3,79	0,14	-197	-4,68	-0,05	-324,93	-10,00	-0,33	59	0,2	0,8	39	83
0,23	278000	588	64925	0,33	84	4,63	0,18	-226	-6,94	-0,11	-403,12	-14,03	-0,45	65	0,1	0,8	34	81
0,24	286000	632	200000	0,32	302	5,54	0,20	-649	-8,89	-0,13	-437,34	-18,41	-0,61	75	0	0,9	32	74

Table 8.11 - Control Volume 1 m³ – Turbulence Factor 4 – Initial Angle 40° - Free Volume 7,5 m³ - Detonación a 632 °K

t	p_i	T_{ui}	q_x	S	a_v	v_v	x_i	a_h	v_h	z_i	ω'	ω	ω . t	θ	C_L	C_D	β	α
0,01	101300	283	0	0,31	-10	0,00	0	0	0,00	0,00	0,00	0,00	0,00	20	0,3	0,7	90	70
0,02	103000	285	1090	0,31	-7	0,00	0	-1	0,00	0,00	0,00	0,00	0,00	20	0,3	0,7	90	70
0,03	103000	285	1224	0,31	-6	0,00	0	-1	0,00	0,00	-6,28	0,00	0,00	20	0,3	0,7	90	70
0,04	103000	285	1146	0,31	-7	0,00	0	-1	0,00	0,00	-7,06	-0,06	0,00	20	0,3	0,7	90	70
0,05	106000	288	3057	0,31	-1	0,00	0,00	-4	0,00	0,00	-6,60	-0,13	0,00	20	0,3	0,7	90	70
0,06	109000	290	6310	0,31	8	0,08	0,00	-8	-0,08	0,00	-17,59	-0,20	0,00	20	0,3	0,7	45	66
0,07	111000	292	9369	0,31	17	0,26	0,00	-11	-0,19	0,00	-33,66	-0,38	-0,01	20	0,3	0,7	54	74
0,08	121000	300	28393	0,31	80	1,05	0,01	-20	-0,38	0,00	-28,72	-0,71	-0,01	21	0,2	0,8	70	90
0,09	134000	312	13438	0,31	39	1,44	0,02	-5	-0,43	-0,01	-117,44	-1,00	-0,02	21	0,1	0,9	73	86
0,10	153000	330	17291	0,31	52	1,96	0,04	-25	-0,68	-0,01	-61,87	-2,17	-0,04	22	0	0,9	70	88
0,11	179000	356	20523	0,31	63	2,59	0,06	-25	-0,94	-0,02	-80,81	-2,79	-0,06	23	0	0,9	70	87
0,12	203000	383	46968	0,32	158	4,18	0,09	-61	-1,55	-0,04	-96,68	-3,60	-0,09	25	0	0,9	69	85
0,13	228000	415	51516	0,32	177	5,95	0,15	-69	-2,24	-0,05	-223,26	-4,57	-0,13	28	0	0,9	69	83
0,14	255000	454	55099	0,33	163	7,58	0,21	-77	-3,01	-0,08	-247,86	-6,80	-0,19	31	0,1	0,8	68	81
0,15	282000	500	57831	0,34	175	9,33	0,30	-102	-4,02	-0,12	-235,47	-9,28	-0,27	35	0,1	0,8	66	78
0,16	305000	554	59233	0,35	173	11,06	0,40	-114	-5,16	-0,16	-250,82	-11,63	-0,38	41	0,2	0,8	65	74
0,17	322000	621	200000	0,37	618	12,91	0,44	-510	-6,69	-0,24	-249,60	-14,14	-0,50	49	0,2	0,8	62	69

Table 8.12 - Control Volume 1 m³ – Turbulence Factor 5 – Initial Angle 20° - Free Volume 7,5 m³

t	p_i	T_{ui}	u_0	q_x	S	a_v	v_v	x_i	a_h	v_h	z_i	ω'	ω	ω . t	θ	C_L	C_D	β	α
0,01	101300	283	0	0	0,31	-10	0,00	0	0	0,00	0,00	0,00	0,00	0,00	30	0,4	0,6	90	60
0,02	103000	285	46	1090	0,31	-7	0,00	0	-2	0,00	0,00	0,00	0,00	0,00	30	0,4	0,6	90	60
0,03	103000	285	52	1224	0,31	-7	0,00	0	-2	0,00	0,00	-3,63	0,00	0,00	30	0,4	0,6	90	60
0,04	103000	285	52	1146	0,31	-7	0,00	0	-2	0,00	0,00	-4,08	-0,04	0,00	30	0,4	0,6	90	60
0,05	106000	288	88	3057	0,31	-2	0,00	0,00	-5	0,00	0,00	-3,82	-0,08	0,00	30	0,4	0,6	90	60
0,06	109000	290	148	6311	0,31	6	0,06	0,00	-11	-0,11	0,00	-10,18	-0,12	0,00	30	0,4	0,6	28	58
0,07	111000	292	233	9371	0,31	14	0,20	0,00	-13	-0,24	0,00	-19,27	-0,22	0,00	30	0,4	0,6	40	70
0,08	121000	300	677	28410	0,31	71	0,91	0,01	-24	-0,48	-0,01	-20,74	-0,41	-0,01	30	0,3	0,7	62	88
0,09	134000	312	444	13460	0,31	32	1,23	0,02	-33	-0,80	-0,01	-100,79	-0,62	-0,01	31	0	0,9	57	87
0,10	153000	330	474	17350	0,31	44	1,67	0,03	-35	-1,16	-0,02	-62,26	-1,63	-0,02	31	0	0,8	55	86
0,11	179000	356	482	20646	0,31	46	2,13	0,05	-39	-1,54	-0,04	-71,32	-2,25	-0,04	32	0	0,9	54	86
0,12	203000	383	692	47424	0,31	132	3,44	0,08	-103	-2,57	-0,06	-95,38	-2,96	-0,07	34	0	0,9	53	87
0,13	228000	415	696	52316	0,31	144	4,89	0,12	-115	-3,72	-0,09	-218,78	-3,91	-0,10	36	0	0,9	52	88
0,14	255000	454	697	56419	0,30	154	6,43	0,18	-125	-4,98	-0,13	-240,61	-6,10	-0,15	39	0	0,9	52	89
0,15	282000	500	164	59789	0,30	161	8,04	0,25	-133	-6,30	-0,19	-257,90	-8,51	-0,23	43	0	0,8	52	85
0,16	305000	554	709	61842	0,30	145	9,50	0,34	-122	-7,52	-0,26	-240,30	-11,09	-0,32	48	0,1	0,8	51	80
0,17	322000	621	718	200000	0,30	535	11,10	0,37	-455	-8,89	-0,36	-238,46	-13,49	-0,45	55	0,2	0,8	51	73

Table 8.13 - Control Volume 1 m³ – Turbulence Factor 5 – Initial Angle 30° - Free Volume 7,5 m³

t	p_i	T_{ui}	q_x	S	a_v	v_v	x_i	a_h	v_h	z_i	ω'	ω	ω . t	θ	C_L	C_D	β	α
0,01	101300	283	0	0,31	-10	0,0	0	0	0,00	0,00	0,00	0,00	0,00	40	0,5	0,6	90	50
0,02	103000	285	1090	0,31	-7	0,0	0	-2	0,00	0,00	0,00	0,00	0,00	40	0,5	0,6	90	50
0,03	103000	285	1224	0,31	-7	0,0	0	-3	0,00	0,00	-8,79	0,00	0,00	40	0,5	0,6	90	50
0,04	103000	285	1146	0,31	-7	0,0	0	-2	0,00	0,00	-9,87	-0,09	0,00	40	0,5	0,6	90	50
0,05	106000	288	3057	0,31	-2	0,0	0,00	-6	0,00	0,00	-9,23	-0,19	0,00	40	0,5	0,6	90	50
0,06	109000	290	6311	0,31	6	0,1	0,00	-13	-0,13	0,00	-24,63	-0,28	0,00	40	0,5	0,6	23	63
0,07	111000	292	9371	0,31	13	0,2	0,00	-15	-0,29	0,00	-49,52	-0,53	-0,01	40	0,4	0,6	33	74
0,08	121000	300	28412	0,31	64	0,8	0,01	-49	-0,78	-0,01	-66,38	-1,02	-0,02	41	0,3	0,7	47	88
0,09	134000	312	13467	0,31	26	1,1	0,02	-34	-1,12	-0,02	-207,80	-1,68	-0,03	42	0	0,9	44	86
0,10	153000	330	17378	0,31	35	1,4	0,03	-46	-1,58	-0,03	-124,58	-3,76	-0,06	43	0	0,9	42	85
0,11	179000	356	20716	0,31	42	1,9	0,05	-57	-2,15	-0,05	-160,80	-5,01	-0,10	46	0	0,9	41	86
0,12	203000	383	47698	0,31	106	2,9	0,07	-134	-3,48	-0,08	-191,90	-6,62	-0,16	49	0	0,9	40	89
0,13	228000	415	52819	0,31	116	4,1	0,10	-150	-4,98	-0,12	-442,07	-8,54	-0,23	53	0	0,9	39	88
0,14	255000	454	57318	0,31	124	5,3	0,15	-163	-6,61	-0,18	-488,18	-12,96	-0,34	59	0	0,9	39	82
0,15	282000	500	61270	0,31	96	6,3	0,21	-171	-8,33	-0,25	-523,39	-17,84	-0,50	68	0,1	0,8	37	75
0,16	305000	554	64167	0,30	73	7,0	0,28	-197	-10,29	-0,35	-498,70	-23,07	-0,70	80	0,2	0,8	34	66
0,17	322000	621	200000	0,30	62	7,2	0,30	-530	-11,88	-0,48	-527,09	-28,06	-0,96	94	0,3	0,6	31	54

Table 8.14 - Control Volume 1 m³ – Turbulence Factor 5 – Initial Angle 40° - Free Volume 7,5 m³

t	p_i	T_{ui}	q_x	S	a_v	v_v	x_i	a_h	v_h	z_i	ω'	ω	ω . t	θ	C_L	C_D	β	α
0,01	101300	283	0	0,31	-10	0,00	0	0	0,00	0,00	0,00	0,00	0,00	40	0,4	0,5	90	50
0,02	103000	285	1090	0,31	-8	0,00	0	-2	0,00	0,00	0,00	0,00	0,00	40	0,4	0,5	90	50
0,03	103000	285	1224	0,31	-7	0,00	0	-2	0,00	0,00	-3,60	0,00	0,00	40	0,4	0,5	90	50
0,04	103000	285	1146	0,31	-8	0,00	0	-2	0,00	0,00	-4,05	-0,04	0,00	40	0,4	0,5	90	50
0,05	106000	288	3057	0,31	-4	0,00	0,00	-5	0,00	0,00	-3,79	-0,08	0,00	40	0,4	0,5	90	50
0,06	109000	290	6311	0,31	3	0,03	0,00	-11	-0,11	0,00	-10,11	-0,11	0,00	40	0,4	0,5	90	50
0,07	111000	292	9373	0,31	9	0,12	0,00	-16	-0,26	0,00	-20,89	-0,22	0,00	40	0,4	0,5	14	54
0,08	121000	300	28431	0,31	50	0,62	0,00	-46	-0,72	-0,01	-31,12	-0,42	-0,01	40	0,4	0,5	29	70
0,09	134000	312	13496	0,31	24	0,85	0,01	-13	-0,85	-0,02	-90,51	-0,74	-0,01	41	0,3	0,7	37	77
0,10	153000	330	17455	0,31	36	1,21	0,02	-27	-1,12	-0,03	-53,92	-1,64	-0,02	41	0,2	0,8	41	82
0,11	179000	356	20857	0,31	41	1,63	0,04	-41	-1,53	-0,04	-78,24	-2,18	-0,04	42	0,1	0,8	43	85
0,12	203000	383	48135	0,31	113	2,76	0,06	-102	-2,55	-0,06	-94,85	-2,96	-0,07	44	0,1	0,8	44	88
0,13	228000	415	53403	0,31	145	4,21	0,09	-111	-3,66	-0,09	-228,62	-3,91	-0,10	46	0,1	0,9	46	88
0,14	255000	454	57950	0,31	129	5,50	0,14	-169	-5,35	-0,14	-305,40	-6,20	-0,15	49	0,1	0,9	46	85
0,15	282000	500	61837	0,32	141	6,92	0,20	-180	-7,15	-0,20	-365,63	-9,25	-0,23	53	0,1	0,9	46	81
0,16	305000	554	64498	0,32	128	8,20	0,28	-191	-9,06	-0,28	-439,48	-12,91	-0,34	59	0,1	0,8	45	76
0,17	322000	621	200000	0,32	292	9,07	0,31	-543	-10,69	-0,40	-464,25	-17,30	-0,49	68	0,2	0,7	37	75

Table 8-15. Control Volume 1 m³ – Turbulence Factor 5 – Initial Angle 40° - Free Volume 7,5 m³ – Distance Oriented

t	p_i	T_{ui}	q_x	S	a_v	v_v	x_i	a_h	v_h	z_i	ω'	ω	ω . t	θ	C_L	C_D	β	α
0,01	101300	283	0	0,31	-10	0,00	0	0	0,00	0,00	0,00	0,00	0,00	40	0,4	0,5	90	50
0,02	103000	285	1090	0,31	-8	0,00	0	-2	0,00	0,00	0,00	0,00	0,00	40	0,4	0,5	90	50
0,03	103000	285	1224	0,31	-7	0,00	0	-2	0,00	0,00	-1,80	0,00	0,00	40	0,4	0,5	90	50
0,04	103000	285	1146	0,31	-8	0,00	0	-2	0,00	0,00	-2,02	-0,02	0,00	40	0,4	0,5	90	50
0,05	106000	288	3057	0,31	-4	0,00	0,00	-5	0,00	0,00	-1,89	-0,04	0,00	40	0,4	0,5	90	50
0,06	109000	290	6311	0,31	3	0,03	0,00	-11	-0,11	0,00	-5,06	-0,06	0,00	40	0,4	0,5	90	50
0,07	111000	292	9373	0,31	9	0,12	0,00	-16	-0,26	0,00	-10,47	-0,11	0,00	40	0,4	0,5	14	54
0,08	121000	300	28431	0,31	49	0,61	0,00	-46	-0,72	-0,01	-15,66	-0,21	0,00	40	0,4	0,5	29	69
0,09	134000	312	13496	0,31	23	0,85	0,01	-13	-0,85	-0,02	-46,09	-0,37	-0,01	40	0,3	0,7	37	77
0,10	153000	330	17455	0,31	36	1,20	0,02	-27	-1,12	-0,03	-27,87	-0,83	-0,01	41	0,2	0,8	41	81
0,11	179000	356	20859	0,30	41	1,61	0,04	-40	-1,52	-0,04	-41,10	-1,11	-0,02	41	0,1	0,8	43	84
0,12	203000	383	48145	0,30	123	2,84	0,06	-100	-2,52	-0,06	-50,79	-1,52	-0,04	42	0,1	0,9	45	87
0,13	228000	415	53397	0,30	125	4,09	0,09	-121	-3,73	-0,09	-141,65	-2,03	-0,05	43	0	0,9	46	91
0,14	255000	454	57956	0,29	137	5,46	0,14	-143	-5,16	-0,13	-173,51	-3,44	-0,08	45	0	0,9	46	89
0,15	282000	500	61892	0,29	145	6,91	0,20	-148	-6,64	-0,19	-214,18	-5,18	-0,12	47	0	0,9	46	87
0,16	305000	554	64569	0,28	147	8,38	0,28	-150	-8,14	-0,27	-263,04	-7,32	-0,19	51	0	0,9	46	83
0,17	322000	621	200000	0,27	356	9,44	0,31	-449	-9,48	-0,37	-315,11	-9,95	-0,27	56	0,1	0,8	39	85

Table 8.16 - Control Volume 1 m³ – Turbulence Factor 5 – Initial Angle 40° - Free Volume 7,5 m³- Distance Pressure Center to Centroid 0,1m

t	p_i	T_{ui}	q_x	S	a_v	v_v	x_i	a_h	v_h	z_i	ω'	ω	ω . t	θ	C_L	C_D	β	α
0,01	101300	283	0	0,31	-10			0			0,00			30	0,5	0,6	90	60
0,02	101300	283	0	0,31	-10			0	0		0,00	0	0	30	0,5	0,6	90	60
0,03	102000	284	895	0,31	-8			-2	0	0,00	0,00	0	0	30	0,5	0,6	90	60
0,04	102000	284	949	0,31	-8			-2	0	0,00	-3,44	0	0	30	0,5	0,6	90	60
0,05	104000	285	3513	0,31	-1	0	0,00	-7	0	0,00	-3,65	0	0	30	0,5	0,6	90	60
0,06	106000	287	6667	0,31	7	0	0,00	-14	-0,14	0,00	-13,51	-0,14	0,00	30	0,5	0,6	21	22
0,07	109000	290	11138	0,31	21	0	0,00	-17	-0,31	0,00	-29,51	-0,43	0,00	30	0,2	0,3	41	41
0,08	111000	292	15664	0,31	12	0	0,01	-6	-0,37	-0,01	-25,11	-0,68	-0,01	31	0,4	0,5	46	47
0,09	114000	295	21221	0,31	46	1	0,01	-5	-0,41	-0,01	-65,11	-1,33	-0,02	31	0,4	0,5	64	64
0,10	117000	298	45615	0,31	107	2	0,03	26	-0,15	-0,01	-86,85	-2,20	-0,04	32	0,5	0,6	85	86
0,11	131000	312	24408	0,31	55	2	0,05	46	0,30	-0,01	-191,61	-4,12	-0,07	34	0,1	0,9	83	49
0,12	149000	332	32237	0,32	114	4	0,08	1	0,32	-0,01	-146,76	-5,58	-0,12	37	0,4	0,5	85	48
0,13	174000	363	38328	0,33	80	4	0,12	-60	-0,28	-0,01	-116,16	-6,75	-0,18	40	0,4	0,5	86	54
0,14	191000	391	86388	0,34	177	6	0,17	-170	-1,98	-0,02	-140,63	-8,15	-0,25	44	0,5	0,5	72	64
0,15	210000	426	90160	0,36	128	7	0,24	-269	-4,67	-0,05	-404,35	-12,20	-0,35	50	0,5	0,6	58	72
0,16	228000	470	93055	0,36	99	8	0,32	-334	-8,00	-0,12	-572,15	-17,92	-0,51	59	0,3	0,7	46	75
0,17	245000	521	94075	0,36	126	10	0,41	-315	-11,15	-0,21	-619,60	-24,11	-0,72	71	0,2	0,8	41	68
0,18	258000	578	93461	0,35	151	11	0,51	-316	-14,32	-0,34	-678,82	-30,90	-0,99	86	0,3	0,7	38	56
0,19	266000	638	200000	0,32	158	11,69	0,63	-633	-16,21	-0,39	-754,70	-38,45	-1,34	106	0,5	0,5		

Tabla 8.17 - Control Volume 1 m³ – Turbulence Factor 5 – Initial Angle 30° - Free Volume 5 m³

t	p_i	T_{ui}	q_x	S	a_v	v_v	x_i	a_h	v_h	z_i	ω'	ω	ω . t	θ	C_L	C_D	β	α
0,01	101300	283	0	0,31	-10			0			0,00			30	0,5	0,6	90	60
0,02	101500	283	258	0,31	-9			-1			0,00	0	0	30	0,5	0,6	90	60
0,03	101500	283	265	0,31	-9			-1	0,00	0,00	-0,99	0	0	30	0,5	0,6	90	60
0,04	102000	284	913	0,31	-8			-2	-0,02	0,00	-1,02	0	0	30	0,5	0,6	90	60
0,05	103000	285	2315	0,31	-4	-0,04	0,00	-5	-0,07	0,00	-3,51	0	0	30	0,5	0,6	90	60
0,06	104000	285	3906	0,31	0	-0,04	0,00	-8	-0,15	0,00	-8,91	-0,09	0,00	30	0,5	0,6	17	0
0,07	104000	286	4075	0,31	1	-0,04	0,00	7	-0,07	0,00	-16,52	-0,25	0,00	30	0,2	0,3	25	0
0,08	105000	286	5070	0,31	-4	-0,07	0,00	4	-0,04	0,00	-8,14	-0,34	-0,01	30	0,2	0,3	63	32
0,09	105000	286	5911	0,31	-1	-0,08	0,00	-1	-0,05	0,00	-11,72	-0,45	-0,01	31	0,3	0,3	61	30
0,10	106000	287	6684	0,31	1	-0,07	0,00	-3	-0,08	0,00	-15,54	-0,61	-0,01	31	0,3	0,3	43	12
0,11	106000	287	8502	0,31	5	-0,03	0,00	1	-0,07	-0,01	-18,28	-0,79	-0,02	31	0,2	0,3	19	0
0,12	108000	289	11278	0,31	3	0,01	0,00	10	0,03	-0,01	-15,78	-0,95	-0,03	32	0,2	0,3	14	0
0,13	109000	290	15500	0,31	7	0,08	0,00	15	0,18	0,00	-19,47	-1,14	-0,04	32	0,2	0,3	23	0
0,14	113000	293	12792	0,31	6	0,13	0,00	10	0,28	0,00	-30,02	-1,44	-0,05	33	0,2	0,3	25	0
0,15	117000	297	16461	0,31	11	0,24	0,00	13	0,41	0,00	-25,34	-1,70	-0,07	34	0,2	0,3	31	0
0,16	122000	302	20444	0,31	18	0,42	0,00	13	0,54	0,01	-34,24	-2,04	-0,09	35	0,2	0,3	38	3
0,17	128000	307	24637	0,31	25	0,67	0,01	12	0,66	0,01	-44,59	-2,49	-0,11	36	0,2	0,3	45	9
0,18	136000	315	29199	0,32	34	1,01	0,02	8	0,74	0,02	-55,62	-3,04	-0,14	38	0,2	0,3	53	16
0,19	144000	323	33330	0,32	42	1,43	0,03	2	0,77	0,03	-67,07	-3,71	-0,17	40	0,2	0,3	61	22
0,20	153000	334	36866	0,33	49	1,91	0,05	-6	0,71	0,03	-76,54	-4,48	-0,21	42	0,2	0,3	69	27
0,21	165000	347	40085	0,34	54	2,45	0,07	-15	0,56	0,04	-83,39	-5,31	-0,26	45	0,3	0,3	77	32
0,22	177000	362	42946	0,35	62	3,08	0,10	-45	0,10	0,04	-94,04	-6,25	-0,32	48	0,3	0,3	88	39
0,23	191000	381	44770	0,36	57	3,65	0,13	-63	-0,52	0,04	-88,93	-7,14	-0,39	52	0,4	0,5	81	47
0,24	199000	394	93786	0,37	194	5,59	0,17	-217	-2,70	0,03	-170,85	-8,85	-0,47	57	0,4	0,5	64	60
0,25	207000	408	93513	0,38	121	6,80	0,24	-274	-5,43	-0,02	-430,90	-13,16	-0,58	63	0,5	0,6	51	66

t	p_i	T_{ui}	q_x	S	a_v	v_v	x_i	a_h	v_h	z_i	ω'	ω	ω . t	θ	C_L	C_D	β	α
0,26	215000	424	91842	0,38	63	7,43	0,31	-357	-9,01	-0,09	-595,55	-19,11	-0,74	72	0,4	0,6	39	69
0,27	223000	441	89476	0,37	22	7,65	0,38	-317	-12,18	-0,19	-591,55	-25,03	-0,96	85	0,3	0,7	32	63
0,28	231000	460	86905	0,35	37	8,03	0,46	-301	-15,19	-0,33	-600,19	-31,03	-1,24	101	0,5	0,6	28	52
0,29	238000	480	84266	0,31	-66	7,37	0,54	-264	-17,83	-0,50	-750,72	-38,54	-1,59	120	0,4	0,5	22	37
0,30	244000	501	81533	0,26	-60	6,77	0,61	-171	-19,54	-0,68	-602,13	-44,56	-2,00	144	0,3	0,4	19	17
0,31	250000	523	79036	0,19	-41	6,36	0,68	-96	-20,50	-0,88	-424,86	-48,81	-2,47	171	0,2	0,3	17	8
0,32	256000	545	76979	0,12	-22	6,14	0,74	-42	-20,92	-1,09	-243,00	-51,24	-2,97	199	0,2	0,3	16	36
0,33	260000	569	200000	0,04	-22	6,07	0,76	-38	-21,03	-1,15	-166,39	-52,90	-3,49	229	0,3	0,3	16	65

Tabla 8.18 - Control Volume 1 m³ – Turbulence Factor 3 – Initial Angle 30° - Free Volume 10 m³

t	p_i	T_{ui}	q_x	S	a_v	v_v	x_i	a_h	v_h	z_i	ω'	ω	ω . t	θ	C_L	C_D	β	α
0,01	101300	283	0	0,31	-10			0			0,00			30	0,5	0,6	90	60
0,02	103000	285	2151	0,31	-5			-4			0,00	0	0	30	0,5	0,6	90	60
0,03	104000	285	3801	0,31	-1			-8			-8,27	0	0	30	0,5	0,6	90	60
0,04	106000	287	6802	0,31	7	0,07	0,00	-14	-0,14	0,00	-14,61	-0,15	0,00	30	0,5	0,6	26	57
0,05	108000	289	11298	0,31	23	0,30	0,00	-15	-0,28	0,00	-31,45	-0,46	0,00	30	0,5	0,6	47	77
0,06	110000	290	17546	0,31	46	0,77	0,01	-3	-0,32	-0,01	-57,09	-1,03	-0,01	31	0,2	0,8	67	82
0,07	113000	293	36267	0,31	89	1,66	0,02	-18	-0,50	-0,01	-93,16	-1,96	-0,03	31	0,1	0,8	73	76
0,08	123000	302	19916	0,31	51	2,16	0,04	-27	-0,77	-0,02	-189,27	-3,86	-0,06	33	0,1	0,8	70	77
0,09	137000	315	27538	0,31	73	2,89	0,06	-42	-1,19	-0,03	-104,85	-4,90	-0,10	36	0,1	0,8	67	77
0,10	157000	335	34437	0,32	92	3,82	0,10	-58	-1,77	-0,04	-147,38	-6,38	-0,16	39	0,1	0,8	65	76
0,11	182000	363	39726	0,32	106	4,88	0,14	-72	-2,49	-0,06	-189,01	-8,27	-0,23	43	0,1	0,8	63	74
0,12	208000	396	88314	0,32	245	7,33	0,20	-173	-4,22	-0,10	-226,22	-10,53	-0,32	48	0,2	0,8	60	72
0,13	237000	439	95287	0,33	238	9,71	0,29	-239	-6,61	-0,15	-564,37	-16,17	-0,46	56	0,3	0,7	55	69
0,14	269000	492	100461	0,33	172	11,43	0,39	-285	-9,47	-0,23	-634,10	-22,51	-0,65	67	0,4	0,7	50	63
0,15	300000	556	103970	0,33	120	12,63	0,51	-346	-12,93	-0,34	-805,94	-30,57	-0,92	82	0,5	0,6	44	54
0,16	329000	629	200000	0,32	43	12,76	0,64	-668	-14,93	-0,38	-938,01	-39,95	-1,27	102	0,4	0,5	40	37

Tabla 8.19 - Control Volume 1 m³ – Turbulence Factor 5 – Initial Angle 30° - Free Volume 10 m³

t	a_v	v_v	x_i	a_h	v_h	z_i
0,5	-10	0,64	0,43	0	-6,33	-1,00
0,6	-10	-0,36	0,44	0	-6,32	-1,63
0,7	-10	-1,36	0,36	0	-6,32	-2,27
0,8	-10	-2,36	0,17	0	-6,31	-2,90
0,9	-10	-3,36	-0,12	0	-6,31	-3,53
1,0	-10	-4,36	-0,50	0	-6,30	-4,16
1,1	-10	-5,36	-0,99	0	-6,30	-4,79
1,2	-10	-6,36	-1,58	0	-6,29	-5,42
1,21	-10	-6,46	-1,64	0	-6,29	-5,48
1,22	-10	-6,56	-1,71	0	-6,29	-5,54
1,23	-10	-6,66	-1,77	0	-6,29	-5,61
1,24	-10	-6,76	-1,84	0	-6,29	-5,67
1,25	-10	-6,86	-1,91	0	-6,29	-5,73
1,26	-10	-6,96	-1,98	0	-6,29	-5,80
						-8,27

Tabla 8.20 - Control Volume 5 m³ – Turbulence Factor 2 – Initial Angle 30° - Free Volume 7,5 m³

t	a_v	v_v	x_i	a_h	v_h	z_i
0,3	135	9,59	1,12		-14,50	-1,37
0,4	-10	8,60	2,03	0,3	-14,46	-2,81
0,5	-10	7,61	2,84	0,3	-14,43	-4,26
0,6	-10	6,63	3,55	0,3	-14,39	-5,70
0,7	-10	5,64	4,17	0,3	-14,36	-7,14
0,8	-10	4,66	4,68	0,3	-14,32	-8,57
0,9	-10	3,68	5,10	0,3	-14,29	-10,00
1,0	-10	2,70	5,42	0,3	-14,25	-11,43
1,1	-10	1,72	5,64	0,3	-14,22	-12,85
1,2	-10	0,74	5,76	0,3	-14,19	-14,27
1,3	-10	-0,24	5,79	0,3	-14,15	-15,69
1,4	-10	-1,22	5,71	0,3	-14,12	-17,10
1,5	-10	-2,20	5,54	0,3	-14,09	-18,51
1,6	-10	-3,18	5,27	0,3	-14,05	-19,92
1,7	-10	-4,17	4,90	0,3	-14,02	-21,32
1,8	-10	-5,15	4,44	0,3	-13,99	-22,72
1,9	-10	-6,13	3,88	0,3	-13,96	-24,12
1,0	-10	-7,12	3,21	0,3	-13,92	-25,51
2,1	-10	-8,10	2,45	0,3	-13,89	-26,91
2,2	-10	-9,09	1,59	0,3	-13,86	-28,29
2,3	-10	-10,08	0,63	0,3	-13,83	-29,68
2,4	-10	-11,07	-0,42	0,3	-13,79	-31,06
2,5	-10	-12,07	-1,58	0,3	-13,76	-32,44
2,51	-10	-12,17	-1,70	0,3	-13,76	-32,57
2,52	-10	-12,27	-1,82	0,3	-13,76	-32,71
2,53	-10	-12,36	-1,95	0,3	-13,75	-32,85
						-44,67

Tabla 8.21 - Control Volume 5 m³ – Turbulence Factor 3 – Initial Angle 30° - Free Volume 7,5 m³

t	a_v	v_v	x_i	a_h	v_h	z_i
0,30	-10	12,44	1,90	0,5	-18,08	-2,18
0,40	-10	11,45	3,10	0,5	-18,02	-3,99
0,50	-10	10,46	4,19	0,5	-17,97	-5,79
0,60	-10	9,47	5,19	0,5	-17,92	-7,58
0,70	-10	8,48	6,09	0,5	-17,86	-9,37
0,80	-10	7,49	6,88	0,5	-17,81	-11,15
0,90	-10	6,50	7,58	0,5	-17,76	-12,93
1,00	-10	5,52	8,18	0,5	-17,71	-14,71
1,10	-10	4,54	8,69	0,5	-17,65	-16,47
1,20	-10	3,56	9,09	0,5	-17,60	-18,24
1,30	-10	2,58	9,40	0,5	-17,55	-19,99
1,40	-10	1,60	9,61	0,5	-17,50	-21,75
1,50	-10	0,62	9,72	0,5	-17,45	-23,49
1,60	-10	-0,36	9,73	0,5	-17,40	-25,24
1,70	-10	-1,34	9,65	0,5	-17,35	-26,97
1,80	-10	-2,32	9,46	0,5	-17,30	-28,70
1,90	-10	-3,30	9,18	0,5	-17,25	-30,43
2,00	-10	-4,28	8,80	0,5	-17,20	-32,15
2,10	-10	-5,26	8,32	0,5	-17,15	-33,87
2,20	-10	-6,24	7,75	0,5	-17,10	-35,58
2,30	-10	-7,21	7,08	0,5	-17,05	-37,29
2,40	-10	-8,18	6,31	0,5	-17,00	-38,99
2,50	-10	-9,16	5,44	0,5	-16,95	-40,69
2,60	-10	-10,13	4,48	0,5	-16,91	-42,38
2,70	-10	-11,09	3,42	0,5	-16,86	-44,07
2,80	-10	-12,06	2,26	0,5	-16,81	-45,76
2,90	-10	-13,02	1,00	0,5	-16,76	-47,43
3,00	-10	-13,98	-0,35	0,5	-16,72	-49,11
3,10	-10	-14,94	-1,79	0,5	-16,67	-50,78
3,11	-10	-15,04	-1,94	0,5	-16,67	-50,95
						-68,31

Tabla 8.22 - Control Volume 5 m³ – Turbulence Factor 4 – Initial Angle 30° - Free Volume 7,5 m³

t	a_v	v_v	x_i	a_h	v_h	z_i
0,17	0	6,1	0,21	0	-8,8	-0,28
0,18	0	6,1	0,27	0	-8,8	-0,37
0,19	0	6,1	0,33	0	-8,8	-0,46
0,2	-10,0	6,0	0,39	0,1	-8,8	-0,55
0,3	-10,0	5,0	0,94	0,1	-8,8	-1,42
0,4	-10,0	4,0	1,39	0,1	-8,8	-2,30
0,5	-10,0	3,0	1,73	0,1	-8,7	-3,17
0,6	-10,0	2,0	1,98	0,1	-8,7	-4,05
0,7	-10,0	1,0	2,13	0,1	-8,7	-4,92
0,8	-10,0	0,0	2,17	0,1	-8,7	-5,79
0,9	-10,0	-1,0	2,12	0,1	-8,7	-6,66
1	-10,0	-2,0	1,97	0,1	-8,7	-7,53
1,1	-10,0	-5,7	0,53	0,1	-8,7	-10,74
1,2	-10,0	-6,7	-0,09	0,1	-8,7	-11,61
1,3	-10,0	-7,7	-0,82	0,1	-8,6	-12,47
1,4	-10,0	-8,7	-1,64	0,1	-8,6	-13,34
1,41	-10,0	-8,8	-1,73	0,1	-8,6	-13,42
1,42	-10,0	-8,9	-1,82	0,1	-8,6	-13,51
1,43	-10,0	-9,0	-1,91	0,1	-8,6	-13,60
						-18,25

Table 8.23 - Control Volume 5 m³ – Turbulence Factor 5 – Initial Angle 30° - Free Volume 7,5 m³

t	a_v	v_v	x_i	a_h	v_h	z_i
0,41	-10	11,39	1,37	0	-10,61	-1,02
0,5	-10	10,46	2,36	0	-10,58	-1,97
0,6	-10	9,43	3,35	0	-10,54	-3,03
0,7	-10	8,40	4,24	0	-10,51	-4,08
0,8	-10	7,38	5,03	0	-10,47	-5,13
0,9	-10	6,37	5,72	0	-10,44	-6,18
1,0	-10	5,36	6,31	0	-10,40	-7,22
2,0	-10	-4,65	6,65	0	-10,07	-17,45
2,9	-9	-13,40	-1,51	0	-9,78	-26,38
2,91	-9	-13,49	-1,64	0	-9,78	-26,48
2,92	-9	-13,59	-1,78	0	-9,78	-26,58
2,93	-9	-13,68	-1,91	0	-9,77	-26,67
						-32,64

Tabla 8.24 - Control Volume 1 m³ – Turbulence Factor 3 – Initial Angle 20° - Free Volume 7,5 m³

t	a_v	v_v	x_i	a_h	v_h	z_i
0,24	-10	8,43	0,45	0,1	-9,34	-0,36
0,30	-10	7,83	0,94	0,1	-9,34	-0,92
0,40	-10	6,81	1,67	0,1	-9,33	-1,85
0,50	-10	5,80	2,30	0,1	-9,32	-2,78
0,60	-10	4,78	2,83	0,1	-9,30	-3,71
0,70	-10	3,77	3,26	0,1	-9,29	-4,64
0,80	-10	2,76	3,59	0,1	-9,28	-5,57
0,90	-10	1,74	3,81	0,1	-9,27	-6,50
1,00	-10	0,73	3,94	0,1	-9,26	-7,43
1,10	-10	-0,26	3,96	0,1	-9,25	-8,35
1,20	-10	-1,25	3,88	0,1	-9,24	-9,28
1,30	-10	-2,24	3,71	0,1	-9,23	-10,20
1,40	-10	-3,22	3,44	0,1	-9,22	-11,12
1,50	-10	-4,21	3,07	0,1	-9,21	-12,04
1,60	-10	-5,19	2,60	0,1	-9,20	-12,96
1,70	-10	-6,18	2,03	0,1	-9,19	-13,88
1,80	-10	-7,17	1,36	0,1	-9,18	-14,80
1,90	-10	-8,15	0,59	0,1	-9,16	-15,72
2,00	-10	-9,14	-0,27	0,1	-9,15	-16,63
2,10	-10	-10,13	-1,24	0,1	-9,14	-17,55
2,11	-10	-10,23	-1,34	0,1	-9,14	-17,64
2,12	-10	-10,32	-1,44	0,1	-9,14	-17,73
2,13	-10	-10,42	-1,54	0,1	-9,14	-17,82
2,14	-10	-10,52	-1,65	0,1	-9,14	-17,92
2,15	-10	-10,62	-1,75	0,1	-9,14	-18,01
2,16	-10	-10,72	-1,86	0,1	-9,14	-18,10
2,17	-10	-10,82	-1,97	0,1	-9,14	-18,19
						-23,41

Tabla 8.25 - Control Volume 1 m³ – Turbulence Factor 4 – Initial Angle 20° - Free Volume 7,5 m³

t	.a_v	v_v	x_i	a_h	v_h	z_i
0,25	-10	8,55	0,54	0,2	-10,96	-0,46
0,30	-10	8,04	0,95	0,2	-10,95	-1,01
0,40	-10	7,02	1,71	0,2	-10,94	-2,10
0,50	-10	6,00	2,36	0,2	-10,92	-3,20
0,60	-10	4,98	2,91	0,2	-10,91	-4,29
0,70	-10	3,96	3,36	0,2	-10,89	-5,38
0,80	-10	2,94	3,70	0,2	-10,87	-6,47
0,90	-10	1,93	3,94	0,2	-10,86	-7,55
1,00	-10	0,91	4,09	0,2	-10,85	-8,64
1,10	-10	-0,08	4,13	0,2	-10,83	-9,72
1,20	-10	-1,06	4,07	0,1	-10,82	-10,80
1,30	-10	-2,04	3,91	0,1	-10,80	-11,89
1,40	-10	-3,03	3,66	0,1	-10,79	-12,97
1,50	-10	-4,01	3,31	0,1	-10,77	-14,04
1,60	-10	-4,99	2,86	0,1	-10,76	-15,12
1,70	-10	-5,97	2,31	0,1	-10,74	-16,19
1,80	-10	-6,95	1,66	0,1	-10,73	-17,27
1,90	-10	-7,93	0,92	0,1	-10,71	-18,34
2,00	-10	-8,92	0,08	0,1	-10,70	-19,41
2,10	-10	-9,90	-0,86	0,1	-10,68	-20,48
2,20	-10	-10,88	-1,90	0,1	-10,67	-21,55
						-28,66

Tabla 8.26 - Control Volume 1 m³ – Turbulence Factor 4 – Initial Angle 20° - Free Volume 7,5 m³ - Detonation 632 °K

t	a_v	v_v	x_i	a_h	v_h	z_i
0,24	-10	4,36	0,19	0,0	-3,45	0,06
0,30	-10	3,76	0,43	0,0	-3,45	-0,15
0,40	-10	2,76	0,76	0,0	-3,45	-0,49
0,50	-10	1,75	0,98	0,0	-3,44	-0,84
0,60	-10	0,75	1,11	0,0	-3,44	-1,18
0,70	-10	-0,25	1,13	0,0	-3,44	-1,53
0,80	-10	-1,25	1,06	0,0	-3,44	-1,87
0,90	-10	-2,25	0,88	0,0	-3,44	-2,21
1,00	-10	-3,26	0,61	0,0	-3,44	-2,56
1,10	-10	-4,25	0,23	0,0	-3,44	-2,90
1,20	-10	-5,25	-0,25	0,0	-3,43	-3,24
1,30	-10	-6,25	-0,82	0,0	-3,43	-3,59
1,40	-10	-7,25	-1,50	0,0	-3,43	-3,93
1,41	-10	-7,35	-1,57	0,0	-3,43	-3,97
1,42	-10	-7,45	-1,64	0,0	-3,43	-4,00
1,43	-10	-7,55	-1,72	0,0	-3,43	-4,03
1,44	-10	-7,65	-1,79	0,0	-3,43	-4,07
1,45	-10	-7,75	-1,87	0,0	-3,43	-4,10
1,46	-10	-7,85	-1,95	0,0	-3,43	-4,14
						-4,87

Tabla 8.27 - Control Volume 1 m³ – Turbulence Factor 4 – Initial Angle 40° - Free Volume 7,5 m³

t	a_v	v_v	x_i	a_h	v_h	z_i
0,25	-10	5,44	0,25	0,1	-8,89	-0,22
0,30	-10	4,93	0,51	0,1	-8,88	-0,66
0,40	-10	3,92	0,95	0,1	-8,87	-1,55
0,50	-10	2,91	1,29	0,1	-8,86	-2,44
0,60	-10	1,89	1,53	0,1	-8,85	-3,32
0,70	-10	0,88	1,67	0,1	-8,84	-4,21
0,80	-10	-0,13	1,71	0,1	-8,83	-5,09
0,90	-10	-1,14	1,65	0,1	-8,82	-5,97
1,00	-10	-2,16	1,48	0,1	-8,81	-6,86
1,10	-10	-3,15	1,22	0,1	-8,80	-7,74
1,20	-10	-4,14	0,85	0,1	-8,79	-8,62
1,30	-10	-5,12	0,39	0,1	-8,78	-9,50
1,40	-10	-6,11	-0,17	0,1	-8,77	-10,37
1,50	-10	-7,10	-0,83	0,1	-8,76	-11,25
1,60	-10	-8,09	-1,59	0,1	-8,75	-12,13
1,61	-10	-8,19	-1,67	0,1	-8,75	-12,21
1,62	-10	-8,28	-1,76	0,1	-8,75	-12,30
1,63	-10	-8,38	-1,84	0,1	-8,75	-12,39
1,64	-10	-8,48	-1,92	0,1	-8,75	-12,48
						-17,26

Tabla 8.28 - Control Volume 1 m³ – Turbulence Factor 4 – Initial Angle 40° - Free Volume 7,5 m³- Detonation 632 °K

t	a_v	v_v	x_i	a_h	v_h	z_i
0,18	-10	11,00	0,48	0	-8,88	-0,44
0,20	-10	10,79	0,70	0	-8,88	-0,62
0,30	-10	9,75	1,72	0	-8,85	-1,51
0,40	-10	9.00	2,65	0	-8,83	-2,39
0,50	-10	8.00	3,47	0	-8,80	-3,27
0,60	-10	7.00	4,19	0	-8,78	-4,15
0,70	-10	6.00	4,81	0	-8,75	-5,03
0,80	-10	5.00	5,32	0	-8,73	-5,90
0,90	-10	4.00	5,74	0	-8,70	-6,78
1,00	-10	3.00	6,06	0	-8,68	-7,64
1,10	-10	2.00	6,27	0	-8,66	-8,51
1,20	-10	1.00	6,39	0	-8,63	-9,38
1,30	-10	0.00	6,40	0	-8,61	-10,24
1,40	-10	-1.00	6,32	0	-8,59	-11,10
1,50	-10	-2.00	6,13	0	-8,56	-11,95
1,60	-10	-3.00	5,85	0	-8,54	-12,81
1,70	-10	-4.00	5,46	0	-8,51	-13,66
1,80	-10	-5.00	4,98	0	-8,49	-14,51
1,90	-10	-6.00	4,39	0	-8,47	-15,36
2,00	-10	-7.00	3,70	0	-8,45	-16,21
2,10	-10	-8.00	2,91	0	-8,42	-17,05
2,20	-10	-9.00	2,02	0	-8,40	-17,89
2,30	-10	-10.00	1,03	0	-8,38	-18,73
2,40	-10	-12.00	-0,07	0	-8,36	-19,57
2,50	-10	-12.00	-1,27	0	-8,33	-20,40
2,51	-10	-13.00	-1,39	0	-8,33	-20,48
2,52	-9	-13.00	-1,52	0	-8,33	-20,57
2,53	-9	-13.00	-1,65	0	-8,33	-20,65
2,54	-9	-13.00	-1,78	0	-8,32	-20,73
2,55	-9	-13.00	-1,90	0	-8,32	-20,82
						-25,15

Tabla 8.29 - Control Volume 1 m³ – Turbulence Factor 5 – Initial Angle 20° - Free Volume 7,5 m³

t	a_v	v_v	x_i	a_h	v_h	z_i
0,18	-10	11,00	0,48	0	-8,88	-0,44
0,20	-10	10,79	0,70	0	-8,88	-0,62
0,30	-10	9,75	1,72	0	-8,85	-1,51
0,40	-10	9	2,65	0	-8,83	-2,39
0,50	-10	8	3,47	0	-8,80	-3,27
0,60	-10	7	4,19	0	-8,78	-4,15
0,70	-10	6	4,81	0	-8,75	-5,03
0,80	-10	5	5,32	0	-8,73	-5,90
0,90	-10	4	5,74	0	-8,70	-6,78
1,00	-10	3	6,06	0	-8,68	-7,64
1,10	-10	2	6,27	0	-8,66	-8,51
1,20	-10	1	6,39	0	-8,63	-9,38
1,30	-10	0	6,40	0	-8,61	-10,24
1,40	-10	-1	6,32	0	-8,59	-11,10
1,50	-10	-2	6,13	0	-8,56	-11,95
1,60	-10	-3	5,85	0	-8,54	-12,81
1,70	-10	-4	5,46	0	-8,51	-13,66
1,80	-10	-5	4,98	0	-8,49	-14,51
1,90	-10	-6	4,39	0	-8,47	-15,36
2,00	-10	-7	3,70	0	-8,45	-16,21
2,10	-10	-8	2,91	0	-8,42	-17,05
2,20	-10	-9	2,02	0	-8,40	-17,89
2,30	-10	-10	1,03	0	-8,38	-18,73
2,40	-10	-12	-0,07	0	-8,36	-19,57
2,50	-10	-12	-1,27	0	-8,33	-20,40
2,51	-10	-13	-1,39	0	-8,33	-20,48
2,52	-9	-13	-1,52	0	-8,33	-20,57
2,53	-9	-13	-1,65	0	-8,33	-20,65
2,54	-9	-13	-1,78	0	-8,32	-20,73
2,55	-9	-13	-1,90	0	-8,32	-20,82
						-25,15

Tabla 8.30 - Control Volume 1 m³ – Turbulence Factor 5 – Initial Angle 30° - Free Volume 7,5 m³

t	a_v	v_v	x_i	a_h	v_h	z_i
0,18	-10	7,1	0,37	0	-11,88	-0,59
0,20	-10	6,9	0,51	0	-11,88	-0,83
0,30	-10	5,9	1,15	0	-11,85	-2,02
0,40	-10	4,9	1,69	0	-11,83	-3,20
0,50	-10	3,9	2,12	0	-11,81	-4,39
0,60	-10	2,9	2,46	0	-11,79	-5,56
0,70	-10	1,9	2,70	0	-11,76	-6,74
0,80	-10	0,9	2,84	0	-11,74	-7,92
0,90	-10	-0,1	2,87	0	-11,72	-9,09
1,00	-10	-1,1	2,81	0	-11,70	-10,26
1,10	-10	-2,1	2,65	0	-11,68	-11,43
1,20	-10	-3,1	2,39	0	-11,65	-12,60
1,30	-10	-4,1	2,02	0	-11,63	-13,76
1,40	-10	-5,1	1,56	0	-11,61	-14,92
1,50	-10	-6,1	1,00	0	-11,59	-16,08
1,60	-10	-7,1	0,33	0	-11,57	-17,24
1,70	-10	-8,2	-0,43	0	-11,55	-18,40
1,80	-10	-9,2	-1,30	0	-11,53	-19,55
1,81	-10	-9,3	-1,39	0	-11,52	-19,67
1,82	-10	-9,4	-1,48	0	-11,52	-19,78
1,83	-10	-9,5	-1,58	0	-11,52	-19,90
1,84	-10	-9,6	-1,67	0	-11,52	-20,01
1,85	-10	-9,7	-1,77	0	-11,51	-20,13
1,86	-10	-9,8	-1,86	0	-11,51	-20,24
1,87	-10	-9,9	-1,96	0	-11,51	-20,36
						-28,64

Tabla 8.31 - Control Volume 1 m³ – Turbulence Factor 5 – Initial Angle 40° - Free Volume 7,5 m³

t	a_v	v_v	x_i	a_h	v_h	z_i
0,18	-10	8,97	0,40	0	-10,69	-0,50
0,20	-10	8,77	0,57	0	-10,68	-0,72
0,30	-10	7,76	1,40	0	-10,67	-1,78
0,40	-10	7.00	2,12	0	-10,65	-2,85
0,50	-10	6.00	2,75	0	-10,63	-3,91
0,60	-10	5.00	3,27	0	-10,61	-4,98
0,70	-10	4.00	3,70	0	-10,59	-6,04
0,80	-10	3.00	4,02	0	-10,58	-7,10
0,90	-10	2.00	4,24	0	-10,56	-8,15
1,00	-10	1.00	4,37	0	-10,54	-9,21
1,10	-10	0.00	4,39	0	-10,52	-10,26
1,20	-10	-1.00	4,31	0	-10,51	-11,31
1,30	-10	-2.00	4,14	0	-10,49	-12,36
1,40	-10	-3.00	3,86	0	-10,47	-13,41
1,50	-10	-4.00	3,48	0	-10,45	-14,46
1,60	-10	-5.00	3,01	0	-10,43	-15,50
1,70	-10	-6.00	2,43	0	-10,42	-16,54
1,80	-10	-7.00	1,75	0	-10,40	-17,58
1,90	-10	-8.00	0,97	0	-10,38	-18,62
2,00	-10	-9.00	0,09	0	-10,37	-19,66
2,10	-10	-10.00	-0,88	0	-10,35	-20,70
2,20	-10	-11.00	-1,96	0	-10,33	-21,73
						-28,40

Tabla 8.32 - Control Volume 5 m³ – Turbulence Factor 5 – Initial Angle 30° - Free Volume 7,5 m³ - Distance Oriented

t	a_v	v_v	x_i	a_h	v_h	z_i
0,18	-10	9,34	0,40	0	-9,48	-0,47
0,20	-10	9,14	0,58	0	-9,48	-0,66
0,30	-10	8,13	1,45	0	-9,46	-1,60
0,40	-10	7.00	2,21	0	-9,45	-2,55
0,50	-10	6.00	2,87	0	-9,43	-3,49
0,60	-10	5.00	3,43	0	-9,42	-4,44
0,70	-10	4.00	3,89	0	-9,41	-5,38
0,80	-10	3.00	4,25	0	-9,39	-6,32
0,90	-10	2.00	4,51	0	-9,38	-7,26
1,00	-10	1.00	4,67	0	-9,36	-8,19
1,10	-10	0.00	4,73	0	-9,35	-9,13
1,20	-10	-1.00	4,69	0	-9,34	-10,06
1,30	-10	-2.00	4,55	0	-9,32	-11,00
1,40	-10	-3.00	4,31	0	-9,31	-11,93
1,50	-10	-4.00	3,97	0	-9,29	-12,86
1,60	-10	-5.00	3,53	0	-9,28	-13,79
1,70	-10	-6.00	2,99	0	-9,27	-14,71
1,80	-10	-7.00	2,35	0	-9,25	-15,64
1,90	-10	-8.00	1,61	0	-9,24	-16,56
2,00	-10	-9.00	0,77	0	-9,23	-17,49
2,10	-10	-10.00	-0,17	0	-9,21	-18,41
2,20	-10	-11.00	-1,21	0	-9,20	-19,33
2,21	-10	-11.00	-1,32	0	-9,20	-19,42
2,22	-10	-11.00	-1,43	0	-9,20	-19,51
2,23	-10	-11.00	-1,54	0	-9,19	-19,61
2,24	-10	-11.00	-1,65	0	-9,19	-19,70
2,25	-10	-11.00	-1,76	0	-9,19	-19,79
2,26	-10	-11.00	-1,88	0	-9,19	-19,88
2,27	-10	-12.00	-1,99	0	-9,19	-19,97
						-25,25

Tabla 8.33 - Control Volume 1 m³ – Turbulence Factor 5 – Initial Angle 40° - Free Volume 7,5 m³

t	a_v	v_v	x_i	a_h	v_h	z_i
0,20	-10	11,59	0,67	0,4	-16,21	-0,43
0,30	-10	11,22	1,01	0,4	-16,20	-0,92
0,40	-10	10,23	1,33	0,4	-16,19	-1,41
0,50	-10	9,24	1,63	0,4	-16,17	-1,89
0,60	-10	8,25	1,89	0,4	-16,16	-2,38
0,70	-10	7,26	2,12	0,4	-16,15	-2,86
0,80	-10	6,28	2,33	0,4	-16,13	-3,35
0,90	-10	5,29	2,50	0,4	-16,12	-3,83
1,00	-10	4,31	2,65	0,4	-16,11	-4,31
1,10	-10	3,33	2,76	0,4	-16,09	-4,80
1,20	-10	2,35	2,85	0,4	-16,08	-5,28
1,30	-10	1,37	2,91	0,4	-16,07	-5,76
1,40	-10	0,39	2,93	0,4	-16,06	-6,24
1,50	-10	-0,59	2,93	0,4	-16,04	-6,72
1,60	-10	-1,57	2,90	0,4	-16,03	-7,21
1,61	-10	-1,67	2,89	0,4	-16,03	-7,25
1,62	-10	-1,77	2,89	0,4	-16,03	-7,30
1,63	-10	-1,87	2,88	0,4	-16,03	-7,35
1,64	-10	-1,97	2,88	0,4	-16,03	-7,40
						-23,45

Tabla 8.34 - Control Volume 1 m³ – Turbulence Factor 5 – Initial Angle 30° - Free Volume 5 m³

t	av	vv	xi	ah	vh	zi
0,50	-10	4,40	1,02	0,7	-20,99	-2,22
0,60	-10	3,42	1,14	0,7	-20,97	-2,85
0,70	-10	2,44	1,23	0,7	-20,95	-3,48
0,80	-10	1,46	1,29	0,7	-20,93	-4,11
0,90	-10	0,48	1,32	0,7	-20,90	-4,74
1,00	-10	-0,50	1,32	0,7	-20,88	-5,36
1,10	-10	-1,48	1,29	0,7	-20,86	-5,99
1,20	-10	-2,46	1,24	0,7	-20,84	-6,62
1,30	-10	-3,44	1,15	0,7	-20,82	-7,24
1,40	-10	-4,42	1,03	0,7	-20,80	-7,87
1,50	-10	-5,41	0,88	0,7	-20,77	-8,49
1,60	-10	-6,39	0,71	0,7	-20,75	-9,11
1,70	-10	-7,37	0,50	0,7	-20,73	-9,73
1,80	-10	-8,36	0,27	0,7	-20,71	-10,36
1,90	-10	-9,35	0,00	0,7	-20,69	-10,98
2,00	-10	-10,34	-0,29	0,7	-20,67	-11,60
2,10	-10	-11,33	-0,61	0,7	-20,65	-12,22
2,20	-10	-12,33	-0,97	0,7	-20,62	-12,84
2,30	-10	-13,32	-1,35	0,7	-20,60	-13,45
2,40	-10	-14,32	-1,77	0,7	-20,58	-14,07
2,41	-10	-14,42	-1,81	0,7	-20,58	-14,13
2,42	-10	-14,52	-1,85	0,7	-20,58	-14,20
2,43	-10	-14,62	-1,90	0,7	-20,58	-14,26
2,44	-10	-14,73	-1,94	0,7	-20,57	-14,32
2,45	-10	-14,83	-1,98	0,7	-20,57	-14,38
						-40,83

Tabla 8.35 - Control Volume 1 m³ – Turbulence Factor 3 – Initial Angle 30° - Free Volume 10 m³

t	av	vv	xi	ah	vh	zi
0,17	-10	12,66	0,77	0,4	-14,93	-0,53
0,20	-10	12,36	1,14	0,4	-14,92	-0,98
0,30	-10	11,37	2,33	0,4	-14,88	-2,47
0,40	-10	10,38	3,42	0,4	-14,84	-3,96
0,50	-10	9,38	4,41	0,4	-14,81	-5,44
0,60	-10	8,40	5,30	0,4	-14,77	-6,92
0,70	-10	7,41	6,09	0,4	-14,73	-8,39
0,80	-10	6,42	6,78	0,4	-14,70	-9,86
0,90	-10	5,44	7,37	0,4	-14,66	-11,33
1,00	-10	4,46	7,87	0,4	-14,63	-12,80
1,10	-10	3,48	8,26	0,4	-14,59	-14,26
1,20	-10	2,50	8,56	0,4	-14,55	-15,72
1,30	-10	1,51	8,76	0,4	-14,52	-17,17
1,40	-10	0,53	8,86	0,3	-14,48	-18,62
1,50	-10	-0,45	8,87	0,3	-14,45	-20,07
1,60	-10	-1,43	8,77	0,3	-14,42	-21,51
1,61	-10	-1,52	8,76	0,3	-14,41	-21,65
1,62	-10	-1,62	8,74	0,3	-14,41	-21,80
1,63	-10	-1,72	8,73	0,3	-14,40	-21,94
1,64	-10	-1,82	8,71	0,3	-14,40	-22,09
1,65	-10	-1,92	8,69	0,3	-14,40	-22,23
						-35,19

Tabla 8.36 - Control Volume 1 m³ – Turbulence Factor 5 – Initial Angle 30° - Free Volume 10 m³

Model	Free Volume	Control Volume	Turbulence Factor	Initial Angle	Horizontal Speed	Vertical Speed	Reach in Air	Ground Displacement	Total Displacement
I	7,5	5	2	30°	6,33	0,64	5,8	2,5	**8,3**
II	7,5	5	3	30°	14,50	9,59	32,9	11,8	**44,7**
III	7,5	5	4	30°	18,08	12,44	50,9	17,4	**68,3**
IV	7,5	5	5	30°	8,8	6,1	13,6	4,7	**18,3**
V	7,5	1	3	20°	10,61	11,39	26,7	5,9	**32,6**
VI	7,5	1	4	20°	9,34	8,43	18,2	4,8	**23,4**
VI	7,5	1	4	20°	10,96	8,55	21,6	7,1	**28,7**
VI	7,5	1	4	40°	3,45	4,36	4,1	0,8	**4,9**
VI	7,5	1	4	40°	8,89	5,44	12,5	4,8	**17,3**
VII	7,5	1	5	20°	6,69	12,81	17,9	2,5	**20,4**
VII	7,5	1	5	30°	8,88	11,00	20,8	4,4	**25,2**
VII	7,5	1	5	40°	11,88	7,1	20,4	8,2	**28,6**
VII	7,5	1	5	40°	10,69	8,97	21,7	6,7	**28,4**
VII	7,5	1	5	40°	9,48	9,34	20,0	5,2	**25,2**
VIII	5	1	5	30°	16,21	11,59	7,4	16,1	**23,5**
IX	10	1	3	30°	20,99	4,4	14,4	26,4	**40,8**
X	10	1	5	30°	14,93	12,66	14,4	20,8	**35,2**

Table 8-37. Height and Displacement Model I to X

Appendix F

ANNEX: Chapter 10 Tables

Angle	Velocity X-axes	Velocity Y-axes
0	1,30	0,10
5	1,30	0,12
10	1,28	0,27
15	1,26	0,43
20	1,22	0,61
25	1,18	0,80
30	1,12	1,01
35	1,06	1,21
40	0,99	1,42
45	0,92	1,63
50	0,83	1,83
55	0,74	2,01
60	0,64	2,19
65	0,54	2,34
70	0,44	2,47
75	0,33	2,57
80	0,22	2,64
85	0,10	2,69
90	-0,01	2,70
95	-0,12	2,68
100	-0,24	2,63
105	-0,35	2,55
110	-0,46	2,44
115	-0,56	2,31
120	-0,66	2,16
125	-0,76	1,98
130	-0,85	1,79
135	-0,93	1,59
140	-1,01	1,38
145	-1,07	1,17
150	-1,13	0,97
155	-1,19	0,77
160	-1,23	0,58
165	-1,26	0,40
170	-1,28	0,24
175	-1,30	0,10
180	-1,30	-0,02
185	-1,29	-0,12
190	-1,28	-0,20
195	-1,25	-0,25
200	-1,21	-0,29
205	-1,17	-0,30

Angle	Velocity X-axes	Velocity Y-axes
225	-0,90	-0,21
210	-1,11	-0,30
215	-1,05	-0,28
220	-0,98	-0,25
230	-0,81	-0,16
235	-0,72	-0,11
240	-0,63	-0,06
245	-0,52	-0,02
250	-0,42	0,02
255	-0,31	0,06
260	-0,20	0,08
265	-0,08	0,10
270	0,03	0,10
275	0,15	0,09
280	0,26	0,07
285	0,37	0,04
290	0,48	0,00
295	0,58	-0,04
300	0,68	-0,09
305	0,77	-0,14
310	0,86	-0,19
315	0,95	-0,23
320	1,02	-0,27
325	1,09	-0,29
330	1,14	-0,30
335	1,19	-0,30
340	1,23	-0,27
345	1,27	-0,22
350	1,29	-0,16
355	1,30	-0,07
360	1,30	0,04

Table 10.1 - Liquid Flowed Through Loading Port X and Y Axes Velocity as an Angle Function

Bibliography

[1] Lee´s Loos Prevention in the Process Industries; 3er Ed Sam Mannan

[2] Gas Explosion Handbook; Bjerketvedt, Bakke, van Wingerden

[3] Mark´s Mechanical Engineer Handbook; Baumister

[4] GreenBook: TNO Methods for the Calculation of the Physical Effects. Resulting from Releases of Hazardous Materials (Liquid and gases) (2nd Edition) Voorburg (Holland), Directorate-General of Labor, Ministry of Social affairs and Employment.

[5] NFPA 68 Guide for Venting of Deflagrations; Edition 2002

[6] UL 142. Steel Aboveground Tanks for Flammable and Combustible Liquids. Underwriters Laboratories Inc. (UL)

[7] Interaction of a Shock Wave with a Water Layer; Andrzej Teodorczyk Institute of Heat Engineering Warsaw University of Technology

[8] Evaluation of de Human Body as an Airfoil by William P. Schane, LTC, MC - U. S. Army Aeromedical Research Laboratory and U. Dean C. Borgman, Research Scientist U.S. Army Aeronautical Research Laboratory Moffett Field, California MAY 1969

[9] Apuntes de Mecánica Newtoniana: Sistemas de Partículas, Cinemática y Dinámica del Rígido. Ariel Fernández. Daniel Marta. Instituto de Física - Facultad de Ingeniería - Universidad de la República

[10] NTP 385: Fugas en Recipientes: Emisión en Fase Gaseosa. Instituto Nacional de Seguridad e Higiene en el Trabajo. Ministerio de Trabajo y Asuntos Sociales de España.

[11] Venting of Gaseous Explosions: Turbulization Aspect, Vladimir V. Molkov. All-Russia Scientific Research Institute for Fire Protection, Ministry of the Interior. VNIIPO, Balashikha-6, Moscow region, Russia,

[12] Estimation of Peak Pressure for Sonic-Vented Hydrocarbon Explosions in Spherical Vessels, Michael Epstain, Ian Swift, Hans Fauske.

[13] A Simple Model for Ski Jump Flight Mechanics Used as a Tool for Teaching Aircraft Gliding Flight. Vassilios McInnes Spathopoulos, Department of Aircraft Technology. Technological Educational Institute of Chalkis. Psachna, Greece

[14] Detonation and the Hydrodynamics of Reactive Shock Waves. Roger A. Strehlow. Department of Aeronautical and Astronautical Engineering. University of Illinois, Urbana, Illinois

[15] Development of a Simplified Theoretical Model for Dynamic Burst Time and Pressure of a Cylindrical Shell. Cunjiang Cheng and G. E. Otto Widera. Bjorksten Research Lab, BIT 7, INC., Madison, Wisconsin. Center for Joining and Manufacturing Assembly, Marquette University, Milwaukee, Wisconsin.

[16] Pressure Vessel Burst Test Study. Maurice R. Cain, General Physics Corporation for 45th Space Wing -Patrick Air Force Base, Florida

[17] Detonation and Transition to Detonation in Partially Water-Filled Pipes. Neal

P. Bitter and Joseph E. Shepherd. Graduate Aeronautical Laboratories. California Institute of Technology.

[18] The physics of Ski Jumping. W. Müller. Department of Biophysics, Medical University of Graz, Austria.

[19] Weight, Volume, and Center of Mass Segments of the Human Body. Charles E. Clauser, et al. Air Force Systems Command. Wright- Patterson Air Force Base, Ohio.

[20] Flashing Liquid Jets and Two-Phase Droplet Dispersion. Henk Witlox and Mike Harper, DNV Software, London, UK, Phil Bowen and Vincent Cleary, Cardiff University, UK

[21] Blast Waves Generated by Accidental Explosions. Roger A. Strehlow. Aeronautical and Astronautical Engineering Department. University of Illinois at Urbana-Champaign, Urbana

[22] General Laws for Propagation of Shock Waves through Matter. Leroy F. Henderson. Department of Mechanical Engineering, University of Sidney, Australia.

[23] Blast Effects of External Explosions. I. Sochet. Ecole Nationale Supérieure d'Ingénieurs de Bourges – Institut PRISME. Bourges, France.

[24] The Influence of Vessel Volume and Equivalence Ratio In Vented Gas Explosions. Kasmani, Andrews, Phylaktou. Faculty of Chemical and Natural Resources Engineering, Universiti Teknologi. Malaysia. Energy and Resources Research Institute, University of Leeds, UK.

[25] Closed Algebraic Expressions for the Adiabatic Limit Value of the Explosion Constant in Closed Volume Combustion. Eric Van den Bulck. Mechanical Engineering Department, Katholieke Universiteit Leuven. Heverlee, Belgium.

[26] Dynamics of a Skydiver. Simulation of Freefall and Parachute Deployment. Nil Valls. Illinois Institute of Technology.

[27] Aircraft Jet Engine Exhaust Atlantic City international Airport Blast Effects on Par-56 Runway. Threshold Lamp Fixtures. Jacob K. Struck, U.S. Army, Armament Research, Development and Engineering Center. Dover, New Jersey. Anthony J. Barile. FAA Technical Center.

[28] Flashing Liquid Jets and Two-phase Dispersion. A Review. Henk W M Witlox. Net Norske Veritas, London. Philip J Bowen Subcontractor to Det Norske Veritas.

[29] Research on Bursting Pressure Formula of Mild Steel Pressure Vessel. Zheng Chuan-xiang, Lei Shao-hui. Institute of Chemical Process Machinery, Zhejiang University. Hangzhou, China.

Figure Index

Figure 1.1 - Free Tank Volume 21

Figure 3.1 - Gas Detector Biosystems - Multipro 45

Figure 4.1 - Effect of Essay Volume K_G Measure for Spherical Tanks 51

Figure 4.2 - Explosions in Closed Tanks: Effect of Volume. Propane Stoichiometric Concentration 54

Figure 4.3 - Variation of Pressure in Wrecked Tank as a Function of Time. Case # 1 : Volume 7.5 m^3 - Factor Turbulence 3 56

Figure 4.4 - Effect of Turbulence on the Maximum Rate Rising in Pressure vs. Time for Mixtures of Methane and Air 60

Figure 4.5 - Sizing for Gas Venting Area. Pstat = 0.1 bar 62

Figure 4.6 - Elongated Tank Correction. Factor B - for Gas 62

Figure 4.7 - Volume Correction. Factor C - for Gas (0 m^3 to 10 m^3) 63

Figure 4.8 - Evolution of Inflamed Mix $\frac{dm_{bi}}{dt}\frac{dm_{bi}}{dt}$. Equation [4.13] 66

Figure 4.9 - Evolution of Inflamed Mix dm_{bi}/dt at the Tank 67

Figure 4.10 - Pressure Variation in Time for a 10 m^3 tank with vent area of 0.20 m^3 for Different Turbulence Factors 71

Figure 4-1 1. Pressure Variation in Time for Wrecked Tank Free Volume is 7,5 m^3 the vent area of 0,20 m^3 and Turbulence Factor is 3 73

Figure 4-12. Burned Gas Volume in the Interval i 78

Figure 4-13. Control Volume at the Vicinity of the Loading Port 79

Figure 5-1. Scaled Overpressure of Tank Burst. (Baker et al. 1975). 97

Figure 5-2. Scaled Impulse for Pentonite. (Baker et al. 1975) 99

Figure 5-3. Scaled Impulse for a Tank Burst. (Baker et al. 1975) 100

Figure 5.4 - Scaled Peak Overpressure at Short Distance for a Tank Burst γ= 1,4 . (Baker et al. 1975) 102

Figure 5.5 - Static Overpressure vs Scaled Distance 105

Figure 5.6 - Dynamic Pressure vs. Scaled Distance 106

Figure 5.7 – Non-Dimensioned Duration of Positive Phase vs. Scaled Distance . 107

Figure 6.1 - Explosion Damage. Survival Curves for a 70 kg Person at Free Flow Body Axis Perpendicular to Pressure Wave Direction. (Bowen IG, Fletcher and

Richmond, 1968) 120

Figure 6.2 - Flow Around a Person Standing at Free Flow Situation with Corporal Axis Perpendicular to the Direction of Pressure Wave 120

Figure 6.3 - Explosions Damage Effects: Lung Injury. Diagram Pressure – Impulse of Survival Applicable to All Standard Postures and Different Body Weights (W.E. Baker et al 1983.) 122

Figure 6.4 - Eardrum Rupture Probability for Overpressure 124

Figure 6-5. Landing Speed of Body Displacement Based on Lateral Pressure and Impulse for a 70 kg Weight Person 127

Figure 8.1 Starting Position of Flame Ignition on the Loading Port Detail . . . 140

Figure 8.2 - Flow Diagram of Gases Trough Loading Port 141

Figure 8.3 - Body Positions, Angles, and Drag and Lift Efforts 146

Figure 8.4 - Sequence of Movement 151

Figure 10.1 Wave Creation Scheme 160

Figure 10.2 - Dispersion Modeling of Liquid Trough Loading Port with Table 10-1 X and Y axes Velocity and Vertical Velocity 27 m/s. Tank and Loading Port Represent in Red. The Limits of Asphalt Diluted RC2 in Dots 162